Oral Presentations

Tuesday, 24 September 2013

Hall & Meeting Room, Kanazawa Bunka Hall

	Tuesday, 24 September				
Time		Hall		Meeting Room	
09:00-09:10	9:00	PL-03	**Plenary**		
09:10-09:20					
09:20-09:30			A. Tuerler		
09:30-09:40	9:30	PL-04	**Plenary**		
09:40-09:50					
09:50-10:00			S. Nagao		
10:00-10:10	10:00	**Coffee Break**			
10:10-10:20					
10:20-10:30	10:20	ENI-01	**Invited**	NCI-01	**Invited**
10:30-10:40					
10:40-10:50			H. Foerstendorf		S. Dmitriev
10:50-11:00	10:50	ENO-01	General	NCI-02	**Invited**
11:00-11:10			Z.J. Guo		
11:10-11:20	11:10	ENO-02	General		Ch.E. Duellmann
11:20-11:30			H. Tuovinen	NCI-03	**Invited**
11:30-11:40	11:30	ENO-03	General		
11:40-11:50			M.- C. Wu		H. Haba
11:50-12:00	11:50	ENO-04	General	NCO-06	General
12:00-12:10			T. Ohnuki		V. Pershina
12:10-13:20	12:10	**Lunch Time**			
13:20-13:30	13:20	ENO-05	General	NCO-07	General
13:30-13:40			S. Sachs		D. Rudolph
13:40-13:50	13:40	ENO-06	General	NCO-08	General
13:50-14:00			Y. Iwahana		A. Yakushev
14:00-14:10	14:00	ENO-07	General	NCO-09	General
14:10-14:20			J. Krmela		J. Even
14:20-14:30	14:20	ENO-08	General	NCO-10	General
14:30-14:40			K. Masumoto		H. Nitsche
14:40-14:50	14:40	ENO-09	General	NCO-11	General
14:50-15:00			H.W. Gaeggeler		R. Eichler
15:00-15:10	15:00	ENO-10	General	NCO-12	General
15:10-15:20			A. Sakaguchi		T.K. Sato
15:20-15:30	15:20	**Coffee Break**			
15:30-15:40					
15:40-15:50	15:40	ENI-02	**Invited**	NEI-01	**Invited**
15:50-16:00					
16:00-16:10			J.V. Krtaz		Z.F. Chai
16:10-16:20	16:10	ENO-11	General	NEI-02	**Invited**
16:20-16:30			J.H. Park		
16:30-16:40	16:30	ENO-12	General		A. Goswami
16:40-16:50			J. Zheng	NEO-01	General
16:50-17:00	16:50	ENO-13	General		E. Loefstroem-Engdahl
17:00-17:10			I. Milanovic	NEO-02	General
17:10-17:20	17:10	FKI-05	**Invited**		Y. Tomobuchi
17:20-17:30				NEO-03	General
17:30-17:40			K. Minato		F. Poineau
17:40-17:50	17:40	FKO-09	General	NEO-04	General
17:50-18:00			Y. Oura		A. Braatz
18:00-18:10	18:00	FKO-10	General	NEO-05	General
18:10-18:20			K. Hirose		R. Chen
18:20-18:30					
18:30-18:40					
18:40-18:50					
18:50-19:00	18:50	**Poster Session**			
19:00-19:20					
19:20-19:40					
19:40-20:00					
20:00-	20:00				

Advances in the Production and Chemistry of the Heaviest Elements

Andreas Türler[1,2]

[1] Laboratory of Radiochemistry and Environmental Chemistry, Paul Scherrer Institute, Villigen-PSI, Switzerland
[2] Laboratory of Radiochemistry and Environmental Chemistry, University of Bern, Bern, Switzerland

Abstract – Now that the discovery of all elements in the 7th period has been announced, has the far end of the Periodic Table of the Elements been reached? What is the heaviest element in the Periodic System? Are there still undiscovered ones which might even be found in nature? Is there an 8th period and how many elements will it contain? Will we need to introduce the g-orbitals and will the current principles governing the groups and periods of the Periodic Table still be valid for the heaviest elements? These intricate questions are the topic of current research in fundamental nuclear chemistry.

Keywords – APSORC'13 Keywords

I. INTRODUCTION

For increasingly heavy nuclei the electrostatic repulsions of protons cannot be sufficiently compensated by the attractive nuclear force through an increasing number of mediating neutrons. Therefore, the heaviest stable known nucleus is already reached with ^{208}Pb. All isotopes of heavier elements, including some elements such as Bi, Th, and U that still can be found in nature as remnants of the last nucleosynthesis process, are radioactive and decay preferentially by successive α-particle and β^--particle emissions back to the last stable element Pb.

A. Synthesis of Heavy Elements

All elements heavier than Pu (Z=94) are man-made. Transactinide elements ($Z \geq 104$) are synthesized currently only in complete heavy ion fusion reactions at high power accelerators on a "one atom at a time" level. Spectacular progress was obtained by using the very tightly bound, doubly magic nucleus ^{48}Ca and actinide target nuclei. Oganessian et al. were able to synthesize single atoms of elements 113 through 118 (with ^{294}118 currently being the heaviest observed nucleus) and observe their radioactive decay [1]. So far, only elements 114 and 116 have been authenticated by IUPAC and the element names flerovium, Fl, and livermorium, Lv, suggested by the team of discoverers, have recently been made official by IUPAC.

The addition of 6 new elements in the past decade was remarkable in several ways. First, the maximum production cross sections of elements Rf through Cn (Z=104-112) could be described rather well by an exponential decay law, where the cross sections dropped by roughly a factor of 10 when increasing the atomic number by 2 units. In the synthesis of ^{277}Cn production cross sections of less than 1 pb (10^{-36} cm^2) were determined. However, by using ^{48}Ca projectiles, this trend was broken and rather constant maximum production cross sections of several picobarns were measured for synthesis of elements Cn through Lv (Z=112-116) and even for elements 117 and 118 values near or slightly below 1 pb were observed. Nevertheless, even under optimum conditions a production cross section of 1 pb translates into the synthesis of only 1 atom of a superheavy nuclide every 36 h on average. Second, of the more than 50 new nuclides produced in these experiments a number of them have $t_{1/2} > 1$ s and, thus, live long enough for chemical investigations. This result is in strong contrast to the previously known, more neutron deficient isotopes of Mt, Ds, Rg, and Cn in the range of few milliseconds.

B. Chemical Investigations of Heavy Elements

The place an element occupies in the Periodic Table is not only defined by its atomic number, i.e. the number of protons in the nucleus, but also by its electronic configuration, which defines its chemical properties. Strictly speaking, a new element is assigned its proper place only after its chemical properties have been sufficiently investigated. In some cases it has been possible to experimentally investigate chemical properties of transactinide elements and even synthesize simple compounds. Due to the predicted strong influence of relativistic effects, the experimental investigation of superheavy elements is especially fascinating.

The difficulties involved in the production and rapid chemical isolation of few single atoms of a transactinide element from numerous other reaction products and the subsequent detection of the nuclear decay require the development of unique separation methods. Chemical studies of transactinide elements and simple transactinide compounds have been accomplished in the liquid as well as in the gaseous phase. For the heavy transactinides, which very likely are volatile in their elemental state, gas phase chemistry is the method of choice [2]. Lately, the required decontamination factors from interfering nuclear reaction products grew so large that chemical experiments were coupled to kinematic preseparators that already remove a substantial fraction of the primary beam and of transfer reaction products.

In this contribution the advances made in the synthesis and chemical investigations of transactinide elements are reviewed [3]. Latest results on attempts to synthesize elements beyond Z=118 and experiments to chemically investigate Fl will be highlighted as well as the first synthesis of volatile transactinide carbonyl complexes.

[1] Yu. Ts. Oganessian, Radiochim. Acta 99, 429 (2011).
[2] R. Eichler et al., Angew. Chem. Int. Ed. 47, 3262 (2008).
[3] A. Türler, V.G. Pershina, Chem. Rev. 113, 1237 (2013).

Study on transport of particulate organic matter in river and coastal marine systems using radiocarbon

Seiya Nagao
Low Level Radioactivity Laboratory, Institute of Nature and Environmental Technology, Kanazawa University

This study applies a combined use of carbon isotope composition ($\Delta^{14}C$ and $\delta^{13}C$) to suspended solids in river waters and surface sediments from the river mouth, continental shelf off the coast of Japan. This study is intended to investigate the fate of terrestrial particulate organic matter that is released from the river to the coastal marine environment at three river-coastal systems. Our results indicate that the combined $\Delta^{14}C$ and $\delta^{13}C$ measurements of the particulate organic matter can provide unique information on the sources and age of sediments and their transport behavior.

Keywords –$\delta^{13}C$, $\Delta^{14}C$, suspended solids, transport

Global riverine discharge of organic matter to the ocean represents a substantial source of dissolved terrestrial matter and organic carbon particulates. Continental margins are recognized as the dominant reservoir for organic carbon burial in the marine environment. An accurate inventory for terrestrial and marine organic carbon in continental margin sediments is important for quantitative understanding of biogeochemical cycles.

A variety of geochemical approaches have been employed to define the mixing ratio of marine and terrestrial organic matter, including $\delta^{13}C$ and lignin biomarker analyses. Radiocarbon abundances have become an additional indicator of terrestrial versus marine sources because nuclear weapons testing in the 1950s and 1960s injected large quantities of ^{14}C into the atmosphere. The $\Delta^{14}C$ values of organic matter in river suspended particles range from −980 to +75‰, but plankton and particulate organic carbon in marine environments have enriched ^{14}C values ranging from −45 to +110‰. Therefore, the simultaneous use of $\Delta^{14}C$ and $\delta^{13}C$ values adds a second dimension to isotopic studies of carbon cycling in surface aquatic environments.

This study investigates the fate of terrestrial particulate organic matter that is released from the river to the coastal marine environment at three research fields in Japan.

We selected a river in wetland, Bekanbeushi River, and rivers in forest and paddy field such as the Ishikari, Kuzuryu and Hino Rivers. The river-coastal systems were set up at the Bekanbeuchi River-Lake Akkeshi, the Tokachi River and the Kumaki River-off the coast of the rivers in Japan.

^{14}C measurements were performed by accelerator mass spectrometry at the Japan Atomic Energy Agency and the Institute for Environmental Studies in Japan. The $\Delta^{14}C$ is defined as the deviation in parts per thousand from the modern standard. $\delta^{13}C$ values were determined for sub-samples of the CO_2 gas generated during graphite production, using an isotope ratio mass spectrometer.

Figure 1 shows the $\Delta^{14}C$ values of organic matter in the riverine suspended solids plotted as a function of $\delta^{13}C$ values. The paired $\Delta^{14}C$ vs. $\delta^{13}C$ distributions vary with sampling site and divided into two groups. Riverine POC in wetland has lower in $\delta^{13}C$ and higher in $\Delta^{14}C$ rather than those of rivers in forest and fluvial plain. This indicates higher contribution of younger organic matter at the wetland river systems.

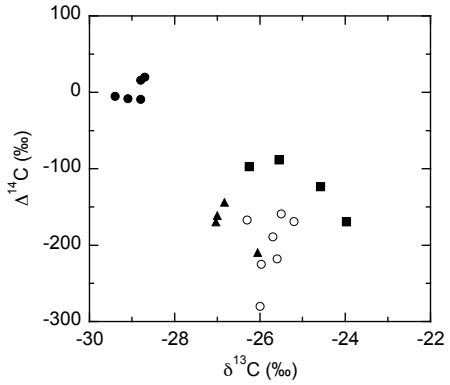

Figure 1 Relationship between $\Delta^{14}C$ and $\delta^{13}C$ of organic matter in the suspended solids for the Bekanbeushi (●), Ishikari (○), Kuzuryu (■) and Hino Rivers (▲).

Figure 2 shows $\Delta^{14}C$ and $\delta^{13}C$ values of organic matter in riverine suspended solids and surface marine sediments at the Kumaki-Nanao Bay system. The $\Delta^{14}C$ decreased from the headwater to the middle sites at the Kumaki River, but increased to the coastal sediments. These results indicate that the middle and lower watershed area has main sources of particulate organic matter exported to the costal marine environments.

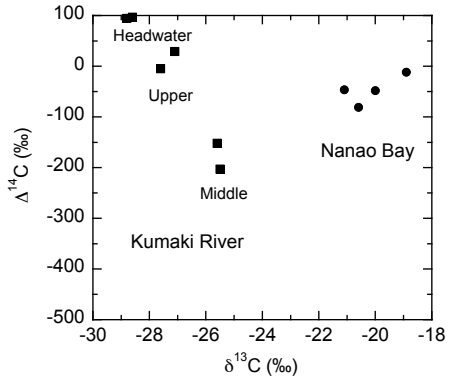

Figure 2 $\Delta^{14}C$ and $\delta^{13}C$ of organic matter in the Kumaki River suspended solids (■) and the Nanao Bay sediments (●).

APSORC'13 - 5th Asia-Pacific Symposium on Radiochemistry
Kanazawa, Japan, 22-27 September 2013

Surface speciation of dissolved radionuclides on mineral phases – A vibrational and X-ray absorption spectroscopic study

H. Foerstendorf[1], K. Gückel[1], N. Jordan[1], A. Rossberg[1,2], V. Brendler[1]
[1]Helmholtz-Zentrum Dresden-Rossendorf, Institute of Resource Ecology, Dresden, Germany
[2]Rossendorf Beamline at the European Synchrotron Radiation Facility (ESRF), Grenoble, France

Abstract – Binary and ternary surface complexes of U(VI) and Np(V) on gibbsite were spectroscopically identified. Se(VI) forms two different types of outer-sphere complexes depending on the solid metal oxide.

Keywords – Surface complexes, minerals, spectroscopy

INTRODUCTION

A detailed description of the molecular interactions of radionuclides with minerals is required for the prediction of their dissemination in the environment. In the past decade, vibrational spectroscopy has been developed to a powerful tool for the study of surface complexes of heavy metal ions on solid phases. In particular, a combined approach of vibrational and X-ray absorption spectroscopy potentially provides comprehensive molecular information. In this study, a survey of very recent results obtained from sorption reactions of radionuclides, namely U(VI), Np(V) and Se(VI) on metal oxides is given.

RESULTS

A. Surface processes of U(VI) and Np(V) on gibbsite

Gibbsite is widely used as a model system for alumosilicate minerals and clays. In addition, it is a ubiquitous weathering product of these minerals and the most common crystalline aluminum hydroxide.

The results of the U(VI) sorption experiments indicate the formation of a monomeric binary inner-sphere surface complex irrespective of the prevailing atmospheric condition and surface loading (Fig. 1A). In addition, it was found that U(VI) surface precipitation occurs at a micromolar concentration level in an inert gas atmosphere. This is circumvented by lowering the initial U(VI) concentration or in the presence of atmospheric CO_2 due to the formation of ternary uranyl carbonato surface complexes. The ternary complex was identified as a dimeric inner-sphere uranyl surface species containing a bidentately coordinated carbonate ligand by EXAFS spectroscopy (Fig. 1B)[1].

Inner-sphere complexation was also derived from spectroscopic results of the Np(V)/gibbsite sorption system. Whilst the neptunyl(V) ion forms a mononuclear surface species under inert gas condition (Fig. 1C), a ternary surface complex in the presence of atmospherically derived CO_2. This ternary species is most likely a mononuclear Al–O–NpO_2–O_2CO-surface species with a bidendately coordinated carbonate ligand (Fig. 1D).

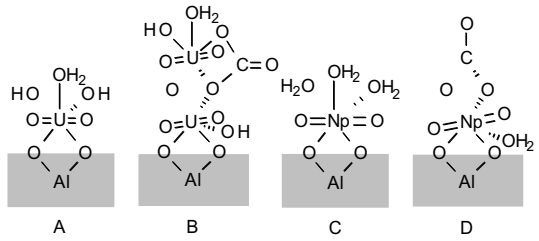

Fig. 1: Proposed surface complexes of U(VI) and Np(V) on gibbsite.

B. Surface speciation of Se(VI)

The sorption of selenate ions on different metal oxide phases exhibits a new type of outer-sphere complexes. As it was already postulated for transition metal cations to form classical and extended outer-sphere complexes [2], this is obviously also true for oxoanions, such as SeO_4^{2-}. With respect to the high sensitivity of vibrational spectroscopy to symmetry properties of molecules, the spectra of the sorption complexes of selenate ions on anatase [3] and maghemite (γ-Fe_2O_3) [4] clearly indicate the formation of different types of outer-sphere complexes (Fig. 2). These findings are corroborated by macroscopic analytical techniques.

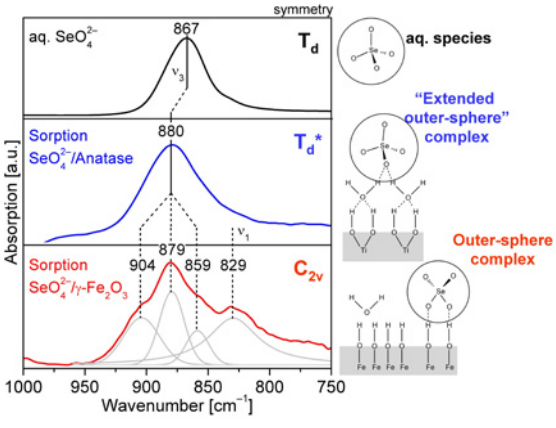

Fig. 2: IR spectra of SeO_4^{2-} species and the derived surface species.

REFERENCES

[1] Gückel, K. et al. (2012) *Chem. Geol.* **326-327**, 27-35.
[2] Lee, S. S. et al. (2010) *Langmuir* **26**, 16647-16651.
[3] Jordan, N. et al. (2011) *Geochim. Cosmochim. Acta* **75**, 1519-1530.
[4] Jordan, N. et al. (2013) *Geochim. Cosmochim. Acta* **103**, 63-75.

APSORC'13 - 5th Asia-Pacific Symposium on Radiochemistry
Kanazawa, Japan, 22-27 September 2013

Adsorption of Eu(III) and Am(III) on granite: Effects of temperature, fulvic acid and background electrolyte

Z.J. GUO, Z.Y. CHEN, Q. JIN, W.S. WU
School of Nuclear Science and Technology, Lanzhou University, Lanzhou, 730000, China
E-mail: guozhj@lzu.edu.cn

Abstract –The adsorption of Eu(III) and Am(III) on crushed Beishan granite (BS03, 600m) was investigated as a function of temperature, background electrolyte and the presence of fulvic acid at different concentrations. It was found that temperature did not affect apparently the distribution coefficient (K_d) of Eu(III) in the range of 25-80 ^oC. At pH < 5.0, the K_d value decreased in $CaCl_2$ solution as compared to that in NaCl solution at the same ionic strength, suggesting cation exchange reactions occurred in low pH range. Whereas in high pH range, the K_d values in $CaCl_2$ and NaCl solutions at the same ionic strength are identical, which indicate inner-sphere surface complexes formed. FA significantly decreased K_d of Eu(III) especially at pH > 4 and the extent of the decrease depended on FA concentration and varied with aqueous pH as well. Aging of freshly crushed granite in synthetic underground water at 150 ^oC for two weeks did not affect apparently Eu(III) K_d values. A surface complexation model (SCM) using Generalized Composite (GC) approach was constructed based on experimental data of Eu(III) in NaCl solutions and verified by experimental data of Eu(III) in $CaCl_2$ solutions as well as in synthetic underground water. The SCM was used to predict Am(III) adsorption on the granite and the calculated results were in accordance with the experimental data of Am(III)

Keywords –Eu(III), Am(III), adsorption, granite, temperature effect, fulvic acid, surface complexation model

I. INTRODUCTION

Beishan granite (Beishan, Gansu province) has been considered as a preliminary selection of host rock for geological disposal of high-level radioactive waste in China, [1]. Considering temperature variation, potential change in electrolytes of underground water, and the presence of humic substances in the near field of a repository, it is necessary to evaluate adsorption of radionuclides on the granite at variable conditions.

II. MATERIAL AND METHODS

$^{152+154}$Eu(III) and ^{241}Am(III) radiotracers were obtained from Chinese Atomic Energy Institute. All other chemicals used were of analytical grade. Beishan granite was sampled from the borehole BS03 at a depth of 600 m. To simplify the adsorption system, carbonates in Beishan granite was removed and the exchangeable cations were transformed into Na-form or Ca-form. Batch sorption was carried out with polyethylene tubes in nitrogen atmosphere glove box.

III. RESULTS AND DISCUSSION

In Generalized Composite (GC) approach [2], a rock is integrally considered and surface reactions on which are assumed to occur on a type of "general sites", although the chemical environmental of surface sites on different minerals and even those on different crystal planes of the same mineral are actually different. In addition, the GC approach ignores electrostatic effect. As a result, a GC model for a radionuclide sorption on a rock is actually the simplest model with the least adjustable parameters.

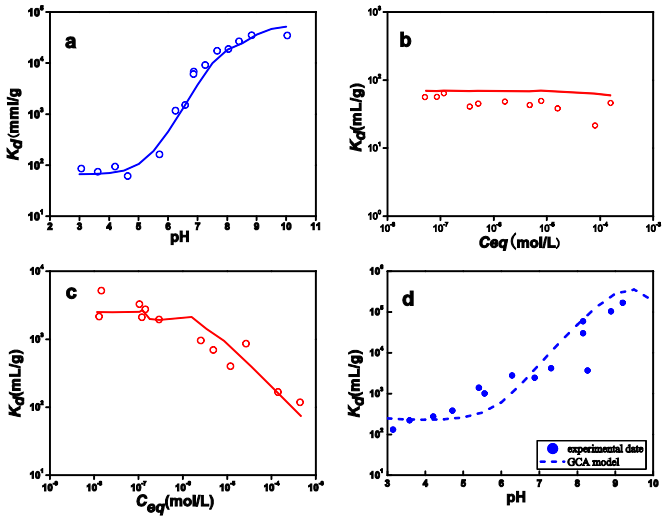

Figure. Eu(III) sorption in $CaCl_2$ and "real" systems, (a) Sorption edge of Eu(III) on Ca-granite, $C_o = 6.74\times10^{-8}$ M, m/V = 1 g/L and $C_{CaCl2} = 0.033$ M; (b) Sorption isotherm of Eu(III) on Ca-granite, $C_{CaCl2} = 0.033$M, m/V = 1g/L and pH = 4.00±0.10; (c) Sorption isotherm of Eu(III) on Ca-granite, C_{CaCl2} = 0.033 M, m/V = 1g/L and pH = 6.50±0.10; (d) Sorption edge of Eu(III) on Na-granite with simulated underground water $C_o = 6.74\times10^{-8}$ M, m/V = 1 g/L and $C_{NaCl} = 0.1$ M.

[1] Guidelines for the R&D for geological disposal of high-level radioactive waste. Beijing: China Atomic Energy Authority (CAEA), Ministry of Environmental Protection, Ministry of Science and Technology, 2006 (in Chinese)
[2] Davis J A, Meece D E, Kohler M, Curtis G P. Approaches to surface complexation modeling of Uranium(VI) adsorption on aquifer sediments. Geochimica et Cosmochimica Acta, 2004, 68: 3621-3641.
[3] Guo Z, Chen Z, Wu W, Liu C, Chen T, Tian W, Li C, The adsorption of Eu(III) on Beishan granite, SCIENTIA SINICA Chimica, 2011, 41: 907-913.

Behaviour of radionuclides and secondary mineral formation in the Talvivaara mining process

Hanna Tuovinen[(1)], Esa Pohjolainen[(2)], Daniela Vesterbacka[(1)], Caroline Kirk[(3)], David Read[(3)], Dina Solatie[(4)], Jukka Lehto[(1)]

[(1)] Laboratory of Radiochemistry, Department of Chemistry, University of Helsinki, P.O. Box 55, FI-00014 University of Helsinki, Finland
[(2)] Geological Survey of Finland, Betonimiehenkuja 4, FI-02151 Espoo, Finland
[(3)] Department of Chemistry, Loughborough University, Loughborough, Leicestershire, LE11 3TU, UK
[(4)] Regional Laboratory of Northern Finland, Finnish Radiation and Nuclear Safety Authority, Lähteentie 2, FI-96400 Rovaniemi, Finland

The Talvivaara nickel deposits are located in Sotkamo, Eastern Finland. The deposits comprise one of the largest known nickel sulphide resources in Europe. Talvivaara is an operational, open cast mine where Talvivaara Mining Company uses bioheap leaching to extract the metals (Ni, Zn, Cu, Co) from the black schist ore. In 2010 the company announced the commencement of uranium production as an addition to its normal mining operations. In heap leaching, uranium dissolves in the pregnant leach solution (PLS) along with main base metals and will be extracted using the solvent extraction (SX) process. The uranium produced will be in the form of yellowcake with an estimated annual production of approximately 350 tons. Currently, the uranium is diverted into a gypsum pond and part of it also ends up in the nickel concentrate as an impurity.

Bioheap leaching is a naturally occurring exothermic process catalysed by indigenous bacteria. The key parameters are particle size (< 8 mm), pH of the pregnant leach solution (2 – 2.5), temperature (20-90 ^{o}C) and the oxidation and aeration rates. The ore is first extracted using conventional large scale open pit drill and blast methods, then crushed and screened in four stages. It is agglomerated in a rotating drum, where recirculated PLS is added to the ore in order to consolidate the finer particles. It is then stacked eight meters high on the primary heap pad for primary leaching. The heap is irrigated from above and the leachate collected from the base of the heaps. The pregnant leach solution is collected in the PLS ponds where a 10% side flow is taken for metals recovery; the remaining 90% per cent is recycled back to irrigation to increase the metal grade. The metals are precipitated from the PLS using hydrogen sulphide and the resulting intermediate products transported for further processing in refineries. After approximately 2 years bioleaching on the primary pad, the leached ore is reclaimed, conveyed and restacked onto secondary heap pads. At this stage, the main part of copper and cobalt is recovered. After secondary leaching, the barren ore will remain permanently in the secondary heaps.

The leaching process oxidizes U(IV) to U(VI) in the form of the uranyl ion (UO_2^{2+}) at low pH. Radioactive progeny from the ^{238}U series are also mobilized and fractionate depending on chemical properties and the ambient conditions. The aim of this study is to generate new data leading to a better understanding of the behaviour of radionuclides, especially ^{226}Ra, ^{210}Pb and ^{210}Po, at each stage of the Talvivaara mining process. In addition the formation of secondary minerals during the leaching process is poorly understood.

Samples were collected from the primary heaps, secondary heaps, the PLS-ponds and gypsum pond in 2011, 2012 and 2013. After pre-treatment, gamma spectrometry was used for direct determination of uranium and thorium progeny. Samples were then analysed by X-ray diffraction (XRD) to determine the main minerals present. The uranium-bearing minerals were determined by electron probe micro-analysis (EPMA). Uranium, thorium and heavy metals were determined by ICP-MS. For alpha spectrometry, uranium and thorium were separated using anion exchange chromatography, ^{210}Po with silver plate precipitation and ^{210}Pb was precipitated from the remaining solution. Leaching experiments were performed in order to determine ^{226}Ra, ^{210}Pb and ^{210}Po – bearing mineral phases.

Preliminary results provide information on the formation of secondary phases and the relative abundance of the initial ore minerals. Uranium in the gypsum pond is found at least in association with goethite (FeO(OH)). The high content of sulphate restricts solubility of radium; ^{226}Ra concentrating in precipitated sulphate minerals. For lead, the formation of anglesite ($PbSO_4$) is probable and polonium is also likely to be bound to secondary minerals in the heaps. The results of this work will play an important role in estimating radiation doses and potential health implications to the local population resulting from past and anticipated disposal. A summary of the main results obtained to date is given in the presentation.

Evaluation of HTO and selenium diffusion behavior in compacted bentonite with different lengths

Chuan-Pin Lee [1], Ming-Chee Wu [1,*],Ching-Yuan Liu [2], Chun-Hua Pan [1], Tsuey-Lin Tsai [3], Hwa-Jou Wei [3], Lee-Chung Men [3]

[1]* Department of Earth Sciences, National Cheng Kung University, Tainan, Taiwan, 70101
[2]Department of Chemical and Materials Engineering, National Central University, Taoyuan, Taiwan, 32001,
[3] Chemistry Divisions, Institute of Nuclear Energy Research, Taoyuan, Taiwan, 32546

Abstract – *n this study, diffusion behavior of selenium(Se) with a concentration of 0.1mM in bentonite (MX80) was investigated using through-diffusion methods with various lengths (0.25, 0.5, 0.75, 1.0, 2.0, 2.5 cm), respectively. Before performing the through-diffusion experiments of Se, a non-reactive tracer (HTO) was applied and achieved to characterize the physical process in compacted MX80 columns with different lengths. It shows that the diffusion process of Se in synthetic seawater (SW) and groundwater (GW) reached equilibrium after 250 and 300 days, respectively. Moreover, both retardation factor (Rf^{cal}) and distribution coefficients (K_d^{cal}) of Se obtained from accumulative concentration's method in through-diffusion test showed an obvious discrepancy in an increasing length/diameter (L/D) ratio. In fact, it presented an agreement of $Rf^{H/Se}$ and $K_d^{H/Se}$ in an increasing L/D ratio in comparison between HTO and Se. It appears that the $Rf^{H/Se}$ and $K_d^{H/Se}$ obtained from the through-diffusion experiments are higher than those derived from the batch experiments. Therefore, it demonstrates that reliable Rf and K_d of Se by through-diffusion experiments could be achieved at a non-reactive radiotracer(HTO) prior to tests and would be more confident for long-term performance assessment.*

Keywords – *Diffusion, Selenium, distribution coefficients, apparent diffusion coefficient*

Sorption Behavior of Dy(III) and Np(V) on microbial consortia

Toshihiko Ohnuki[1], Naofumi Kozai[1], Fuminori Sakamoto
[1]Japan Atomic Energy Agency, Tokai, Ibaraki, 319-1195 Japan

Abstract – To elucidate sorption of trivalent and pentavalent actinides by the consortia of microorganisms sampled at Horonobe, Hokkaido, Japan. In the sorption experiments of Nd(III), Dy(III) (analogue of trivalent actinides), and Np(V) were contacted with the consortia in the solution at pH between 3 and 7 in resting condition. The coordination environment of the sorbed Dy by the consortia was analyzed by EXAFS. For the sorption of Nd and Dy on the consortia, the K_d increased with increasing pH, and was nearly the same as that by single species of *S. putrefaciens*. For the sorption of Np on the consortia, the K_d was higher than that for a single species of *S. putrefaciens*, indicating that the sorption behavior of Np on the consortia is different from that by a single species of *S. putrefaciens*. These results indicate that the consortia poses higher affinity to Np than a single species of S. putrefaciens.

Keywords – Neptunium, trivalent actinides, sorption, consortia of microorganisms

I. INTRODUCTION

The presence of actinides (ANs) in radioactive wastes is a major environmental concern due to their long radioactive half-lives, and its chemical toxicity. The high capacity of microbial surfaces to bind ANs may affect the migration of ANs in the environment. Unfortunately, we have only limited knowledge of the role of microorganisms in the migration of ANs in the environment.

Many researches have been carried out to study adsorption of ANs on the cell surface o microorganisms. Usually in the adsorption experiment single species of microorganism was used, even though microorganisms habit in consortia in environment. The adsorption of divalent cations of Cd, Cu, Ca, Pb, Sr, and Zn by the consortia was nearly the same as that by a single species. However, sorption behavior of ANs by consortia has not been elucidated.

In the present study, sorption behavior of trivalent lanthanides of Nd(III) and Dy(III) (alternative use for Am(III) and Cm(III), and of Np(V), by consortia of microorganisms using batch type sorption experiments..

II. EXPERIMENTAL

Sample locations were at 140 m in depth in the site of JAEA Horonobe Deep Geological Research Center, Horonobe, Hokkaido, Japan. Samples were collected 3 different points on February, 2011. The samples were inoculated in the Fe-reducing bacteria growth medium containing $NaHCO_3$ 1g: NH_4Cl 0.6g: KH_2PO_4 0.24g: KCl 0.04 g: Na-acetate 1 g: Na-citrate 0.4 g: $Fe(OH)_3$ 0.4g in 1 L distilled water under anaerobic condition. The pre-grown consortia were cultured in the medium containing beef extract or shewanella medium under aerobic condition. Culture in the consortia were analyzed by 16S rRNA analysis.

For the sorption experiments of Nd(III), Dy(III), and Np(V) by the consortia were conducted in resting condition. The solution sampled at 4 and 24 hrs after the exposure were centrifuged for 10 min at 4000 rpm. The supernatant was filtered through a membrane filter of 0.2 μm to measure concentrations of the dissolved elements. The concentration of Nd and Dy was 0.1 mM, and Np was 0.01 mM. The sorption experiments were performed in aerobic condition.

The concentrations of Nd and Dy were measured by ICP-AES, and that of Np by liquid scintillation analyzer. The coordination environments of the sorbed Dy(III) by consortia were determined by XAFS analysis using KEK PF.

III. RESULTS AND DISCUSSION

The consortia contained many kind sof bacteria involving Pseudomona and *Shewanella* family by random clone analysis.

For the sorption of Nd and Dy on the consortia, distribution coefficients (K_d) were between 10^4-10^5 ml/g at pH between 3-7. The K_d for Nd and Dy increased with increasing pH. Higher Kd in Dy than Nd was determined. The K_d of Nd and Dy for the single species of *Shewanella putrefaciens*, was approximately 10^4 ml/g at pH around 4, and increased with increasing pH. XAFS analysis showed that the FT spectrum of Dy sorbed on the consortia resembled to that of Dy sorbed on a single species of *Shewanella putrefaciens*, but not to $DyPO_4$, indicatng that the coordination environment of Dy was nearly the same as that on *P. putrefaciens*. These results indicate that the sorption behavior of Nd and Dy on the consortia is nearly the same as that by a single species of *S. putrefaciens*.

For the sorption of Np on the consortia, the K_d was approximately 10^4 ml/g at pH 4. The K_d remained constant with increasing pH of the solution. The K_d for a single species of *S. putrefaciens* was about 10^2 ml/g at pH between 4 and 6.5. The Kd increased with increasing pH. These results indicate that the sorption behavior of Np on the consortia is different from that by a single species of *S. putrefaciens*. Since higher K_d is measured in the consortia than a single species of *S. putrefaciens*, the consortia poses higher affinity to Np than a single species of S. putrefaciens.

This research project has been conducted as the regulatory supporting research funded by the Nuclear Regulation Authority (NRA), Japan.

APSORC'13 - 5th Asia-Pacific Symposium on Radiochemistry
Kanazawa, Japan, 22-27 September 2013

Interaction of Eu(III) with Mammalian Cells as a Function of Eu(III) Concentration and Nutrient Composition

Susanne Sachs, Anne Heller, Gert Bernhard
Helmholtz-Zentrum Dresden-Rossendorf e.V., Institute of Resource Ecology, P.O. Box 510 119, 01314 Dresden, Germany

The Eu(III) toxicity onto FaDu cells is influenced by its chemical speciation that is determined by the composition of the culture medium. However, independent from its speciation, Eu(III) seems to be bound to the cell surface and does not significantly enter the cells.

Eu(III), interaction, mammalian cells, toxicity, speciation

I. INTRODUCTION

In case of the release of long-lived radionuclides, e.g., actinides, into the environment, knowledge about their behavior in biosystems is necessary to assess and prevent health risks for humans. This includes knowledge about bioavailability and toxicity of actinides for/onto cells, which are governed to a large extent by their speciation [1]. In order to enable a better understanding of these processes, we study interaction processes of trivalent actinides/lanthanides with mammalian cells on a cellular level combining biochemical and spectroscopic methods. In the present work we studied the cellular tolerance of FaDu cells (human squamous cell carcinoma cell line) toward Eu(III), as an analog for trivalent actinides, and its uptake into the cells as a function of the metal concentration and the nutrient composition. In parallel, the Eu(III) speciation in the culture media was studied by time-resolved laser-induced fluorescence spectroscopy (TRLFS) to correlate Eu(III) toxicity and uptake with its chemical speciation.

II. EXPERIMENTAL

FaDu cells were grown in Dulbecco's modified eagle medium supplemented with fetal bovine serum (FBS), non-essential amino acids, HEPES buffer, penicillin/streptomycin, sodium pyruvate (37°C, 5% CO_2, 95% humidity) and subcultivated as described in [2]. The Eu(III) toxicity onto FaDu cells ([Eu]: 5-2000 µM) and its uptake into the cells ([Eu]: 10, 1000 µM) was studied in the presence and absence of FBS as described in [2,3]. In addition, the impact of citrate was studied. To differentiate between chemotoxic and radiotoxic effects of Eu(III), first experiments were performed in the presence of FBS ([Eu]: 10, 1000 µM) applying ^{152}Eu as radioactive tracer. The Eu(III) speciation was studied by TRLFS as described in [4].

III. RESULTS

As an example, the viability of FaDu cells after 24 h of incubation with 5-2000 µM Eu(III) in the presence and absence of FBS (no citrate present) is shown in Fig. 1. The Eu(III) toxicity is higher in the absence of FBS than in its presence. This discrepancy is attributed to the different Eu(III) species in the media and points to an unequal bioavailability of Eu(III). In the presence of FBS, Eu(III) is stabilized in solution by complexation with FBS constituents, most probably serum proteins, which was verified by ultrafiltration. In contrast, in the absence of FBS, the Eu(III) solubility is very low. ICP-MS analysis of Eu(III) precipitates as well as TRLFS point to the occurrence of ternary or higher Eu(III) complexes with phosphate as the dominant ligand. The additional presence of citrate does not significantly affect the Eu(III) toxicity onto the cells in the presence of FBS. However, in its absence, an excess of citrate decreases the Eu(III) toxicity most probably due to a change of the chemical speciation.

Independent from the initial Eu(III) speciation, the Eu(III) uptake by the cells is low. It is predominantly located on the cell surface.

Under the studied experimental conditions, the tolerance of FaDu cells versus Eu(III) appears to be not significantly influenced by the presence of ^{152}Eu, i.e., there seems to be no additional radiotoxic effect.

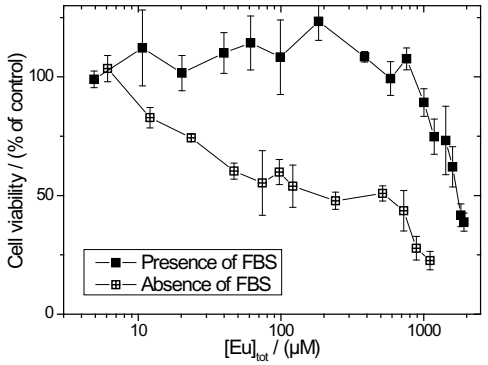

Fig. 1: Cell viability after 24 h of incubation with Eu(III).

ACKNOWLEDGMENTS

We thank J. Seibt, S. Heller, A. Ritter, C. Eckardt, and S. Weiß for experimental and technical support as well as J. Pawelke and E. Leßmann for the first batch of FaDu cells, FBS and training in cell cultivation techniques.

[1] Ansoborlo, E. et al., Biochimie 88 (2006), 1605.
[2] Sachs, S., Bernhard, G., *Annual Report 2011, HZDR-013.* Helmholtz-Zentrum Dresden-Rossendorf, Dresden (2012), p. 12.
[3] Sachs, S., Heller, A., *Annual Report 2012, HZDR-030.* Helmholtz-Zentrum Dresden-Rossendorf, Dresden (2013), p. 26.
[4] Heller, A. et al., *Annual Report 2011, HZDR-013.* Helmholtz-Zentrum Dresden-Rossendorf, Dresden (2012), p. 13.

ENO-06

Monitoring and Elution Characteristics of Radioactive Cs in Incinerator Fly ashes of Municipal Solid Waste

Yuki Iwahana, Yuya Koike, Masaru Kitano, Toshihiro Nakamura
Meiji University

Abstract – Radioactive Cs in incinerator fly ash was monitored and Notification No. 13 test was applied to the ashes in order to estimate the Cs elution. In monitoring, ^{40}K, ^{134}Cs, ^{137}Cs, ^{226}Ra, ^{228}Ra, and ^{228}Th were detected in fly ashes. These concentrations were ^{40}K, 445 – 2,556 Bq kg^{-1}; ^{134}Cs,0 – 10.0 Bq kg^{-1}; ^{137}Cs, 4.2 – 18.4 Bq kg^{-1}; ^{226}Ra,15.0 – 20.1 Bq kg^{-1}; ^{228}Ra, 24.2 – 33.9 Bq kg^{-1}; and ^{228}Th, 23.4 – 33.3 Bq kg^{-1}; respectively. ^{134}Cs was only detected in sample of January, while ^{137}Cs existed in all measured samples, but activity concentrations tended to decrease. As results of pure water and Notification No. 13 elution test, 50–60% of radioactive Cs moved to liquid phase in each case. Since no γ-ray peaks of radioactive Cs were detected on the spectra of elution residues, it was indicated that radioactive Cs in incinerator fly ashes had high water solubility.

Keywords – Radioactive Cs, Notification No. 13 Test, Incinerator Fly Ashes Monitoring

I. INTRODUCTION

Incinerator ashes of municipal solid wastes contain a large amount of hazardous heavy metals and dioxins. They are known as 'specially controlled industrial wastes', and the concentration of hazardous materials in the ashes and leachate from disposal sites are strictly controlled. In Japan, a certification of elution procedure is provided by the Environment Agency of Japan as Notification No. 13 test. In the certification, pH 6.0 of HCl and/or pH8.0 of NaOH solutions were applied to elution. In addition, Fukushima nuclear power plant accident was caused by the Great East Japan Earthquake on March 11, 2011; subsequently radioactive contamination with released radioactive Cs was reported. Following the accident, the Japanese Government established 100, 000 Bq kg^{-1} as the activity concentration limit for radioactive Cs in the incinerator ashes of the MSW that were destined for the landfill. In this report, radioactive Cs in incinerator fly ash was monitored and Notification No. 13 test was applied to the ashes in order to estimate Cs elution.

II. EXPERIMENTAL

The γ-ray measurement were performed with γ-ray spectrometer (γ-PGT) equipped high purity Ge semi-conductor detector. The incinerator fly ashes were obtained in an incinerator plant, located in northern Kyushu, from January to August, 2012.

The elution procedure was followed by the Notification No. 13 test. Eluted materials were added to 2 mL of conc. HNO_3 to rip eluted materials from glass beaker. These solutions were evaporated on evaporation dish to make dried salt. Elution residues and salt were dried at 110°C for a period of 24 h in the drying oven.

About 4 g of solid samples were placed in tin containers (3.8 cmϕ, 1.1 cmh). The containers were made gas tight by sealing with an epoxy resin adhesive and stored for three weeks at least in order to achieve radioactive equilibrium among ^{226}Ra and its daughters. These measurement samples were set away from the Ge-detector to prevent considering the coincidence sum effect. The γ-rays were measured for 48 h.

III. RESULTS AND DISCUSSION

A. *Cs monitoring*

In the fly ahses, ^{40}K, ^{134}Cs, ^{137}Cs, ^{226}Ra, ^{228}Ra, and ^{228}Th were identifed. These concentrations of nuclides were ^{40}K, 445 – 2,556 Bq kg^{-1}; ^{134}Cs,0 – 10.0 Bq kg^{-1}; ^{137}Cs, 4.2 – 18.4 Bq kg^{-1}; ^{226}Ra,15.0 – 20.1 Bq kg^{-1}; ^{228}Ra, 24.2 – 33.9 Bq kg^{-1}; and ^{228}Th, 23.4 – 33.3 Bq kg^{-1}; respectively. ^{134}Cs was only detected in sample of January, while ^{137}Cs existed in all measured samples, but activity concentrations tended to decrease. Therefore, it was considered that the influence of ^{134}Cs, which had been released from Fukushima nuclear power plant, faded away. By contrast, concentrations of natural radioactive nuclides were constant.

B. *Results of Notification No. 13 Test*

To estimate Cs elution, Notification No. 13 test was applied to fly ashes collected on January and August. Pure water elution was also performed under the same condition of official certification. About 50% of ^{134}Cs and 60% of ^{137}Cs eluted when pure water had been used. Comparable results were obtained as the pH 6.0 of HCl and pH 8.0 of NaOH solutions were used for elution. While no γ-ray peaks of radioactive Cs were detected on spectra of each elution residues. Hence, it was indicated that radioactive Cs in incinerator fly ashes had high water solubility.

IV. CONCRUSIONS

Radioactive Cs in incinerator fly ashes tends to decrease from January to August, 2012. From Result of pure water and Notification No. 13 elution test, radioactive Cs in incinerator fly ashes had high water solubility for deposit site of incinerator fly ashes.

APSORC'13 - 5th Asia-Pacific Symposium on Radiochemistry
Kanazawa, Japan, 22-27 September 2013

The Issue of Separation of Uranium from Drinking Water in the Czech Republic

Jan Krmela[1]
[1]UJV Řež a.s., Hlavní 130, Řež, 250 68 Husinec, The Czech Republic, jan.krmela@ujv.cz

Abstract

Natural ground water used for the preparation of drinking water contains a number of cations, anions, elements and other substances depending on the bedrock composition (Ca, Mg, Fe, Mn, heavy metals, radioactive elements, arsenic, chromium, carbonates, sulfates, phosphates, silicates, fulvic and humic acids etc.). Information about composition of drinking water is important to comply with all the requirements on sanitary of drinking water.

The elements that affect the quality of drinking water mainly from groundwater, also includes radioactive elements contained in bedrock sections where water is extracted. These are the elements with long half-lives, mainly alpha emitters (U, Ra, Rn, Th, and elements of the decay series).

Uranium and its decay products are found in all environmental compartments. Radionuclides come to the environment both naturally - weathering and leaching of the rocks, and as a consequence of human activities in connection with the use of raw materials.

Uranium occurs naturally in four oxidation states. The most mobility has hexa-valent state (uranyl ion). Uranyl is highly soluble form of uranium in water. Mobility of uranium in soil and water is affected by many factors.

Complex processes in soil and rock lead to redox reactions forming both insoluble compounds (lower valence forms of uranium) and soluble form of U (VI) (forming by reoxidation), which is again leachable into groundwater. The content of uranium in groundwater depends on the geological composition of the ground, and can reach up to hundreds of μg/L.

At present the issue associated with removing uranium from drinking water is solved in the Czech Republic. New limit for the concentration of natural uranium (^{234}U, ^{235}U and ^{238}U) was recommended at a level of 15 μg/L as the highest limit based on the World Health Organization (WHO). Advice of the Chief Health Officer of the Czech Republic came into force on 1st January 2010, which decreased the limit for uranium in drinking water from original 30 μg/L to new 15 μg/L recommended by WHO. However, the WHO reported a new limit value of 30 μg/L in 2011 based on a new studies, which proved that 30 μg/L uranium in drinking water has not negative effect on the human organism (chemical toxicity) [1]. Limit in the Czech Republic remained at the same level 15 μg/L.

Change the limit leaded to solving the issue on the waterworks in the Czech Republic, which had not any experiences with radioactivity. Some waterworks installed a new device from Germany (ion exchanges), but did not solve what they do with saturated ion exchanges. Ion exchanges as the most suitable material for removing of uranium from drinking water is not reused (without regeneration), but it is used in the uranium industry, where is putted to start of processing of uranium ore. Ion exchanges are replaced with a new one in the waterworks and saturated ion exchanges are discarded in the uranium industry.

Regeneration of ion exchanges could be cheaper, because ion exchanges could be reused and processing of ion exchangers could be cheaper, because it is possible to put the regenerant before the process of precipitation of "yellow cake" in the processing of uranium ore.

This project TA02010044 was supported by TA CR.

Key words - Uranium, Drinking water, Ion exchanger

[1] WHO: Uranium in Drinking-water, Background document for development of WHO guidelines for Drinking-water Duality, WHO/SDE/WSH/03.04/118/Rev/1, 2011.

Air-born contamination caused in a high-energy proton accelerator room

K. Mausmoto[1], A. Toyoda[1], H. Matsumura[1], T. Kunifuda[2]
[1]High Energy Accelerator Research Organization, Tsukuba, 305-0801, Japan
[2]Tokyo Nuclear Service, Tsukuba, 300-2646, Japan

Abstract – Surface contamination caused during the operation of 12-GeV proton synchrotron, KEK have been studied by gamma-ray spectrometry and imaging plate technique. The surface of accelerator component was wiped with the filter paper. PSL value of imaging plate contacted on the filter paper decreased according to the half-life of 2 weeks. Therefore, it was assumed that ^{32}P might be produced from Ar by the high-energy protons and neutrons and deposited on the accelerator components.

Keywords – Air-born activity, High-energy accelerator, ^{32}P, Imaging plate

I. INTRODUCTION

It is well known that various radioisotopes are induced in the stratosphere by cosmic rays. During the operation of a high-energy proton accelerator, air components are also activated by primary protons and secondary neutrons and similar radioisotopes are produced. It is interesting to know the behavior of radioisotopes in an accelerator room. The radioisotopes are deposited on the surface of accelerator components and cause surface contamination problem. In this work, these radioisotopes were wiped with a filter paper. The radioactivity was measured by the gamma-ray spectrometry and the imaging plate technique.

II. EXPERIMENTAL

This work was performed at the 12-GeV proton synchrotron, KEK. After stopping, smeared samples were obtained from on beam pipes, magnets, wall and floor in the accelerator room. In order to measure the activity of beta and gamma nuclides, a GM-counter, a liquid scintillation counter, a Ge-detector and an imaging plate were used.

III. RSULTS AND DISCUSSIONS

(1) A liquid scintillation counter

Tritium was only observed. Carbon-14 could not detected by the background effect.

(2) GM-counter and Imaging plate

Figure 1 shows the decay curves of seven filter papers sampled from the beam line. It was found that the half-life of major activity was 2 weeks. Therefore, it was assumed that ^{32}P was produced and deposited. As the similar result was obtained by a GM-counter, Imaging plate was also detected beta activity. A polyethylene film pasted on the wall and surface was wiped with a filter after beam stopping. In this case, ^{32}P was also observed as a major activity.

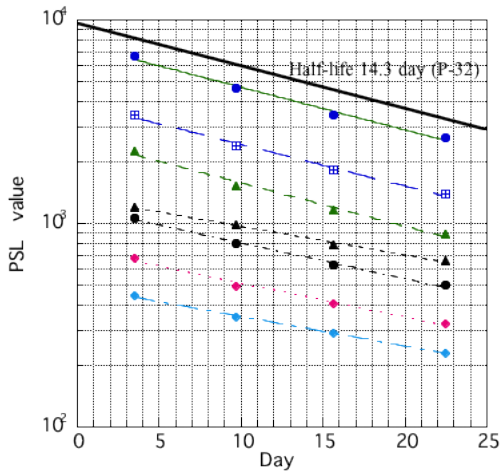

Fig. 1 Decay curves of radioactivity collected on filter

(3) Ge-detector

Many radioisotopes such as ^{7}Be, ^{54}Mn, were observed. ^{7}Be was produced by the spallation reactions of oxygen and nitrogen in air and deposited on the surface of beam line. The gamma activity obtained by the Ge-detector was not correlated with the result of imaging plate technique. Therefore, beta activity is important for surface contamination.

IV. CONCLUSION

An imaging plate technique is very useful to measure the radioactive decay of many samples simultaneously on the same condition.

Induced radioisotopes in air were deposited on the beam line. Because, the radioisotopes attached to aerosol and deposited on the surface of beam line. A major acitivity was ^{32}P, which might be produced by the spallation reaction of Ar in air.

In case of high-energy and high-intensity accelerators, radioactive aerosol formation will become important problem of radiation control. And this phenomenon was interesting subject to achieve the cosmic ray reaction in the stratosphere on the ground level.

APSORC'13 - 5th Asia-Pacific Symposium on Radiochemistry
Kanazawa, Japan, 22-27 September 2013

Application of ^{210}Pb in Glaciology

H.W. Gäggeler, L. Tobler, M. Schwikowski
Paul Scherrer Institut, Labor für Radio- und Umweltchemie, 5232 Villigen, Switzerland

Keywords – ^{210}Pb dating, climate research, environmental pollution, non-dating application of ^{210}Pb

I. *ABSTRACT*

Glaciers are increasingly used as proxies for climate change. Advances and retreats of these ice bodies are prime information on climate variability. Moreover, glaciers have found widespread application as archive of current and past atmospheric information. To fully benefit from such information, the glaciers have first to be dated. ^{210}Pb is one of the most frequently used radionuclide that enables dating for one to two centuries BP (before present). ^{210}Pb is ubiquitous in atmosphere, since it is a decay product of natural radon (^{222}Rn). Attached to aerosol particles ^{210}Pb is then scavenged by precipitation and deposited on the Earth surface. ^{210}Pb has proven to be much more versatile as information species besides dating. This contribution summarizes some examples that includes (besides dating, see e.g. figure 1);

Determination of annual snow accumulation rates at remote sites using the ^{210}Po/^{210}Pb disequilibria.

Thinning of glaciers as a function of depth caused by the increasing mass of overlying fresh snow and ice.

Folding of low lying ice layers due to topographic conditions that lead to non regular age-depth relationships.

Variability of seasonal deposition at high altitudes due to convective processes in summer.

Study of heavy metal percolation in temperate glaciers

Determination of sublimation rates at glacier sites in arid areas such as the Andes.

^{210}Pb activity concentrations as indicator of air masses, with low values for precipitation from marine air and high values for continental air, respectively.

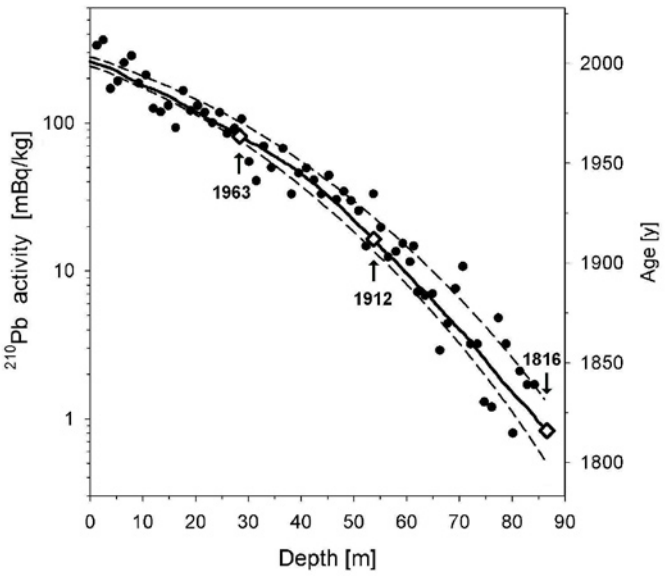

Fig. 1: ^{210}Pb activity concentrations along an ice core from the Belukha saddle in the Altai mountains (Siberia, Russia) together with three additional time horizons from the nuclear weapons testing (1963: measured via tritium), and the well known volcanic eruptions from Katmai (1912) and Tambora (1816) identified via increased excess sulphate concentrations. The right axis depicts the age deduced from the ^{210}Pb measurement (deduced from [1])

Presented examples originate from glaciers studied at our institute. Ice core drillings were performed in the European Alps, the South American Andes, the Russian and Mongolian Altai, the Mt. Cook area in New Zealand and in Svalbard (Norway).

References

[1] Olivier, S.., C. Blaser, S. Brütsch, N. Frolova, H.W. Gäggeler, K.A. Henderson, A.S. Palmer, T. Papina, M. Schwikowski, Temporal variations of mineral dust, biogenic tracers and anthropogenic species during the past two centuries from Belukha ice core, Siberian Altai, J. Geophys. Res. Atmospheres, 111, DO5309, doi:10.1029/2005/Doo5830 (2006)

APSORC'13 - 5th Asia-Pacific Symposium on Radiochemistry
Kanazawa, Japan, 22-27 September 2013

Depth distributions of uranium-236 and cesium-137 in the Japan Sea; toward the potential use as a new oceanic circulation tracer

Aya Sakaguchi[1], Akinobu Kadokura[1], Peter Steier[2], Yoshio Takahashi[1], Kiyoshi Shizuma[3], Tomoeki Nakakuki[1], Masayoshi Yamamoto[4]
[1] Graduate School of Science, Hiroshima Univ.
[2] VERA-Laboratory, Univ. of Vienna
[3]Graduate School of Engineering, Hiroshima Univ.
[4]Low Level Radioactivity Laboratory, Kanazawa Univ.

We present a feasibility study for using ^{236}U as an oceanic circulation tracer based on depth profiles of ^{236}U and ^{137}Cs in the Japan/East Sea. The concentration of the predominantly anthropogenic ^{236}U, measured with Accelerator Mass Spectrometry (AMS), decreased from the order of 10^7 atom/kg in surface water to 10^6 atom/kg close to the sea floor (3000 m). The profile has a smooth trend with depth and concentration values are generally proportional to that of ^{137}Cs for the same water sample. The cumulative inventory of dissolved ^{236}U in the water column was estimated to be 10^{12}-10^{13} atom/m^2, which is similar to the global-fallout level ($17.8x10^{12}$ atom/m^2) in Japan. Additional analyses of suspended solids (SS) and bottom sediments yielded negligible amounts of ^{236}U. Our results suggest that ^{236}U behaves as a conservative nuclide in seawater, with potential advantages over other tracers of oceanic circulation.

Keywords – *the Japan Sea, GEOTRACES, U-236, Cs-137, globalfallout*

I. INTRODUCTION

^{137}Cs ($T_{1/2}$=30.2 y) has been spread all over the world as a fission product of atmospheric nuclear weapons tests in the 1960s. This nuclide has been used as a powerful tool for oceanography due to the well-defined origin and conservative behaviour in water. However, the number of atoms has decayed already to one thirds compared with its initial levels, and it will become more difficult to measure. In this situation, we focus on ^{236}U ($T_{1/2}$=2.342×10^7 y) as a candidate for a new isotopic tracer for oceanography. The detection of ^{236}U in the environment has become possible only recently, by the development of measuring techniques with high sensitivity based on AMS. Our group showed that global fallout from bomb tests contains ^{236}U, which might be produced as nuclear reactions of $^{235}U(n,\gamma)$ and/or $^{238}U(n,3n)$[1]. So ^{236}U has been therefore globally distributed in the surface environment. Thus, ^{236}U has a similar potential as a tracer for environmental dynamics as ^{137}Cs, especially for oceanography.

In this study, a comprehensive attempt was made to measure the concentration of ^{236}U in marine samples such as water, suspended solid and bottom sediments to clarify the environmental behaviour of this isotope. Furthermore, the discussion of the circulation of deep and bottom water in "Miniature Ocean", the Japan Sea, has been attempted.

II. MATERIAL AND METHOD

Bottom sediments (4 sites) and seawater samples (7 sites) were collected from the Japan Sea in the research cruise with R/V Hakuhomaru, 2010 . The sediment core was cut into 1 cm segments from the surface to 5 cm in depth within a few hours after the sampling. About 20 L of seawater samples were collected from some depths in each site, and immediately after the sampling, the water was filtered with 0.45 μm pore-size membrane-filters. After the appropriate pre-treatment for each sample, uranium isotope and ^{137}Cs were measured with AMS and Ge-detector, respectively. The detail of these methods were published in Sakaguchi et al., (2012)[2].

III. RESULTS AND DISCUSSION

^{236}U was successfully detected for all seawater samples, and $^{236}U/^{238}U$ atom ratios in seawater were in the range of (0.19-1.75)×10^{-9}. The dissolved ^{236}U concentration showed a subsurface maximum and decreased steeply with depth. The minimum value was found at a depth of 2500 m and bottom (about 3000 m in depth) in the northern and the southern areas, respectively. These profiles are markedly different from that of natural ^{238}U which is nearly constant over the depth, suggesting that ^{236}U has not yet reached steady state. For the SS sample, ^{236}U could not be detected in significant levels. The total ^{236}U inventory of the water column was estimated at 10^{12}-10^{13} atom/m^2. This value is nearly the same as the global fallout level (17.8×10^{12} atom/m^2)[1][2]. ^{236}U was also found in the bottom sediments, and the inventory was about 1/40 compared with that in water column. All above characters are comparable with ^{137}Cs which is anthropogenic conservative nuclide in ocean. Actually, the diffusion coefficients for both nuclides show the nearly same value. The detail discussion of this study has been shown in Sakaguchi et al., (2012)

[1] A. Sakaguchi, K. Kawai, P. Steier et al. Science of the Total Environment. 407, 4238-4242, 2009.
[2] A. Sakaguchi, K. Kawai, P. Steier, et al., Science of the Total Environment, 408, 5392-5398, 2010.
[3] A. Sakaguchi, A. Kadokura, P. Steier,et al, Earth and Planetary Science Letters, 333-334, 165-170, 2012.

Ultratrace Analysis of Long-lived Radionuclides by Resonance Ionization Mass Spectrometry (RIMS)

J.V. Kratz
Institute for Nuclear Chemistry, Johannes Gutenberg-University, Mainz, Germany

Keywords – Ultratrace analytical method, resonant laser ionization, isotopic composition, plutonium analyses, actinide ionization potentials, optical spectroscopy with ^{255}Fm, IONTOF-SIMS coupled with RIMS

Abstract For long-lived radionuclides such as actinides, conventional radioanalyses by α spectroscopy suffer from unsatisfactory limits of detection (LOD). Resonance ionization mass spectrometry, on the contrary, achieves limits of detection of 10^6 atoms and is free from isobaric interferences [1,2]. The multiple step resonant excitation of evaporated atoms with laser light and the mass selective detection is presented for isotopes of plutonium as an example. We use a frequency-doubled Nd:YAG laser with a repetition rate of 10 kHz to pump three titanium-sapphire lasers delivering wave lengths of 420.76 nm, 847.28 nm, and 767.53 nm to resonantly excite plutonium into a Rydberg state from where ionization is achieved by applying an electric field [3]. For isotopic composition measurements, the wavelengths of lasers 1 and 2 must be readjusted for each isotope while laser 3 can be maintained at the same wavelength. The accuracy of isotopic ratios determined this way is demonstrated with a certified NIST standard. Applications are presented for fallout plutonium, reactor plutonium, samples from the Chernobyl area, wapons plutonium from the Mururoa island, seawater plutonium from the Northern Sea, and from the Irish Sea. Migration of plutonium through a granite fracture in the Grimsel underground laboratory has also been investigated [4].

By detecting ionization thresholds as a function of the applied electric field, accurate ionization potentials IP of Ac, Th, U, Np, Pu, Am, Cm, Bk, Cf, and Es have been determined by extrapolation to zero field strength [5, 6, 7]. In a first attempt to determine also the IP of Fm, a sample of 20.1-h ^{255}Fm produced at the HFIR at Oak Ridge has been investigated. By resonance excitation with a dye laser and ionization with an excimer laser in a buffer gas cell, two excited states of Fm ($5f^{12}$ 7s 7p) have been identified and mass spectra of $^{255}Fm^+$ and the daughter $^{251}Cf^+$ have been measured by a quadrupole mass spectrometer coupled to a channeltron detector [8]. By measuring the drift times of these ions and of $^{238}UO^+$, ion mobilities in the electric field could be determined. These are potentially useful to determine ionic radii of the heavy actinides and superheavy elements.

By using a commercial IONTOF-SIMS apparatus, analyses of hot micro particles with high lateral resolution in the sub-micron range have been exploited [9]. For the determination of the location of these hot particles (x,y coordinate on the target holder) their content of fissile material via fission track analysis [10] has been used. In order to avoid isobaric interferences, the sputtered ions (SIMS) were suppressed by a pulsed counter voltage applied to the target holder, and the abundantly sputtered neutral particles were resonantly excited and ionized by RIMS. The resulting ions were directed by an alternating acceleration voltage into the TOF mass spectrometer.

[1] N. Erdmann, G. Herrmann, G. Huber, S. Köhler, J.V. Kratz, A. Mansel, M. Nunnemann, G. Passler, N. Trautmann, A. Turchin, A. Waldek
Fresenius J. Anal. Chem. 359, 378 (1997)
[2] M. Nunnemann, N. Erdmann, H.-U. Hasse, G. Huber, J.V. Kratz, P. Kunz, A. Mansel, G. Passler, O. Stetzer, N. Trautmann, A. Waldek
J. Alloys and Compounds 271-273, 45 (1998)
[3] C. Grüning, G. Huber, P. Klopp, J.V. Kratz, P. Kunz, G. Passler, N. Trautmann, A. Waldek, K. Wendt
Int. J. Mass Spectrometry 235, 171 (2004)
[4] S. Bürger, R.A. Buda, H. Geckeis, G. Huber, J.V. Kratz, P. Kunz, Ch. Lierse von Gostomski, G. Passler, A. Remmert, N. Trautmann
in: Radioactivity in the environment – Volume 8, series editor: M.S. Baxter, Elsevier 2006, 581
[5] S. Köhler, R. Deißenberger, K. Eberhardt, N. Erdmann, G. Herrmann, G. Huber, J.V. Kratz, M. Nunnemann, G. Passler, P.M. Rao, J. Riegel, N. Trautmann, K. Wendt
Spectrochimica Acta, Part B 52, 717 (1997)
[6] J.R. Peterson, N. Erdmann, M. Nunnemann, K. Eberhardt, G. Huber, J.V. Kratz, G. Passler, O. Stetzer, P. Thörle, N. Trautmann, A. Waldek
J. Alloys and Compounds 271-273, 876 (1998)
[7] N. Erdmann, M. Nunnemann, K. Eberhardt, G. Herrmann, G. Huber, S. Köhler, J.V. Kratz, G. Passler, J.R. Peterson, N. Trautmann, A. Waldek
J. Alloys and Compounds 271-273, 837 (1998)
8] H. Backe, A. Dretzke, K. Eberhardt, S. Fritzsche, C. Grüning, G. Gwinner, R. G. Haire, G. Huber, J.V. Kratz, G. Kube, P. Kunz, J. Lassen, W. Lauth, G. Passler, R. Repnow, D. Schwalm, P. Schwamb, M. Sewtz, P. Thörle, N. Trautmann, A. Waldek
J. Nucl. Sci. Tech., Suppl. 3, 86 (2002)
[9] N. Erdmann, J. V. Kratz, N. Trautmann, G. Passler
Anal. Bioanal., Chem. 395, 1911 (2009)
[10] O. Stetzer, M. Betti, J. van Geel, N. Erdmann, J.V. Kratz, R. Schenkel, N. Trautmann
Nucl. Instr. and Meth. in Physics Research A525, 582 (2004)

APSORC'13 - 5th Asia-Pacific Symposium on Radiochemistry
Kanazawa, Japan, 22-27 September 2013

The Bulk Analysis with TIMS Measurements Performed in KAERI for Nuclear Safeguards

Jong-Ho Park, Sunyoung Lee, Young-Geun Ha, Seon A Lee, Kahee Jeong, Kyuseok Song
Nuclear Chemistry Research Division, Korea Atomic Energy Research Institute, Daejeon 305-353, Korea.

Abstract

KAERI has been developing the techniques for bulk analysis of environmental samples to support the international society for nuclear safeguards purpose. The analytical procedure, which consists of screening, ashing, acid digestion, chemical separation, and isotopic measurements by TIMS, was established. The analytical results of simulated environmental samples prepared from certified reference materials fell into the criteria that the IAEA requires for the NWAL qualification.

Environmental Sample, Safeguards, Isotopic Analysis, TIMS

I. INTRODUCTION

Highly accurate and precise analysis of nuclear materials in environmental samples plays essential roles in monitoring undeclared nuclear activities.[1] The IAEA has been maintaining a Network of Analytical Laboratories (NWAL) for nuclear safeguards. Since 2009, Korea Atomic Energy Research Institute (KAERI) has been developing the techniques for bulk analysis of environmental samples to support the international society as one of the members of NWAL. The analytical techniques that KAERI is utilizing with TIMS measurements for bulk analysis are briefly introduced in this paper.

A. Sample Analysis Procedure

Decomposition and acid digestion of environmental samples were carried out to prepare sample solutions in nitric acid, called as the mother solution. The solutions were weighed precisely, and then divided into three for determination of U isotope ratios and Pu quantity, for determination of U quantity and Pu isotope ratio, and for archive, respectively. Appropriate spike isotopic reference materials were added to the corresponding mother solution portion. IRMM 040a (^{233}U) and IRMM 085 (^{242}Pu) were used for quantification of uranium and plutonium, respectively.

The Pu isotopes were eluted into the conical PFA vial through the UTEVA columns with 2M HNO_3/0.02M ascorbic Acid/0.02M $NH_2OH \cdot HCl$ after loading the sample solution adjusted with 8M HNO_3/0.3% H_2O_2 on the UTEVA columns. The uranium isotopes were eluted through the columns with 0.007M ammonium oxalate solution. The purified Pu and U solutions were evaporated to dryness with concentrated nitric acid, HF and $HClO_4$ until any residue was not found in the PFA vial. Each sample was loaded on a pre-degassed rhenium filament with minimized residue. A thermal ionization mass spectrometer (TRITON, Thermo Fisher Scientific) was utilized for isotopic measurement.

A simulated samples were prepared with cotton swipe containing known amounts of uranium (CRM 112-A) and plutonium (REIMEP 16D) reference materials. The routine procedure was applied for the bulk analysis of the simulated samples.

B. Result

The analytical results of simulated environmental samples prepared from certified reference materials are shown in Table 1. The accuracy and the precision of the result fell into the criteria that the IAEA requires for the NWAL qualification. The measured n(^{235}U)/n(^{238}U) of the samples agreed with the certified value within less than 1% of accuracy.

Table 1. The result of bulk analysis of simulated environmental samples

	n(^{234}U)/n(^{238}U)	n(^{235}U)/n(^{238}U)	n(^{240}Pu)/n(^{239}Pu)
Cert.	5.2841e-5	7.2543e-3	1.110e-1
#1	5.32[±0.52]e-5	7.27[±0.18]e-3	1.150[±0.005]e-1
#2	6.71[±0.97]e-5	7.28[±0.11]e-3	1.140[±0.002]e-1

Numbers in parentheses indicate expanded uncertainties $U = k \cdot u_c$

[1] D. L. Donohue, *J. Alloy Compd.* **1998**, 271-273, 11.

APSORC'13 - 5th Asia-Pacific Symposium on Radiochemistry
Kanazawa, Japan, 22-27 September 2013

Determination of plutonium isotopes at ultratrace level in seawater samples by sector-field ICP-MS combined with chromatographic separation

Wenting Bu[1,2], Jian Zheng*[2], Qiuju Guo*[1], Tatsuo Aono[2], Keiko Tagami[2], Shigeo Uchida[2]
[1]School of Physics, Peking University, China
[2]National Institute of Radiological Sciences, Japan

Plutonium isotopes are released into the environment as a consequence of human nuclear activities including nuclear weapon testing, nuclear fuel reprocessing and nuclear accident. As the world's ocean covers ca. 70 % of the earth surface, it received majority of Pu isotopes released into the environment by atmospheric nuclear weapons tests. For example, it has been estimated that the total global fallout $^{239+240}$Pu released into the environment was about 10.87 PBq, and 6.6 PBq entered the world's ocean[1]. Besides, a significant amount of Pu isotopes were injected directly to the world's ocean by close-in fallout from the nuclear explosions conducted at the Pacific Proving Ground by US and the French Polynesia by France.

Due to their radiotoxicity and long half-lives, Pu isotopes are regarded as highly hazardous pollutants in the marine environment and are of great research interest. Accurate and precise determination of plutonium isotopes in marine samples is important for radioecological assessment. In addition, Pu isotopes have also been used for tracing of oceanographic processes, such as water mass circulation, transport and scavenging of particulate matter, etc.

The concentration of Pu in seawater is extremely low ($^{239+240}$Pu, 1.2-7.4 mBq/m^3 in the surface seawater of the NW Pacific Ocean).[2] By the traditional alpha spectrometry method, usually large volume (~ 200 L) of seawater sample is needed for the analysis of Pu, and the ^{240}Pu/^{239}Pu atom ratio, which is an important fingerprint for Pu source identification and for tracing of oceanographic processes, cannot be obtained.[3] Due to the low detection limit and the relatively simple sample preparing procedures, ICP-MS has been treated as a promising method for the analysis of Pu in environmental samples in recent years. However, when using ICP-MS, the detection of ^{239}Pu and ^{240}Pu can be affected by spectral interferences caused by $^{238}UH^+$ and $^{238}UH_2^+$ formations, especially for the environmental samples with high U concentrations. The concentration of U in seawater in the Pacific Ocean is about several μg/L and the atom ratio of ^{238}U/^{239}Pu can be up to 10^{11}.[4] Thus, complex procedures for the preconcentration of Pu and separation of Pu from U were employed for the determination of Pu in seawater prior to the analysis by ICP-MS, which somehow may lead to a low Pu recovery.

In this work, we presented a simple method for the analysis of Pu concentration and its isotopic composition in seawater samples by sector field ICP-MS combined with chromatographic separation technique. High precision and accuracy were achieved by using this method. The detailed analytical procedures and the merits of this method will be discussed at the conference.

Acknowledgments
This work was supported by the Ministry of Education, Culture, Sports, Sciences and Technology (MEXT) (24110004), Japan, and partly supported by the Agency for Natural Resources and Energy, the Ministry of Economy, Trade and Industry (METI), Japan.

References
[1] Aarkrog, A., Deep-Sea Res. II, 50, 2597-2606, 2003.
[2] Povinec, P. P., Livingston, H. D., Shima, S. et al., Deep-Sea Res. II, 50, 2607-2637, 2003.
[3] Yamada, M. and Zheng, J., Appl. Radiat. Isot., 66, 103-107, 2008.
[4] Chen, J. H., Edwards, R. L., Wasserburg G. J., Earth Planet. Sci. Lett., 80, 241-251, 1986.

APSORC'13 - 5th Asia-Pacific Symposium on Radiochemistry
Kanazawa, Japan, 22-27 September 2013

Semi-automated Procedure for the Determination of ^{89,90}Sr in Environmental Samples by Cherenkov Counting

Ivana Milanović, Željko Grahek
Division for marine and environmental research, Ruđer Bošković Institute, Zagreb, Croatia

Abstract - Development of new chromatographic resins in the last two decades Sr resin, AnaLig-01 and SuperLig 620 has significantly simplified separation of strontium from various types of samples. These resins, that have principles based on molecular recognition, are highly selective for strontium binding. In combination with appropriate detection methods they enable automatic determination of radioactive strontium. Sequential injection analysis and equilibration based sensor column analysis were developed for the determination of long lived ^{90}Sr (28.8 y) in liquid radioactive waste and water samples.[1-3] However, ^{89}Sr that has short half-life (50.5 d), can also be present in samples, especially in those exposed to fresh fallout from nuclear reactor. Classical analysis of ^{89}Sr requires isolation of ^{90}Y, usually after attaining of secular equilibrium of ^{90}Sr-^{90}Y and the whole procedure takes at least 16 days. However, by using Cherenkov counting technique, determination time may be significantly reduced. Unlike ^{90}Sr that emits low energy electrons, its daughter ^{90}Y as well as ^{89}Sr, generates Cherenkov photons in aqueous media. Consequently, by successive counting within 64 hours, ^{89}Sr and ^{90}Sr via ^{90}Y can be determined. Therefore, the main aim of this research is development of semi-automated procedure for the determination of ^{89,90}Sr. It includes solid phase extraction (SPE) of strontium from liquid samples and Cherenkov counting of its isotopes. The procedure is based on sample - column equilibration and off-line detection of bound ^{89,90}Sr on the column. Sample is pumped through column at constant flow rate until the breakthrough or saturation point is achieved. The ^{89,90}Sr is determined by counting on column in PE vial. It will be shown how strontium can be selectively bound on the Sr resin, AnaLig-01 and SuperLig 620 resins and separated from interfering radionuclides. Also, influence of column geometry, amount of resin and media in PE vial around the column on quantity determination, detection efficiency and achievable lower detection limits will be discussed. The method is tested in proficiency testing samples and natural water samples.

Keywords – semi-automated procedure, solid phase extraction, Cherenkov counting, ^{89,90}Sr determination

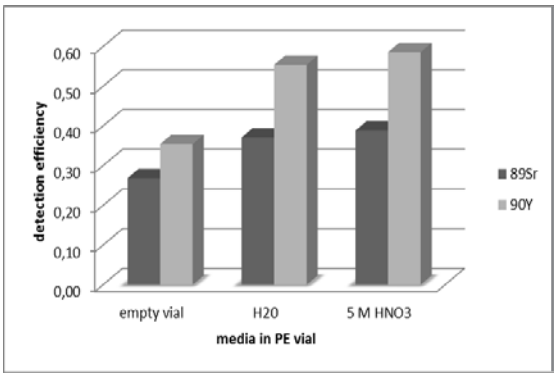

Figure 1. Detection efficiency of ^{89}Sr and ^{90}Y bound on AnaLig-01 resin depending on surrounding media (TriCarb 3180)

REFERENCES

[1] O. B. Egorov, M. J. O'Hara, J. W. Grate, Equilibration-Based Preconcentrating Minicolumn Sensors for Trace Level Monitoring of Radionuclides and Metal Ions in Water without Consumable Reagents. *Anal. Chem.* **2006** 78(15) 5480-5490.

[2] J. W Grate, O. B. Egorov, M. J. O'Hara, T. A. Devol, Radionuclide Sensors for Environmental Monitoring: From Flow Injection Solid-Phase Absorptiometry to Equilibration-Based Preconcentrating Minicolumn Sensors with Radiometric Detection. *Chem. Rev*. **2008** 108(2) 543-562.

[3] M. J. O'Hara, S.R. Burge, J. W. Grate, Automated radioanalytical system for the determination of Sr-90 in environmental water samples by Y-90 Cherenkov radiation counting. *Anal. Chem.* **2009** 81(3) 1228-1237.

Research and Development towards Decommissioning of Fukushima Daiichi Nuclear Power Plants

Kazuo Minato
Nuclear Science Research Institute, Tokai Research and Development Center,
Japan Atomic Energy Agency
Tokai-mura, Ibaraki-ken 319-1195, Japan

Abstract – Towards the decommissioning of Fukushima Daiichi Nuclear Power Plants, science-based research and development is important and useful, as well as technology and engineering development. Research and development activities based on radiation chemistry, radiochemistry, thermodynamics, etc., have contributed to safe and efficient decommissioning of the plants.

Keywords – Fukushima Daiichi, Decommissioning, Radiation Chemistry, Radiochemistry, Thermodynamics

I. INTRODUCTION

Two and a half years have passed since the accident at Fukushima Daiichi Nuclear Power Station Units 1-4, Tokyo Electric Power Company, Inc. (TEPCO). The research and development towards decommissioning of the plants, concerning the removal of fuels from spent fuel pools, removal of fuel debris, processing and disposal of radioactive waste, and remote control equipment and devices, have been being made as national projects, which are based on the Mid-and-Long-Term Roadmap towards the Decommissioning of TEPCO's Fukushima Daiichi Nuclear Power Station Units 1-4 [1]. Besides TEPCO, plant makers, research institutes, etc., jointly participate in the projects. Among them the Japan Atomic Energy Agency is playing an important part in science-based research and development to support the decommissioning of the plants.

II. RADIOLYSIS OF SEAWATER

One of the distinguishing features of the accident is that seawater was injected to the damaged reactor cores and spent fuel pools in the early stage of actions. The accumulated radioactive water, including seawater, in the reactor and turbine buildings has been being processed for decontamination and desalination. This process generates spent zeolites highly contaminated with radioactive cesium. For safe storage of the spent zeolites, hydrogen generation should be clarified.

Gamma-ray irradiation experiments revealed that the yield of hydrogen from seawater was larger than that from pure water and comparable to the primary yield, indicating that oxidation of hydrogen by radical products of water radiolysis is not effective in seawater due to the presence of Cl^- and Br^- ions. Furthermore, hydrogen generation was increased by addition of the zeolite to seawater. This means that the radiation energy deposited on zeolite is involved in hydrogen formation [2].

Based on the experimental data, hydrogen generation in the vessels was evaluated, and the procedures to repress hydrogen generation in the spent zeolite were suggested.

III. RADIOCHEMICAL ANALYSIS OF WASTE

The radioactive materials were released into the environment by the accident. A huge amount of the waste contaminated with the radioactive materials was generated. To classify the waste and to establish ways of processing and disposal of the waste, inventory of radioactive materials in the waste should be clarified.

The analysis of rubbles, trees, and accumulated water sampled in the site of the nuclear power station revealed that the main radionuclide was ^{137}Cs (and ^{134}Cs) with very small amounts of fission products, actinides, and activation products, which is quite different from those of the radioactive waste generated from ordinary nuclear power stations and reprocessing plants. The development of separation method of a target nuclide before radiochemical analysis was inevitable, and the analytical scheme and methods have been developed for the nuclides, such as ^{3}H, ^{14}C, ^{36}Cl, ^{79}Se, ^{90}Sr, ^{99}Tc, ^{129}I, ^{60}Co, ^{94}Nb, ^{137}Cs, ^{152}Eu, ^{154}Eu, ^{238}Pu, ^{239}Pu, ^{240}Pu, ^{241}Am, and ^{244}Cm.

IV. THERMODYNAMIC ANALYSIS OF FUELS

A large amount of seawater was injected into the reactor pressure vessels in the accident. Several elements contained in seawater possibly reacted with degraded fuel debris and molten corium. These reactions may have affected volatilization of fission products, property of fuel debris, and formation of corrosive gases.

Thermodynamic evaluation indicated that volatility of Cs, Sr, and Te was potentially increased due to the change in stable chemical species, and that corrosive gases, such as HCl and H_2S, were possibly generated, depending on temperature and oxygen potential [3].

Experiments on the high temperature reaction between sea salt deposit and $(U,Zr)O_2$ simulated fuel debris (sim-debris) were also made. A dense layer of calcium and sodium uranate formed on the surface of a sim-debris under airflow. When the oxygen partial pressure was low, calcium was dissolved into the cubic sim-debris phase to form solid solution $(Ca,U,Zr)O_{2+x}$ [4].

REFERENCES

[1] http://www.meti.go.jp/english/earthquake/nuclear/decommissioning/index.html
[2] Y. Kumagai, R. Nagaishi, et al., At. Energy Soc. Jpn., 10, 235-239 (2011).
[3] M. Kurata, N. Shirasu and T. Ogawa, Trans. At. Energy Soc. Jpn., in press.
[4] M. Takano and T. Nish, J. Nucl. Mater., 443, 32-39 (2013).

APSORC'13 - 5th Asia-Pacific Symposium on Radiochemistry
Kanazawa, Japan, 22-27 September 2013

Determination of atmospheric radiocesium on filter tapes used at automated SPM monitoring stations for estimation of transport pathways of radionuclides from Fukushima Daiichi Nuclear Power Plant

Yasuji Oura[1], Mitsuru Ebihara[1], Haruo Tsuruta[2], Teruyuki Nakajima[2], Toshimasa Ohara[3]
Mitsunori Ishimoto[4], Yosuke Katsumura[4]
[1]Department of Chemistry, Tokyo Metropolitan University
[2]Atmosphere and Ocean Research Institute, The University of Tokyo
[3]Center for Regional Environmental Research, National Institute for Environmental Studies
[4]Nuclear Professional School, The University of Tokyo

I. INTRODUCTION

Enormous amount of artificial radionuclides were emitted into the atmosphere by a nuclear accident at Fukushima Daiichi nuclear power plant (FDNPP) in March 2011. The radionuclide in the atmosphere was transported with atmospheric stream into eastern Japan area widely. Since some institutes in Kanto region monitored atmospheric radioactivity periodically, it was partially evident that when radioactive plumes passed through Kanto region. However, data on atmospheric radioactivity during an initial period in Tohoku region in where FDNPP presents is nothing, thus passing routes of radioactive plumes in Tohoku region and how radioactivity went though is not clear.

A lot of automated air pollution monitoring stations are placed by local governments around in Japan. Suspended particulate matters (SPM) are also monitored hourly in the station. SPM collected during the accicdent at the stations in Tohoku and Kanto region must play an important role to solve when and how much atmospheric radionuclides passed through in Tohoku and Kanto regions. So we determined ^{134}Cs and ^{137}Cs contents in SPM collected on filer tapes at SPM monitoring stations. The determined contents are also expected to help a development of air pollution transport model calculation.

II. EXPERIMENTAL

Filter tapes used at 3 stations in Miyagi, 19 stations in Fukushima, 8 stations in Ibaraki, 4 stations in Saitama, and 6 stations in Chiba prefectures were subjected to gamma spectroscopy. SPM was collected on roll paper tape continuously and SPM on a paper tape was visible as a black circle (we call it spot in this article). Spots of SPM collected from 15 to 16 March and from 20 to 23 March in 2011 were cut one-by-one. Each spot was sandwiched between medical papers, and it was fixed on a thin plastic sheet by an adhesive tape. Gamma rays from samples were measured for 1 to 3 hours with a Ge detector.

III. RESULTS AND DISCUSSION

We observed the different arrival time of radioactive plume on 15 and 20-21 March among stations. For example, ^{137}Cs concentrations at 3 stations in Fukushima city and 4 stations in Ibaraki prefecture are shown in Figs. 1 and 2, respectively. It was found that high ^{137}Cs concentration (> 10 Bq/m^3) continued for about 12 hours in Fukushima city. This peak was not observed by radiation dose monitoring around that time. In Ibaraki prefecture, a high ^{137}Cs concentration (> 200 Bq/m^3) appeared at 8 am, 21 March at 2 stations in Tsuchiura but not observed in both Shimozuma and Tsukuba. This difference is expected to be helpful for solving passways of radioactive plume in Ibaraki. Analysis of radioactive Cs on filter tapes collected by automated SPM monitoring stations even at 1 - 2 years after FDNPP accident is concluded to give very valuable information.

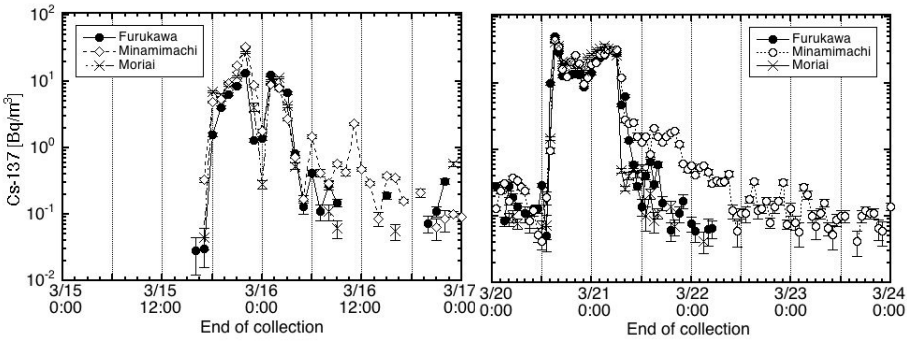

Fig.1 Atmospheric ^{137}Cs concentration at 3 stations in Fukushima city.

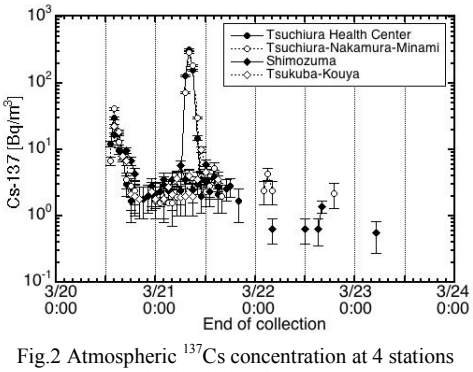

Fig.2 Atmospheric ^{137}Cs concentration at 4 stations in Ibaraki prefecture.

FKO-10

Two-Years Trend of Monthly ^{137}Cs Deposition Observed within 300 km of the Fukushima Dai-ichi Nuclear Plant

Katsumi Hirose [1,2]

[1] *Department of Materials and Life Sciences, Faculty of Science and Technology, Sophia University, 7-1 Kioicho, Chiyodaku, Tokyo 102-8554, Japan*

[2] *Geosphere Research Institute, Saitama University, 255 Shimo-okubo, Sakura-ku, Saitama, 338-8570, Japan*

Abstract – Monthly depositions, which directly reflect atmospheric processes including emission from the Fukushima Daiichi nuclear power plant (FDNPP), are an important tool to re-construct accident sequence. In order to elucidate deposition behavior of the FDNPP-derived radionuclides after the major emission in March 2011, two-years trends of the monthly ^{137}Cs deposition at monitoring stations within 300 km of the FDNPP were examined. The monthly ^{137}Cs deposition showed marked peaks in winter 2012 and winter 2013 at the Futaba site about 5 km of the FDNPP, whereas 2013 winter the peak at the sites in south Kanto and Tohoku regions was not pronounced. We discuss two-years trend of the monthly ^{137}Cs deposition taking into account its spatial variation and effect of precipitation amount.

Keywords – Fukushima Dai-ichi nuclear power plant, monthly deposition, ^{137}Cs, temporal variation, emission history

I. INTRODUCTION

The 2011 Great East Japan Earthquake and resulting tsunami caused severe accident in the Fukushima Dai-ichi nuclear power plant (FDNPP). As a result, large amounts of radionuclides have been released in the environment. In order to trace long-term trend of FDNPP-derived radionuclides emitted into atmosphere, it is important to do continuous monitoring of radionuclides in surface air and deposition. Especially monthly deposition of the FDNPP-derived radionuclides is one of the powerful tools to elucidate long-term environmental effects of the FDNPP accident. The results of monthly ^{137}Cs deposition [1,2] revealed that the effects of the FDNPP accident at least continued until the early 2012. In this paper, we describe two-years trend of the monthly ^{137}Cs deposition observed in the Kanto and Tohoku regions and discuss processes controlling temporal variation of the monthly ^{137}Cs deposition.

II. SAMPLING AND METHOD

Monthly deposition samples (rainwater and falling dust) were collected by rainwater samplers with surface areas of 0.5 m^2, respectively, which are usually installed on the roof of main monitoring building in each monitoring site. Monthly deposition sampling in 45 monitoring sites covering Japanese Island has been stationary performed to monitor basic levels of radioactivity deposition. Monthly rainwater and falling dust samples was collected in appropriate bottles on the first day morning of every month. Water sample was transferred into an evaporation dish and dried on a hot plate. The resultant residues were weighted after drying in an oven at 110°C and then transferred to a plastic container. Dried residue sample in a plastic container was subjected by gamma spectrometry. Gamma spectrometry was performed in each measurement laboratory of local government. Major radionuclides in monthly deposition samples were radiocesium (^{134}Cs and ^{137}Cs). In this analysis, we focused ^{137}Cs deposition because at initial stage, the ^{134}Cs/^{137}Cs activity ratio was constant (Hirose, 2012). All of monthly deposition data has been recorded in NRA homepage.

III. RESULT AND DISCUSSION

Two-years trend of the monthly ^{137}Cs deposition at the monitoring stations within 300 km of the FDNPP was examined. The FDNPP-derived ^{137}Cs has been still measured in January 2013 at most of the monitoring stations within 300 km of the FDNPP. A typical time sequence of the monthly ^{137}Cs deposition is as follows: 1. Pronounced high ^{137}Cs deposition (3.34 MBq m^{-2}) occurred in March 2011 at the Futaba monitoring station, where is located about 5 km of the FDNPP. 2. The monthly ^{137}Cs deposition at Futaba rapidly decreased in April 2011 as a result of cease of major radioactivity emission from the FDNPP. 3. A minimum monthly ^{137}Cs deposition (1.55 kBq m^{-2}) appeared in October 2011 and then gradually increased to a maximum (19.5 kBq m^{-2}) in February 2012. 4. A cause of higher ^{137}Cs deposition in winter, 2012 was presumed to be resuspension of ^{137}Cs-enriched particles [2]. 5. After a peak in February 2012, the monthly ^{137}Cs deposition deceased and reached a minimum in August 2012. However, the monthly ^{137}Cs deposition increased in winter, 2013 (January 2013: 18.9 kBq m^{-2}).

The temporal variations of the monthly ^{137}Cs deposition at the monitoring stations within 300 km of the FDNPP spatially differed from each other. In order to have better understanding of temporal variations of the monthly ^{137}Cs deposition and its spatial difference, we calculate ^{137}Cs concentrations in rainwater from the ^{137}Cs deposition and precipitation amount to eliminate effect of precipitation amount. The temporal variation of the ^{137}Cs concentration in rainwater at Hitachinaka is similar to that at Futaba. This finding suggests that the temporal change of the ^{137}Cs concentration in rainwater at Hitachinaka was predominantly affected by that at Futaba, in other words, source intensity at the FDNPP.

REFERENCES

[1] Hirose, K., *J. Environ. Radioact*., **111**, 13-17, 2012.
[2] Hirose, K., Appl. Radiat. Isot. doi.org/10.1016/j.apradiso.2013.03.076

NCI-01

Synthesis and study of properties of superheavy elements status, problems, and prospects

S. Dmitriev
The Flerov Laboratory of Nuclear Reactions, JINR, Dubna,
dmitriev@jinr.ru

The study of nuclear physical and chemical properties of recently discovered superheavy elements (SHE, Z = 112–118) as well as synthesis of new elements (Z>118) remain one of the most crucial tasks in modern science. Over the past decade, the unique results [1] have been obtained that are of utmost importance both in nuclear physics and astrophysics (experimental evidence of existence of islands of increased stability of SHE) as well as in chemistry (influence of relativistic effects on the chemical properties of the elements 112–114). As per the IUPAC decision, the two new elements are now officially called Fl - Flerovium (element 114) and Lv - Livermorium (element 116). The discovery of elements 117 [2] and 118 closed the 7th period of Mendeleev's Periodic Table of the Elements. Possibilities to study synthesis of heavier elements in reactions with the double-magic ^{48}Ca nucleus are exhausted because production of actinides with Z>98 (Es, Fm, etc.) in necessary quantity (several mg) is impossible in neutron-capture reactions within the framework of existing today reactor technologies. One needs to use ions heavier than ^{48}Ca, for example, ^{50}Ti, ^{58}Fe, and ^{64}Ni; however, production cross sections with these ions are expected to be at least one order of magnitude less. Implementation of the large-scale program on the study of earlier synthesized SHE requires, in turn, significant experiment efficiency improvement.

Further development implies the construction of a first-ever SHE factory at JINR FLNR, which shall include the following:

- a new accelerator complex with the average-mass ion beam intensity 10-20 times higher than that of today;
- physical and chemical new-generation experimental set-ups (highly effective gas-filled recoil separator, gas catcher, selective laser ionization, etc.).

The work was carried out with the financial support from the Russian Foundation of Basic Research (project code # 13-03-12058-ofi-m-2013).

[1] Yu. Ts. Oganessian, S. N. Dmitriev, Russian Chem.Review, 78, 1077, 2009.
[2] Yu. Ts. Oganessian et al., Phys. Rev. Lett., 104, 142502, 2010.

APSORC'13 - 5th Asia-Pacific Symposium on Radiochemistry
Kanazawa, Japan, 22-27 September 2013

The Search for New Chemical Elements and the Possibilities to Synthesize Transactinide "Chemistry" Isotopes

Christoph E. Düllmann[1,2,3]
[1]Johannes Gutenberg-Universität Mainz, 55128 Mainz, Germany
[2]GSI Helmholtzzentrum für Schwerionenforschung, 64291 Darmstadt, Germany
[3]Helmholtz Institute Mainz, 55099 Mainz, Germany

On overview on nuclear reactions leading to isotopes of the transactinide (Z≥104) elements with sufficiently long half-lives for chemical study will be presented.

Transactinides, Superheavy elements, Nuclear fusion reactions

Elements up to Z=112 as well as 114 and 116 are officially recognized as discovered and have been named [1]. The current literature contains reports about the synthesis of all elements up to Z=118 [2], meaning that more than 10% of all elements are members of the transactinide series with Z=104-118. Search experiments for the new elements with Z=119 and Z=120 have been performed, e.g., at the GSI Darmstadt. Elements up to Hs (Z=108) as well as Cn (Z=112) and Fl (Z=114) have been chemically investigated [3], using isotopes with half-lives of at least about one second, which is the current limit for chemical studies. The figure shows the cutout of the current chart of nuclei of the more than 100 transactinide isotopes, synthesized in nuclear fusion reactions. Selecting the optimum nuclear reaction to synthesize a certain isotope is a sensible topic, which requires proper attention in any experiment with the heaviest elements, regardless of the specific aspect under study. The figure shows that isotopes suitable for chemistry studies with current technology exist for all elements up to Fl (Z=114).

I will first present the search for new elements using the recoil separator TASCA [4] at GSI and then discuss the optimum reactions leading to the relatively long-lived isotopes of the transactinides as they are frequently used in chemical studies of these elements, including elements which were not studied chemically to date.

[1] R. D. Loss and J. Corish, Pure Appl. Chem. **84**, 1669 (2012).
[2] Y. Oganessian, Radiochim. Acta **99**, 429 (2011).
[3] A. Türler and V. Pershina, Chem. Rev. **113**, 1237 (2013).
[4] A. Semchenkov et al., Nucl. Instrum. Meth. B **266**, 4153 (2008)

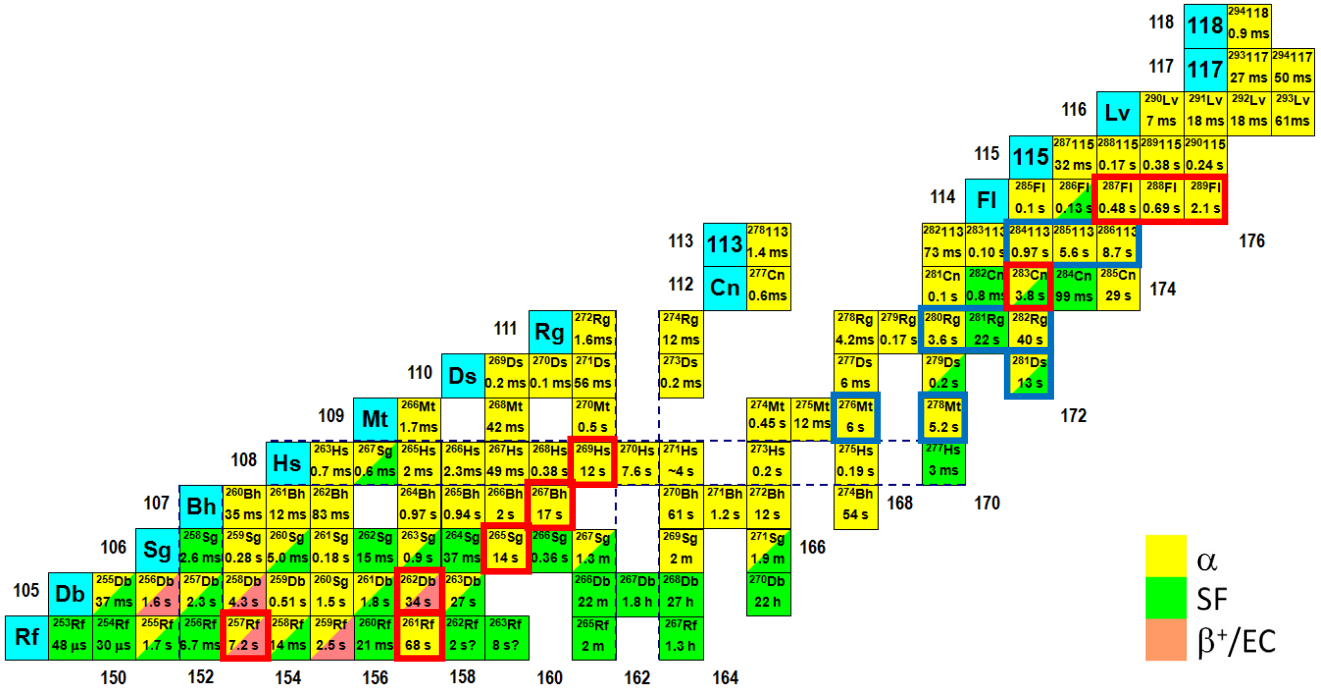

Chart of nuclei of transactinide elements. Half-lives are given, and decay modes color coded. Isotopes often used in chemical studies are shown in a red border. Long-lived isotopes of elements that were not studied chemically so far are shown in a blue border. Dashed lines show nuclear shell closures.

Production and Decay Studies of Transactinide Nuclides with GARIS at RIKEN

Hiromitsu Haba
Nishina Center for Accelerator-Based Science, RIKEN, Wako, Saitama 351-0198, Japan

Abstract – The isotopes of ^{261}Rf, ^{262}Db, and ^{265}Sg were produced in the ^{248}Cm(^{18}O,5n)^{261}Rf, ^{248}Cm(^{19}F,5n)^{262}Db, and ^{248}Cm(^{22}Ne,5n)^{265}Sg reactions, respectively, using a gas-jet transport system coupled to the gas-filled recoil ion separator, GARIS at RIKEN. Production and decay properties of those nuclides were investigated in detail with a rotating wheel apparatus for α and spontaneous fission spectrometry under low background conditions.

Keywords – Superheavy elements; RIKEN gas-filled recoil ion separator, GARIS; ^{261}Rf; ^{262}Db; ^{265}Sg

Chemical characterization of superheavy elements (SHEs, atomic numbers $Z \geq 104$) is an extremely interesting and challenging research subject in modern nuclear and radiochemistry [1,2]. We have been developing a gas-jet transport system coupled to the RIKEN gas-filled recoil ion separator GARIS as a novel technique for the next-generation SHE chemistry [3–5]. With this method, breakthroughs in SHE chemistry are expected: (i) the background radioactivities originating from unwanted by-products are strongly suppressed, (ii) the intense primary heavy-ion beam is absent in a gas-jet chamber and hence high gas-jet yield is achieved, and (iii) the beam-free conditions also make it possible to investigate new chemical reactions. In this work, we investigated production and decay properties of isotopes of ^{261}Rf (Z = 104), ^{262}Db (Z = 105), and ^{265}Sg (Z = 106) available for chemical studies using the GARIS gas-jet system.

A schematic of the experimental setup is shown in Fig. 1. Oxygen-18, ^{19}F, and ^{22}Ne beams were extracted from the RIKEN Linear Accelerator, RILAC. The isotopes of ^{261}Rf^{a,b}, ^{262}Db, and ^{265}Sg^{a,b} were produced in the reactions of ^{248}Cm(^{18}O,5n)^{261}Rf, ^{248}Cm(^{19}F,5n)^{262}Db, and ^{248}Cm(^{22}Ne,5n)^{265}Sg, respectively. The evaporation residues of interest were separated in flight from the beam and the majority of the nuclear transfer products by GARIS and were guided to a gas-jet chamber at the focal plane of GARIS. The evaporation residues were thermalized in He gas, attached to KCl aerosol particles, and were transported through a Teflon capillary to a chemistry laboratory. Alpha and spontaneous fission (SF) decays of ^{261}Rf^{a,b}, ^{262}Db, and ^{265}Sg^{a,b} were then investigated with the rotating wheel apparatus MANON (Measurement system for Alpha-particle and spontaneous fissioN events ON line) under low background conditions.

The 1.9-s isomeric state (^{261}Rf^{b}) in ^{261}Rf was directly populated in the ^{248}Cm(^{18}O,5n)^{261}Rf^{b} reaction for the first time [6]. The identification of ^{261}Rf^{b} was based on six α-α correlations linking α decays of ^{261}Rf^{b} and its daughter ^{257}No. The α-particle energy of ^{261}Rf^{b} was measured to be E_α = 8.52 ± 0.05 MeV. The half-life was determined to be $T_{1/2}$ = 1.9 ± 0.4 s based on both 8.52-MeV α and SF decays. The SF branch is b_{SF} = 0.73 ± 0.06. The cross section for the ^{248}Cm(^{18}O,5n)^{261}Rf^{b} reaction is σ(^{261}Rf^{b}) = 11 ± 2 nb at 95.1 MeV, which gives a cross section ratio of σ(^{261}Rf^{a})/σ(^{261}Rf^{b}) = 1.1 ± 0.2. In the ^{265}Sg experiment [7], eighteen and twenty four events were assigned to ^{265}Sg^{a} and ^{265}Sg^{b}, respectively, based on α-α(-α) and α-SF correlations. The half-life and α-particle energy of ^{265}Sg^{a} were measured to be $T_{1/2} = 8.5^{+2.6}_{-1.6}$ s and E_α = 8.84 ± 0.05 MeV, respectively, and those of ^{265}Sg^{b} were $T_{1/2} = 14.4^{+3.7}_{-2.5}$ s and E_α = 8.69 ± 0.05 MeV. As a daughter product of ^{265}Sg^{a,b}, the decay properties of ^{261}Rf^{b} were derived: $T_{1/2} = 2.6^{+0.7}_{-0.5}$ s, E_α = 8.51 ± 0.06 MeV, and b_{SF} = 0.82 ± 0.09. These results confirm and refine the complicated decay pattern suggested for the decay chain ^{265}Sg^{a,b} → ^{261}Rf^{a,b} → ^{257}No → in [8]. The production cross sections for ^{265}Sg^{a} and ^{265}Sg^{b} were determined to be σ(^{265}Sg^{a}) = 180^{+80}_{-60} pb and σ(^{265}Sg^{b}) = 200^{+60}_{-50} pb at 117.8 MeV. Recently, decay properties of ^{262}Db and its α-decay daughter ^{258}Lr were investigated [9]: E_α = 8.46 ± 0.04 MeV (α intensity I_α = 70 ± 6%) and 8.68 ± 0.04 MeV (I_α = 30 ± 6%), $T_{1/2} = 34^{+4}_{-3}$ s, and b_{SF} = 55 ± 4% for ^{262}Db; $T_{1/2} = 3.5^{+0.5}_{-0.4}$ s and b_{SF} (and/or b_{EC}) = 2.6 ± 1.8% for ^{258}Lr. Based on those decay properties, the cross section for the ^{248}Cm(^{19}F,5n)^{262}Db reaction in [10,11] was revised to σ(^{262}Db) = 2.2 ± 0.7 nb at 103 MeV. In the conference, perspectives of SHE nuclear chemistry opened by GARIS will be also presented.

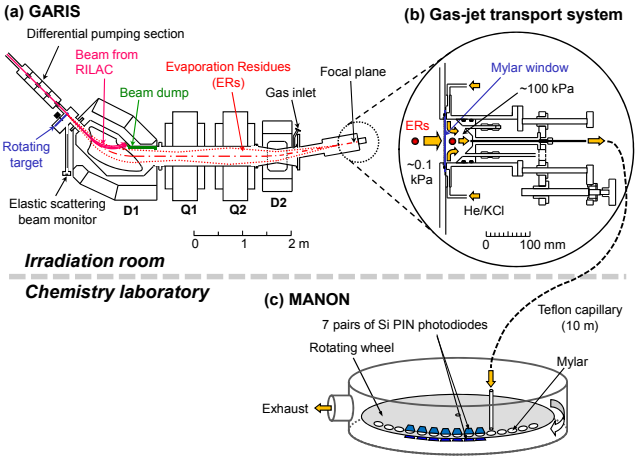

Fig.1. (a) RIKEN gas-filled recoil ion separator, GARIS. (b) Gas-jet transport system coupled to the focal plane of GARIS. (c) The rotating wheel apparatus MANON for α/SF-spectrometry.

[1] M. Schädel, Angew. Chem. Int. Ed. **45**, 368 (2006).
[2] A. Türler and V. Pershina, Chem. Rev. **113**, 1237 (2013).
[3] H. Haba *et al.*, J. Nucl. Radiochem. Sci. **8**, 55 (2007).
[4] H. Haba *et al.*, J. Nucl. Radiochem. Sci. **9**, 27 (2008).
[5] H. Haba *et al.*, Chem. Lett. **38**, 426 (2009).
[6] H. Haba *et al.*, Phys. Rev. C **83**, 034602 (2011).
[7] H. Haba *et al.*, Phys. Rev. C **85**, 024611 (2012).
[8] Ch. E. Düllmann and A. Türler, Phys. Rev. C **77**, 064320 (2008).
[9] H. Haba *et al.*, EuCheMS International Conference on Nuclear and Radiochemistry (NRC8), Sept. 18, 2012, Como, Iraly.
[10] Y. Nagame *et al.*, J. Nucl. Radiochem. Sci. **3**, 85 (2002).
[11] K. Tsukada *et al.*, Radiochim. Acta **97**, 83 (2009).

APSORC'13 - 5th Asia-Pacific Symposium on Radiochemistry
Kanazawa, Japan, 22-27 September 2013

Theoretical Predictions of the Electronic Structure and Properties of the Heaviest Elements

Valeria Pershina[1]
[1]Helmholtzzentrum für Schwerionenforschung, Planckstr. 1, D-64291 Darmstadt, Germany

Abstract - Recent theoretical works on predictions of chemical properties and experimental behaviour of the heaviest elements are presented and critically compared

Keywords – Superheavy elements/Electronic structure/Relativistic calculations

I. INTRODUCTION

One of the main aims of studies in the area of the chemistry of the heaviest elements is to place a newly produced element in the proper position of the Periodic Table [1]. It is achieved by comparing behaviour of the new element with that of its lighter homologs in the chemical group. Having this in mind, a large number of interesting and important chemical experiments on the heaviest elements were performed in the recent years [2]. Theoretical investigations in this area have also been very fruitful and resulted in some remarkable achievements [2, 3]. In the presentation, recent advances in the relativistic electronic structure calculations for the heaviest elements and predictions of their experimental behaviour are overviewed. An emphasis is put on the reliability of the theoretical approaches and models with respect to the experimental outcome.

II. THEORETICAL METHODS AND RESULTS

For the heaviest elements, electronic structure calculations should be made with the use of methods that treat relativistic and electron correlation effects at the highest possible level of theory. In the recent years, the relativistic quantum theory and computational algorithms received tremendous developments [4]. As a result, very accurate calculations of the electronic structure and properties of superheavy atoms and molecules became possible. On their basis, reliable predictions of experimental behaviour of these elements in the sophisticated and expensive experiments with single species have been made [5].

For atoms, Dirac-Coulomb-Breit (DCB) calculations with electron correlation at the highest level of theory, i.e., a coupled-cluster (CC) method, were performed for elements till Z=122 [6]. Accurate predictions of such properties like electronic configurations, ionization potentials, polarizabilities, that are important for the placement of the elements and for the chemical experiments, have been made.

In the molecular theory, fully relativistic (4-component) and 2-component wave-function (*ab initio* Dirac-Fock) [7] and Density-Functional-Theory (DFT) [8] methods have been developed to such an extent that very accurate predictions of binding molecular energies, optimized geometry, electronic density distributions, etc. are now available. On their basis, predictions of experimental behaviour for gas-phase and aqueous chemistry chromatography experiments have been made [2, 3, 5]. For the gas-phase experiments, direct calculations of adsorption energy of atoms and molecules on metal or other surfaces using relativistic DFT methods are now possible via a cluster approach [9].

In the presentation, we will overview results of atomic calculations till Z=122 that are important for placing these elements in the Periodic Table. They are also used for predictions of adsorption of atoms of these elements on neutral surfaces to guarantee their transportation from an accelerator to the chemistry set up.

For the gas-phase chemistry experiments, predictions of volatility of group-4 through 8 compounds are presented and compared. General trends and a common character of the chemical behaviour are outlined. Predictions of volatility of elements in the atomic state, like of element 112, Cn, element 113, and element 114, Fl, as adsorption on neutral and metal surfaces are also described and compared [9]. Interesting cases of volatility of even heavier elements, like 115, or 119 and 120 are considered.

Influence of relativistic effects on properties and experimental behaviour of the heaviest elements is elucidated.

Future perspectives for the chemical studies on the heaviest elements from the theoretical point of view are outlined.

Acknowledgment: The author is thankful to her free-will collaborators J. Anton, T. Jacob, A. Borschevsky, E. Eliav and U. Kaldor. She also thanks her colleagues, experimentalists, for valuable discussions of experimental results.

REFERENCES

[1] *The Chemistry of Superheavy Elements*, M: Schädel ed., Kluwer, Dorderecht, 2003.
[2] A. Türler and V. Pershina, Chem. Rev. **113**, 1237 (2013).
[3] V. Pershina, Radiochim. Acta **99**, 459 (2011).
[4] *Relativistic Electronic Structure Theory*, P. Schwerdtfeger ed., Parts I and 2, Elsevier, Dordrecht, 2002 and 2004.
[5] V. Pershina, In: *Relativistic Methods for Chemists*, Y. Ishikawa, M. Barysz, eds., Springer, Dordrecht (2010), pp. 452-520.
[6] U. Kador, E. Eliav, In: Ref. [4], Part 2, pp. 279-350.
[7] K. G. Dyall and K. Faegri, *Relativistic Quantum Chemistry*, Oxford University Press, 2007.
[8] J. Anton, B. Fricke, E. Engel, Phys. Rev. A **69**, 012505 (2004).
[9] V. Pershina, J. Anton and T. Jacob, J. Chem. Phys. **131**, 084713 (2009).

APSORC'13 - 5th Asia-Pacific Symposium on Radiochemistry
Kanazawa, Japan, 22-27 September 2013

Spectroscopy of Element 115 Decay Chains

D. Rudolph[1], U. Forsberg[1], P. Golubev[1], L.G. Sarmiento[1], A. Yakushev[2], L.-L. Andersson[3], Ch.E. Düllmann[2,3,4], J.M. Gates[5], K.E. Gregorich[5], F.P. Heßberger[2,3], R.-D. Herzberg[6], J. Khuyagbaatar[2,3], J.V. Kratz[4], K. Rykaczewski[7], M. Schädel[2,8], S. Åberg[1], D. Ackermann[2], M. Block[2], H. Brand[2], B.G. Carlsson[1], D. Cox[6], X. Derkx[3,4], A. Di Nitto[4], K. Eberhardt[4], J. Even[3], C. Fahlander[1], J. Gerl[2], C.J. Gross[7], E. Jäger[2], B. Kindler[2], J. Krier[2], I. Kojouharov[2], N. Kurz[2], B. Lommel[2], A. Mistry[6], C. Mokry[4], H. Nitsche[5], J.P. Omtvedt[9], P. Papadakis[6], I. Ragnarsson[1], J. Runke[2], H. Schaffner[2], B. Schausten[2], P. Thörle-Pospiech[4], T. Torres[2], A. Türler[10], A. Ward[6], D. Ward[1], N. Wiehl[3,4]

[1]Lund University, S-22100 Lund, Sweden
[2]GSI Helmholtzzentrum für Schwerionenforschung GmbH, D-64291 Darmstadt, Germany
[3]Helmholtz Institute Mainz, D-55099 Mainz, Germany
[4]Johannes Gutenberg-Universität Mainz, D-55099 Mainz, Germany
[5]Lawrence Berkeley National Laboratory, Berkeley, CA 94720, USA
[6]University of Liverpool, Liverpool L69 7ZE, United Kingdom
[7]Oak Ridge National Laboratory, Oak Ridge, TN 37831, USA
[8]Advanced Research Center, Japan Atomic Energy Agency, Tokai, Japan
[9]University of Oslo, NO-0315 Oslo, Norway
[10]Paul Scherrer Institute and University of Bern, CH-5232 Villingen, Switzerland

During the past decade, a number of correlated α-decay chains, which all terminate by spontaneous fission, have been observed in several independent experiments using ^{48}Ca-induced fusion-evaporation reactions on actinide targets [1]. These are interpreted to originate from the production of neutron-rich isotopes with proton numbers Z = 113 to 118. However, neither their mass, A, nor their atomic number, Z, have been measured directly.

In November 2012, a three-week experiment was conducted at the GSI Helmholtzzentrum für Schwerionenforschung GmbH in Darmstadt, Germany, using high-resolution α-, electron, X-ray and γ-ray coincidence spectroscopy to observe α-X-ray events to identify uniquely atomic numbers of isotopes in Z = 115 decay chains. The reaction ^{48}Ca+^{243}Am was used, with fusion-evaporation products being focused into the TASISpec set-up [2-4], which was coupled to the gas-filled separator TASCA [5,6].

A beam integral of roughly $7 \cdot 10^{18}$ ^{48}Ca particles led to the observation of about 25 correlated α-decay chains with characteristics similar to those previously published [7,8].

Results from the ongoing data analysis will be presented.

[1] Yuri Oganessian, J. Phys. G **34**, R165 (2007).
[2] L.-L. Andersson *et al.,* Nucl. Instrum. Meth. A **622,** 164 (2010).
[3] L.G. Sarmiento, L.-L. Andersson and D. Rudolph, Nucl. Instrum. Meth. A **667**, 26 (2012).
[4] U. Forsberg *et al.*, Acta Phys. Pol. B **43**, 305 (2012).
[5] A. Semchenkov *et al*., Nucl. Instrum. Meth. B **266**, 4153 (2008).
[6] J.M. Gates *et al.*, Phys. Rev. C **83**, 054618 (2011).
[7] Yu. Ts. Oganessian *et al*., Phys. Rev. C. **69**, 021601 (2004).
[8] Yu. Ts. Oganessian *et al*., Phys. Rev. Lett**. 108**, 022502 (2012).

APSORC'13 - 5th Asia-Pacific Symposium on Radiochemistry
Kanazawa, Japan, 22-27 September 2013

Chemistry at a one-atom-per-week level

A. Yakushev
GSI Helmholtzzentrum für Schwerionenforschung GmbH, 64291 Darmstadt, Germany

Keywords – superheavy elements, element 114, flerovium, gas chromatography, adsorption

INTRODUCTION

Long-lived isotopes of superheavy elements (SHE) with atomic number $Z \geq 108$ can be produced via fusion reactions between heavy actinide targets and neutron-rich projectiles at a rate of single atoms per day or per week only. Investigating the neutron-rich SHE nuclei using rapid chemical separation and subsequent on-line detection provides an independent chemical characterization and an alternative separation technique to electromagnetic recoil separators. The highly efficient separation of Hs in the form of HsO_4 is an impressive example for such studies of the nuclear reaction mechanism and nuclear structure [1,2]. Approaching the heaviest elements, copernicium (Cn), element 113 and flerovium (Fl), which are accessible for chemistry experiments, the coupling of chemistry setups to a recoil separator promises extremely high sensitivity due to strong suppression of background from unwanted species.

FL: NOBLE GAS OR VOLATILE METAL?

Electron shells of SHE are influenced by strong relativistic effects caused by the high value of *Z*. Early atomic calculations for Fl predicted this to have quasi-closed electron shell configuration $6d^{10}7s^27p_{1/2}^2$, and to be noble gas-like due to very strong relativistic effects [3]. Recent fully relativistic calculations studying Fl in different environments suggest this to be less reactive compared to its lighter homologues in the group, but still exhibiting metallic character [4]. The dilemma, is Fl a noble gas or a noble metal, calls for experiments. Comparative studies of the interaction of Fl, Cn, Pb, Hg and Rn in the elemental state with metal surfaces are a powerful tool for distinguishing between metallic and noble-gas-like chemical behaviour. This was shown in experiments with Cn [5]. For Fl, the formation of a weak physisorption bond upon adsorption on gold was inferred from first experiments [6].

GAS-SOLID CHROMATOGRAPHY OF FL AT TASCA

The present gas chromatography study on Fl upon the adsorption on gold was performed at a gas-filled separator TASCA [7]. Flerovium isotopes were produced in the nuclear reaction ^{244}Pu(^{48}Ca;3,4n)^{288,289}Fl. Thez were separated in TASCA and stopped in a gas-filled chamber and flushed by a He/Ar gas mixture within 0.8 s to a detection setup COMPACT [1,2]. Two detector arrays connected in series were used, both covered with a thin gold layer. The first detector array was connected directly to the exit of TASCA and kept at room temperature. A negative temperature gradient from +20 to −162 °C was applied along the second detector array placed downstream of the first one. The use of two detectors in series allowed the detection of species in a wide volatility range – from the non-volatile Pb to the noble gas Rn.

RESULTS

Two decay chains, one from ^{288}Fl and one ^{289}Fl were detected. Both decays from Fl isotopes occurred in the first detector array at room temperature. The positions of decay chain members are shown in Fig. 1 together with distributions of Pb, Hg, and Rn and the Monte–Carlo simulated deposition peak for ^{285}Cn (dashed line). The observed behavior of Fl in the chromatography column is indicative of Fl being less reactive than the nearest homolog Pb. The evaluated lower limit of the adsorption enthalpy $-\Delta H_{ads}$(Fl) > 48 kJ/mol reveals the formation of a metal-metal bond with Au, which is at least as strong as that of Cn, and thus demonstrates the metallic character of Fl.

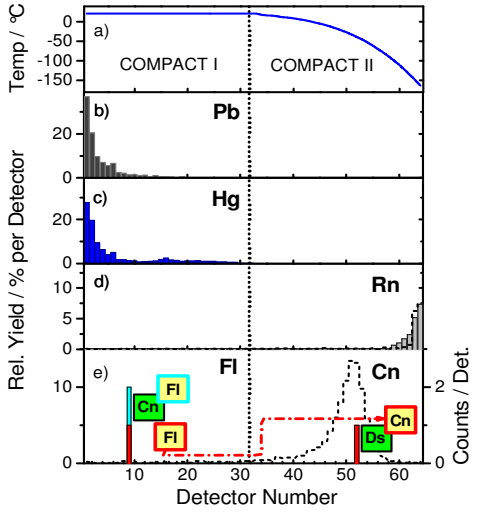

Fig.1: The observed gas-chromatography behavior of Fl and Cn in COMPACT compared to those of Pb, Hg and Rn.

[1] J. Dvorak *et al. Phys. Rev. Letters* **97**, 242501 (2006).
[2] J. Dvorak *et al. Phys. Rev. Letters* **100**, 132503 (2008).
[3] K.S. Pitzer. *J. Chem. Phys*. **63**, 1032 (1975).
[4] V. Pershina *et al. J. Chem. Phys*. **131**, 084713 (2009).
[5] R. Eichler *et al. Angew. Chem, Int. Ed.* **47**, 3262-3266 (2008).
[6] R. Eichler *et al. Radiochim. Acta* **98**, 133-139 (2010).
[7] A. Semchenkov et al. *NIM B* **266**, 4153-4161 (2008).

APSORC'13 - 5th Asia-Pacific Symposium on Radiochemistry
Kanazawa, Japan, 22-27 September 2013

$Sg(CO)_6$ – The First Organometallic Transactinde Complex opening a Window to a New Compound Class

J. Even [1], A. Yakushev[2], Ch.E. Düllmann[1,2,3], H. Haba[4], M. Asai[5], T.Sato[5], H. Brand[2], A. Di Nitto[3], R. Eichler[6,7], F. Fangli[8], W. Hartmann[2], M. Huang[4], E. Jäger[2], D. Kaji[4], J. Kanaya[4], Y. Kaneya[5], J. Khuyagbaatar[1], B. Kindler[2], J.V. Kratz[3]; J.Krier[2],Y. Kudou[4], N. Kurz[2], B. Lommel[2], S. Miyashita[5], K. Morimoto[4], K. Morita[4], Y. Nagame[5], H. Nitsche[9,10], K. Ooe[11], M. Schädel[5], J. Steiner[2], T. Sumita[4], K. Tanaka[4], A. Toyoshima[5], K. Tsukada[5], A. Türler [6,7], I. Usoltsev [6,7], Y. Wakabayashi[4], Y. Wang[8], N. Wiehl[1,3], S. Yamaki[4,12], Q. Zhi[8]

[1]Helmholtz-Institut Mainz, Johannes Gutenberg-Universität, 55099 Mainz, Germany;
[2] GSI – Helmholtzzentrum für Schwerionenforschung, Planckstr. 1, 64291 Darmstadt, Germany;
[3]Johannes Gutenberg-Universität Mainz, 55099 Mainz, Germany;
[4]Nishina Center for Accelerator-Based Science, RIKEN, Wako, Saitama 351-0198, Japan;
[5]Advanced Science Research Center, Japan Atomic Energy Agency, Tokai, Ibaraki 319-1195, Japan;
[6]University of Berne, Freiestrasse 3, CH-3012 Berne, Switzerland;
[7]Paul Scherrer Institute, CH-5232 Villigen, Switzerland;
[8]Institute of Modern Physics Lanzhou; Chinese Academy of Sciences, 509 Nanchang Road, CN-730000 Lanzhou, China;
[9]University of California, Berkeley, CA 94720-1460; U.S.A.;
[10] Lawrence Berkeley National Laboratory, Berkeley, CA 94720-8169 U.S.A.,
[11]Niigata University, Niigata, Niigata 950-2181, Japan,
[12]Saitama University, Saitama 338-8570, Japan.

Abstract – We report on the synthesis and chemical investigation of the first organometallic compound of a transactinide element, namely seaborgium hexacarbonyl.

Keywords – Seaborgium, Carbonyl Complex, Adsorption, Hot chemistry

In the last decades, simple inorganic compounds of the transactinde elements (TAN) were studied in gas phase chemical reactions [1]. Accessing, e.g., metal complexes with organic ligands or organometallic compounds was impossible due to technical restrictions, like the destructive plasma present behind the target created by the intense heavy ion beam. Thanks to the novel approach of physical preseparation in a recoil separator to reject the beam [2], these limitations could be overcome [3]. In previous experiments, we demonstrated the formation of volatile d-element carbonyl complexes with recoiling ions thermalized in a carbon monoxide containing atmosphere [4]. Short-lived isotopes of the lighter homologs of seaborgium – molybdenum and tungsten showed this to be an appropriate method to study group 6 elements under conditions relevant for a transactinide chemistry experiment.

Seaborgium hexacarbonyl has been predicted to be stable [5]. The π-back bonding, characteristic for the metal-carbon bond in carbonyl complexes, is expected to be stronger than in the complexes of the lighter homologues due to the relativistic expansion of the d-orbitals. Furthermore, $Sg(CO)_6$ is predicted to be as volatile as tungsten hexacarbonyl and therefore suitable for, e.g., thermochromatography studies [6]. Based on previous studies with molybdenum and tungsten, an experiment aiming at the study of seaborgium hexacarbonyl was conducted at the gas-filled recoil ion separator GARIS at RIKEN. In our experiment, $^{265a,b}Sg$ ($t_{1/2}$=8.5 s, 14.4 s) [7] was synthesized in the reaction $^{248}Cm(^{22}Ne,5n)$. Seaborgium was separated within GARIS from the primary beam and was guided to the recoil transfer chamber (RTC) mounted in the focal plane of GARIS [8]. The ^{265}Sg was thermalized within the RTC in a helium carbon-monoxide mixture under ambient conditions. This way it formed volatile carbonyl complexes and was transported in the gas stream to the radiochemistry laboratory. There, its adsorption on silicon dioxide was studied with the thermochromatography detector COMPACT. The combination of preseparation with GARIS and detection in COMPACT allowed the study of seaborgium under background-free conditions.

Our results indicate the observation of $Sg(CO)_6$ and allow to compare its behavior to that of $W(CO)_6$ and to theoretical predictions. At the moment, the data analysis is ongoing. Experimental details and results will be presented at the conference.

[1] A. Türler and V. Pershina, *Chem. Rev*. **2013**, *113*, 1237−1312.
[2] Ch E. Düllmann et al., *Nucl. Instr. Meth. A* **2005**, *551*, 528–539.
[3] Ch.E. Düllmann et al., *Radiochim. Acta* **2009**, *97*, 403-418.
[4] J. Even, et al., *Inorg.Chem.* **2012**, *51*, 6431-6422.
[5] C.S. Nash, B. E. Bursten, *J. Am. Chem. Soc.* **1999**,*121*, 10830-10831.
[6] V. Pershina and J. Anton, *submitted to J. Chem Phys.* **2013**.
[7] H. Haba et al., *Phys. Rev. C* **2012**, *85*, 024611.
[8] H. Haba et al, *Chem. Lett.* **2009**, *38*, 426-427.

This experiment was performed at RI Beam Factory operated by RIKEN Nishina Center and CNS, University of Tokyo. We thank the ion source and RILAC operators Financial support from the German BMBF under contract 06MZ7164 and from JAEA Tokai, Advanced Science Research Center's Reimei research program is gratefully acknowledged..

APSORC'13 - 5th Asia-Pacific Symposium on Radiochemistry
Kanazawa, Japan, 22-27 September 2013

Superheavy Element Z and A Measurements at the Berkeley Gas-Filled Separator

H. Nitsche [1, 2], G. K. Pang [2], J. M. Gates [2], K. E. Gregorich [2] N. E. Esker [1], O. R, Gothe [1]
[1] University of California, Berkeley, Department of Chemistry, Berkeley, CA 94720-1460, USA
[2] Lawrence Berkeley National Laboratory, Nuclear Science Division, Berkeley, CA 94720-8169, USA

Since the dawn of the new Millenium, six new superheavy elements (SHE) (113, 114, 115, 116, 117, and 118) have been produced in reactions of ^{48}Ca beams with actinide targets. So far, these experiments have led to the discovery of 52 new isotopes [1,2]. Several independent confirmation experiments led to the recent naming of flerovium, Fl, and livermorium, Lv, for elements 114 and 116, respectively [3-6]. The α-decay chains of these SHE terminate by spontaneous fission, before reaching the part of the Chart of the Nuclides where Z and A are well-established. The SHE Z and A assignments have been made by comparing experimental α-particle decay energies with model calculations [7], supplemented with cross-bombardment information. Thus, neither Z nor A have been directly measured. Before using measured α-decay energies to adjust mass models, these Z and A assignments must be proven to be correct. Otherwise a situation could arise where data from incorrect assignments are used to modify mass models which, in turn, reinforce the incorrect assignments. Identifying Z by detecting α - K x-ray coincidences [9], known as x-ray fingerprinting, is an already established process. The first results of x-ray finger printing experiments conducted for element 115 produced in the ^{243}Am(^{48}Ca,3n)^{288}115 reaction using the Berkeley Gas-Filled Separator (BGS) at the 88-inch cyclotron at Lawrence Berkeley National Laboratory will also be presented.

However, to simultaneously identify both Z and A with the BGS, we are making several upgrades to its detection setup, design and construct a new mass analyzer, as well a gas catcher and a radiofrequency quadrupole ion trap (RFQ) to match the output of the BGS to the acceptance of the mass analyzer. The first SHE to be studied using these new upgrades at the BGS will be ^{289}Fl [9] produced in the fusion evaporation reaction of ^{244}Pu(^{48}Ca,3n). Z-identification is conducted in the same manner as described above and coupling of the x-ray fingerprinting setup with a mass analyzer, then provides a simultaneous determination of A and Z.

[1] Y.T. Oganessian, J. Phys. G 34, R165 (2007).
[2] Y.T. Oganessian, Radiochim. Acta 99, 429 (2011)
[3] L. Stavsetra, K. E. Gregorich, J. Dvorak, P. A. Ellison, I. Dragojevic´, M. A. Garcia, and H. Nitsche, Phys. Ref. Let. 103, 132502 (2009).
[4] Ch. E. Düllmann et al., Phys. Ref. Let. 104, 252701 (2010).
[5] P. A. Ellison, K. E. Gregorich, J. S. Berryman, D. L. Bleuel, R. M. Clark I. Dragojevic´, J. Dvorak, P. FallonC. Fineman-Sotomayor, J. M. Gates, O. R. Gothe, I.Y. Lee, W. D. Loveland, J. P. McLaughlin, S. Paschalis, M. Petri, J. Qian, L. Stavsetra, M. Wiedeking, and H. Nitsche, Phys. Ref. Let. 105, 182701 (2010).
[6] J. M. Gates et al., Phys. Rev. C 83, 054618 (2011).
[7] A. Sobiczewski et al., Prog. Part. Nucl. Phys. 58, 292 (2007).
[8] C.E. Bemis et al., Phys. Rev. Lett. 31, 647 (1973).
[9] Y.T. Oganessian et al., Phys. Rev. C 69, 054607 (2004).

Acknowledgement:
This work is supported by U.S. Department of Energy, Office of Science, Nuclear Physics, Low Energy Physics Program, and was performed at Lawrence Berkeley National Laboratory under Contract No. DE-AC02-05CH11231.

Intermetallic Actinide compounds for SHE Production Targets

R. Eichler[a,b], I. Usoltsev[a,b], J.P. Omtvedt[d], O. V. Petrushkin[c], D. Piguet[a], A. V. Sabel'nikov[c], A. Türler[a,b], G. K. Vostokin[c] , A. V. Yeremin[c]

[a] Laboratory for Radiochemistry and Environmental Chemistry, Paul Scherrer Institute, CH-5232 Villigen, Switzerland
[b]Department of Chemistry & Biochemistry, University of Berne, Freiestrasse 3, CH-3012 Berne, Switzerland
[c]Flerov Laboratory of Nuclear Reactions, Joint Institute for Nuclear Research, 141980 Dubna, Russia
[d]University of Oslo, 0316 Oslo, Norway

*R*ecent experiments with superheavy elements require high intensive heavy ion beams and highly sophisticated target technologies able to stand the harsh irradiation conditions. Especially, stationary target technologies based on painting and molecular plating of actinide oxides onto thin Ti foils reveal severe target degradation by the intensive beams. These effects lead to a considerable drop in the production rates and transport yields of SHE to chemical setups. Seeking for better target material possibilities we focused our research onto metallic targets. These metallic targets are expected to be superior to the widely used nowadays solely electroplated targets due to higher thermal conductivity, electrical conductivity, chemical stability, and mechanical stability. We proposed a simple method which allows producing Pd-based intermetallic targets for high intensity irradiations [1]. Based on the molecular plating technique [2] followed by coupled reduction [3] this method was successfully applied to different lanthanide and actinide isotopes [1]. First irradiation experiments with intermetallic targets were carried out at the Oslo Cyclotron Laboratory, University of Oslo, Norway. Here, a 3.5 µm ^{238}U/Pd target was irradiated at the MC-35 Scanditronix cyclotron using a 0.5 □A proton beam with cyclotron energy of 30 MeV. This experiment showed the possibility of safe handling of such targets in accelerator environments. Two ^{243}Am/Pd intermetallic targets have been prepared and irradiated at the U-400 cyclotron at the Flerov Laboratory for Nuclear Reactions for several days. Both ^{243}Am targets were characterized by alpha-particle spectroscopy and light microscopy before and after irradiation with high intensity beams of ^{48}Ca. For direct comparison, the performance of a 'classical' electroplated $^{243}AmO_2$/Ti target was investigated. Figure 1 shows optical micrographs revealing the clear superiority of intermetallic targets. Challenges and possibilities connected to the use of intermetallic compounds as high power irradiation targets will be presented.

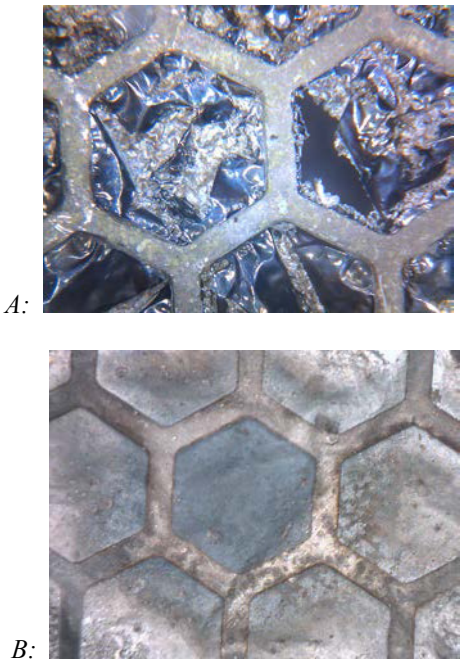

A:

B:

Figure 1: Micrographs of irradiated targets. A) titanium based target after irradiation with ^{48}Ca particles at intensities of up to $7\cdot10^{12}$ ^{48}Ca per second for about 120 hours; B) palladium based target after irradiation with ^{48}Ca particles at almost two times higher intensities compared to the titanium based target of up to $1.2\cdot10^{13}$ ^{48}Ca per second for about 60 hours. The Pd foil and the actinide distribution remain nearly unchanged.

Acknowledgments: We thank the crews form the ion source and U-400 cyclotron of FLNR Dubna for providing intense beams of ^{48}Ca. This research was supported by Swiss National Science Foundation grant 200020_126639.

References

[1]I. Usoltsev, et al., Preparation of Pd-based intermetallic targets for high intensity irradiations, Nucl. Instr. and Meth. Phys. Res.A691, 5–9 2012.
[2]W. Parker, et al., Nucl. Instr. and Meth. 26, 61 (1964).
[3]S. Möbius, L. Hellwig, C. Keller, J. Less-Common Met. 121, 43 (1986).

The First Successful Observation of Mass-separated Lawrencium (Lr, Z = 103) Ions with ISOL Technique

T. K. Sato[1], M. Asai[1], N. Sato[2], Y. Kaneya[1,3], K. Tsukada[1], A. Toyoshima[1], S. Miyashita[1], Y. Nagame[1], M. Schädel[1], A. Osa[3], S. Ichikawa[1,4], K. Ooe[5], T. Stora[6], J. V. Kratz[7]

[1]Advanced Science Research Center, Japan Atomic Energy Agency, Tokai, Ibaraki 319-1195, Japan
[2] Nuclear Science and Engineering Directorate, Japan Atomic Energy Agency, Tokai, Ibaraki 319-1195, Japan
[3]Graduate School of Science and Engineering, Ibaraki University, 2-1-1, Bunkyo, Mito, Ibaraki 310-8512, Japan
[3]Department of Research Reactor and Tandem Accelerator, Japan Atomic Energy Agency, Tokai, Ibaraki 319-1195, Japan
[4]Nishina Center for Accelerator-Based Science, RIKEN, 2-1 Hirosawa, Wako, Saitama 351-0198, Japan
[5]Institute of Science and Technology, Niigata University, Niigata 950-2181, Japan
[6]ISOLDE, CERN, CH-1211 Geneva 23, Switzerland
[7]Institut für Kernchemie, Universität Mainz, D-55099 Mainz, Germany

*Abstract – In order to determine the first ionization potential of the heaviest actinide lawrencium (Lr, Z=103), we have developed a surface ionization ion-source as part of the JAEA-ISOL (**I**sotope **S**eparator **O**n-**L**ine) setup, which is coupled to a He/CdI_2 gas-jet transport system. We will report on the first successful ionization and mass separation of 27-s ^{256}Lr produced in the ^{249}Cf+^{11}B reaction.*

Keywords – Lawrencium (Lr), Heavy actinide, Ionization potential, ISOL, Surface ionization, Ion source

I. INTRODUCTION

The ground-state electronic configuration of lawrencium (Lr, Z = 103) that is the heaviest actinide element is predicted to be [Rn]5f^{14}7$s^2$7$p_{1/2}$, which is different from that of the lanthanide homolog lutetium (Lu) [Xe]4f^{14}6$s^2$5d. The reason for this change in the ground state configuration is that the 7p orbital of Lr is stabilized below the 6d orbital by strong relativistic effects [1]. The weakly-bound outermost electron results in a significantly lower first ionization potential of Lr as compared to its neighboring heavy actinides [2]. The ionization potential of Lr, however, has not been determined experimentally owing to its low production rate and short half-life. In order to determine the ionization potential of Lr, we have developed a surface ionization type ion-source for the JAEA-ISOL coupled to a gas-jet transport system [3]. As a step to determination of the ionization potential of Lr, we conducted to ionize a short-lived Lr isotope by using the ion-source in several ionization conditions.

II. EXPERIMENTAL

The isotope ^{256}Lr ($T_{1/2}$ = 27 s) was produced in the reaction of ^{249,250,251}Cf(^{11}B, xn)^{256}Lr [4]. A ^{249,250,251}Cf target (^{249}Cf: 63%, ^{250}Cf: 12%, and ^{251}Cf : 25%) with 185 ± 25 μg/cm^2 on a 1.85 mg/cm^2 thick Be backing foil was irradiated with a 67.9-MeV (63 MeV in the middle of the target) $^{11}B^{4+}$ beam from the JAEA tandem accelerator. For comparison the lutetium isotopes ^{168m}Lu and ^{168g}Lu, with half-lives of 6.7 min and 5.5 min, respectively, were synthesized in the ^{162}Dy(^{11}B, 5n) reaction. The nuclear reaction products recoiling from the targets were transported to the ion-source by a He/CdI_2 gas-jet transport system. The products were ionized in the ion-source, accelerated with 30 kV, and then mass-separated with a mass-separator in ISOL. The amount of ions collected at the end of the ISOL after mass-separation was determined by α- or γ-ray measurements. To calculate ionization efficiencies, nuclear reaction products transported from a target recoil chamber were collected directly and measured prior to the ionization experiments. To compare the ionization efficiencies on different surface material of the ion-source, a rhenium (Re) surface and a tantalum (Ta) surface were employed in this study.

III. RESULTS AND DISCUSSION

We successfully ionized and mass-separated ^{256}Lr for the first time by using the developed ion-source and applying the ISOL technique. The Ionization efficiencies of Lr and Lu on the Re surface were obtained to be 42^{+20}_{-19} % and 19.9 ± 7.0 %, respectively. In the case of the Ta surface, the efficiency of Lr was 19^{+9}_{-8} % while that of Lu was 4.0 ± 1.4 %. The ionization efficiency of each element on the Re surface was larger than that on the Ta surface because the work function of Re is higher than that of Ta.

Under both conditions, the ionization efficiencies of Lr are larger than those of Lu. The results indicate that the ionization potential of Lr must be lower than that of Lu. This is consistent with the theoretical prediction from a coupled cluster (CC) calculation that takes into account relativistic effects [3].

In the presentation, we will report on the first experimental determination of the first ionization potential of Lr based on our latest results.

[1] Zou, Y. and Fischer, C. F. Phys. Rev. Lett. **88** (2002) 183001.
[2] Borschevsky, A. et al. Eur. Phys. J. D**45** (2007) 115.
[3] Sato, T. K. et al. Rev. Sci. Instrum. **84** (2013) 023304.
[4] Sato, N. et al. JAEA Rev. **2010-056** (2010) 52.

NEI-01

Nuclear Energy Chemistry in China: Present Status and Future Perspectives

Zhi-Fang Chai
Nuclear Energy Chemistry Group, Key Laboratory of Nuclear Analytical Techniques
Institute of High Energy Physics, Chinese Academy of Sciences, Beijing 100049, China
E-mail: chaizf@ihep.ac.cn

Nuclear energy chemistry is one of the most challenging subjects in modern science, and its development is tightly related to the advanced nuclear fuel cycle and persistent development of nuclear energy. Nuclear energy chemistry in China is now experiencing a renaissance, which is being strongly motivated by China's huge energy demand. In this talk, the recent progresses in nuclear energy chemistry of China are selectively highlighted, with emphasis on the front-end chemistry, actinide solid-state chemistry associated with nuclear fuel fabrication, actinide solution chemistry and nuclear fuel reprocessing as well as chemistry in nuclear waste disposal and management. Some positive measures about how to promote the nuclear energy chemistry in China are discussed, and future perspectives are briefly outlined as well.

Acknowledgement – This work was supported by Natural Science Foundation of China (Grants 91026007, 91226201 and 11275219) and the "Strategic Priority Research Program" of the Chinese Academy of Sciences (Grants.XDA030104).

[1] WQ Shi, YL Zhao, ZF Chai. *Radiochim Acta*. 2012, 100: 529.

Evaluation of new extractants relevant to the back-end of nuclear fuel cycle

A. Goswami

Radiochemistry Division, Bhabha Atomic Research Centre, Trombay, Mumbai – 400 085, INDIA

E-mail: agoswami@barc.gov.in

Abstract:. *Conventionally, PUREX and THOREX processes have been proposed for the reprocessing of U and Th based spent fuels employing tri-n-butyl phosphate (TBP) as extractant. However, some major limitations of TBP have been identified and need to be addressed. Evaluation of alternative extractants is, therefore, desirable which can overcome at least some of these problems. Extensive studies have been carried out on the evaluation of N,N-dialkyl amides as extractants in the back-end of the nuclear fuel cycle for addressing the issues related to the reprocessing of U and Th based spent fuels. Similarly, efforts have been made on the evaluation of new solvents for the partitioning of minor actinides (MA) from high-level waste (HLW) solutions. This talk presents an overview of studies carried out at Radiochemistry Division on (a) spent fuel reprocessing of U/Th based spent fuels employing N,N-dialkyl amides as extractants, and (b) partitioning of minor actinides using novel solvents .*

Keywords – Reprocessing; Actinide partitioning; Tributyl phosphate; Dialkyl amides; Diglycolamides

The challenging task of recovery and purification of ^{239}Pu from irradiated U and of ^{233}U from irradiated Th are accomplished presently by the well known PUREX and THOREX processes, respectively [**1**]. These processes employ tri-n-butyl-phosphate (TBP) in n-dodecane as solvent. However, a few drawbacks associated with the use of TBP have been identified: (i) deleterious nature of its degradation products (ii) relatively lower distribution coefficient of Pu(IV) as compared to that of U(VI) (iii) significant solubility of TBP towards aqueous phase, and (iv) non-incinerable nature of the spent solvent yielding large volumes of secondary radioactive waste. These shortcomings may pose a serious challenge particularly during the reprocessing of short-cooled (MOX) thermal reactor, Advanced Heavy Water Reactor (AHWR, being developed in India based on Th) as well as fast reactor spent fuels with larger Pu content and significantly higher burn up [**2**]. In this context, large number of eco-friendly *N,N*-dialkyl amides were evaluated as alternative extractants at Radiochemistry Division, BARC, Mumbai, India. Amongst these amides, N,N-dihexyloctanamide (DHOA) and *N,N*-di(2-ethylhexyl)isobutyramide (D2EHIBA) received considerable attention as potential alternatives extractants for the reprocessing of U and Th based spent nuclear fuels, respectively [**3**]. Batch extraction, mixer settler/ centrifugal contactor runs were carried out with these reagents under Pu rich feed (relevant to fast reactor) and AHWR feed conditions, respectively. These data were compared with those obtained with TBP as extractant under identical experimental conditions and a flow sheet for AHWR spent fuel reprocessing has been proposed [**4**].

Actinide partitioning is the proposed strategy for effective mitigation of the long term hazards associated with high-level waste (HLW). Octyl-(phenyl)–*N,N*-diisobutyl carbamoyl methyl phosphine oxide (CMPO) has been studied extensively during eighties for actinide partitioning from wastes of different origin. However, the last two decades, substituted malonamide extractants such as *N,N'*-dimethyl-*N,N'*-dibutyl tetradecyl malonamide (DMDBTDMA) and *N,N'*-dimethyl-*N,N'*-dioctyl hexylethoxy malonamide (DMDOHEMA) have emerged as viable green alternatives to phosphine oxides. Recently, diglycolamide based extractants such as *N,N,N′,N′*-tetraoctyl diglycolamide (TODGA) and *N,N,N′,N′*-tetra-2-ethylhexyl diglycolamide (TEHDGA) have received considerable attention due to overwhelmingly favorable extraction and stripping efficiencies of minor actinides from different types of transuranium (TRU) wastes (**Fig.1**) [**5,6**]. We have carried out comparative evaluation of the key physical and chemical properties (including extraction/stripping) of these extractants for hydrometallurgical applications. A flow sheet has been proposed using DHOA as extractant. Merits of flow-sheets proposed for the separation and recovery of minor actinides from HLW have also been discussed. Detailed batch as well as mixer settler studies have shown that tridentate diglycolamide based ligands such as TODGA and TEHDGA have excellent properties for the partitioning of actinides from HLW solution.

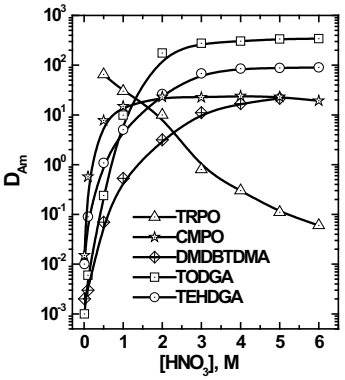

Fig.1: Variation of D_{Am} with HNO_3 concentration; Extractants: 30% TRPO, 0.2M CMPO+1.2M TBP, 1M DMDBTDMA, 0.1M TODGA + 0.5M DHOA and 0.2M TEHDGA + 30% *iso*-decanol; Diluent: *n*-dodecane; Temperature: 25°C

Acknowledgement: Author thanks Dr. P.K. Mohapatra and Dr. P.N. Pathak for their help in preparing this paper.

References

1. "Reactor Hand Book", S.M. Stoller and R.B. Richards (Eds.), v. 2, "*Fuel reprocessing*", Interscience Publishers & Inc., New York, 1961.
2. R.K. Sinha, A. Kakodkar, A. *Nucl. Engg. Design*, 2006, 236, 683.
3. V.K. Manchanda, P.N. Pathak, *Sep. & Purif. Technol.*, 35 (2004) 85.
4. N. Kumari, D.R. Prabhu, A.S. Kanekar, P.N. Pathak. *Ind. Engg. Chem. Res.,* 51 (44) (2012) 14535.
5. S.A. Ansari, P.N. Pathak, Prasanta K. Mohapatra, Vijay K. Manchanda. *Chemical Reviews*, 112(3) (2012) **1751**.
6. Seraj A. Ansari, Priyanath Pathak, Prashant K. Mohapatra and Vijay K. Manchanda. *Sep.& Purif. Reviews*, 40 (2011) 43.

Hexanoic acid as alternative diluent in a GANEX process based on TBP and CyMe4-BTBP

Elin Löfström-Engdahl[1], Emma Aneheim[1], Christian Ekberg[1], Hanna Elfversson[1] and Gunnar Skarnemark[1]

Nuclear chemistry[1], Industrial Materials Recycling[2], Department of chemical and Biological Engineering, Chalmers University of Technology, SE 412 96 Gothenburg, Sweden

Abstract – Used nuclear fuel is radiotoxic for mankind and its environment for a long time. However, if it can be transmuted the radiotoxicity can be reduced. Simultaneously the long term heat load is decreased, making a final storage more volume efficient. Before the transmutation the actinides within the used fuel need to be separated from the fission, corrosion and activation products. This separation can be achieved by using the technique liquid-liquid extraction.

One extraction process that can be used for such a separation is the GroupActiNideEXtraction (GANEX) process. In a GANEX process all the actinides are to be separated from the rest of the fuel as one group. This extraction leaves all the fission, corrosion and activation products in the aqueous stream. One GANEX process that can successfully accomplish the An(III)/Ln(III) separation utilizes the diluent cyclohexanone in combination with the extractant tributylphosphate (TBP) (30 % vol) and a second ligand, CyMe4-BTBP (10 mM). However, there are some issues when using cyclohexanone as diluent, for example; it has a low flash point and it degrades in contact with the acidic aqueous phase. In this work an alternative diluent has therefore been tried in order to rule out if it can replace cyclohexanone. The diluent used was hexanoic acid. In the system containing 12 mM CyMe4-BTBP and 30 % vol TBP in hexanoic acid and the aqueous phase being 4 M HNO_3 the distribution ratio for plutonium is high (D_{Pu} = 76 ± 17), while the one for uranium is lower (D_U = 2.2 ± 0.25). The distribution ratios for americium and curium are unfortunately much lower than that of plutonium (D_{Am}= 1.1 ± 0.27, D_{Cm}=1.6 ± 1.81). The concentration CyMe4-BTBP ligand, the extractant of curium and americium, could unfortunately not be increased, because of limited solubility in hexanoic acid. The distribution ratios for fission, corrosion and activation products were low for mostly metals; however, silver, cadmium, palladium and molybdenum all have distributions ratios above 1 is therefore troublesome. Europium is used as a representative lanthanide, which are similar to the trivalent actinides and therefore hard to separate. The distribution ratio for europium is low in this system (D Eu = 0.12 ± 0.016). However, to conclude, the low americium and curium extractions indicate that hexanoic acid cannot replace cyclohexanone in a GANEX process.

APSORC'13 - 5th Asia-Pacific Symposium on Radiochemistry
Kanazawa, Japan, 22-27 September 2013

Effect of alcohols on separation behavior of rare earth elements using benzimidazole-type anion-exchange resin in nitric acid solutions

Tomobuchi Yusuke[1], Yu Tachibana[1], Masao Nomura[2] and Tatsuya Suzuki[1]
[1]Department of Nuclear System Safety Engineering, Graduate School of Engineering, Nagaoka University of Technology,
[2]Laboratory for Nuclear Reactors, Tokyo Institute of Technology

Abstract - Chromatographic separation experiments of trivalent rare earth elements were performed using benzimidazole type anion-exchange resin in nitric/alcohol mixed solvent systems at room temperature. As a result, it was found those trivalent rare earth elements are able to be separated mutually in a 20 % HNO_3 and 80 % MeOH mixed solvent. Based on these results, we systematically examined using various alcohols to make clear the role of alcohols in anion-exchange reactions at various temperatures.

Keywords - rare earth elements, alcohols, benzimidazole-type anion-exchange resin, mutual separation

I. INTRODUCTION

As a final disposal method for the high level liquid waste(abbreviated as HLLW) generated by spent-nuclear-fuel reprocessing plants, the geologic disposal concept of the vitrified HLLW has been proposed and investigated globally. Especially, from the viewpoint of minimizing the long-term radiological risk and facilitating the management of HLLW, a separation of the long-lived minor actinides(MA = Am and Cm) from HLLW is strongly desired.[1)] Moreover, a mutual separation of Am and Cm is also required after the separation of MA from HLLW because the relatively high decay heat of Cm makes it difficult to fabricate nuclear fuels reproduced from spent nuclear fuels.[2)] On the other hand, it has been well known that the difficulty of a mutual separation between trivalent Am and Cm is due to similar chemical properties.[2)] In fact, although a few reports by Hale et al. using diethylenetriaminepentaacetic acid and Suzuki et al. with tertiary pyridine have been reported, little systematic information is available on the mutual separation mechanisms between Am and Cm.[2,3)] Therefore, as a part of the fundamental researches to innovate conventional separation technologies, we have studied on the chromatographic separation of trivalent rare earth elements(abbreviated as REE (REE = La, Ce, Pr, Nd, Sm, Eu, and Gd)) which have the same valence level in solutions and the similar ion radii as compared with those of MA, using benzimidazole type anion-exchange resin (abbreviated as AR-01) embedded in high-porous silica beads in nitric acid/alcohol mixed solvent systems.

II. EXPERIMENTAL

All REE were used without further purification. The purity of all REE was more than 98.0%. All chemicals for sample preparations were of special pure grade. AR-01 resin consisted of styrene-divinylbenzene copolymers with 4-(1-methylbenzoimidazole-2-yl)phenyl and 4-(1,3-dimethyl-benzoimidazole-2-yl)phenyl, was supplied from Asahi Kasei Corporation. Each concentration of REE species in the solutions were determined by ICP-MS(7700x, Agilent).

III. RESULTS

Chromatographic separation experiments of trivalent REE were performed using AR-01 resin in a nitric acid solvent system and a nitric/alcohol mixed solvent system at room temperature. As a result, it was found that mutual separations of REE cannot be achieved completely in HNO_3 solutions(data no shown), but REE are able to be separated mutually in a 20 % HNO_3 and 80 % MeOH mixed solvent(see Figure 1). In addition, retention times obtained from these chromatograms of the REE increase with increasing the ion radii in order of Gd, Eu, Sm, Nd, Pr, Ce, and La, *i.e.*, it could be estimated that the separation mechanisms proceed through anion-exchange reactions between 4-(1,3-dimethyl-benzoimidazole-2-yl)phenyl groups of AR-01 and $[Ln(NO_3)_n]^{3-n}$ ($n \geq 4$). Based on these results, we concluded that the examined separation technique is applied to mutual separation of Am and Cm.

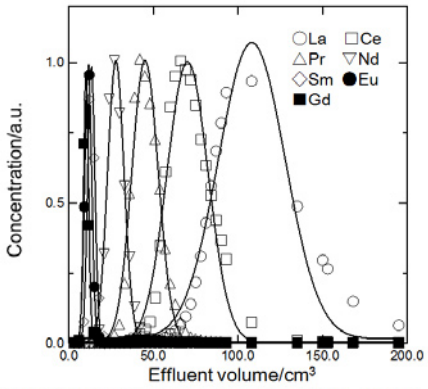

Figure 1. Chromatograms of La, Ce, Pr, Nd, Sm, Eu, and Gd species with AR-01 in 20 % HNO_3 and 80 % MeOH mixed solvent.

ACKNOWLEGEMENT

This work was partially supported by the Grant-in-Aid for Scientific Research (B) (KAKENHI No. 23360423).

REFERENCES

[1] Kolarik, Z., Journal of Nuclear Fuel Cycle and Environment, 5, 21-35 (1998)
[2] Suzuki, T., Otake, K., Sato, M., Ikeda, A., Aida, M., Fujii, Y., Hara, M., Mitsugashira, T.,Ozawa, M., Journal of Radioanalytical and Nuclear Chemistry, 272, 257-262 (2007)
[3] Hale, W.H., Lowe, J.T., Inorganic and Nuclear Chemistry Letters, 5, 363-368 (1969)

APSORC'13 - 5th Asia-Pacific Symposium on Radiochemistry
Kanazawa, Japan, 22-27 September 2013

Speciation and Reactivity of Heptavalent Technetium in Concentrated Acids.

Frederic Poineau[1], Philippe Weck[2], Benjamin P. Burton-Pye[3], Alesya Maruk[4], Gayane Kirakosyan[4], Ibthihel Denden[5], Daniel. B Rego[1], Erik V. Johnstone[1], William Kerlin[1], Eunja Kim[1], Mairlynn Ferrier[1], Alfred P. Sattelberger[7], Wayne Lukens[6], Massoud Fattahi[5], Lynn C. Francesconi[3], Konstantin E. German[4], and Kenneth R. Czerwinski[1].

[1] Department of Chemistry, University of Nevada Las Vegas, Las Vegas, NV, USA.
[2] Sandia National Laboratories, Albuquerque, NM 87185, USA.
[3] Department of Chemistry, Hunter college of the City University of New York, NY, USA
[4] A. N. Frumkin Institute of Physical Chemistry and Electrochemistry, Russian Academy of Sciences, Moscow, Russian Federation
5 Laboratory Subatech, Ecoles des Mines de Nantes, Nantes, France
[6] Energy Engineering and Systems Analysis Directorate, Argonne National Laboratory, Lemont, IL, USA.
[7] Chemical Sciences Division, Lawrence Berkeley National Laboratory, Berkeley, 94720, USA

Keywords – Technetium, Speciation, EXAFS spectroscopy.

Discovered 75 years ago, technetium is the lightest radioelement. Thirty four isotopes are known; the most common isotopes being ^{99}Tc ($t_{1/2}$ = 2.1 x 10^5 y) and ^{99m}Tc ($t_{1/2}$ = 6 h). The isotope ^{99}Tc is a fission product of the nuclear industry, while the isotope ^{99m}Tc is used in nuclear medicine as an imaging agent. Current researches focus on the development of ^{99m}Tc radiopharmaceuticals, and on the development of separation process and waste form storage for ^{99}Tc. Technetium exhibits nine oxidation states (-1 to +7). Under oxidizing conditions, the aqueous chemistry of Tc(+7) is dominated by the pertechnetate anion, TcO_4^-. In high acid concentration, TcO_4^- can be protonated and pertechnetic acid, $HTcO_4$, is formed. The structure and reactivity of $HTcO_4$ is poorly studied. Studying the chemistry of Tc(+7) in concentrated acids is relevant to the fundamental and applied chemistry of technetium; it will allow to better understand the behavior of Tc(+7) in separation processes where concentrated acids are used. In this work, the speciation and reactivity of Tc(+7) in concentrated HNO_3, H_2SO_4 and $HClO_4$ is investigated. The resulting complexes are characterized by NMR, UV-visible and EXAFS spectroscopy and DFT calculations. Results show the formation of $TcO_3(H_2O)_2(OH)$ in concentrated H_2SO_4 and $HClO_4$ while TcO_4^- in concentrated HNO_3. The complex $TcO_3(H_2O)_2(OH)$ reacts in 13 M H_2SO_4 with MeOH to produce $TcO(HSO_4)_3(OH)^-$. In HNO_3 > 7 M , the pertechnetate anion reacts with hydrogen peroxide to produce $TcO(O_2)_2(H_2O)OH$. The results demonstrate the complex and little explored chemistry of Tc in concentrated acids.

NEO-04

Fluorescence Studies of Complex Stoichiometry of Metal ions in Extraction Systems Combining Dibutyl Phosphoric Acid and Tri-n-butyl Phosphate

Alexander Braatz and Mikael Nilsson
University of California, Irvine
Department of Chemical Engineering & Materials Science
916 Engineering Tower
Irvine, CA 92697-2575
abraatz@uci.edu

Advanced nuclear fuel cycles are dependent on successful chemical separation of the various elements present in the used fuel. Numerous extraction systems have been developed for the recovery and separation of the various metal ions present in the used fuel. Extraction of lanthanides and actinides by tri-n-butyl phosphate (TBP) and dibutyl phosphoric acid (HDBP) is of importance for one of these processes, the PUREX process. The combination of these two extraction reagents have been shown to synergistically enhance metal ion extraction and display characteristics of microemulsion aggregates of reverse micelle type. To improve our understanding of the complexes formed in this system we further studied the extraction of lanthanides and actinides, in our case dysprosium, Dy, and uranium, U, with TBP and HDBP in conjunction with 2D fluorescence spectrometry. Aqueous samples containing Dy^{3+} and UO_2^{2+} in nitric acid were contacted with organic phases containing varying ratios of TBP and HDBP in n-dodecane and the distribution was followed by neutron activation analysis. 2D Fluorescence spectra were examined for all lanthanides and uranium. Typically, europium is used as a benchmark for lanthanides in fluorescence studies but we show here that several other lanthanides exhibit excellent spectroscopic characteristics using this technique. The effects of acid on the fluorescence spectra will be investigated. Possible explanations of phenomena and comparison to existing Eu studies found in literature will also be presented.

Column study on electrochemical separation of cesium ions from wastewater using copper hexacyanoferrate film

Rongzhi Chen [1)], Hisashi Tanaka [1)], Miyuki Asai [1)], Chikako Fukushima [1)], Tohru Kawamoto [1)], Manabu Ishizaki [2)], Masato Kurihara [1,2)], Makoto Arisaka [3)], Takuya Nankawa [3)] and Masayuki Watanabe [3)]

[1)] Nanosystem Research Institute, AIST, Tsukuba central 5, 1-1-1 Higashi, Tsukuba, Ibaraki 305-8565, Japan

[2)] Department of Material and Biological Chemistry, Faculty of Science, Yamagata University, 1-4-12 Kojirakawa-machi, Yamagata 990-8560, Japan

[3)] Japan Atomic Energy Agency, 2-4 Shirane Shirakata, Tokai-mura, Naka-gun, Ibaraki 319-1195, Japan

Abstract – We coated the copper hexacyanoferrate (CuHCF) on the gold electrodes, and then performed the Cs removal by electrochemical separation (ES). The prepared CuHCF nanoparticles can be simply and uniformly coated on electrodes by wet process like conventional printing methods, so any sizes or patterns are feasible at low cost, which indicated the potential as a promising sorption electrode of large size in the columns for sequential removal and recycle of Cs from wastewater.

Keywords: Metal hexacyanoferrate complex, Electrochemical separation, Cesium, Radioactive waste, Nanoparticle ink, Prussian blue complex.

Introduction

Transition metal hexacyanoferrates (HCFs) are preferred to be competitive ion exchangers over other materials due to their selectivity and high capacity. Among them, copper (II) hexacyanoferrate (III) (CuHCF) is often selected as the agent in practical analysis. This compound has been much used as precipitants for alkali metal cations, especially cesium, to remove them from aqueous radioactive wastes [1].

However, small sized CuHCF particles can easily contaminate water, which restricts its direct use for column operations. Herein, we developed and coated the water-dispersible CuHCF nanoparticles on the electrode substance, and then performed Cs removal. This study evaluates the electrochemical Cs sorbability of CuHCF NPs film and estimates the potential as a promising sorption electrode of large size in the columns for sequential removal and recycle of Cs from wastewater.

Experimental & Results

The Cs adsorption was performed in a three-electrode cell in which an $Hg/Hg_2Cl_2/KCl$ (saturated solution) as reference electrode, a platinum electrode (as counter electrode), and the CuHCF film coated adsorbent electrode were used as the working electrodes. The redox reaction for Cs separation process is proposed as follows [1]:

$$Cu_3[Fe^{III}(CN)_6]_2) + 2e^- + 2Cs^+ \leftrightarrow Cs_2Cu_3[Fe^{II}(CN)_6]_2$$

To examine the effect of temperature, electrochemical characterization of CuHCF film and its Cs adsorptions were conducted at 298, 313, and 323 K, respectively. Cs removal decreased with the increase in temperature for CuHCF film (Fig. 3b). Namely, the Cs adsorption process was exothermic in nature.

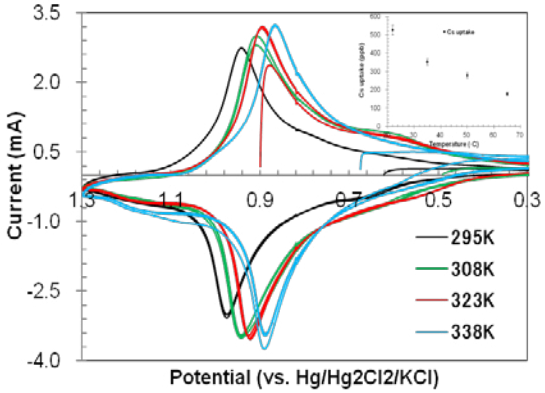

Fig. CV of a Cu-HCF film under different temperatures (from 298 to 338 K), and effect of temperature on Cs sorption using CuHCF film

In order to using our film for practical analysis in the field-scale applications, column study is needed. We synthesized water-dispersed nanoparticle CuHCF ink and then coated its nanoparticles on SUS316L sheet electrodes. The Cs adsorption and desorption were alternately repeated for 5 cycles (30 min/cycle), initial Cs conc. is 9.858 ppm.

The well balance of Cs desorption and adsorption, indicated the CuHCF film has a long life in the columns for sequential removal and recycle of Cs from wastewater.

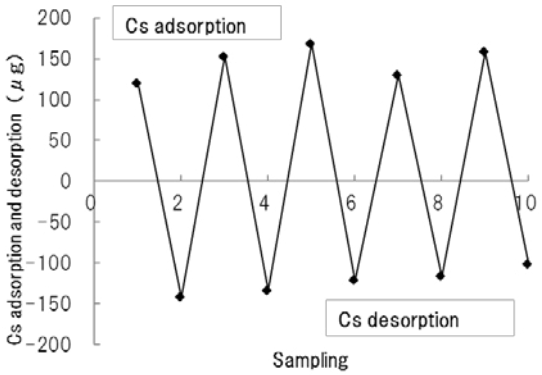

Fig. Cs alternate adsorption and desorption performance using CuHCF film

Effective regeneration and large surface coating will allow it to be used in the column for sequential removal processes.

[1] RZ. Chen, et al., *Electrochimica Acta,* **2013**, *87* 119

Poster Session 2

Tuesday, 24 September 2013

18:50 ~ 20:00

Scientific Topics (Abbrev.)

1. Fukushima issues (FK)
2. Education in nuclear and radiochemistry (ED)
3. Nuclear forensics (NF)
4. Nuclear energy chemistry (NE)
5. Nuclear chemistry (NC)
6. Actinide chemistry (AC)
7. Environmental radiochemistry (EN)
8. Radiopharmaceutical chemistry and Nuclear medicine (RP)
9. Nuclear probes for materials science (NP)
10. Activation analysis (AA)
11. Application of nuclear and radiochemical techniques (AP)

APSORC'13 - 5th Asia-Pacific Symposium on Radiochemistry
Kanazawa, Japan, 22-27 September 2013

Determination of short-lived ^{241}Pu in environmental samples by inductively coupled plasma mass spectrometry

Jian Zheng*, Keiko Tagami, Shigeo Uchida
Office of Biospheric Assessment for Waste Disposal, National Institute of Radiological Sciences

Plutonium isotopes have been released into the environment mainly from the atmospheric nuclear weapons tests in last century, the discharges from nuclear fuel reprocessing facilities, and the nuclear accidents, such as the Chernobyl and the Fukushima Daiichi Nuclear Power Plant (FDNPP) accidents [1-3]. Accurate determination of Pu isotopic composition is important for the source identification of radioactive contamination in the environment since Pu isotopic composition is characteristic for various Pu sources. Among Pu isotopes (^{238}Pu, ^{239}Pu, ^{240}Pu, and ^{241}Pu) observed in the environment, the short-lived ^{241}Pu ($t_{1/2}$ = 14.4 y), a beta emitter, is a sensitive indicator for the identification of any new contamination of Pu isotopes resulted from nuclear power plant accident. For ^{241}Pu originated from the global fallout, the activity of ^{241}Pu in the environment is quite low due to the dacay with time. The activity ratio of ^{241}Pu/$^{239+240}$Pu is ca. 1.2 in 2011 for the global fallout-sourced Pu isotopes. Therefore, higher activity ratio of ^{241}Pu/$^{239+240}$Pu in the environment will provide evidence of additional Pu input.

Due to its short half-life and beta emission, determination of ^{241}Pu in environmental samples has been a great analytical challege. Conventional technique is the low level liquid scintillation counting, which requires tedious sample preparation and long measurement time (typically 13-24 h). In the past years, we have developed sensitive analytical method using inductively coupled plasma mass spectrometry for the determination of ^{241}Pu in various environmental samples, such as atmospheric fallou material, marine sediments, and seawater reference material [4-6]. In this work, we report the determination of ^{241}Pu in environmental samples, such as litter, soil and marine sediments collected in Fukushima Prefecture after the FDNPP accident in 2011. Fig. 1 shows the results of ^{241}Pu activity in litter and surface soils collected in 20-30 km zone of the FDNPP, and in Cities of Mito, Kamagaya and Chiba. High activities of ^{241}Pu ranging from 4.5 to 34.8 mBq/g were detected in the J-Village surface soil (0-2 cm) and two litter samples. This finding of high ^{241}Pu activities in environmental samples after the FDNPP accidnet provided evidence of the release of Pu isotopes from the accident.

Acknowledgement: This study was partially supported by the Agency for Natural Resources and Energy, Ministry of Economy, Trade and Industry (METI), Japan.

References

[1] J. M. Kelley, L. A. Bond, T. M. Beasley. Sci. Total Environ. 237/238 (1999) 483-500.
[2] M. E. Ketterer, K. M. Hafer, J. W. Mietelski. J. Environ. Radioact. 73 (2004) 183-201.
[3] J. Zheng, K. Tagami, Y. Watanabe et al. Sci. Rep. 2:304; DOI:10.1038/srep00304. 2012
[4] J. Zheng, M. Yamada. J. Oceanogr. 64 (2008) 541-550.
[5] J. Zheng, M. Yamada, Appl. Radio. Isot. 70 (2012) 1944-1948.
[6] Y. S. Zhang, J. Zheng, M. Yamada et al. Sci. Total Environ. 408 (2010) 1139-1144.

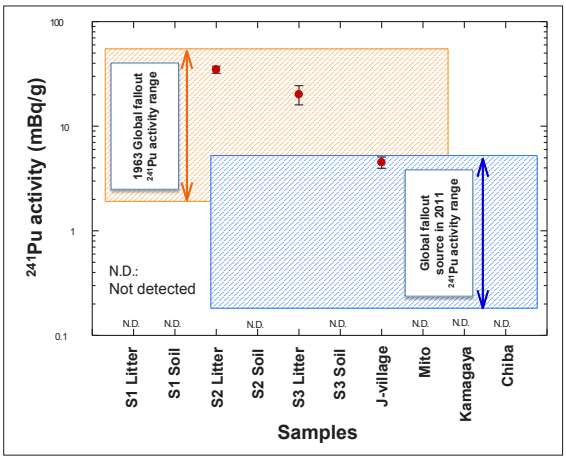

Figure 1. Results of activities of ^{241}Pu detected in the environmental samples collected after the FDNPP accident.

Numerical evaluation of Cs adsorption in PB column by extended Langmuir formula and one-dimensional adsorption model

Hiroshi Ogawa, Akiko Kitajima, Hisashi Tanaka, and Tohru Kawamoto
Nanosystem Research Institute, Advanced Industrial Science and Technology (AIST), Tsukuba, 305-8568, Japan.

Abstract – Amount of Cs adsorption in PB column was numerically evaluated based on extended Langmuir formula and one-dimensional adsorption model. The extended Langmuir formula successfully reproduced the experimental K_d distribution coefficient of Cs adsorption that cannot be explained by traditional Langmuir model. The time-variation of the Cs adsorption in column experiment was also explained by one-dimensional adsorption model.

Keywords – Cs decontamination, Cs adsorption, extended Langmuir formula, column experiment, simulation

I. INTRODUCTION

The accident of the Fukushima-daiichi nuclear plant in March, 2011 has caused heavy radioactive pollution in surrounding regions. Decontamination of radioactive elements, especially Cs-134 and Cs-137, is an urgent issue. One of the most effective procedures for the Cs-decontamination from contaminated water is to use Prussian-Blue (PB) as a Cs adsorbent [1,2]. In this paper, the authors propose a numerical method for expecting the amount of Cs reduction by PB adsorbent based on extended Langmuir formula and one-dimensional adsorption model.

II. METHOD

The Langmuir formula is extended as,

$$w = \Sigma_{i \le Ni}\, w_i\,, \qquad (1)$$

$$w_i = K_i\, c\, (w_i^{\max} - w_i), \qquad (2)$$

where w is the total amount of the adsorbed Cs in the adsorbent, N_i the number of adsorption site, w_i the amount of the adsorbed Cs at i-th adsorption site, K_i the equilibrium constant between liquid and adsorbent at the i-th site, $w_i^{\max}$ the saturation value of the Cs adsorption at the i-th site, and c the Cs concentration in the liquid.

Time-variation of Cs reduction in a column experiment was calculated by one-dimensional adsorption model as,

$$dc\,(x, t) / dt' = -\,c\,(1 - \zeta\,(x, t)) / \zeta^{\max}\,\tau, \qquad (3)$$

where x, t, t', $\zeta^{(\max)}$, and τ are the one-dimensional position in the column, wall-clock time, contact time of the water with the adsorbent, (maximum capacity of) Cs-concentration in the adsorbent, and time constant of Cs-concentration reduction, respectively.

The column and shaking experiments were carried out by using granular adsorbent with PB nanoparticle supplied by Kanto Chemical Co. Inc. [2]

III. RESULTS

In Fig. 1 the experimental K_d values are shown as a function of initial Cs concentration in comparison with the results of Langmuir fittings of N_i = 1 and 2. Large discrepancy is found in the case of N_i = 1 (dashed line) especially at high Cs concentration. The fitting is, however, drastically improved if the second adsorption site is included (solid line).

Figure 2 gives the comparison between experimental and calculated time-variation of Cs concentration in column experiment. Our one-dimensional model gives time-variation of the Cs concentration after column adsorption accurately. It is expected that precise simulation of the Cs adsorption in actual plant will be possible by combining extended Langmuir formula and one-dimensional adsorption model.

[1] Kitajima et al., Chem. Lett., 41, 1403 (2012).
[2] Kitajima et al., in APSORC 13 abstract.

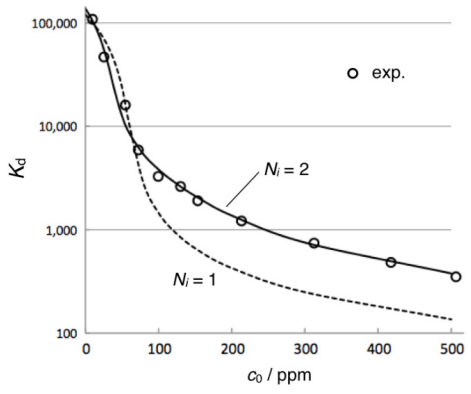

Fig. 1 Experimental and calculated K_d values of the adsorbent used in this study.

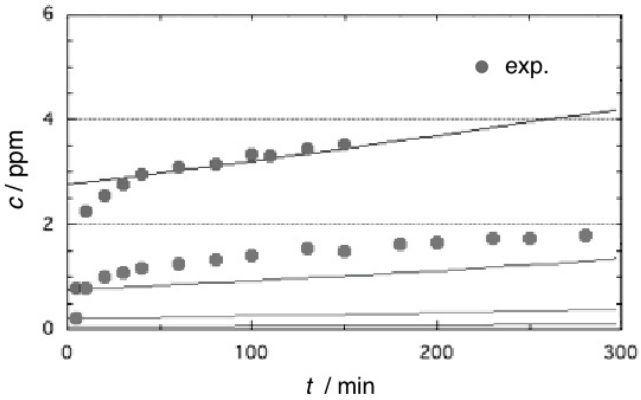

Fig. 2 Experimental and calculated (solid lines) time-variation of Cs concentration in liquid after column adsorption.

Secular distribution of radioactive concentration in the atmosphere at Fukushima, Hitachi and Marumori

ZiJian Zhang[1], Shunsuke Kakitani[1], Kazuhiko Ninomiya[1], Naruto Takahashi[1], Yoshiaki Yamaguchi[2], Takashi Yoshimura[2], Kazuyuki Kita[3], Akira Watanabe[4], Atsushi Shinohara[1]

[1] Graduate School of Science, Osaka University, [2] Radioisotope Research Center, Osaka University,
[3]Faculty of Symbiotic Systems Science, Fukushima University,
[4]College of Science, Ibaraki University

Abstract - Our group started gamma ray measurement of air dust sample after the Fukushima Dai-ichi nuclear power station accident. Air dust filters was collected at Hitachi, Fukushima and Marumori. The activity of Cs-134 and Cs-137 was determined by germanium semiconductor detector. The radiocesium activity concentration in air dust(Bq/m^3) after October 2011 were stable and 6.2×10^{-6} at Hitachi, 3.0×10^{-4} at Fukushima and 1.3×10^{-4} at Marumori.

Key word –radioactive cesium, air dust

I. INTRODUCTION

On 11th March 2011, the earthquake occurred and a large tsunami destroyed coasts of Eastern Japan. As a result, the nuclear accident of Fukushima Dai-ichi nuclear power station (in the following FD-NPS) was arisen. The accident caused massive release of radioactivity into the atmosphere. Many material transportation models were used for simulating the behavior of radioactive nuclides in environment. From these simulations, we can estimate the amount of radioactive deposition to land and sea, and calculate the internal exposure. However, there are some unclear points about nuclides transportation in the environment, and the accuracy of precision simulation was limited by these problems. We need accurate measurement data of radioactive nuclides in the atmosphere. Our group started collection of air dust after the accident of FD-NPS at three locations. In this study, we discuss about the seculer distribution of radioactive concentration in the atmosphere.

II. MEASUREMENT

Our group has been collecting air dust in Fukushima City, in 68 km east of FD-NPS, Hitachi, in 87 km south and Marumori, in 50 km north. Sampling duration was 3-4 days. All gamma ray measurements were carried out at Osaka University in low background condition with 1-2 days. Radioactivities in air (Bq/m^3) of I-131, Cs-134 and Cs-137 were determined. We also measured Be-7 that is one of index of cosmogenic radionuclides, to discuss transportation process of Cs-137.

III. RESULT AND DISCUSSION

The time variation of activity concentration in Hitachi and Fukushima is shown in Fig.1. In Hitachi, activity concentrations for Cs-134 and Cs-137 were very high at April 2011(～Bq/m^3).They were rapidly decrease with time passing, and in October, they were about one-thousandth of the concentration in April. The average of radiocesium activity concentration after October 2011 were 6.2×10^{-6} Bq/m^3 at Hitachi, 3.0×10^{-4} Bq/m^3 at Fukushima and 1.3×10^{-4} Bq/m^3 at Marumori. Ratios of Cs-134/Cs137 were about 1 in three locations. There are many studies that observe the same results in environmental samples.

The activity concentration of beryllium-7 was always about 10^{-3} Bq/m^3. The seasonal variation was likely some previous report [1]. Beryllium-7 is known for attaching to aerosol and being transported to all over the world. We could not find out some correlation between Be-7 and Cs-137. Therefore, main sources of Cs-137 in environment behave differently with cosmic ray radionuclides. We suggest that most of radiocesium in the atmosphere come from some local sources, likely releasing from soil and forest.

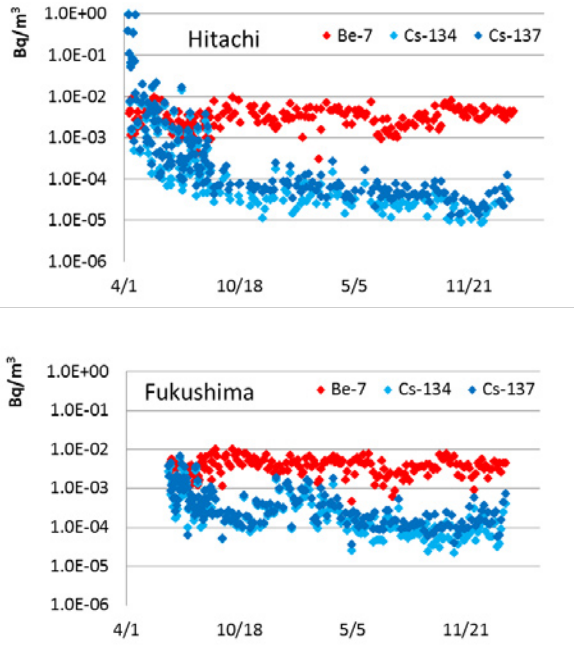

Fig.1. Cs-134, Cs-137 and Be-7 activity concentration. Upper one is data of Hitachi and Under one is data of Fukushima

[1]R.Winkler and F.DIETL, Atmospheric Environment 32, No6, 983-991(1998)

APSORC'13 - 5th Asia-Pacific Symposium on Radiochemistry
Kanazawa, Japan, 22-27 September 2013

Concentration of ^{137}Cs in atmospheric coarse and fine particles collected in Fukushima

Kyo Kitayama[1], Hirofumi Tsukada[1], Kenji Ohse[1], Chika Suzuki[1], Akira Kanno[1], Kencho Kawatsu[1],
[1]Fukushima University Future Center for Regional Revitalization

Abstract – Concentration of ^{137}Cs in atmospheric coarse and fine particles was determined in Fukushima city and Date city collected every 2 weeks from August 2012 to January 2013. Total average concentration of ^{137}Cs in Fukushima and Date were 182 and 173 μBq m^{-3}, respectively and the range was within a factor of 2. The concentration of ^{137}Cs in the coarse fraction was higher than that in the fine fraction except for one sample collected in Fukushima city. The variation of ^{137}Cs concentration in the fine fraction was smaller than that in the coarse fraction and the concentration ratio of ^{137}Cs in the fine fraction to that in the total was approximately 1/3.

Keywords – ^{137}Cs, fine particle, coarse particle, Fukushima city, Date city

I. INTRODUCTION

On 11 March, 2011, the Fukushima Dai-ichi Nuclear Power Plant accident was caused by the tsunami following the earthquake to release radioactive nuclides into the atmosphere. Cesium-137 is a major radionuclide released into the environment and is important to estimate radiation dose for the public. In order to estimate radiation dose from inhalation, the particle size distribution of ^{137}Cs in the atmosphere is required. In this study, concentration of ^{137}Cs in atmospheric coarse and fine particles was determined in Fukushima city and Date city.

II. METHOD

Coarse and fine particles were collected from two sites such as 62 km (Fukushima) and 55 km (Date) distant from Fukushima Dai-ichi Nuclear Power Plant from August 2012 to January 2013. Fukushima is in the urban site and Date is in the rural site. Coarse and fine particles were divided at 50 % cutoff diameter of 1.1 μm with an Andersen sampler (AH-600, Tokyo Dylec), and were collected on polytetrafluoroethylen filters at flow rate of 566 L min^{-1}. The filters were exchanged every two weeks.

The sampled filters were cut into small pieces and compress into a plasitic bottle. Radioactivety of ^{137}Cs in the samples was measured for 0.5-2 days by Ge detector.

III. RESULTS AND DISCUSSION

Total concentration of ^{137}Cs in coarse and fine particles in Fukushima was ranged from 84 to 347 μBq m^{-3} with an average of 182 μBq m^{-3} (Fig. 1-a). The total ^{137}Cs concentration of Date was in the range of 103 to 311 μBq m^{-3} where the average was 173 μBq m^{-3} (Fig. 1-b). The range of

a) Fukushima city

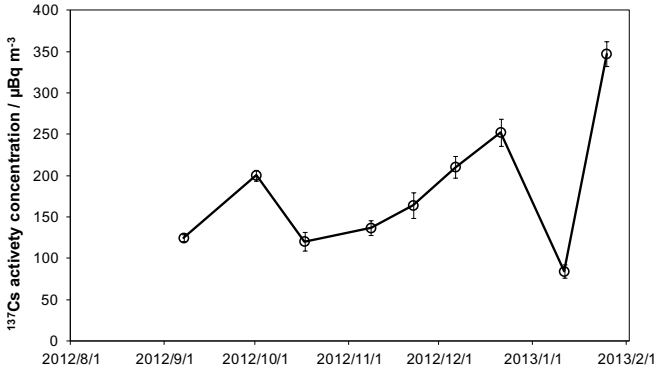

b) Date city

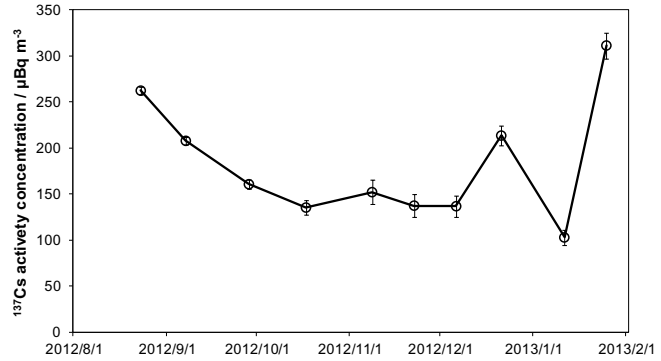

Fig. 1 Concentration of ^{137}Cs in atmospheric coarse and fine particles. Error bars indicate one sigma of deviation.

the concentration of ^{137}Cs in the total particles was within a factor of 2. Tsukada et al. (2012) reported that ^{137}Cs concentration in Fukushima city was 164 mBq m^{-3} in early April 2011 and the value decreased to one thousandth in September 2011. The observed values in the study also maintained a similar order of magnitude to the value in September 2011.

The concentration of ^{137}Cs in the coarse fraction was higher than that in the fine fraction except for one sample collected in Fukushima. The variation of ^{137}Cs concentration in the fine fraction was smaller than that in the coarse fraction and the concentration ratio of ^{137}Cs in the fine fraction to that in the total was approximately 1/3. However, mass concentration ratio in the fine fraction to the total was approximately 1/2. It may attribute that the sources of coarse and fine particles were different.

[1] Tsukada H. et al. (2012) Atomic Energy Society of Japan, Hiroshima.

APSORC'13 - 5th Asia-Pacific Symposium on Radiochemistry
Kanazawa, Japan, 22-27 September 2013

Electrochemical cesium sorption under coexisting other ions using nanoparticle film of copper hexacyanoferrate

Hisashi Tanaka [1)], Rongzhi Chen [1)], Miyuki Asai [1)], Chikako Fukushima [1)], Tohru Kawamoto [1)], Manabu Ishizaki [2)], Masato Kurihara [1,2)], Makoto Arisaka [3)], Takuya Nankawa [3)] and Masayuki Watanabe [3)]

[1)] Nanosystem Research Institute, AIST, Tsukuba central 5, 1-1-1 Higashi, Tsukuba, Ibaraki 305-8565, Japan

[2)] Department of Material and Biological Chemistry, Faculty of Science, Yamagata University, 1-4-12 Kojirakawa-machi, Yamagata 990-8560, Japan

[3)] Japan Atomic Energy Agency, 2-4 Shirane Shirakata, Tokai-mura, Naka-gun, Ibaraki 319-1195, Japan

Abstract – Copper hexacyanoferrate (CuHCF) is known as a good adsorbent for Cs. We developed water-dispersible CuHCF ink by nanoparticulation and surface treatment, and fabricated the thin film of CuHCF on metal electrodes. Cs adsorption/desorption can be controlled electrochemically using this thin film CuHCF electrode, repetitively. Cs sorption capability under coexisting other ions were examined for alkali metals, alkali earth metals, transition metals, etc, and determined to be few affected.

Keywords – Copper hexacyanoferrate, Prusian blue analogues, Nanoparticle ink, Electrochemical adsorption/desorption, Cs adsorption, Nuclear waste water, Fukushima daiichi nuclear disaster

I. INTRODUCTION

The radioactive cesium such as ^{137}Cs ($T_{1/2}$ ~ 30.1 years) is one of heat sources in radioactive wastes. To remove the radioactive nuclide, extensive studies have been done using metal hexacyanoferrates (MHCFs), which have a selective affinity for Cs^+ over a wide pH range and good resistance to radiation. Especially, copper hexacyanoferrate (CuHCF, $Cu_3[Fe(CN)_6]_2$) is stable for electrical use. We fabricated the thin films of CuHCF on metal electrodes by conventional spin coating and succeeded in developing electrochemical Cs^+ recovery system. Here we report the electrochemical Cs^+ adsorption/desorption control and Cs sorption capability under coexisting other ions.

II. EXPERIMENTAL & RESULTS

The nanoparticle CuHCF ink was synthesized according to our previous paper [1]. Uniform film about 100-150 nm thickness was fabricated by spin coating on Au substrate. After insolubilizing process, the CuHCF electrode was able to treat in aqueous electrolyte solution. The Cs^+ concentration in solution was measured with inductivity coupled plasma mass spectrometry (ICP-MS, NexION 300D, Perkin Elmer).

The electrochemical Cs^+ adsorption/desorption was executed by three-electrode system, nanoparticle CuHCF film electrode (20x25 mm^2) as working electrode, saturated calomel electrode (SCE) as reference electrode, and Pt wire as counter electrode. The aqueous electrolyte solution for adsorption contained 10 ppm Cs^+ and 1 ppm Na^+, and for desorption contained 1 ppm Na^+. In the case of coexisting Sr, the adsorption solution contained 10 ppm Cs^+, 10 ppm Sr^{2+} and 1 ppm Na^+. After executing 5 cycle adsorption and desorption, the Cs^+ concentration decreased about 2.5 ppm in adsorption and increased 2.5 ppm in desorption solutions, in the only Cs case and Cs+Sr coexisting case (Fig. 1). In contrast, the Sr concentration kept about 10 ppm in adsorption and 0 ppm in desorption solution. That means the coexisting of Sr ion does not affect the electrochemical Cs sorption capability of CuHCF thin film, and it suggests the possibility of selective recovery of Cs. We also checked it for other alkali metals, alkali earth metals, transition metals, etc.

[1] A. Gotoh, et al., Nanotechnology **2007**, *18*, 345609

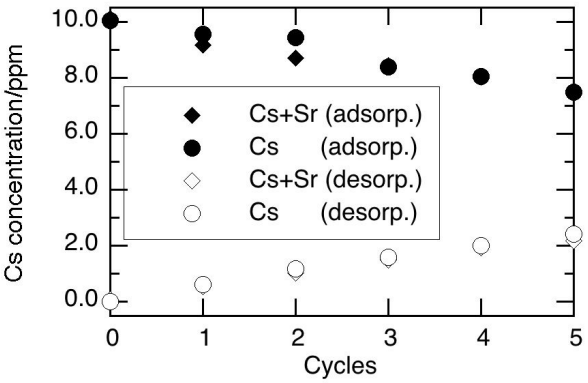

Figure 1. Cs concentration in adsorption solution and desorption solution.

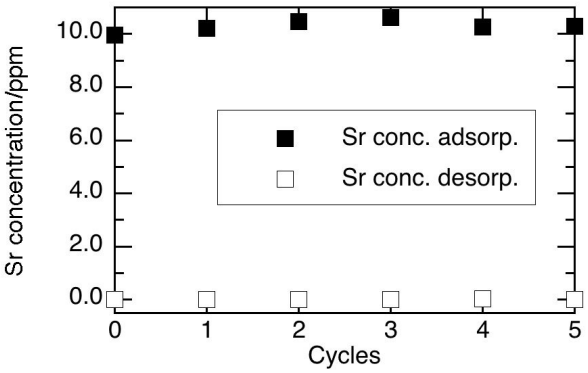

Figure 2. Sr concentration in adsorption solution and desorption solution.

APSORC'13 - 5th Asia-Pacific Symposium on Radiochemistry
Kanazawa, Japan, 22-27 September 2013

Determination of ^{129}I in Fukushima Soil Samples by ICP-MS

Takeshi Ohno[1], Yasuyuki Muramatsu[1], Hiroyuki Matsuzaki[2]
[1]Faculty of Science, Gakushuin University
[2]School of Engineering, The University of Tokyo

Abstract – A method was developed for the determination of ^{129}I in soil samples, which uses a ICP-MS with an octopole reaction system, permitting the investigation of radioiodine released by the Fukushima Daiichi nuclear power plant (FDNPP) accident. The determination of ^{129}I by ICP-MS is capable of providing a high sample throughput compared to other methods.

Keywords – Radioiodine, Fukushima Daiichi nuclear power plant accident, ^{129}I, ICP-MS, Octopole reaction system

I. INTRODUCTION

The accident at the Fukushima Daiichi nuclear power plant (FDNPP) resulted in a substantial release of radionuclides into the environment, including atmospheric of radioiodine and radioceium.[1, 2] The distribution of radio-cesium has been studied, and a map of the radiocesium contamination was made. On the other hand, ^{131}I could only be determined within a couple of months, due to its short half life (8 days), resulting in a lack of data on the deposition of this nuclide. Because iodine is an essential element, and plays an important role in thyroid development, radioiodine that is ingested readily and becomes enriched in the human thyroid. In the event of a nuclear plant accident, an effective dose estimation of released ^{131}I is important.

Another iodine isotope, ^{129}I (half-life: 1.57×10^7 y), was released simultaneously with ^{131}I, although the amount was very small. To reconstruct the early distribution of ^{131}I in the environment, ^{129}I has been used as a follow-up tracer due to its much longer half-life. The determination of ^{129}I in soils in Fukushima is of importance to investigate the distribution of radioiodine released from the FDNPP. Recent advances in inductively coupled plasma mass spectrometry (ICP-MS) using a octopole reaction cell have enabled us to determine the long-lived radionuclide ^{129}I in soil samples.[3]

II. EXPERIMENTAL

The analytical method used in this study is based on the method for AMS measurements.[4] Soil samples (about 2 g) were mixed with V_2O_5 in a ceramic boat before being placed in a quartz tube. The sample was heated at 1000°C in a tube oven for 30 min under a flow of oxygen with water vapor. The iodine released by heating was collected with a trap containing 10 ml of a solution of 1% TMAH. The iodine fraction was then purified by a combination of solvent-extraction and back extraction using carbon tetrachloride as the solvent. The back-extracted solution was concentrated to about 1 mL on a hotplate at 100°C. The purified samples were subjected to measurements of ^{129}I/^{127}I by the ICP-MS. Any mass-discrimination effect in the mass spectrometer was monitored using NIST SRM 3231 Level 1.

III. RESULTS AND DISCUSSION

In order to improve the precision and accuracy of the ^{129}I/^{127}I isotopic ratio measurements, interfering signals, such as $^{129}Xe^+$, must be reduced. In this study, $^{129}Xe^+$ was suppressed by O_2 as a reaction gas using the following reaction: $Xe^+ + O_2 \rightarrow Xe + O_2^+$. The oxygen flow rate was optimized while aspirating an iodine solution (10 ppb, ^{129}I/^{127}I=10^{-13}) so as to maximize the ^{127}I intensity/background (m/z = 129) ratio. When increasing the oxygen flow rate from 0 L/min to the optimum value at 0.8 mL/min, a twenty-fold improvement of ^{129}I background-equivalent concentration was observed.

We investigated the production ratio of $^{127}IH_2^+/^{127}I^+$ while aspirating iodine solution (100 ppm, ^{129}I/^{127}I=10^{-13}). The results demonstrated that the production ratio of $^{127}IH_2^+/^{127}I^+$ in the ICP-MS was about 3×10^{-8}. The contribution from this interference could be corrected by subtracting of $^{127}IH_2^+$ according to the production ratio. The production ratio was monitored before and after measuring the samples, and the contribution of $^{127}IH_2^+$ was subtracted from the signal intensity of ^{129}I when calculating the ^{129}I/^{127}I isotopic ratios.

In order to confirm the applicability to measurements of the ^{129}I/^{127}I ratios of soils we measured ^{129}I in six samples which were collected from an orchard in Ohkuma-machi (about 5 km from the FDNPP), a rice paddy in Iitate-mura and Namie-machi (about 30 km from the FDNPP) and an orchard in Koriyama-shi (about 60 km from the FDNPP). The measured ^{129}I/^{127}I ratios in the samples by ICP-MS are consistent with the value determined by AMS within the analytical error, suggesting the applicability of this method to measurements of ^{129}I/^{127}I in Fukushima soil samples. Our results indicate that ^{129}I can also be determined outside of the 30 km districted area, i.e. 60 km or more from the FDNPP. This method could provide a powerful tool for the investigation of the radioiodine contamination.

[1] M. Chino, H. Nakayama, H. Nagai, H. Terada, G. Katata, and H. Yamazawa, J. Nucl. Sci. and Tech., 2011, 48, 1129.
[2] N. Kinoshita, K. Sueki, K. Sasa, J. Kitagawa, S. Ikarashi, T. Nishimura, Y.-S. Wong, Y. Satou, K. Handa, T. Takahashi, M. Sato, and T. Yamagata, PNAS, 2011, 108, 19526.
[3] T. Ohno, Y. Muramatsu, C. Toyama, K. Nakano, S. Kakuta, and H. Matsuzaki, Anal. Sci., 2013, 29, 271.
[4] Y. Muramatsu, Y. Takada, H. Matsuzaki, and S. Yoshida, Quarter. Geochronol., 2008, 3, 291.

APSORC'13 - 5th Asia-Pacific Symposium on Radiochemistry
Kanazawa, Japan, 22-27 September 2013

Measurement of soil-to-crop transfer factor of tellurium for estimation of potential radiotellurium ingestion from crops

Guosheng Yang, Keiko Tagami*, Jian Zheng, Shigeo Uchida
Office of Biospheric Assessment for Waste Disposal, National Institute of Radiological Sciences

The Fukushima Daiichi Nuclear Power Plant (FDNPP) accident discharged large amounts of radionuclides into the environment, including ^{127m}Te ($T_{1/2}$=109 d), ^{129m}Te ($T_{1/2}$=33.6 d), ^{131m}Te ($T_{1/2}$=30 h) and ^{132}Te ($T_{1/2}$=3.204 d) [1]. Since relatively long-lived ^{127m}Te could transfer from soil to crops through roots, people would ingest ^{127m}Te; however, the isotope is a beta-emitter and the concentration data in food crops were unavailable. Now, ^{127m}Te has been decayed out and it is difficult to measure ^{127m}Te in crops samples. However, it is still important to estimate how much amount of ^{127m}Te might have been ingested from food for public safety purpose. The soil-to-crop transfer factor (TF) is a useful tool to estimate Te concentrations in crops. Unfortunately, the TF data of Te are scarce in the world [2] and there are no data for crops native to Japan.

In order to obtain the TF data of Te for crops, we focused on stable Te as an analogue of radioactive Te. We measured 79 soil and associated crop samples collected nationwide to calculate TFs of Te. Te concentrations in soil and crop samples were measured by using sector field inductively coupled plasma mass spectrometry (SF-ICP-MS) after *aqua regia* digestion and appropriate dilution to reduce the matrix effect [3]. The Te contents in Japanese soil and crops ranged from 12.6 to 479 ng g^{-1} (mean: 55.3 ng g^{-1}) and from 0.06 to 3.8 ng g^{-1} (mean: 0.7 ng g^{-1}), respectively. The Te concentrations in soil were higher than previous report in Japan (10–109 ng g^{-1}), while Te contents in plant samples were much lower than those (18–33 ng g^{-1}) in Japanese plants [4]. Then, TF values from 8.7×10^{-4} to 1.1×10^{-1} (mean: 1.8×10^{-2}) were obtained for the first time in Japan (Figure 1), which were relatively low compared to those reported by IAEA-TRS-472 (0.1–1) [2]. These data could be used to estimate the internal radiation dose from ^{127m}Te after the FDNPP accident.

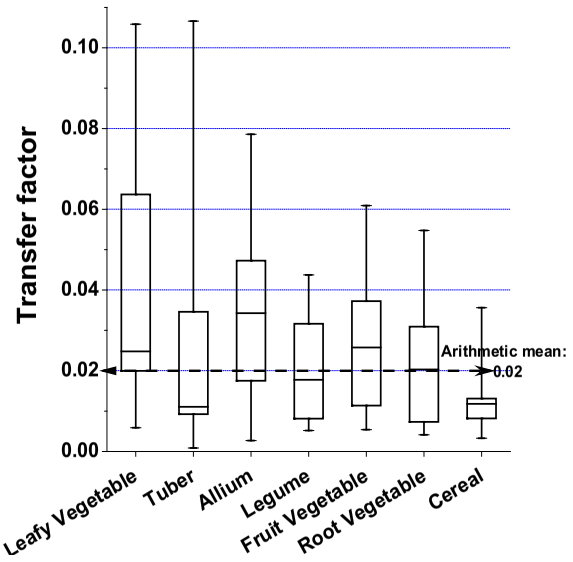

Figure 1. The variations of soil-to-crop transfer factors of Te from different crop groups in Japan. Bars show maximum and minimum values. Boxes show the 75% and 25% values.

Acknowledgement: This work was partially supported by the Agency for Natural Resources and Energy, the Ministry of Economy, Trade and Industry (METI), Japan.

[1] METI (Ministry of Economy, Trade and Industry), Data on the amount of released radioactive materials, http://www.meti.go.jp/press/2011/08/20110826010/20110826010-2.pdf. 2011.
[2] IAEA. *Handbook of Parameter Values for the Prediction of Radionuclide Transfer in Terrestrial and Freshwater Environments*. Technical Reports Series No. 472, IAEA, 2010.
[3] G. Yang, J. Zheng, K. Tagami, S. Uchida, Direct determination of tellurium in Japanese soil and plant samples by sector-field inductively coupled plasma mass spectrometry (submitted).
[4] T. Asami, Metal pollution in Japanese soils (in Japanese), Heiwa Kogyo Co., Ltd., Tokyo, Japan, 2010, p. 447.

* Corresponding author. Tel: +81 43 206 3268; fax: +81 43 206 3267. E-mail address: k_tagami@nirs.go.jp (K. Tagami).

APSORC'13 - 5th Asia-Pacific Symposium on Radiochemistry
Kanazawa, Japan, 22-27 September 2013

Retention of radiocesium incorporated in tree leaves contaminated by fallout of the radionuclides emitted from the Fukushima Daiichi Nuclear Power Plant

Kazuya Tanaka[1], Hokuto Iwatani[2], Aya Sakaguchi[2], Yoshio Takahashi[2], Yuichi Onda[3]
[1] Institute for Sustainable Sciences and Development, Hiroshima University, 1-3-1 Kagamiyama, Higashi-Hiroshima, Hiroshima 739-8530 Japan
[2] Department of Earth and Planetary Systems Science, Graduate School of Science, Hiroshima University, 1-3-1 Kagamiyama, Higashi-Hiroshima, Hiroshima 739-8526 Japan
3 Graduate School of Life and Environmental Sciences, University of Tsukuba, 1-1-1 Tennodai, Tsukuba, Ibaraki, 305-8572, Japan

Abstract – We analyzed fresh and dead leaves collected in forests in Fukushima after the Fukushima Daiichi Nuclear Power Plant (FDNPP) accident using autoradiography. We examined how strongly radiocesium was incorporated in contaminated leaves of Cryptomeria japonica, Quercus serrata and Pinus densiflora. More than half of radiocesium in the contaminated leaves remained in leaf tissues after leaching treatment using pure water, surfactant and acetone.

Keywords – Fukushima, radioactivity, radiocesium, tree leaves, autoradiography

I. INTRODUCTION

A large amount of radionuclides was emitted by the Fukushima Daiichi Nuclear Power Plant (FDNPP) accident. Tree canopies and underlying litters above the soil layers are critical parts when forests are directly contaminated by fallout of radionuclides. Considering cycles of radiocesium in ecosystems, it is very important to know the distribution of radionuclides that were deposited directly on litters or intercepted by tree canopies [1-3]. In this study, we investigated the distribution of radioactivity in various samples of fresh and dead leaves contaminated by the fallout of radionuclides after the FDNPP accident, and examined how strongly radiocesium was incorporated in the leaves [4].

II. SAMPLES AND METHODS

We collected fresh and dead leaf samples (*Cryptomeria japonica*, *Quercus serrate* and *Pinus densiflora*) from Kawamata Town in Yamakiya District, in the northern part of Fukushima Prefecture on December 15, 2011. Leaching experiments were carried out to examine how strongly radiocesium was incorporated in leaf tissues. Leaching experiments consisted of three steps using leachates in the order of pure water, 0.14% of fatty acid potassium salt (surfactant) solution and 100% acetone. Leaf samples were immersed in each leachate and sonicated in an ultrasonic water bath at room temperature for 30 min. Leaf samples before and after each treatment were analyzed using autoradiography. All the samples were treated in the same way to obtain comparable autoradiographs. Reduction of radioactivity by each leaching treatment was evaluated using the differences in signal intensity of autoradiographs before and after leaching treatments.

III. RESULTS AND DISCUSSION

It was clearly observed in autoradiographs that both fresh and dead leaves of *C. japonica* were contaminated by radionuclides (^{134}Cs and ^{137}Cs). Contamination of the fresh leaves was possibly attributed to interception of radionuclides by tree canopies, whereas the dead leaves indicated the direct deposition of radionuclides by fallout and/or washout of radionuclides intercepted by tree canopies. Fallen leaves of *Q. serrata*, which started growing after the FDNPP accident, did not show radioactivity. This means that significant amounts of translocation from other parts to new leaves did not occur. Fallen leaves of *Q. serrata* collected from a litter showed hot spots originating from direct fallout. Needles of *P. densiflora* were also contaminated by fallout. Leaching with pure water removed soluble fractions of radiocesium and radiocesium-bearing particles from the surface of the contaminated leaves, but significant amounts of radioactivity remained. This suggests that foliar absorption occurred in both fresh and dead leaves. The surfactant was used to remove the wax coating from leaf surfaces. This treatment showed that 10 to 20% of radiocesium was removed as a wax fraction of leaf surface. However, the further treatment using acetone did not effectively removed radiocesium. After the three step leaching experiments using pure water, surfactant and acetone, more than half of radiocesium remained in the contaminated leaves. In conclusion, our results indicate that radiocesium in the contaminated leaves is strongly fixed in leaf tissues and is not readily released unless leaf tissues are decomposed.

REFERENCES

[1] Desmet G, Myttenaere C (1988) J Environ Radioact 6:197-202
[2] Bunzl K, Schimmack W, Kreutzer K, Schierl R (1989) Sci Total Environ 78:77-87
[3] Ronneau C, Sombre L, Myttenaere C, Andre P, Vanhouche M, Cara J (1991) J Environ Radioact 14:259-268
[4] Tanaka K, Iwatani H, Sakaguchi A, Takahashi, Y, Onda Y (2013) J Radioanal Nucl Chem 295:2007–2014

Decontamination of Radioactive Cesium in the Soil

Makoto YANAGA, Ayumi OISHI
Department of Chemistry, Graduate School of Science, Shizuoka University

Abstract – Decontamination of radioactive cesium from the agricultural soil was attempted by extraction method using potassium solution. The result of experiments using the soil artificially contaminated with ^{137}Cs showed that radioactive cesium was extracted by potassium solution. However, the extraction rate decreased when time after contamination passed.

Keywords – Decontamination, Radioactive cesium, Nuclear power plant accident, soil

I. INTRODUCTION

A huge amount of radioisotopes was released by the Fukushima Daiichi Nuclear Power Plant accident in March 2011. The radioactive materials released in the atmosphere contaminated not only air but also the earth surface. Decontamination of the radioactive cesium from the soil is one of the current serious problems. In the present work, the decontamination of radioactive cesium from soil, especially agricultural soil, was attempted using the contaminated soil which was made artificially.

II. EXPERIMENTAL

Many commercial plastic containers usually for storing and preserving food were prepared. About 400 grams of commercially obtained mixture of many kinds of soil, used for gardening, was put into each plastic container. Then, 5 ml of ^{137}Cs solution (1 kBq/ml) was dropped in each container. After selected time (from several hours to dozens of weeks) was passed, one container was opened and homogenized in another container.

The homogenized soil was separated to by 60 grams, and each radioactivity was measured. Then, 200 ml of pure water, 1M KNO_3, 1M KI, or 2M KI solution was poured into the beaker which soil was in and the mixture was stirred. After two days standstill, radioactivity of each extract was measured.

III. RESULTS AND DISCUSSION

Relation between the removal rate and time after contamination is shown in Fig. 1. As shown in Fig. 1, it was hardly extracted in pure water. The extraction rate for 1M KI solution and the 1M KNO_3 solution was about the same, and the extraction rate for the 2M KI water solution was higher than them. This indicates that radioactive cesium in the soil was extracted by ion exchange with potassium.

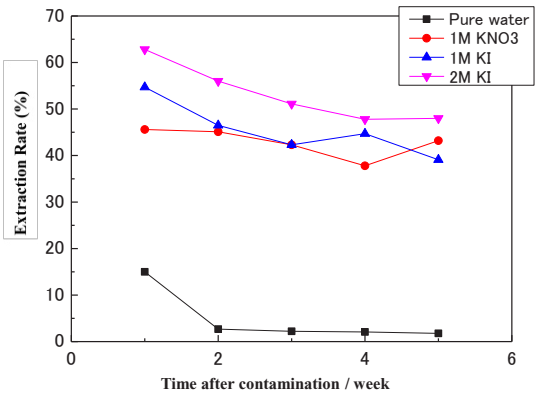

Fig. 1 Time variation of removal rate of ^{137}Cs from the gardening soil.

On the other hand, when time after soil was contaminated by radioactive cesium passed, in the case of any solution used in the present work, the removal rate decreased. It is thought that cesium ion moved to the site that is strongly combined with cesium ion in minerals.

APSORC'13 - 5th Asia-Pacific Symposium on Radiochemistry
Kanazawa, Japan, 22-27 September 2013

Altitude distribution of radioactive cesium at Mt. Fuji due to Fukushima No.1 nuclear power plant accident.

T. Saito[1], Y. Kurihara[2], Y. Koike[2], I. Tanihata[3], M. Fujiwara[3], H. Sakaguchi[3], A. Shinohara[4], H. Yamamoto[5]
[1]Faculty of Comprehensive Human Sciences, Shokei Gakuin University
[2] School of Science and Technology, Meiji University
[3] Research Center for Nuclear Physics, Osaka University
[4]Graduate School of Science, Osaka University
[5]Department for the Administration of Safety and Hygiene, Osaka University

Abstract – Altitude distributions of radioactive cesium (^{134}Cs and ^{137}Cs) fallout at Mt. Fuji due to Fukushima No.1 nuclear power plant accident have been investigated. Radioactive cesium from Fukushima No.1 nuclear plant is found to reach at the height of 2700 m. It is inferred that some amounts of radioactive cesium are attributable to the global fallout due to the nuclear weapons tests in the atmosphere.

Keywords – radioactive cesium, altitude distribution, Mt. Fuji

I. INTRODUCTION

Radioactive materials, released by the Fukushima No.1 nuclear power plant accident have been spread through the atmosphere, and have deposited on the soil surface all over Japan. Over the past two years, a considerable number of studies have been conducted on deposition of radioactive materials on the soils, but very few attempts have been made for measuring the altitude distribution of radioactive materials. In this study, the altitude distribution of radioactive cesium (^{134}Cs and ^{137}Cs) at Mt. Fuji, and floated height of radioactive plume from the power plant have been investigated.

II. EXPERIMENTALS

The soil samples at Mt. Fuji were collected in Sep. 2011 and Sep. 2012, and its details are given in Table. Each sample was packed in the U-8 container, and activities were determined by means of γ-ray spectrometry with a HPGe semiconductor detector. The 605 keV and 662 keV γ-rays from ^{134}Cs and ^{137}Cs, respectively, were used for the determination of radioactivity fallout, and the decay correction of measured activities were made for the date of Mar. 11, 2011.

Table Sampling point information of Mt. Fuji.

Sampling date	Climbing route	Altitude (m)	Remarks
Sep.23. 2011	Fujinomiya	3720 - 2502	scoriaceous lava
Sep.10. 2012	Gotenba	2800 - 1491	scoriaceous lava

III. RESULT AND DISCUSSIONS

The altitude distribution of radioactive cesium inventory (Bq/m^2) and the activity ratios of ^{134}Cs/^{137}Cs are given in Fig.1. Figure 1 shows that the ^{134}Cs and ^{137}Cs inventories are in the range of triple-digit, being higher in the lower altitude.

The significant amount of radioactive cesium at the place lower than the altitude of 2500 m was detected, while radioactivity levels at the altitude higher than 2700 m was extremely low, especially for the ^{134}Cs activity. Therefore, it is suggested that the radioactive plume, which was caused due to Fukushima No.1 nuclear power plant accident, was floated at the upper limit of about 2500 m around of Mt. Fuji.

The activity ratio of ^{134}Cs/^{137}Cs is known as about 1, but in this study, most of the ratio is less than 1. It is inferred from these data that some amounts of radioactive cesium is attributable to the global fallout due to the nuclear weapons tests in the atmosphere.

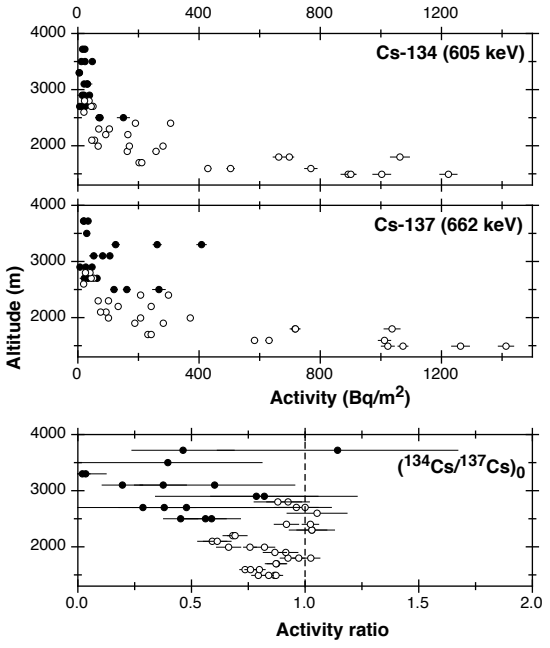

Fig.1: Radioactivities of ^{134}Cs and ^{137}Cs and the activity ratios of ^{134}Cs/^{137}Cs in scoriaceous lava at Mt. Fuji.
(filled cycle: Fujinomiya route, open cycle: Gotenba route)

APSORC'13 - 5th Asia-Pacific Symposium on Radiochemistry
Kanazawa, Japan, 22-27 September 2013

Isotope Compositions of Strontium in Environmental Samples in Fukushima Prefecture

Y. Shibahara[1], S. Fukutani[1], T. Fujii[1], T. Kubota[1], M. Yoshikawa[2], T. Shibata[2], T. Ohta[3], K. Takamiya[1], N. Sato[1], M. Tanigaki[1], Y. Kobayashi[1], R. Okumura[1], H. Yoshinaga[1], H. Yoshino[1], A. Uehara[1], S. Mizuno[4], T. Takahashi[1], and H. Yamana[1]

[1]Research Reactor Institute, Kyoto University
[2]Institute for Geothermal Sciences, Kyoto University
[3]Faculty of Engineering, Hokkaido University
[4]Nuclear Power Safety Division, Fukushima Prefectural Government

Abstract – Strontium was recovered from environmental samples in Fukushima prefecture. The isotopic composition of ^{84}Sr, ^{86}Sr, ^{87}Sr, ^{88}Sr, and ^{90}Sr was evaluated by mass spectrometry and β spectrometry. The source of radioactive strontium released during the Fukushima Daiichi nuclear power plant accident was discussed.

Keywords– strontium-90, strontium isotope ratio, mass spectrometry

On the accident of Fukushima Daiichi nuclear power plant, huge amount of fission product containing radioactive strontium were widely released. The most important radioactive strontium are ^{89}Sr and ^{90}Sr, whose half-lives are 50.5 days and 28.90 years, respectively. The cumulative yields of thermal neutron induced fission of ^{235}U are 4.73% (^{89}Sr) and 5.77% (^{90}Sr) [1]. As shown in Fig. 1, the isotopic composition of Sr via fission of uranium and plutonium [1] are totally different from the natural abundance. The information on the origin of radioactive strontium release would also be obtained from the analytical data.

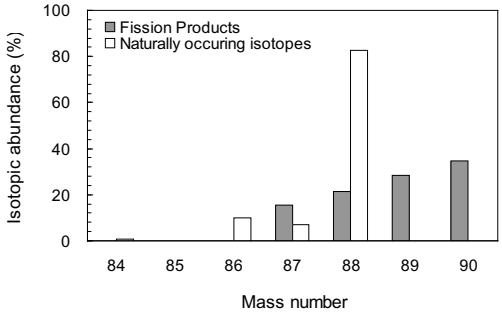

Fig. 1 Isotopic abundances of Sr. The sum of cumulative fission yields of Sr isotopes from ^{235}U by thermal neutron irradiation [1] was set to 100% for comparing them with the natural abundance. The natural abundance of ^{84}Sr is 0.56%. The fission yields of ^{84}Sr and ^{86}Sr are less than 10^{-4}%.

The purpose of the present study is to enhance the analysis of Sr isotopes in environmental samples in Fukushima prefecture for safety assessment about ^{90}Sr dose. Generally, concentration of ^{90}Sr is determined by β spectrometry. Since this method gives no data of stable isotopes, the thermal ionization mass spectrometry (TIMS) was applied for high precision isotopic analysis in parallel. The isotopic composition of ^{84}Sr, ^{86}Sr, ^{87}Sr, ^{88}Sr, and ^{90}Sr was evaluated

Environmental samples (soils, plants, and so on) were immersed in concentrated HNO_3 and heated at 413 K. After evaporation of HNO_3, diluted HNO_3 was added and this was used as the source material. Strontium was recovered from the samples by extraction chromatography with UTEVA-resin and Sr-resin following ion-exchange chromatography with ion-exchange resin. Concentration of recovered strontium was analyzed with a quadrupole inductively coupled plasma mass spectrometer, and that of ^{90}Sr was analyzed by β spectrometry. Correlation between ^{90}Sr and ^{137}Cs was also checked. These samples were supplied for TIMS.

Isotopic ratios of Sr were measured with a TIMS (Triton-T1, Thermo Fisher Scientific). About 100 ng of strontium was loaded on a rhenium single filament with TaO activator. The isotopic reference material SRM987 was used as the standard. Our analytical result of SRM987 agreed with the certified value within 2σ analytical error. As a possible source of ^{89}Sr and ^{90}Sr, on the other hand, 10 mg of UO_2 of natural uranium was irradiated at the Kyoto University Research Reactor. Similar to the environmental samples, strontium was recovered from UO_2 irradiated and analyzed. Since the amounts of ^{89}Sr and ^{90}Sr were much smaller than those of stable Sr isotopes, their mass spectra were obtained with a secondary electron multiplier detector. The isotopic data obtained are discussed by conjunction with the results of β spectrometry.

[1] K. Shibata *et al.*, *J. Nucl. Sci. Technol.*. **48**, 1 (2011).

Distribution of radioactive caesium in the North Pacific one year and a half after the Fukushima Dai-ichi Nuclear Power Plant accident

K. Tsujita[1], A. Hasegawa[1], N. Harada[2], T. Yamagata[2], H. Nagai[2], M. Aoyama[3]
[1]Graduate School of integrated Basic Sciences, Nihon University
[2]College of Humanities and Sciences, Nihon University
[3]Geochemical Research Department, Meteorological Research Institute

Abstract – In stations off Fukushima, ^{137}Cs concentration in surface seawater were 3.9±0.2 and 2.7±0.2 mBq/kg. Between stations off Fukushima and open ocean station (K2; 47°N, 160°E), average ^{137}Cs concentration was 2.9±0.2 mBq/kg. From 160°E to 170°W along 47°N in the North Pacific, average ^{137}Cs concentration was 4.9±0.2 mBq/kg. It was higher than that off Fukushima, and ^{134}Cs was also detected. Thus, the effects of the Fukushima Dai-ichi Nuclear Power Plant accident were observed. But it was not observed in Bering Sea and east of 170°W.

Keywords – Fukushima Dai-ichi Nuclear Power Plant; ^{137}Cs; ^{134}Cs; North Pacific

I. INTRODUCTION

On 11 March 2011, the accident occurred at the Fukushima Dai-ichi Nuclear Power Plant (F1NPP) due to the Tohoku earthquake and tsunami. A large amount of ^{134}Cs ($T_{1/2}$=2.06 y) and ^{137}Cs ($T_{1/2}$=30.07 y) were released to the environment. The estimated total amounts of ^{137}Cs released from the F1NPP reactors to the atmosphere and ocean were 15 [1] and 3.5±0.7 PBq [2], respectively. In this study, we measured the distributions of ^{134}Cs and ^{137}Cs in seawater off Fukushima and in the North Pacific to investigate the spread of the radionuclides about a year and a half after the accident.

II. EXPERIMENTAL

Seawater samples (20 L) were collected with an underway pump and a large-volume water sampler during the KH-12-4 cruise (23 Aug. to 3 Oct. 2012). The sample was acidified to pH1.8 by adding concentrated nitric acid, stirred for 1 hour after adding 200 mg of stable cesium, then stirred again for 1 hour after adding 4 g of ammonium phosphomolybdate (AMP). The sample was settled for 12 hours and filtrated to collect AMP-Cs compound onto a membrane filter (0.45 μm). The AMP-Cs compound was dried for 12 hours at 100 °C, transferred to a counting tube, then measured ^{134}Cs (Eγ=604 keV, 795 keV) and ^{137}Cs (Eγ=661 keV) gamma rays using a well-type HPGe detector.

III. RESULTS AND DISCUSSION

In regions off Fukushima, ^{137}Cs concentration in surface water from BD-02 and 03 located 30 km east of F1NPP were 3.9±0.2 and 2.7±0.2 mBq/kg, respectively. The ^{137}Cs concentrations reduced by two orders of magnitude from those observed in MR-11-03 cruise (Apr. 2011) [3] and KOK cruise (Jun. 2011) [4]. For distant stations about 190 km south (BD-01) and 250 km east (BD-04) of F1NPP were 1.4±0.1 and 1.3±0.1 mBq/kg, respectively. It was almost same as those before the accident (1.5 mBq/kg) [5]. Between off Fukushima and open ocean (47°N, 160°E, BD-05~07), average ^{137}Cs concentration in surface water was 2.9±0.2 mBq/kg, still high compared to that before the accident (1.8 mBq/kg) [6]. From 160°E to 170°W along 47°N (BD-08~14), average ^{137}Cs concentration was 4.9±0.2 mBq/kg. It is higher than those off Fukushima. For all stations of high ^{137}Cs concentration, ^{134}Cs were also detected. In those regions the effects of the F1NPP accident were observed. In Bering Sea and east of 170°W (BD-15~17), ^{137}Cs concentration in surface water were equal to or lower than those before the accident and ^{134}Cs were not detected. In those regions the effects of the F1NPP accident were not observed.

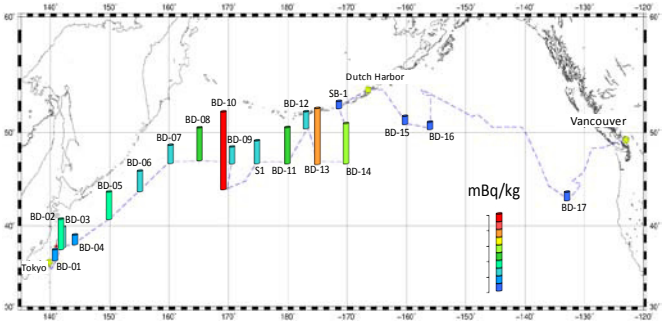

Fig.1 The surface ^{137}Cs concentration in the North Pacific and the KH-12-4 cruise track

REFERENCES

[1] NERH (Nuclear Emergency Response Headquarters, Government of Japan) (2011) Report of Japanese Government to the IAEA Ministerial Conference on Nuclear Safety—The Accident at TEPCO's Fukushima Nuclear Power Stations.
[2] D. Tsumune et al., J. of Environ. Radioact., **111** (2012) 100e108.
[3] M. C. Honda et al., Geochemical J., 46 (2012) e1- e9.
[4] N. Harada, Bachelor thesis (2011).
[5] K. Buesseler et al., Environ. Sci. Technol., 45(2011) 9931-9935.
[6] K. Hirose et al., Deep-Sea Res. II, 50 (2003) 2675-2700.

APSORC'13 - 5th Asia-Pacific Symposium on Radiochemistry
Kanazawa, Japan, 22-27 September 2013

Image analysis for the study of radiocesium distribution in coniferous trees: two years after the Fukushima Daiichi Nuclear Power Plant accident

Haruka Minowa
Radioisotope Research Facility, The Tokyo Jikei University School of Medicine

Abstract – The accident at the Fukushima Daiichi Nuclear Power Plant in March 2011 resulted in the deposition of radioactive fallout over wide area in eastern Japan. Environmental samples were examined with an imaging plate to investigate the characteristics and the behavior of fallout deposits. In the autoradiographs, so-called "hot particles" were evident in many samples. There were no particulate contamination on new leaves which grown after the accident. The state and adsorption amount of fallout was different depending on the locality and the timing of sampling. The results of this study confirm that deposition on the leaves and the barks would remain several years and radiocesium concentration would be decrease with the growing of new leaves.

Keywords – radiocesium, autoradiography, coniferous tree

I. INTRODUCTION

Radioactive fallout from the March 2011 disaster at the Fukushima Daiichi Nuclear Power Plant (NPP) spread across much of eastern Japan. Deposition of fallout on land was affected by rain, wind, and geographical features [1]. The purpose of this research is to investigate the characteristics and behavior of the fallout. Because it was early spring in eastern Japan at the time of the accident, many trees were bare of leaves except for evergreen trees include coniferous trees. Radioactivity on the perennial leaves of coniferous trees would be an appropriate indicator for the monitoring of the radionuclides in the environmental system.

II. SAMPLES AND METHODS

Samples were collected at Naraha-machi, Hirono-machi and Iwaki city in Fukushima prefecture, which are located approximately 20 to 50km in south or southwest side from Fukushima Dai-ichi NPP. It was considered that the dried deposition were more principal than the wet deposition in these area [2]. As a typical coniferous tree, Pine trees (*Pinus thunbergii, Pinus densiflora*), Japanese cypress (*Chamaecyparis obtusa*), Japanese cedar (*Cryptomeria japonica*), and Chinese juniper (*Juniperus chinensis*) were selected.

Samples were flattened and covered with a wrapping film and exposed to an imaging plate BASIII 2040 (Fujifilm Co., Tokyo, Japan) for time periods ranging from overnight to one week. Autoradiographs were scanned using an image analyzer Typhoon FLA7000 (GE Healthcare Japan Co., Tokyo, Japan).

III. RESULTS AND DISCCUSION

Autoradiographs are shown in Figure 1 and 2. Samples were collected from Naraha-machi at Nov. 2012. It was observed that the fallout seemed to be granular, so-called "hot particles". These radioactive particles had not moved from the initial site of adhesion on the leaf despite repeated exposure to rain. Particulate contaminations were distributed only the bottom leaves spread before the accident and did not seen in the top leaves grown after the accident. This confirms that particulate deposition on the leaves and the barks would remained several years and radiocesium concentration would be decrease with the growing of new leaves.

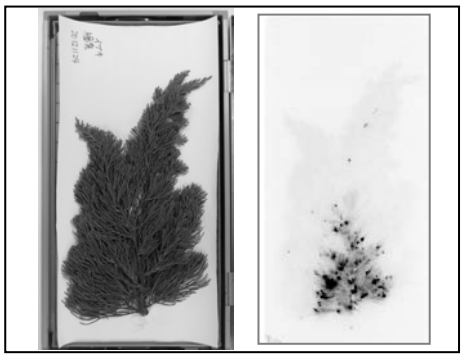

Fig. 1. Leaves of *Juniperus chinensis* from Naraha-machi at Nov. 2012. Particulate contaminations were seem only on the bottom leaves and not seem on the top leaves.

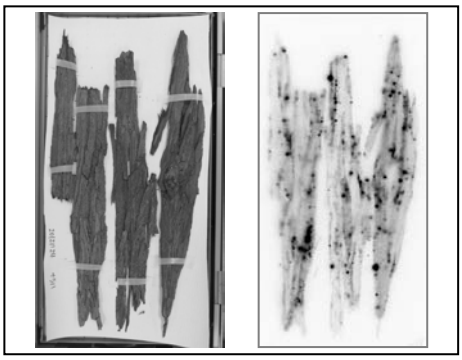

Fig. 2. Tree barks of *Chamaecypars obtusa* from Naraha-machi at Nov 2012. Heterogeneously contaminations were visible throughout on the bark.

[1] Kinoshita et al. (2011) PNAS 108, 19526-19529
[2] Katata et al. (2012) J. Environ. Radioact. 109, 103-113

Distribution of Iodine-129 in off Fukushima and the North Pacific one year and a half after the Fukushima Dai-ichi Nuclear Power Plant accident

A. Hasegawa[1], T. Yamagata[2], H. Nagai[2], M. Aoyama[3], H. Matsuzaki[4]
[1]Graduate School of integrated Basic Sciences, Nihon University
[2]College of Humanities and Sciences, Nihon University
[3]Geochemical Research Department, Meteorological Research Institute
[4]School of Engineering, the University of Tokyo

Abstract – High ^{129}I concentrations were observed in samples from stations off Fukushima (BD02, 03) located 30 km away from Fukushima Dai-ichi Nuclear Power Plant (F1NPP). In these stations, ^{129}I inventory down to 100 m water depth was not decrease since three month after the F1NPP accident. In adjacent stations off Fukushima (BD01, 04), ^{129}I concentrations were almost identical to those observed in seawater collected in the Kuroshio region before the F1NPP accident. In the North Pacific (BD05~17), ^{129}I concentrations in surface seawater were 2 times higher than those in the Kuroshio region.

Keywords – Iodine-129, seawater, Fukushima Daiiti Nuclear Power Plant, North Pacific

I. INTRODUCTION

The Fukushima Dai-ichi Nuclear Power Plant (F1NPP) was damaged by the great earthquake of magnitude 9.0 and the associated tsunami on 11 March 2011. As a result, Many radionuclides such as, ^{134}Cs (2.06 yr), ^{137}Cs (30.2 yr), ^{131}I (8.01 d), ^{129}I (1.57 x 10^7 yr) were discharged from F1NPP into the ocean. These nuclides were transported by the Oyashio current and the Kuroshio current, and supposed to spread along the Kuroshio extension. Many data for ^{137}Cs discharged into ocean from F1NPP in seawater has already reported[1][2] but few data for ^{129}I have reported[3][4].

A large amount of ^{129}I discharged from nuclear activities such as, weapons testing until the 1970's, nuclear power plant accidents, nuclear fuel reprocessing plants, into the environment. As a result, most of ^{129}I present in the environment is anthropogenic, and ^{129}I concentrations in seawater are higher than pre-nuclear activities. Due to the F1NPP accident, ^{129}I concentration in seawater may enhanced. In this study, we measure of ^{129}I concentration in seawater, to investigate the influence of the F1NPP accident in the North Pacific.

II. EXPERIMENTAL PROCEDURE

Seawater samples (1L) were collected with an underway pump and a large-volume water sampler during the cruise of the R/V Hakuho-maru in 23 Aug. to 3 October 2012 (KH-12-4). The cruise track and positions of the station are shown in Fig. 1. First, seawater samples were filtered through a membrane filter (0.45 μm), them iodine carrier (I^- : 1 mg) were added to filtered seawater samples. Secondly, separation of iodine from seawater samples has carried out solvent extraction and back-extraction. The molecular iodine extracted into carbon tetrachloride (CCl_4), then back-extracted into aqueous layer. Finally, silver nitride solution was added to make silver iodide precipitation. The $^{129}I/^{127}I$ ratios of samples were measured by Accelerator Mass Spectrometry (AMS) at MALT, the University of Tokyo. All measured ratios were normalized to the standard reference material having $^{129}I/^{127}I=63.6 \times 10^{-12}$(S-Puredue2).

III. RESULTS AND DISCUSSION

^{129}I concentrations in surface seawater in the Western North Pacific (BD05~09) and Eastern North Pacific (BD11~17) were almost constant (12.7~17.1 x 10^6 atoms/kg). On the other hand, ^{129}I concentrations in stations off Fukushima were higher than those in the North Pacific. Maximum ^{129}I concentration 71.4 x 10^6 atoms/kg was observed at BD03 (about 30 km away from F1NPP). ^{129}I inventory down to 100 m water depth at BD03 was 35.3 x 10^{11} atoms/m^2, which is comparable to those observed three month after the F1NPP accident (KOK cruise). Therefore, the effects of the F1NPP accident still remain in this region. In other stations off Fukushima (BD01 and BD04), ^{129}I concentrations were almost identical to those observed in seawater collected in the Kuroshio region before the F1NPP accident (KT-09-13). In the North Pacific (BD05~17), ^{129}I concentrations were 2 times higher than those in the Kurosio region. It considered with high ^{129}I concentration seawater inflow from the Bering Sea.

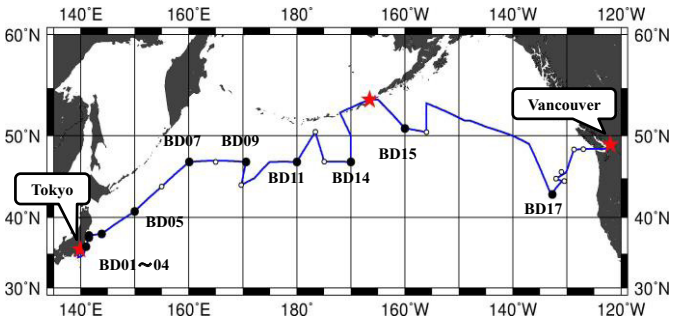

Fig. 1 The KH-12-4 cruise track and sampling stations

[1] http://www.mri-jma.go.jp/Topics/hotyouhi/houtyouhi_sea.html
[2] P. P. Povinec et al., Biogeosciences Discuss, 10, 6377-6416, 2013
[3] T. Suzuki et al., Biogeosciences Discuss, 10, 1401-1419, 2013
[4] X. Hou et al., Environ. Sci. Technol. 47, 3091-3098, 2013

APSORC'13 - 5th Asia-Pacific Symposium on Radiochemistry
Kanazawa, Japan, 22-27 September 2013

Agricultural Implications for Fukushima Nuclear Accident

Tomoko M. Nakanishi

Graduate School of Agricultural and Life Sciences, The University of Tokyo

Abstract – The overview of our research projects for Fukushima is presented including how they were derived. Then, where the fallout was found, right after the accident, is briefly summarized for soil, plants, trees, etc. The time of the accident was late winter, there were hardly any plants growing except for the wheat in the farming field. Most of the fallout was found at the surface of soil, tree barks, etc., which were exposed to the air at the time of the accident. The fallout found was firmly adsorbed to anything and did not move for months from the site when they first touched. Therefore, the newly emerged tissue after the accident showed very low radioactivity. The fallout contamination was not uniform, therefore, when radiograph of contaminated soil or leaves were taken, fallout was shown as spots. Generally, plants could not absorb radiocesium adsorbed to soil. Some of the results we obtained will be presented.

Keywords – *Fukushima nuclear accident, research in agiriculture, research project, research site, fallout, the way of contamination*

Introduction

After the accident of Fukushima Daiichi nuclear power plant, thousands of measuring data have been piling up, especially in the web sites of government agencies. However, most of them are two kinds of the data. One is the radio activities of the places, including soil, air dust or sea water and the other is the measurement of the foods. These are just the monitoring data and it is difficult to find out the research data related to agriculture, such as, how much amount of radioactivity was found or estimated when the plants were grown in the contaminated field or how much radioactivity was accumulated in mountains and what about the contamination of river water coming from the mountain, etc.

Research groups

Right after the accident, about 40 academic staffs in our Graduate School had started the research project for Fukushima in plants, soil, animals, fish, etc. Our activities were classified into several groups as follows but most of them were developed based on voluntary activities. research project for Fukushima for plants, soil, animals, fish, etc. Our activities were classified into several groups as follows but most of them were developed based on voluntary activities.

Research projects

Influence of fallout (distribution & movement)

1. crop plants and soils
2. stock raising & dairy products
3. fishery
4. environment, including wild life
5. radiation measurement & radiochemistry
6. science communication

Research sites

Results & discussion

The Cs movement in soil showed that Cs is so firmly adsorbed on soil and there was no further washout of Cs by rain, therefore, Therefore, it was suggested that this thin contaminated surface soil can thus be collected and buried on site, leaving the land safe to work again, as the radionuclides are unlikely to be leached from the soil. The downward movement of the radiocesium in soil was further monitored. The study of fruit tree showed that Cs was transferred from bark surface to fruits and there was not any radiocesium taken up from roots. Animals are now investigated how radiocesium is distributed among the tissues. We have now expanded our investigations into a long-term study that will also cover trees and fisheries.

Reference

Agricultural Implications for Fukushima Nuclear Accidents. Nakanishi, T.M. and Tanoi, K. ed. Springer (2013)

APSORC'13 - 5th Asia-Pacific Symposium on Radiochemistry
Kanazawa, Japan, 22-27 September 2013

Concentration of Radiocesium in Rice, Vegetables, and Fruits Cultivated in Evacuation Area at Okuma Town, Fukushima

Kenji Ohse[1], Kyo Kitayama[1], Seiich Suenaga[2], Kiyoyuki Matsumoto[2], Akira Kanno[1], Chika Suzuki[1], Kencho Kawatsu[1], Hirofumi Tsukada[1]
[1]Fukushima Future Center for Regional Revitalization, Fukushima University
[2] Okuma Government Office

Abstract – Rice, vegetables, and fruits were cultivated in the evacuation area at Okuma town, and the radiocesium concentration of the crop samples cultivated in contaminated and decontaminated soil was compared. Decrease of the concentration in every crop by decontamination was observed. The TF of brown rice was higher than previous reports.

Keywords – evacuation area, test cultivation, radiocesium

I. INTRODUCTION

Okuma Town which Fukushima Daiichi nuclear power plant locates, the whole region contaminated severely by radioactive nuclides including ^{134}Cs and ^{137}Cs and was designated the evacuation area. The prospect for reactivate of agriculture was not found in the regions. However, in order to obtain the scientific data for recultivation in the future, test cultivations of several crops in the contaminated and decontaminated soils and collected fruits grown in the town were carried out. In this study, the concentration and translate factor of radiocesium in rice, vegetables, and fruits cultivated in the contaminated and decontaminated sites are reported.

II. MATERIALS AND METHODS

Test cultivation site, which had paddy and upland field, was located about 6 km far from Fukushima Daiichi Nuclear Power Plant. Each paddy and upland field was divided into two parts, which was contaminated and decontaminated by removing surface soil. Several crops including rice plant, eggplant, green soybean, sweet potato, pumpkin, and cabbage were cultivated in both sites. After harvest, the crops were washed and separated in several parts. They were dried and pulverized to powder. An ancient black rice plant was also harvested from other paddy field. Soil samples were corrected for the depth of 30 cm, cut into sections 0-2, 2-5, 5-10, 10-15, 15-20, 20-25, 25-30 in depth, oven dried and sieved 2 mm mesh. ^{134}Cs and ^{137}Cs in the samples were determined by germanium semiconductor detector.

III. RESULTS AND DISSCUSSION

The abundance of radiocesium in the soils at contaminated upland, decontaminated upland, contaminated paddy, decontaminated paddy and ancient black rice paddy field was 3680, 877, 1820, 1640, and 1070 kBq m^{-2}, respectively and the weighted average of the concentration for the depth of 15 cm was 31.6, 7.46, 15.4, 13.7, and 14.8 kBq kg^{-1},. The concentration of radiocesium in the decontaminated upland soil decreased 1/4 by removing the soil of 0-15 cm depth. However, the radiocesium concentration in decontaminated paddy soil was slightly decrease compared to the contaminated paddy soil because the paddy field was disturbed by animals and radiocesium mixed in deeper before cultivation.

The radiocesium concentration in crops and their transfer factor (TF) were shown in Table 1. The concentration of radiocesium in every crop cultivated in the decontaminated field was lower than that cultivated in the contaminated field. The concentration of radiocesium in eggplant and pumpkin of edible part cultivated in the decontaminated field was lower than standard limit (100 Bq kg^{-1}). However, the TF values of the crops cultivated in the contaminated fields were within a factor of 3 to those cultivated in the decontaminated fields. More techniques are required to decrease the radiocesium concentration in crops.

Table 1 Concentration and translate factor of radiocesium in crops.

Crop	Sampling date	contaminated field			decontaminated field		
		Cs-134 (Bq kg^{-1} fresh weight)	Cs-137 (Bq kg^{-1} fresh weight)	TF	Cs-134 (Bq kg^{-1} fresh weight)	Cs-137 (Bq kg^{-1} fresh weight)	TF
rice plant							
brown rice	3-Oct-12	117	195	0.0203	82.7	139	0.0162
rice hull	3-Oct-12	264	438	0.0456	197	322	0.0379
reaf and straw	8-Aug-12	89.0	132	0.0144	39.2	57.5	0.0071
reaf and straw	3-Oct-12	185	300	0.0315	113	187	0.0219
ancient black rice							
brown rice	3-Oct-12	258	424	0.0461			
rice hull	3-Oct-12	474	762	0.0835			
reaf and straw	22-Aug-12	178	271	0.0303			
reaf and straw	3-Oct-12	285	464	0.0506			
eggplant							
edible part	8-Aug-12	58.5	90.0	0.0047	7.01	11.0	0.0024
edible part	3-Oct-12	32.4	52.9	0.0027	7.39	11.5	0.0025
stalk	3-Oct-12	69.1	116	0.0059	12.2	20.4	0.0044
reaf	3-Oct-12	161	262	0.0134	46.4	77.1	0.0166
green soybean							
bean	3-Oct-12	161	257	0.0132	69.4	116	0.0249
pod	3-Oct-12	240	395	0.0201	97.0	158	0.0342
stalk	3-Oct-12	302	492	0.0251	91.8	153	0.0329
reaf	3-Oct-12	627	992	0.0512	136	226	0.0486
sweet potato							
edible part	3-Oct-12	151	261	0.0130	84.4	139	0.0300
coat	3-Oct-12	223	356	0.0183	68.6	115	0.0246
vine	3-Oct-12	171	284	0.0144	101	163	0.0354
reaf	3-Oct-12	215	361	0.0182	137	226	0.0487
pumpkin							
edible part	3-Oct-12	113	184	0.0094	13.4	21.7	0.0047
coat	3-Oct-12	145	234	0.0120	16.0	24.5	0.0054
gut	3-Oct-12	191	319	0.0161	14.6	22.6	0.0050
vine and reaf	3-Oct-12	143	234	0.0119	41.7	62.8	0.0140
cabbage							
head	3-Oct-12	250	402	0.0206	148	241	0.0522
un-head reaf	3-Oct-12	375	634	0.0319	321	520	0.1129

APSORC'13 - 5th Asia-Pacific Symposium on Radiochemistry
Kanazawa, Japan, 22-27 September 2013

Isotopic U, Pu, Am and Cm signatures in environmental samples from the Fukusima Dai-ichi Nuclear Power Plant accident

Masayoshi Yamamoto[1], Aya Sakaguchi[2], Shinya Ochiai[1],Takahiro Takada[1], Seiya Nagao[1], Peter Steier[3]
[1] Low Level Radioactivity Laboratory, KINET, Kanazawa University, Nomi, Ishikawa 923-1224, Japan
[2] Graduate School of Science, Hiroshima University, Higashi-Hiroshima, 739-8526, Japan
[3] VERA-Laboratory, Faculty of Physics, University of Vienna, Währinger Str. 17, A-1090 Vienna, Austria

Abstract – Alpha-ray spectrometry and AMS measurements of U, Pu Am and Cm isotopes isolated from black materials of roadsides collected at areas within the 20-km exclusion zones (Minami-Souma, Namie, Futaba and Okuma Towns) and Iitate Village are reported. For most of the samples, low levels of ^{236}U, ^{238}Pu, $^{239,240}Pu$, ^{241}Am, ^{242}Cm and $^{243,244}Cm$ were successfully determined. The results provide a coherent isotopic data set, indicating that traces of U and transuranic nuclides were released into the environment without their large fractionations, probably with forms of fine particles. These data are also very important in order to check the validity of estimation of fuel compositions in the FDNPP.

Keywords – FDNPP accident, ^{236}U, transuranic elements, black materials of roadside, alpha-ray spectrometry, AMS

I. INTRODUCTION

In the Fukushima Dai-ichi Nuclear Power Plant (FDNPP) accident which occurred in connection with the *M9* Great East Japan Earthquake and subsequent tsunami on 11 March 2011, large amounts of radionuclides, especially volatile ones such as ^{131}I, ^{134}Cs and ^{137}Cs, have been accidently released into the environment from the FDNPP. By broadly survey of these nuclides and researches, whole picture about levels and spreading areas of contaminants has been becoming clear, together with the situation of plant accident. However, information on releases of U and transuranic nuclides as refractory elements in fuel core was extremely limited due to the difficulties of analyzing these nuclides. In this paper, we intended to clarify a full picture about these elements released into the environment. For this purpose, ^{236}U, Pu isotopes (^{238}Pu, ^{239}Pu and ^{240}Pu), ^{241}Am and Cm isotopes (^{242}Cm and $^{243,244}Cm$) were measured for roadside dust collected at the Fukushima areas heavily contaminated. Their released levels and isotopic compositions will be discussed, compared with the fuel compositions in FDNPP estimated by Nishihara et al. (2012).

II. MATERIAL AND METHODS

The road dusts, called "Black Materials", whose color is apparently black, are browned in a corner and/or dip of residential streets and roadside by wind and rain. These materials are composed with fine aerosol particles, fine car-cut asphalt materials, residue of lichens, soil and so on, and contaminated with extremely high levels of radionuclides released. They seemed to be suitable for getting information on isotopic composition of trace amount of U and transuranic elements. The samples were mainly collected from areas within the 20-km exclusion zones (Minami-Souma, Namie, Futaba and Okuma Towns) in Sep.- Nov., 2012. Also were samples taken from Iitate Village heavily contaminated. The collected samples were air-dried, and sieved through a 2-mm mesh to remove pebbles and big plant remains, and pulverized in an agate mortar to obtain homogeneous samples. After chemical separation of each element, Pu (^{238}Pu and $^{239,240}Pu$), ^{241}Am and Cm (^{242}Cm and $^{243,244}Cm$) were determined by alpha-ray spectrometry, respectively. Uranium-236 was determined by AMS installed at VERA-Laboratory, University of Vienna (Vienna, Austria).

III. RESULTS AND DISCUSSION

The collected black materials samples were found to be contaminated with extremely high levels of ^{134}Cs and ^{137}Cs over 1000 kBq/kg by the FDNPP accident. More than 100 samples from areas within the 20 km-exclusion zones were determined for ^{238}Pu, $^{239,240}Pu$, ^{241}Am. ^{242}Cm and $^{243,244}Cm$ by α–ray spectrometry. Furthermore, in some samples, ^{236}U was successfully determined by AMS.

The results provided a coherent isotopic data set as follows: 1) traces of $^{239,240}Pu$ (range: 0.0n-1.8 Bq/kg) and high levels of $^{238}Pu/^{239,240}Pu$ activity ratios (range; ca.1-2.7, but mostly around 2.1-2.4) were detected; for samples showing $^{238}Pu/^{239,240}Pu$ ratios of more than 2 (most (or all) of Pu detected is due to the accident); 2) $^{241}Am/^{239,240}Pu$ activity ratios were in the range from 0.32-0.75 with the mean value of 0.53 ± 0.12 (n=35); 3) $^{242}Cm/^{243,244}Cm$ activity ratios (decay-corrected to 11 March, 2011) were 25.1 ± 8.9 (n=61) on average; 4) $^{242}Cm/^{239,240}Pu$ activity ratios (decay-corrected to 11 March, 2011) were 33.6 ± 10.6 (n=52) on average; and 5) $^{236}U/^{239,240}Pu$ activity ratios were in the range of (1.96-18.4) $x10^{-4}$ with the weighted mean value of $7.87x10^{-4}$ (n=12).

When these activity ratios are compared with those of fuel compositions in the FDNPP estimated by Nishihara et al (2012) of the JAEA group, fairly good agreement was found, indicating that traces of U and transuranic nuclides, probably with forms of fine particles, were released into the environment without their large fractionations.

K. Nishihawa et al. (2012), JAEA-Data/Code, 2012-018.

Influence of the Fukushima Daiichi nuclear disaster on the tritium concentration in the precipitation of Kanazawa city

Yoshimune Yamada[1], Kaeko Yasuike[1], Toshiyuki Kawabata[2], Akihiro Fujii[2], Hitoshi Kakimoto[2]
[1]Faculty of Pharmaceutical Sciences, Hokuriku University, Kanagawa-machi, Kanazawa, 920-1181, Japan
[2]Ishikawa Prefectural Institute of Public Health and Environmental Science, Taiyogaoka, Kanazawa, 920-1154, Japan

Abstract – The variation in tritium concentration in the precipitation of Kanazawa city was measured the day after the Fukushima Daiichi nuclear disaster, which occurred on 11 March, 2011. The most interesting result in the period from March to August 2011 is that a secondary peak of 4.6 Bq/L was observed on 22 March after the maximum peak of 15.0 Bq/L on 16 March. This fact suggests that a sudden release of a large amount of tritium from the Fukushima Daiichi nuclear power plant occurred between 21 March and 22 March, followed by the release from 11 March to 15 March. Another interesting result is that dramatic increases in the tritium concentration of 131.6 Bq/L and 99.9 Bq/L were observed on 30 May and 13 June in the variation patterns of the tritium concentration in the precipitation of Kanazawa city. These increases may have been caused by wind blowing down from the upper atmosphere during a storm. A large amount of tritium which had been released by hydrogen explosions from the Fukushima Daiichi nuclear reactors was considered to exist in the bulk air in the upper atmosphere.

Keywords – Tritium, Fukushima Daiichi nuclear disaster, precipitation of Kanazawa city

I. INTRODUCTION

Tritium distribution in nature is mainly the result of continuous production by cosmic rays in the upper atmosphere and prolonged exposure from thermonuclear bomb tests carried out during the 1950's and early 1960's.

The tritium concentration of the precipitation in Ishikawa Prefecture, Japan, showed the highest annually averaged value of 74.1 Bq/L[1] in 1963, which corresponded to the year of the maximum fallout of tritium in the northern hemisphere. After the maximum, it decreased year by year for the past four or five decades, and returned to levels lower than 1 Bq/L in 2007.

Tritium is generated by various nuclear reactions and presents as tritiated water (HTO), tritiated hydrogen gas (HT) and other chemical forms in nuclear reactors. A large amount of tritium was released from the Fukushima Daiichi nuclear power plant caused by the damage of the nuclear reactors in consequence of the Great East Japan Earthquake on 11 March 2011. In this paper, the variations in tritium concentration in the precipitation of Kanazawa city are reported for the period from March to August 2011. This was done to determine the influence of the tritium released into the environment by the Fukushima Daiichi nuclear disaster on the tritium concentration in the precipitation of Kanazawa city.

II. MATERIAL AND METHODS

The precipitation of Kanazawa city (36.52°N, 136.71°E) Ishikawa Prefecture, Japan, was collected during every rainfall in a stainless tray of 560 mm x 405 mm, and then distilled after the addition of $KMnO_4$ and Na_2O_2 to remove any acidic contaminants. The counting source for a liquid scintillation spectrometer was prepared by mixing 40 mL of distilled water with 60 mL of cooled sol-gel emulsifier-type scintillating cocktail, ULTIMA GOLD LLT （PerkinElmer Inc.） in a 100 mL Teflon vial. It was allowed to stand under cool, dark conditions for three days before counting to suppress chemical luminescence. The tritium activity was measured under temperature-stabilized conditions at 12°C using a low background liquid scintillation counter, Aloka LB-5. The counting was carried out for at least four cycles of 1,150 min (50 min x 23) run. The background count rate was 2.22-2.48 cpm at an efficiency of 30.0-30.8 %, which was determined by the external standard channels ratio method.

III. RESULTS AND DISCUSSION

The first rainfall in Kanazawa city after the occurrence of the Fukushima Daiichi nuclear disaster was observed on 15 March 2011 (from 15:50) and it changed to intermittent snow the next day. The tritium concentration in the precipitation of Kanazawa city (36.52°N, 136.71°E) Ishikawa Prefecture, Japan was at levels of 0.35-0.54 Bq/L during the period from February to early March in 2011. It began to increase following the snow of 4:10-9:00 on 16 March, and through to a maximum peak of 15.0 Bq/L after the snow of 9:00-19:00 on 16 March. It decreased to the normal level of 0.5 Bq/L in the rainfall of 9:00-13:30 on 21 March, and thereafter increased again rapidly to 4.6 Bq/L in the sleet from 19:10 on 22 March to 9:00 on 23 March. These facts suggests that a sudden release of a large amount of tritium from the Fukushima Daiichi nuclear power plant occurred between 21 March and 22 March, followed by the accidental or uncontrolled release of tritium from 11 March to 15 March.

A dramatic increase in tritium concentrations of 131.6 Bq/L and 99.9 Bq/L was observed in the rainfalls of 9:30-13:40 on 30 May and those from 21:30 on 13 June to 9:00 on 14 June in the variation patterns of tritium concentration in the precipitation of Kanazawa city, although no marked change was observed in the period from April up to the end of May. This may have been caused by the wind violently blowing down from the upper atmosphere during a storm. A large amount of tritium which had been released by hydrogen explosions from the Fukushima Daiichi nuclear reactors is considered to exist in the bulk air in the upper atmosphere.

[1] Y. Yamada, K. Yasuike, K. Komura, J. Nucl. Radiochem. Sci., 6, 17-20 (2005)

Sediment transport processes in reservoir-catchment system inferred from sediment trap observation and fallout radionuclides

Shinya Ochiai[1], Seiya Nagao[1], Masayoshi Yamamoto[1], Taeko Itono[2], Kenji Kashiwaya[3]
[1]Low Level Radioactivity Laboratory, Institute of Nature and Environmental Technology, Kanazawa University, Japan
[2]Graduate School of Natural Science & Technology, Kanazawa University, Japan
[3]Institute of Nature and Environmental Technology, Kanazawa University, Japan

Abstract – Sediment trap observation of ^{210}Pb, ^{137}Cs, and ^{134}Cs in an artificial reservoir located in central Japan indicates that the discharge rate of these radionuclides from the catchment is largely influenced by the precipitation, with high precipitation in typhoon and snow season. The annual discharge rate of ^{134}Cs from the catchment is larger than that of ^{137}Cs, suggesting that FDNPP-derived ^{134}Cs is concentrated at the erodible surface soil and it is a major sediment source for the annual timescale. The $^{137}Cs/^{210}Pb_{ex}$ activity ratio was high during rainy season and typhoon season, corresponding to the change in 10 mm/h excess rainfall. The soil erosion during the heavy rainfall may extend to the high ^{137}Cs accumulated part in the catchment where is not erodible in the normal condition. This result suggests that heavy rainfall affects the source of eroded sediment and the erosion process in the catchment.

Keywords – sediment transport, sediment trap, ^{210}Pb, $^{134,137}Cs$, Fukushima Dai-ichi NPP

I. INTRODUCTION

The sediment transport processes in the catchment are important to understand the landform development and material transport to downstream rivers, lakes and ocean. The fallout radionuclides ^{137}Cs and ^{210}Pb have been widely used to investigate soil erosion and sediment transport processes. ^{210}Pb is continuously supplied on the soil through atmospheric deposition, while the supply of ^{137}Cs is negligible at the present and its distribution has been changed by downward migration and erosion during the past several decades. Additionally, ^{134}Cs was newly accumulated on the surface soil by the Fukushima Dai-ichi Nuclear Power Plant (FDNPP) accident in 2011. The difference in horizontal and vertical distribution of these radionuclides in the catchment may provide the information on the eroded sediment sources and its response to erosional forces (e.g., hydrological and geomorphological conditions).

This study aims to investigate the sediment transport processes in the reservoir-catchment system based on the continuous sediment trap observation and these fallout radionuclides.

II. SAMPLES AND METHOD

Study site is an artificial reservoir Takidani-ike for agricultural irrigation located in Ishikawa Prefecture in central Japan. Sediment trap observations have been performed since 2000 in Takidani-ike. Deposited sediments collected monthly using a sediment trap on the bottom were oven dried at 110°C to obtain their dry weights and sedimentation rates. Samples collected during the period from February 2010 to December 2011 were used for the radioactivity measurements. Soil samples were also obtained in the catchment using a steel tube (30 cm length) to estimate inventory of the radionuclides. The activity concentration of ^{210}Pb (peak energy: 46 keV), ^{214}Pb (352 keV), ^{137}Cs (661.6 keV), and ^{134}Cs (604.7 keV) were determined by gamma-ray spectrometry using low background Ge detectors. The activity of excess $^{210}Pb_{ex}$ was estimated by subtracting the activity of ^{214}Pb from that of ^{210}Pb.

III. RESULTS AND DISCUSSION

Sedimentation fluxes of $^{210}Pb_{ex}$ and ^{137}Cs in Takidani-ike range 3.5–80 and 0.1–2.6 Bq/m^2/day, respectively, and were high during autumn and winter than in spring and summer. ^{134}Cs was first observed just after the FDNPP accident and showed the similar seasonal fluctuation ranging n.d.–0.15 Bq/m^2/day. These fluctuations correspond to the changes in precipitation, with high precipitation in typhoon and snow season, indicating that the discharge of these radionuclides from the catchment is largely influenced by the precipitation.

Based on the average sedimentation flux, the annual $^{210}Pb_{ex}$, ^{137}Cs, and ^{134}Cs discharge rates from the catchment were estimated as 222, 7.1, and 0.62 Bq/m^2/year, respectively. These values correspond to 0.72, 0.25, and 4.2 %/year of the inventory of $^{210}Pb_{ex}$ (31 kBq/m^2), ^{137}Cs (2.8 kBq/m^2), and ^{134}Cs (14.7 Bq/m^2). The annual discharge rate of ^{134}Cs is much larger than that of ^{137}Cs, suggesting that FDNPP-derived ^{134}Cs was accumulated at the erodible surface soil and it is a major sediment source for the annual timescale.

The $^{137}Cs/^{210}Pb_{ex}$ activity ratio of the trap samples temporally changes from 0.02 to 0.045, and was high during rainy season and typhoon season. This fluctuation well corresponds to the change in 10 mm/h excess rainfall (total rainfall exceed 10 mm/h for each sampling interval) reflecting the heavy rainfall events. This fluctuation may result from the soil erosion at the high ^{137}Cs accumulated part in the catchment during the heavy rainfall where is not erodible in the normal condition. This result suggests that heavy rainfall affects the source of eroded sediment and the erosion process in the catchment.

Transfer of Radiocesium to Crops Cultivated in Fukushima

Shinji Sugihara[1], Toshio Hara[2], Akihiro Maekawa[3], Noriyuki Momoshima[1]
[1]Radioisotope Center, Kyushu University, 6-10-1 Hakozaki, Higashi-ku, Fukuoka 812-8581, Japan
[2]Molecular Engineering Institute, Kinki University, 11-6 Kayanomori, Iizuka, Fukuoka 820-8555, Japan
[3]Graduate School of Sciences, Kyushu University, 6-10-1 Hakozaki, Higashi-ku, Fukuoka 812-8581, Japan

Abstract – Several kinds of crops were cultivated by using the contaminated soil in the field of Fukushima Prefecture and the radioactivity of soil and crops was measured. The soil-to-crops transfer factor of a radiocesium was calculated, and a different value was calculated by corps and the part of crops. But the level of the calculated value is almost equal to already reported.

Keywords – Transfer factor, Radiocesium, Crop, Fukushima Dai-ichi Nuclear Power Plant

I. INTRODUCTION

A large amount of radioactive materials were discharged into the atmosphere during the Fukushima Dai-ichi Nuclear Power Plant accident. As a consequence, a wide region of Japan has been contaminated by mainly radiocesium.

As part of the proof examination of the revival model after the Fukushima nuclear disaster, several kinds of crops were cultivated and the effect of decontamination and desalinization of the contaminated farmland were inspected. The soil-to-plant transfer factor (TF) of radiocesium is extremely variable among soils.

Radionuclides can reach the human body through several food chains in the environment. A lot of data in the targeted environment such as TF is necessary to evaluate the influence on the human body.

II. METHOD

The cultivation examination ground was set by two places (A area: Harashita, B area: Kekaya) in Tomioka, Fukushima Prefecture. B area had received the flood damage of the tsunami. After the disaster, the area was left because these areas were specified for the no-go zone though both areas were originally rice fields. The radiation measurement, the ploughing and the sowing were done in May, 2013. Crops were sorghum (*Sorghum bicolor*), corn (*Zea mays*), rapeseed (*Brassica napus*) and Sugar beet (*Beta vulgaris ssp*). Sorghum and corn were harvested in the middle of November, 2013 at A area. Because the cultivation period was different, the flowering of the rapeseed was difficult. Only the sugar beet grew and it harvested in December, 2013 though sorghum and corn were fruitless on B area due to the salt damage. The radioactivity of the soil before and after the ploughing and the harvested crops sample was measured. The soil sample was cut at intervals of 1cm. The samples of Crops were made separately for the leaf, the stalk and the seed. A dry sample was put in the U8 container, and the Cs concentration was measured with the Ge solid state detector. The radioactivity of the sunflower (Helianthus annuus) grown at the field in A area was measured similarly.

III. RESULTS AND DISCUSSION

Figure 1 shows the depth distribution of the Cs in the soil before the ploughing of A area. Cs that deposited to surface on the field by the Fukushima nuclear disaster remained in the surface layer after two years passed, and most was detected within 5cm in depth. The radiation dose rate at A area was 1.14 μSv/h by 1m on the ground. The Cs concentration was about 1/3 of that of A area, and the dose rate was 0.71 μSv/h on B area.

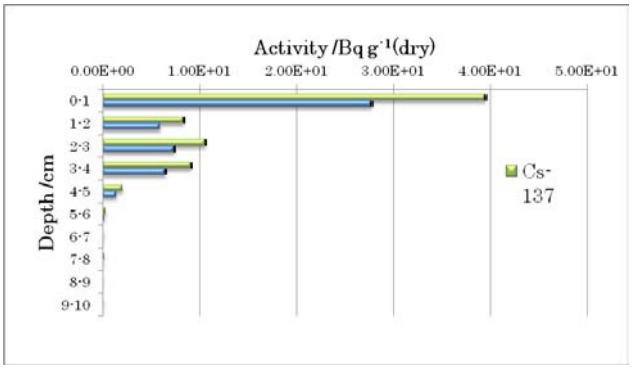

Fig.1 Depth distribution of Cs in A area before the ploughing

Soil-to-crop transfer factor (TF) was calculated as the ratio of the radionuclide concentration in crops (Bq/kg dry weight) to its concentration in soil (Bq/kg dry weight). Both the dry weight and the fresh weight were used as for the numerator, and the dry weight was used here. TF differed according to the part of the crop, and existed in the range of 0.01 to 0.1. Because TF of the seed was small, the seed might be able to use as fodder.

It will be necessary to obtain the basic data for the revival by changing the kind of the soil and crops in addition and accumulating the vast scope of data in the future.

Dynamics of radiocesium in bamboo forests after the accident of Fukushima Daiichi nuclear power plant

Tsutomu KANASASHI, Mitsutoshi UMEMURA, Yuki Sugiura , Chisato TAKENAKA

Graduate School of Bioagricultural Sciences, Nagoya University

Abstract – To understand the dynamics of radiocesium in bamboo forests, we compared the ^{137}Cs concentrations in one-year old bamboo with older ones. The leaves from one-year bamboo contained ^{137}Cs at similar concentration to those of older bamboos. Since bamboo shoot of 2012 also contained ^{137}Cs, cesium should be actively transported in bamboo body.
Keywords – bamboo, radiocesium, leaves, branch, shoot

I. INTRODUCTION

The accident of Fukushima daiichi nuclear power plant on 2011 caused serious problems through the deposition of radionuclide in a large area of Fukushima prefecture. Bamboo forests, which have been familiar to peoples as producing area of various livelihoods like bamboo shoots, were also contaminated with radionuclide, especially ^{137}Cs. The decontamination of ^{137}Cs from bamboo forests has been expected but supposed to be difficult because of the existence of a large amount of subterranean stems. In order to design an effective decontamination procedure of ^{137}Cs and resume the usage of bamboo forests in Fukushima, it is essential to understand the dynamics of ^{137}Cs in bamboo forests. We aimed to clarify the absorption and transport of ^{137}Cs in bamboo by comparing the ^{137}Cs concentration in one-year old bamboo with older one.

II. MATERIAL & METHODS

Bamboo samples were collected from three moso bamboo (*Phyllostachys pubescens*) forests in Fukushima prefecture during spring season of 2012. At one site (site A), since the age of each bamboo could be defined, not only an one-year old bamboo, which sprouted after the accident of FNPP, but also 2,4,5,10,11-years old bamboos were collected. At the other two sites (sites B and C), three one-year old bamboos and three bamboos older than one year were sampled. A bamboo shoot was also collected at site C. Litters and soils were collected from three sites.

Each bamboo was divided into stem, branch and leaves. For the samples from site C, branch and leave samples were prepared from top and middle parts of a stem.

Every plant samples were pulverized after drying. The activity of ^{137}Cs was counted by a Ge- semiconductor detector (Seiko EG & G). Each counting was continued until the count error becomes below 10%.

III. RESULTS & DISCUSSION

Table 1 shows the concentration of ^{137}Cs per area in litter and soil layers at three moso bamboo forest sites. From these data, the radioactivity at site A was almost a third of those at sites B and C. In addition, at the sites A and B, the concentrations of ^{137}Cs in soil layer were higher than those in litter layer, whereas the activity of litter was almost twice of that of soil layer at site C. These observations suggested that the degree of ^{137}Cs infiltration into root system were different among three sites.

The concentrations of ^{137}Cs in leaves and branches collected at site A were shown in Fig.1. The ^{137}Cs concentration in leaves from one-year bamboo, which sprouted on 2011 after the accident, was not so different from the values of leaves in the other samples (2 to 11-years old bamboos), whereas the data in branch of one-year bamboo was quite low comparing with those of the other bamboos. Since the bamboos older than one year adsorbed ^{137}Cs on their surface at the accident of FNPP, the difference of concentrations among branches with various aged bamboo should reflect the direct deposition. On the contrary, the similar concentrations of ^{137}Cs in leaves of one-year bamboo with the others might indicate the uptake of ^{137}Cs through root system. The same results were obtained from the data of site B and C. The bamboo shoot sprouted on 2012 also contained ^{137}Cs at the same level as leaves.

Table 1. Acticity of Cs-137 in litter and soil at three moso forests (kBq/m2)

	A	B	C
Litter	44	161	254
Soils	66	186	132

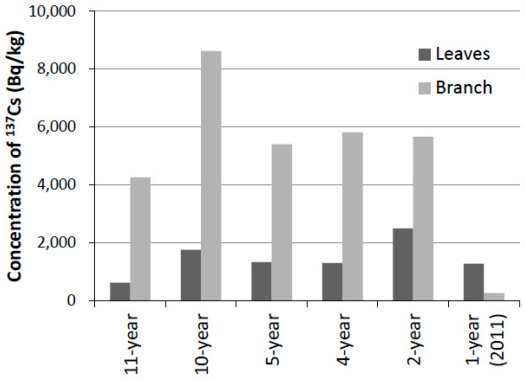

Figure 1. Concentration of ^{137}Cs of leaves and branches in various aged bamboos

Reaction Behavior of Uranium and Zirconium Oxides in Oxidative and Reductive Conditions

Nobuaki Sato, Kohei Fukuda and Akira Kirishima
Institute of Multidisciplinary Research for Advanced Materials, Tohoku University,
2-1-1, Katahira, Aoba-ku, Sendai,980-8577, Japan

To investigate the treatment of fuel debris formed in the damaged reactors at Fukushima Daiichi NPP, study on the reaction behavior of main constituents in the reactor is essential. The main component in the damaged reactor is the mixture of uranium and zirconium since there are the fuel and cladding. As for the reaction between fuel oxide and fission products in oxidative condition, the phase relation of the oxides in the U_3O_8 and Nd_2O_3 system was reported [1]. Then the reaction behavior of the uranium and zirconium oxides at elevated temperatures in oxidative and reductive atmospheres was studied by XRD method. After the heat treatment of the mixture of UO_2 and ZrO_2 with a Zr amount of 50 mol % under vacuum at elevated temperature, the UO_2 solid solution phase such as $Zr_yU_{1-y}O_{2+x}$ seemed to be formed at temperatures lower than 1273 K. However, phases similar to U_3O_8 structure appeared in the temperature range from 1073 K to 1473 K. Over this temperature, a new phase similar to the UO_2 phase seemed to be formed showing the decomposition of U_3O_8 phase at high temperature. When the mixture of zirconium to uranium oxides was treated by mechanochemical method under reducing condition , the X-ray pattern of the products showed that they were the same fluorite structure and the lattice parameter of linearly decreased with increasing zirconium ratio. This suggests that the UO_2 and ZrO_2 form the solid solution from low Zr/U ratio to high one. These results were also discussed with the phase diagram.

Keywords: Fuel debris, Uranium oxides, Zirconium, UO_2 solid solution, Phase relation

[1] N. Sato, G. Shinohara, A. Kirishima and O. Tochiyama, *High Temp. Mat. Proc.,* **29** (2010) 461–468.

Radiocesium in zooplankton in seawaters off Miyagi, Fukushima, and Ibaraki Prefectures

H. Takata[1], M. Kusakabe[2], S. Oikawa[1]
[1]Central Laboratory, Marine Ecology Research Institute
[2]Head Office, Marine Ecology Research Institute

Abstract – Zooplankton samples in seawaters were collected off Miyagi, Fukushima, and Ibaraki prefectures from May 2012 to January 2013. Activity concentrations of ^{134}Cs and ^{137}Cs in zooplankton varied from 0.1to 9.1 Bq/kg-wet weight, and from 0.1 to 12.8 Bq/kg-wet weight, and were higher in May 2012 than in the other sampling months. We also estimated the zooplankton-to-water activity ratio of ^{137}Cs to be 20-754 L/kg.

Keywords – zooplankton, radiocesium, concentration ratio, Fukushima Dai-ichi nuclear power plant

I. INTRODUCTION

The East Japan earthquake and tsunami of March 11, 2011, resulted in unprecedented radioactivity releases from the Fukushima Dai-ichi nuclear power plant (FDNPP) to the Northwest Pacific Ocean. Radionuclides (e.g., ^{134}Cs ($t^{1/2}$ =2 y), and ^{137}Cs ($t^{1/2}$=30 y)) originated from the FDNPP migrated horizontally (e.g., Aoyama et al., [1]); however, the vertical transport mechanisms for radiocesium in the coastal areas off Japan are not fully understood. Zooplankton activity such as excretion and vertical migration can be one of candidates to play an important role in vertical transport of man-made radionuclides (e.g. Fowler et al. [2]).

We report here the results from a radiochemical analysis of zooplankton for raiocesium (^{134}Cs and ^{137}Cs) collected in the waters off Miyagi, Fukushima, and Ibaraki prefectures in 2012 and 2013.

II. MATERIALS AND METHODS

Zooplankton were collected at seven stations during four cruises (May 2012, Aug. 2012, Oct. 2012, and Jan. 2013) at the depths of around 20-80 m with a large ring net (160 cm mouth diameter, 0.5 mm mesh) during daytime by a 30-min horizontal towing. To ensure sufficient amounts of sample for radionuclide analyses, 2–3 hauls per station were combined into one sample. After the collection, samples on the mesh were transferred to plastic buckets. A small amount of samples were preserved immediately in 5% (v/v) formalin–seawater buffered with borax for microscopic observation, and the rest of the sample was stored in a freezer at -20°C.

Zooplankton samples were weighed (wet weight), ovendried (105°C), and weighed again to obtain dry weight. The activity of radiocesium in dried samples was measured with coaxial type Ge detectors for a few hours. The radioactivities of ^{134}Cs and ^{137}Cs in the samples were decay-corrected to the sampling date.

III. RESULTS AND DISCUSSION

Activity concentrations of radiocesium in zooplankton ranged from 0.1 to 9.1 Bq/kg-wet weight, and from 0.1 to 12.8 Bq/kg-wet weight for ^{134}Cs and ^{137}Cs, respectively during May 2012 to January 2013 (Fig. 1). In addition, relatively high activity concentrations of radiocesium were observed near off Ibaraki prefecture during May 2012 cruise, and near off Fukushima prefecture during January 2013 cruise (Fig. 1). The variation in activity concentrations would be due to changes in activity concentrations of radiocesium in their ambient waters. However, there was no significant correlation between radiocesium activity concentration in the ambient water and in the zooplankton.

Another possible reason is probably due to the difference in the composition of zooplankton at each station; however, so far it is unclear as to the relationship between planktonic species and their ^{137}Cs contents.

We also estimated the zooplankton-to-water activity ratio of ^{137}Cs to be 20-754 L/kg; most of them are higher than the one (40 L/kg) published by the IAEA[3].

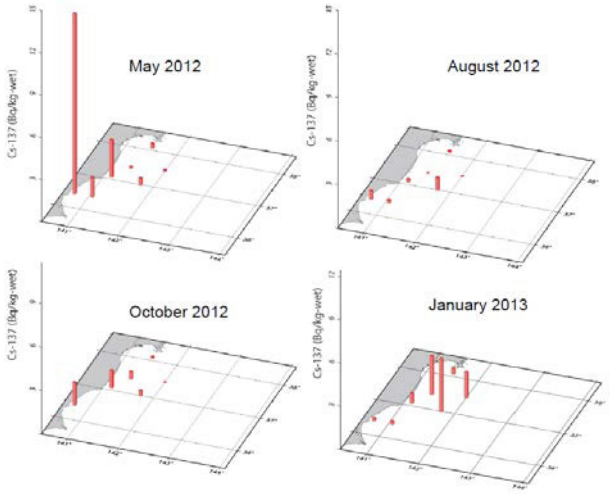

Fig. 1 Activity concentrations of ^{137}Cs in zooplankton at 7stations during each sampling cruise.

REFFERENCES

[1] Aoyama, M., Uematsu, M., Tsumune, D., and Hamajima, Y.: Surface pathway of radioactiveplume of TEPCO Fukushima NPP1 released 134Cs and 137Cs, *Biogeosciences Discuss.,* 10, 265–283, doi:10.5194/bgd-10-265-2013, 2013.

[2] Fowler, S.,W., Buat-Menard, P., Yokoyama, Y., Ballestra, S., Holm, E., and Nguyen, H.,V.: Rapid removal of Chernobyl fallout from Mediterranean surface waters by biological activity, *Nature* 329, 56–58, 1987.

[3] IAEA: Sediment distribution coefficients and concentration factors for biota in the marine environment, Technical Report Series no. 422, IAEA, Vienna, 1–95, 2004.

This work was part of a research project contracted from the Ministry of Education, Culture, Sports, Science and Technology, Tokyo, Japan.

Plutonium isotopes and ^{241}Am in surface sediments off the coast of the Japanese islands after the Fukushima accident

S. Oikawa[1], T. Watabe[2], H. Takata[1], J. Misonoo[2], M. Kusakabe[2]
[1] Central Laboratory, Marine Ecology Research Institute
[2] Head Office, Marine Ecology Research Institute

Abstract – We determined concentrations of Pu isotopes and ^{241}Am in surface (upper 3cm) bottom sediments collected in a sea area along the coast of the Japanese islands after the Fukushima Dai-ichi Nuclear Power Plant (FDNPP) accident. The concentration in the sediments collected immediately after the accident was at almost the same levels as those obtained before the accident.

Keywords – plutonium; ^{241}Am; bottom sediment; Fukushima Dai-ichi Nuclear Power Plant accident

I. INTRODUCTION

As a result of the FDNPP accident on March 11, 2011, a large amount of ^{131}I (half-life: 8 d), ^{134}Cs (2 y), ^{137}Cs (30 y) and other radionuclides were released into the atmosphere. In addition, a remarkable amount of radionuclides was also released directly from the plant as the leakage of coolant seawater poured into the reactor. Comprehensive survey projects were immediately initiated after the accident for clarifying the distribution of radionuclides especially with high volatility such as ^{131}I, ^{134}Cs and ^{137}Cs in the environment. However, a survey of actinides derived from the accident in the marine environment has been yet to be sufficient to evaluate their impact. This paper represents the results of a nationwide survey project to figure out the extent of the accident impact in the levels of Pu isotopes and ^{241}Am in the bottom sediments collected from the 15 sampling areas. And a comparison was made of the pre-accident data to the post-accident ones.

II. MATERIALS AND METHODS

The radioactivity survey project was implemented in nationwide 15 sampling areas (Fig. 1). Bottom sediment samples were collected by a box-type sampler, which retrieves a 1600 cm^2 of sediment from the ocean floor without disturbing their surface. The upper 3 cm of the sediments were taken for analysis. Plutonium and ^{241}Am analysis was performed using 50 g aliquot of dried sample, and alpha spectrometry and beta counting method was used to measure $^{239+240}$Pu (alpha), ^{241}Pu (beta) and ^{241}Am (alpha). We also used SF-ICP-MS to measure ^{240}Pu/^{239}Pu atom ratio.

III. RESULTS AND DISCUSSION

The activity concentrations of $^{239+240}$Pu found in these surface sediment samples collected in May-July 2011, immediately after the accident ranged from 0.42 to 3.7 Bq/kg-dry, which was comparable to those reported by Zheng et al. [1] and Oikawa et al. [2]. The highest $^{239+240}$Pu activity concentration of 3.7 Bq/kg-dry was found in the clayey sediment collected in the Aomori area and the lowest of 0.42 Bq/kg-dry in the sandy sediment in the Ehime area. Although the ^{241}Pu was detected from some samples having relatively high $^{239+240}$Pu concentration (*ca.* >0.7 Bq/kg-dry), the ^{241}Am was detected from all of the sediments. The ^{241}Pu/$^{239+240}$Pu activity ratio found in the sediments varied among the sites even if the sediments collected in the same period of time and ranged from 0.75 to 1.2. The ^{241}Am/$^{239+240}$Pu activity ratio in the sediments were nearly constant (*ca.* 0.6), and the ^{240}Pu/^{239}Pu atom ratios were also nearly constant (*ca.* 0.24) throughout the nationwide sites. The concentrations of Pu isotopes and ^{241}Am, and their ratios found even in the sediments taken in the vicinity of the FDNPP accident have no significant differences between prior to and after the accident. Thus, our nationwide survey results showed that the accident at the FDNPP did not contribute so greatly to the inventory of Pu isotopes and ^{241}Am even in the coastal area off Fukushima Prefecture.

Fig. 1 Locations of sampling areas.

REFERENCES

[1] Zheng, J. et al., Distribution of Pu isotopes in marine sediments in the Pacific 30km off Fukushima after the Fukushima Daiichi nuclear power plant accident. *Geochem. J.* 46, 361-369 (2012).
[2] Oikawa, S. et al., Plutonium isotopes concentration in seawater and bottom sediment off the Pacific coast of Aomori sea area during 1991-2005. *J. Environ. Radioact.* 102, 302-310 (2011).

This work was a part of a research project contracted from the Ministry of Education, Culture, Sports, Science and Technology, Tokyo, Japan.

APSORC'13 - 5th Asia-Pacific Symposium on Radiochemistry
Kanazawa, Japan, 22-27 September 2013

A theoretical study of actinide and lanthanide extraction with carbamoylmethylphosphine oxide ligands

Cong-Zhi Wang, Jian-Hui Lan, Yu-Liang Zhao, Zhi-Fang Chai, Wei-Qun Shi*
Nuclear Energy Nano-Chemistry Group, Key Laboratory of Nuclear Analytical Techniques and Key Laboratory For Biomedical Effects of Nanomaterials and Nanosafety, Institute of High Energy Physics, Chinese Academy of Sciences, Beijing 100049, China
E-mail: shiwq@ihep.ac.cn

Abstract – With the development of nuclear energy, safe disposal of the spent nuclear fuel especially high level liquid waste (HLLW) generated during the PUREX (Plutonium Uranium Extraction) process has become the key factors affecting the sustainable development of nuclear energy. The n-octyl(phenyl)-N,N-diisobutyl-methylcarbamoyl phosphine oxide (CMPO) used in the so-called TRUEX (Transuranium Extraction) process was found to possess excellent extracting ability for actinide and lanthanide cations in acidic media.[1,2] In this work, The UO_2^{2+}, NpO_2^{+}, Pu^{4+}, Am^{3+} and Eu^{3+} extraction complexes with CMPO and diphenyl-N,N-diisobutyl carbamoyl phosphine oxide (Ph_2CMPO) have been investigated by density functional theory (DFT) in conjunction with relativistic small-core pseudopotentials. For most extraction complexes, the CMPO and Ph_2CMPO molecules are coordinated as bidentate chelating ligands through the carbonyl oxygen and phosphoric oxygen atoms. The metal-ligand bonding is mainly ionic for all of these complexes. The neutral $UO_2L_2(NO_3)_2$, $NpO_2L_2(NO_3)$, $PuL_2(NO_3)_4$, $AmL_3(NO_3)_3$ and $EuL_3(NO_3)_3$ complexes are predicted to be the most thermodynamically stable molecules according to the metal-ligand complexation reactions. As reported in the literature,[3-5] the extractability of these actinides decrease in the order of $Pu^{4+} > UO_2^{2+} > Eu^{3+} \approx Am^{3+} > NpO_2^{+}$. In addition, hydration energies may play an important role in the extractability of CMPO and Ph_2CMPO for these actinide ions. In most cases, the complexes with CMPO and Ph_2CMPO ligands have comparable metal-ligand binding energies, i.e., the substitution of a phenyl ring for the n-octyl at the phosphoryl group of CMPO has little influence on the extraction of these actinides and lanthanides.

Keywords – actinide, lanthanide, extractant, relativistic quantum chemistry

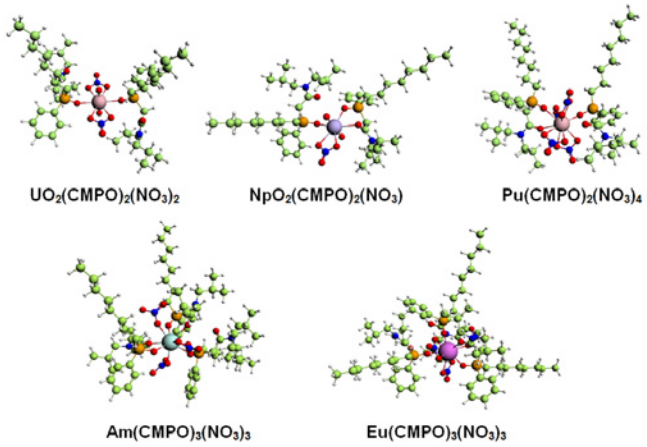

Fig. 1 Extraction complexes of UO_2^{2+}, NpO_2^{+}, Pu^{4+}, Am^{3+} and Eu^{3+} from nitric acid solutions with CMPO

[1] Horwitz, E. P.; Kalina, D. G.; Diamond, H.; Vandegrift, G. F.; Schulz, W. W. *Solvent Extr. Ion Exch.* 1985, 3, 75.
[2] Horwitz, E. P.; Kalina, D. G.; Diamond, H.; Kaplan, L.; Vandegrift, G. F.; Leonard, R. A.; Steindler, M. J.; Schulz, W. W. DE85 010251, 1985.
[3] Visser, A. E.; Jensen, M. P.; Laszak, I.; Nash, K. L.; Choppin G. R.; Rogers, R. D. *Inorg. Chem.* 2003, 42, 2197.
[4] Wisnubroto, D. S.; Nagasaki S.; Enokida Y.; Suzuki A. *J. Nucl. Sci. Technol.* 1992, 29, 263.
[5] Mathur, J. N.; Murali, M. S.; Natarajan P. R. *Taianta* 1992, 39, 493.

APSORC'13 - 5th Asia-Pacific Symposium on Radiochemistry
Kanazawa, Japan, 22-27 September 2013

The role of microorganisms during the wet nuclear fuel storage in Slovak Republic

Martin Pipíška[1], Lenka Tišáková[2], Miroslav Horník[1], Jozef Augustín[1]
[1]Department of Ecochemistry and Radioecology, University of SS Cyril and Methodius, J. Herdu 2, Trnava, SK-917 01, Slovak Republic (pipiska@ucm.sk)
[2]Institute of Molecular Biology, Slovak Academy of Sciences, SK-845 51, Bratislava, Slovak Republic

Abstract

The role of short-term and long-term effects of microbial activity on the wet disposal of spent nuclear fuel in storage facilities is relatively discussed question. Deionized water in storage pools serves as a coolant and, at the same time, as a protection against radiation. However, microorganisms have been shown to survive and grow in high levels of radiation and in highly pure water and they can tolerate both high and low osmolarity and extreme pH and temperature values [1, 2]. This work is focused on a characterization of bacterial contamination in pool water of the Interim spent nuclear fuel storage (ISFS, JAVYS Inc.) in Slovakia. The ISFS consists of 4 interconnecting pools: 3 fuel storage pools and 1 reserve pool built from austenitic steel and permanently filled with deionized water (Fig 1). The mean specific radioactivity of pool water for β emitters was 3.910 ^{5} Bq/L, for γ emitters 3.7 $\times 10^5$ Bq/m^3. Tritium participated by the activity 1.3 $\times 10^5$ Bq/m^3 and contribution of radionuclides increased in the order: ^{60}Co < ^{134}Cs < ^{3}H < ^{137}Cs. From the microbiological point of view, the pool water represents oligotrophic environment which enables the growth of mesophilic bacteria, where chronic radiation exerts selective pressure, altering both the diversity and abundance of bacteria.

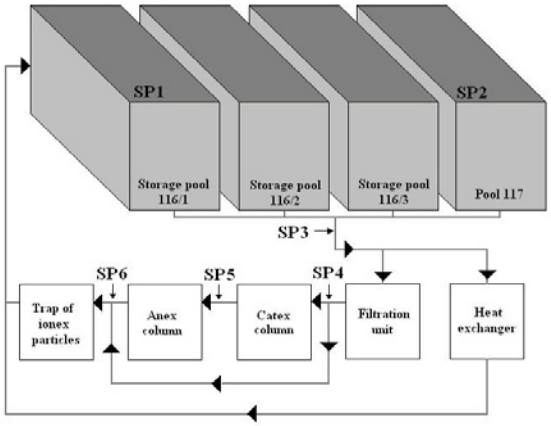

Fig. 1 Circulation system of pool water in spent nuclear fuel storage facility at ISFS. Samples of water were collected from fixed 6 sampling points: SP1 and SP2 – near the water surfaces, SP3 – from the bottom, SP4, SP5 and SP6 – after filtration unit, after catex and anex columns, respectively.

Bacterial content in pool waters is kept on very low level by extremely low concentration of solutes in deionized water and by both the efficient water and air filtration systems. During the monitoring from 2009 to 2012, bacterial densities in the water samples from the surface of pools (SP1, 2) were within the range from 50 to 4 525 CFU/L. Viable counts in the water from the bottom of the pool SP 3 and SP4 to SP6 fluctuated between 100 and 5 500 CFU/L, although noticeable higher values were observed in August and October 2011 and from April to June 2012. Observed higher values up to 250 000 CFU/L can be caused by manipulation procedures such as filling the new fuel assemblies or manipulation in filtration units and by the facility reconstruction. In our primary screening 7 different bacterial isolates from spent nuclear fuel pools were obtained. Only 4 isolates showed stable growth on DEV nutrient agar. Subsequently, these isolates were identified by 16S rDNA as *Kocuria palustris, Micrococcus luteus, Ochrobactrum* spp. and *Pseudomonas aeruginosa.*

In laboratory experiments, the bioaccumulation of ^{137}Cs and ^{60}Co by isolated bacteria were also studied [3]. The maximum specific uptake of Cs^+ after 48 h cultivation in mineral medium (MM) reached 7.54 ± 0.48 µmol/g dw. (*Ochrobactrum* spp.), 19.6 ± 0.1 µmol/g dw. (*M. luteus*) and 20.1 ± 2.2 µmol/g dw. (*K. palustris*). The maximum specific uptake of Co^{2+} after 24 h cultivation in MM reached 31.1 ± 3.5 µmol/g dw. (*Ochrobactrum* spp.), 86.6 ± 12.2 µmol/g dw. (*M. luteus*) and 16.9 ± 1.2 µmol/g dw. (*K. palustris*).

Analyzing of bacterial communities inhabiting an environment exposed to radiation gives opportunities to find bacterial strains with interesting properties such as radioresistance and radionuclide sequestering, able to survive in extremely nutrient deficient environment. We found that bacteria *K. palustris*, *Ochrobactrum* spp. and *M. luteus* isolated from ISFS pool water effectively accumulate both ^{137}Cs and ^{60}Co under growth conditions indicating that these bacteria affect the fate of radionuclides in pool water. Presented results should serve also as the basis for further studies relating to the microbial safety of wet nuclear waste storage in Slovak Republic.

Keywords spent nuclear fuel, storage pools, bacteria, bioaccumulation, ^{60}Co, ^{137}Cs

References

[1] Wolfram JH, Dirk, WJ (1997) Biofilm development and the survival of microorganisms in water systems of nuclear reactors and spent fuel pools. In: Wolfram JH, Rogers RD, Gaszó LG (Eds) Microbial degradation process in radioactive waste repository and in nuclear fuel storage areas. Dordrecht, Kluwer Academic Publishers, pp. 139-147
[2] Diósi G, Telegdi J, Farkas G, Gazso LG, Bokori E (2003) Corrosion influenced by biofilms during wet nuclear waste storage. Int Biodeterior Biodegrad 51: 151-156
[3] Tišáková L, Pipíška M, Godány A, Horník M, Vidová B, Augustín J (2013) Bioaccumulation of ^{137}Cs and ^{60}Co by bacteria isolated from spent nuclear fuel pools. J Radioanal Nucl Chem 295: 737-748

APSORC'13 - 5th Asia-Pacific Symposium on Radiochemistry
Kanazawa, Japan, 22-27 September 2013

Single centrifugal contactor test of a proposed group actinide extraction process for partitioning and transmutation purposes

Emma Aneheim[1,2], Christian Ekberg[1], Giuseppe Modolo[3], Andreas Wilden[3]
[1]Nuclear Chemistry, Department of Chemical- and Biological Engineering, Chalmers University of Technology, SE41296 Gothenburg, Sweden
[2]Targeted Alpha Therapy group, Department of Radiation Physics, Sahlgrenska Academy at Gothenburg University, SE41345 Gothenburg Sweden
[3]Forschungszentrum Jülich GmbH (FZJ), Institut für Energie- und Klimaforschung, Nukleare Entsorgung und Reaktorsicherheit (IEK-6), 52428 Jülich, Germany

Partitioning and Transmutation (P&T) is one of the future strategies for handling of used nuclear fuel. Within P&T, compared to conventional reprocessing, not only uranium and plutonium are to be recycled, but also the rest of the actinides present in the used fuel. By doing this, the idea is to decrease the storage time needed for the residual waste as well as to lower the strain on the final repository. Group Actinide Extraction (GANEX) is a process scheme for P&T where the actinides are extracted as a group directly from the dissolution liquor, after removal of bulk uranium. A solvent intended for GANEX purposes, utilizing two well-known extractants (tri-butyl phosphate and bis-triazine,bi-pyridine) in cyclohexanone has previously been intensely investigated. The extraction system has in batch tests been found to extract the actinides as a group and, with some modifications, separate them from most of the fission products. The solvent was also found to be resistant both towards strong nitric acid and irradiation up to ca 200 kGy. Due to these positive findings, the extraction system has in this work been used in a single centrifugal contactor test on a simulated high active raffinate solution, spiked with radiotracers. The kinetics of the system was found to be relatively slow in the equipment of choice, especially regarding the stripping. However, it was still possible to recover more than 87% of all actinides in one extraction step with a flowrate of 30ml/h.

Keywords – GANEX, TBP, BTBP, Centrifugal contactor

Application of Flow Analytical Methods for Determination of Radionuclides in Cooling Water and Wastes from Nuclear Plants

Anna Bojanowska-Czajka[1], Kamila Kołacińska[1], Marek Trojanowicz[1]
[1]Institut of Nuclear Chemistry and Technology, Dorodna 16, 03-195 Warsaw, Poland

I. INTRODUCTION

Flow analytical systems can be described as measuring devices, in which all operations of sample pretreatment and detection of analyte are carried out in flowing streams. This concept of analytical measurements is widely employed in process analysis, and for laboratory measurements was primarily developed for clinical analysis. In last decades these methods have gained a lot of interest especially for environmental applications [1]. This is proved by vast number of research papers and developed methods, increasing number of commercially available instruments and increasing number of methods, which are recognized by national and international authorities as standard methods.

The methodology of flow-injection analysis (FIA), being developed since 1970-ties, has gained numerous technical modifications such as *e.g.* systems with sequential injection of sample and reagents into a single line system (named as *sequential injection analysis* - SIA), flow measurements with direct injection to the detector sensing surface (named as *batch injection analysis* – BIA), or application in flow-injection systems with a moveable solid particles, also named as *bead-injection analysis*. [2]. Commonly, as major advantages of flow methods of analysis are considered possibility of efficient on-line methods of sample processing prior to the detection step, and improvement of precision and efficiency compared to batch procedures. From the point of view of application of flow analysis in determination of trace level of selected radionuclides especially valuable is possibility of effective on-line preconcentration of trace analytes [3], and carrying out elemental speciation analysis.

Flow methods are mainly developed for non-gamma or low-energy gamma emitters with application for detection of individual radioisotopes mainly α– and β-spectrometry (gas proportional counters, liquid-scintillation counters) [4]. Some developments reported so far include determinations of such radioisotopes as ^{90}Sr, ^{99}Tc, ^{226}Ra or ^{231,240}Pu and ^{241}Am. For design of flow-injection setups different configurations of instrumentation can be employed, including FIA, SIA, and also multi-syringe and multi-pumping devices. Most commonly both in environmental samples or cooling waters from nuclear plants those isotopes are determined in trace or ultra-trace levels, hence, in flow systems especially efficient preconcentration steps are developed. As the most efficient is considered extraction chromatography, but among other methods possible for this purpose are sorption on solid sorbents including recently also nanostructured materials, and precipitation or co-precipitation processes. Those operations can be especially efficient in flow conditions, hence construction of such monitoring systems is very advantageous for monitoring of selected radionuclides in nuclear power reactors.

APSORC'13 HEADING (WITHOUT NUMBER)

[1] M. Trojanowicz (Ed.), *Advances in Flow Analysis*, Wiley-VCH, Weinheim, 2008.
[2] M. Trojanowicz, *Flow Injection Analysis. Instrumentation and Applications*. World Scientific Publishing, Singapore, 2000APSORC'13 Reference
[3] Z. Fang, Flow Injection Separation and Preconcentration, VCH, Weinheim, 1993
[4] Y. Fajardo, J. Avivar, L. Ferrer, E. Gomez, M. Casas, V. Cerda, *Trends Anal. Chem*., 29 (2010) 1399.

Acknowledgments:
Research task No. 8 „Study of processes occurring under regular operation of water circulation systems in nuclear power plants with suggested actions aimed at upgrade of nuclear safety" financed by the National Research and Development Centre in the framework of the strategic research project entitled „Technologies Supporting Development of Safe Nuclear Power Engineering".

APSORC'13 - 5th Asia-Pacific Symposium on Radiochemistry
Kanazawa, Japan, 22-27 September 2013

Determination of low level ^{99}Tc in the primary coolant water by ICP-MS. Analysis of potential interferences.

Ewelina Chajduk[1], Sylwia Witman-Zając[1], Halina Polkowska-Motrenko[1]
[1]Institute of Nuclear Chemistry and Technology, Dorodna 16, 03-195 Warsaw, Poland

Keywords – technetium-99, primary coolant water, inductively coupled plasma mass spectrometry (ICP-MS)

Tc-99 is produced by the fission of U-235 and Pu-239. Information on technetium and other fission and activation product content in the primary coolant and at various locations in the purification system can be of considerable value in assessing fuel integrity and performance of purification system component. Nowadays, mass spectrometry methods are complementary to radiometric techniques for radionuclide determination. Using inductively coupled plasma mass spectrometry (ICP-MS) for long-lived radionuclides improves detection limit and accuracy. However, in accurate measurements by ICP-MS method, the contribution of isobaric interferences from atomic- and molecular ions created by plasma gas and/or solvent used should be defined and appropriate ways of their elimination should be introduced. During the determination of Tc-99, the following interferences can be taken into account: $^{99}Ru^{+}$, $^{64}Zn^{35}Cl^{+}$, $^{98}Mo^{1}H^{+}$, $^{198}Hg^{2+}$, $^{198}Pt^{2+}$, $^{157}Gd^{40}Ar^{2+}$, $^{40}Ar_{2}{}^{18}O^{1}H^{+}$ etc. In this work, possibility of presence isobaric inferences has been investigated. From obtained results, it could be concluded, that some of interference examined can be recognized as insignificant. However, a careful chemical separation of Tc species before the measurements, for the removal of interfering elements, such as Ru traces, as well as for the high recovery of Tc is necessary.

Acknowledgments:

Research task No. 8 „Study of processes occurring under regular operation of water circulation systems in nuclear power plants with suggested actions aimed at upgrade of nuclear safety" financed by the National Research and Development Centre in the framework of the strategic research project entitled „Technologies Supporting Development of Safe Nuclear Power Engineering".

APSORC'13 - 5th Asia-Pacific Symposium on Radiochemistry
Kanazawa, Japan, 22-27 September 2013

Extraction of Homologous Elements of Dubnium and Seaborgium from HCl Solution

T. Yokokita[1], K. Nakamura[1], A. Kino[1], Y. Komori[1], K. Toyomura[1], Y. Kasamatsu[1], N. Takahashi[1], T. Yoshimura[2], K. Ooe[3], Y. Kudou[4], K. Takamiya[5], A. Shinohara[1]
[1]Graduate School of Science, Osaka University
[2]Radioisotope Research Center, Osaka University
[3]Faculty of Science, Niigata University
[4]Nishina Center for Accelerator Based Science, RIKEN
[5]Research Reactor Institute, Kyoto University

Abstract – We aim at studying aqueous chemistry of element 105, dubnium (Db), and element 106, seaborgium (Sg). In this work, we carried out extraction experiments of Nb, Mo, Ta, W, and Pa which are homologous elements of Db and Sg by batch method. These data are significant to investigate the chemical properties of Db and Sg and to determine the experimental conditions of these experiments.

Keywords – Hydrochloric acid, Niobium, Molybdenum, Tantalum, Tungsten, Protactinium

I. INTRODUCTION

It is predicted that the chemical properties of transactinide elements, atomic numbers $Z \geq 104$, show some difference from periodicity in the Periodic Table due to increasingly strong relativistic effect. These elements are produced only by nuclear reactions with very low production rates as one atom at a time, and their half-lives are short, μs to ca. 1 min. Therefore, we must repeat rapid chemistry by such as partition method and alpha-particle measurement. In these studies, the complex formation and chemical species of the transactinides were investigated based on the comparison of their chemical behaviors with those of lighter homologues and pseud homologues. To the chemistry of element 104 (Rf), 105 (Db), and 106 (Sg), we have studied extraction experiments of homologous of Rf, Db, and Sg. Moreover, we have developed rapid extraction apparatuses. In this presentation, we report on solid-liquid and liquid-liquid extraction of Nb, Mo, Ta, W, and Pa as homologous elements of Db and Sg in HCl solution. For Db only one result obtained in HCl solution, so far, and Sg is expected to show different behavior with oxidation states.

II. EXPERIMENTAL

We carried out extraction experiments using carrier-free radiotracers of ^{95}Nb, ^{99}Mo, ^{179}Ta, ^{181}W, and ^{233}Pa. Two kinds of macro amounts of Mo(V) samples were used; one is $[MoCl_5]$ and the other is prepared by electrochemical reduction of $Na_2[MoO_4]$ solution. Macro amounts of W(V) was prepared by reducing $Na_2[WO_4]$ containing ^{181}W tracer by $SnCl_2$. Liquid-liquid extraction was performed by mixing 1–2 mL of the 0.1–11 M HCl solutions containing RI tracers or Mo(V) or W(V) with the same volumes of Aliquat 336 in chloroform or carbon tetrachloride solutions. The mixture was mechanically shaken at 25 °C. After centrifuging the solution, both the phases were pipetted in separate tubes and then subjected to γ- or X-ray spectrometry. The quantity of Mo(V) was determined by thiocyanate method. In solid-liquid extraction, cation-exchange resin (DOWEX^{TM} 50W×8) or MCI GEL CHP20/P30 powder sorbed by Aliquat 336 and 0.5–1 mL of 0.1–11 M HCl solution containing ^{95}Nb, ^{179}Ta, and ^{233}Pa tracers was mixed. The aqueous solution was pipetted into another tube and the sample was subjected to γ- or X-ray spectrometry. In all solid-liquid extraction, control experiments without the resin were performed to determine the radioactivities on the resin indirectly. We also carried out solvent extraction with a flow-type extraction apparatus. Distribution ratio (D) and distribution coefficient (K_d) were determined from radioactivity of RI tracer or concentration of Mo(V).

III. RESULTS AND DISCUSSION

In the results of the cation-exchange of Nb, Ta, and Pa, the K_d value was in the sequence of Ta > Pa > Nb. In the liquid-liquid extraction and solid-liquid extraction of the anionic complexes of Nb, Ta, and Pa using Aliquat 336, the D value and K_d value were in the sequence of Pa > Nb > Ta. From HCl concentration dependences of the K_d and D values, Nb forms neutral and anionic complexes in 0.1–4 M and 5–11 M HCl, respectively. The Ta forms cationic and neutral complexes in 0.1–5 M and 6–11 M HCl, respectively. The Pa forms cationic, neutral, and anionic complexes in 0.1–1 M, 1–3 M, and 4–11 M HCl, respectively. Based on the comparison with these elements, we are planning to investigate the chloride complex formation of Db. In the liquid-liquid extraction of group-6 elements using Aliquat 336, the D values of Mo(VI) were higher than those of W(VI). The D values of Mo(V) were higher than those of Mo(VI). The D values of Mo(V) obtained by the reduction of Mo(VI) were in good agreement with those obtained with $[MoCl_5]$. These results suggest that reduction behavior of Sg can be observed by solvent extraction in Aliquat 336/HCl system. In contrast, the D values of W(VI) and W(V) were similar to each other. This suggests that the behavior of W(V) is similar of that of W(VI). The alternative interpretation is that W(VI) could not be reduced or W(V) was rapidly oxidized to recover W(VI) species.

Evaluation of Stopping Powers of Superheavy Ions in Al and U

Y. H. Chung
Department of Chemistry, Hallym University, 1 Hallymdaehak-gil, Chuncheon 200-702, Korea
yhchung@hallym.ac.kr

Electronic and nuclear stopping powers of superheavy ions with Z>120 in Al and U were estimated in the energy range of 0.01-0.20 MeV/u. In the previous study [1], the corresponding stopping powers of a superheavy ion with Z=120 and A=300 in several media were estimated using stopping powers of ions with 6≤Z≤92 obtained from SRIM [2]. Results were compared with those deduced from Northcliffe and Schilling's stopping-power tables [3]. In the lower energy regime the contribution of nuclear stopping powers is substantially significant in both media while it is not negligible even in the higher energy regime.

[1] Y. H. Chung, Int. J. Mod. Phys. E **19**, 1117 (2010).
[2] http://www.srim.org.
[3] L. C. Northcliffe and R. F. Schilling, Nuclear Data Tables A **7**, 233 (1970).

Separation of tungsten from LEU fission-produced ^{99}Mo solution to improve technological performance in both the processes of ^{99}Mo and ^{99m}Tc generator production

Van So Le[1] , Cong Duc Nguyen[2]
[1]Medisotec, NSW, Australia
[2]ChoRay Hospital , HCM, Vietnam

I. INTRODUCTION

^{99}Mo is a parent nuclide of the ^{99m}Tc radioisotope generator which is used in diagnostic imaging procedures in nuclear medicine world-wide. The ^{99}Mo production is mainly based on the ^{235}U fission using HEU and/or LEU targets and on the ^{98}Mo (n, γ) ^{99}Mo reaction. The conversion of present HEU-based technology to those using LEU requires a 5-6 fold increase in total uranium target weight. Consequently, LEU target possibly contains approximately five times more W contaminant than HEU target, assuming the same purity of the both types of the targets. The large amount of W is seriously challenging the performance of both the processing of ^{99}Mo stock solution and the ^{99m}Tc generator production. So the development of the method of W separation from LEU-produced ^{99}Mo solution should be addressed.

II. METHODS

A ^{99}Mo/^{188}W-spiked simulator of the fission ^{99}Mo solution containing (0.05 mg Mo + 0.06 mg W) per mL and the contaminant ions was used for W/Mo separation method development. The element composition of the simulator solution is mimicked based on an elemental analysis result of a real ^{99}Mo solution sample which is obtained from the chemical processing steps in which a base-dissolution-processed ^{99}Mo solution of LEU (20% ^{235}U) target is passed through anion exchange (AG-1 X8 and AGMP) and Chelex resin columns to remove the majority of fission products.

K_d values of molybdate and tungstate ions adsorption on the acidic alumina in the above mentioned simulator solution of variable acidity were first studied as described in the literature [1]. The separation process was then performed using a chromatographic column of 1.0 g acidic alumina sorbent, on which a given amount of the simulator solution was loaded. The elution of ^{99}Mo-molybdate ions was performed by sulphuric and/or nitric acid solutions with an acidity optimised based on the K_d measurement results. Tungstate ions were then striped out of the column with 5 mL 1.0 M NH_4OH solution. The elution fractions of 5 mL were collected and their ^{99}Mo/^{188}W radioactivity was measured using an Ortec gamma-ray spectrometer coupled with HpGe detector.

III. RESULTS

The K_d values versus acidity of H_2SO_4 solutions and the elution profile of ^{99}Mo/W separation are shown in Fig.1 and Fig. 2, respectively. Based on the obtained results it is stated that the separation of ^{99}Mo from W contaminant can be effectively performed using a small acidic alumina column and H_2SO_4 eluant. This process can be conveniently integrated with the base-dissolution technology process of LEU target-based ^{99}Mo production. This additional alumina column separation step, following the step of AG-1 X8/AGMP anion exchange and Chelex resin column separation, is proposed to eliminate or reduce W contaminant content from ^{99}Mo solution. A typical design of a chromatographic column loaded with 5-10 g acidic alumina and the elution of ^{99}Mo with 50-70 mL 4 M H_2SO_4 solution can be effectively used to remove more than 80% W contaminant content (~ 100 mg W) from a 3665 Ci activity (E.O.B) ^{99}Mo solution (~ 70 mg Mo) produced using 18.4 g ^{235}U LEU target neutron-activated for 120 hours in the OPAL reactor. The ^{99}Mo recovery yield is >96 %.

REFERENCE

[1] Le, VS, Morcos N. (2008) New SPE column packing material: Retention assessment method and its application for the radionuclide chromatographic separation, J Radioanal nucl Chem, 277: 651-661

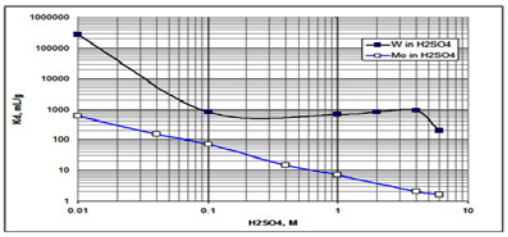

Fig. 1. Weight distribution coefficient of WO_4^{2-} and MoO_4^{2-} ions vs. H_2SO_4 solution acidity for alumina sorbent

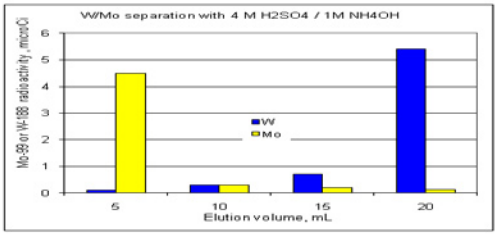

Fig. 2. Elution profile of WO_4^{2-} and MoO_4^{2-} ions (Column: 1 g alumina; Eluent: 4 M H_2SO_4 for MoO_4^{2-} and 1 M NH_4OH for WO_4^{2-}; Loading solution: Simulator solution containing 8 mg Mo + 10 mg W.

APSORC'13 - 5th Asia-Pacific Symposium on Radiochemistry
Kanazawa, Japan, 22-27 September 2013

Effecting Separation of Fission Products from the Actinides By Direct Reaction with Diketones

Daniel B. Rego, Paul M. Forster, Kenneth R. Czerwinski
University of Nevada, Las Vegas

Abstract – The use of diketone ligands, such as hexafluoroacetylacetone (Hhfac) and tetramethylheptandione (Htmhd), can react in solvent -free and solvent-minimal routes to effect separation fission products from uranium matrices without any pre-preparation of the isotopes in question, and provides a path to drastically simplify the separations process and limits the potential for contamination and waste formation due to extensive handling, while increasing the rapidity of separation and isolation of target elements. In particular, the reactivity cesium, barium, strontium, silver, and lead [1] with Hhfac can allow for rapid separations from uranium matrices such as oxide mixtures, in some cases in a matter of minutes.

Keywords – Fission Products, Uranium, Cesium, Strontium, Volatility, Separations.

I. INTRODUCTION

Current radioelement separations necessitate the dissolution of solids in either an acidic aqueous solution or a molten salt. The resulting solutions must be manipulated through a variety of means to achieve the desired separation. These manipulations can involve a complex set of conditions (e.g., the UREX+ suite of separations). Volatile dikeotones, such as hexafluoroacetylacetone (Hhfac) and tetramethylheptandione (Htmhd), have been used to react with, and isolate with crystalline purity, fission products [2,3] and actinides [4,5] such as uranium (figure 1) and neptunium.

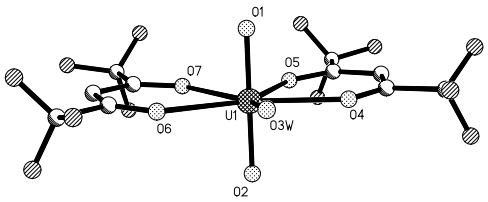

Ball and stick diagram of $UO_2(hfac)_2(H_2O)$.

Initial studies have focused on characterizing the coordination with the diketone ligands. The use of coordinating ethers to help break up matrices in order to maximize volatility has been examined and can increase the volatility and separatability of species from uranium matrices: For example, cesium hexafluroacetylacetonate forms an extended polymeric structure with extensive Cs-O and Cs-F coordination; in contrast, the use of diglyme or 18-crown-6 reduces this extensive cross-coordination significantly.

Direct separation of reactive species from uranium containing oxide mixtures has been demonstrated. The additional ability of exploiting differences in volatility of these diketone complexes themselves serves as a secondary method of separating the isotopes in question with limited handling and processing. [6] The flexibility of this system can allow for customization to fit specific scenarios and situations. Single solvent extraction from solid material, or volatilization of treated solid samples, are utilizable routes. An additional route is that these metal complexes are often used as metal vapor deposition precursors. [7] Thus, a pure metal could be obtained directly from vapor phase volatile complexes formed directly in the reaction mixture from the oxides and vaporous ligands *in situ*, which would allow for the potential combination of separations with metal formation in a single step.

[1] (a) Evans, W. J.; Rego, D. B.; Ziller, J. W. *Polyhedron* **2006**, *25*, 2691-2697. (b) Malandrino, G.; Nigro, R. L.; Rossi, P.; Dapporto, P.; Fragalá, I. L. *Inorg. Chim. Acta* **2004**, *357*, 3927. (c) Rego, D. B. Lanthanide Reduction Chemistry of the LnZ_3/M and LnZ_2Z'/M Systems and Related Coordination Chemistry Dissertation, University of California, Irvine, **2007**.
[2] (a) Evans, W. J.; Giarikos, D. G.; Johnston, M. A.; Greci, M. A.; Ziller, J. W. *J. Chem. Soc., Dalton Trans.* **2002**, 520-526. (b) Fragalà, L.; Maladrino, G.; Benelli, C.; Castelli *Chem. Mater.* **1998**, *10*, 3434. (c) Fragalà, L. Maladrino, G.; Incontro, O.; Castelli, F. *Chem. Mater*, **1996**, *8*, 1292.
[3] (a) Krisyuk, V.V.; Sysoev, S. V.; Fedotova, N. E.; Igumenov, I. K.; Grigorieva, N. V. *Thermochim. Acta* **1997**, *307*, 107-115. (b) Drake, S. R.; Hursthouse, M. B.; Abdul Malik, K. M.; Miller, S. A. S. *Inorg. Chem.* **1993**, *32*, 4653-4657. (c) Darr, J. A.; Poliakoff, M.; Blake, A. J.; Li, W.-S. *Inorg. Chem.* **1998**, *37*, 5491-5496. (d) Strasser, A.; Vogler, A. *Inorg. Chem. Comm.* **2004**, *7*, 528-530. (e) Azad Malik, M.; O'Biren, P.; Motevalli, M.; Jomes, A. C.; Leedham, T. *Polyhedron* **1999**, *18*, 1641-1646. (f) Fenton, D. E.; Newman, R. *J. Chem. Soc., Dalton Trans.* **1974**, 655-657. (g) Cotton, F. A.; Holm, R. H. *J. Am. Chem. Soc.* **1960**, *82*, 2979-2983.
[4] (a) Nikitenko, S. I.; Moisy, Ph.; Tcharushnikova, I. A.; Blanc, P.; Madic, C. *Ultrasonics Sonochemistry*, **2000**, *7*, 177-182. (b) Danford, M. D.; Burns, J. H.; Higgins, C. E.; Stokely, J. R., Jr.; Baldwin, W. H. *Inorg. Chem.* **1970**, *9*, 1953-1955. (c) Morris, M. L.; Moshier, R. W.; Sievers, R. E. *Inorg. Chem.* **1962**, *1*, 411-412.
[5] (a) Giarikos, D.G. Dissertation. University of California, Irvine, **2003**. (b) Yamamura, T.; Shiokawa, Y.; Yamana, H.; Moriyama, H. *Electochim. Acta* **2002**, *48*, 43-50. (c) Kramer, G. M.; Dines, M. B.; Kaldor, A.; Hall, R.; McClure, D. *Inorg. Chem.* **1981**, *20*, 1421-1426. (d) Kramer, G. M.; Dines, M. B.; Hall, R. B.; Kaldor, A.; Jacobson, A. J.; Scanlon, J. C. *Inorg. Chem.* **1980**, *19*, 1340-1347.
[6] Sedai, B.; Heeg, M. J.; Winter, C. H. *Organometallics*, **2009**, *28*, 1032-1038.
[7] Lin, W., Warren, T.H., Nuzzo, R.G., and Girolami, G.S.: J. Am. Chem. Soc., **115 (24),** 11644–11645 (1993).

APSORC'13 - 5th Asia-Pacific Symposium on Radiochemistry
Kanazawa, Japan, 22-27 September 2013

Muonic Atom Formation by Muon Transfer Process in C_6H_6 / C_6H_{12} + CCl_4 Mixtures

M. Inagaki[1], K. Fujihara[1], G. Yoshida[1], K. Ninomiya[1], Y. Kasamatsu[1], A. Shinohara[1], M. K. Kubo[2], W. Higemoto[3], Y. Miyake[4], T. Miura[5]
[1]Graduate School of Science, Osaka University
[2]Colleage of Liberal Arts, International Christian University
[3]Advanced Science Research Center, Japan Atomic Energy Agency
[4]Institute of Materials Structure Science, High Energy Accelerator Research Organization (KEK)
[5]Radiation Science Center, High Energy Accelerator Research Organization (KEK)

Abstract – Negative muon transfer process in the mixtures of C_6H_6 / C_6H_{12} + CCl_4 was studied. The muonic Cl X-ray structure of C_6H_6 + CCl_4 mixture sample was similar to that of pure CCl_4 sample. However, the muonic Cl X-ray structure of C_6H_{12} + CCl_4 mixture sample was different from that of pure CCl_4 sample. This result can be explained by assuming that the number of muons transferred to chlorine atoms in C_6H_6 + CCl_4 mixture sample is smaller than that in C_6H_{12} + CCl_4 mixture sample. This fact suggests that the muon transfer rate for carbon atoms of C_6H_6 is higher than that for carbon atoms of C_6H_{12}.

Keywords – Muonic Atom, Exotic Atom, Muon Transfer, Muonic X-ray

I. INTRODUCTION

A muonic hydrogen is one of the simplest exotic atom that consists of a muon and a proton. The charge of a proton is strongly shielded by a muon in the muonic hydrogen because the mass of a muon is 206 times larger than that of an electron. The muonic hydrogen can diffuse in the substance like a neutron and transfer the muon to the other heavier atoms. This process is known as muon transfer process. The transfer process occurs also in the case of a pionic hydrogen, which consists of a pion and a proton.

It is reported that the structure of molecule affects the formation or transfer process of the exotic atom. This effect is called as chemical effect. In the previous study on pion transfer process, we investigated the chemical effect in mixtures of C_6H_6 / C_6H_{12} + CCl_4. The pion transfer rate for carbon atoms of C_6H_6 is twice higher than that for C_6H_{12} [1]. In this study, we examined the chemical effect on the muon transfer in the same sample system.

II. EXPERIMENTAL

The muon irradiation experiments were performed at the MUSE D2 beam line of Materials and Life Science Experimental Facility in Japan Proton Accelerator Research Complex (J-PARC). We selected the following samples for measurement; C_6H_6 + CCl_4 (33%) mixture, C_6H_6 + CCl_4 (3%) mixture, C_6H_{12} + CCl_4 (33%) mixture, C_6H_{12} + CCl_4 (3%) mixture, pure C_6H_6, pure C_6H_{12}, and pure CCl_4. Muonic X-rays, which are emitted after formation of muonic atoms, were measured by Ge detectors.

III. RESULTS AND DISCUSSION

The experimental muonic Cl X-ray structure (muonic X-ray intensity ratios) in pure CCl_4, C_6H_{12} + CCl_4 (33%) mixture and C_6H_6 + CCl_4 (33%) mixture samples are shown in Fig. 1.

The relative intensity of Cl (5–3) / Cl (4–3) and Cl (4–2) / Cl (3–2) in C_6H_{12} + CCl_4 mixture sample was smaller than that in pure CCl_4 sample. The difference indicates that initial state (principal and angular momentum quantum number) of the muon captured by chlorine atoms in C_6H_{12} + CCl_4 mixture sample is different from that in pure CCl_4 sample. Because the muon transfer occurs in C_6H_{12} + CCl_4 mixture sample while no muon transfer in pure CCl_4 sample, it seems that the muon transfer process changes the initial state of the muon captured by chlorine atoms in C_6H_{12} + CCl_4 sample. On the other hand, although the muon transfer also occurs in C_6H_6 + CCl_4 sample, the muonic X-ray structure of that was similar to pure CCl_4 sample. This can be explained by assuming that the number of muons transferred to chlorine atoms in C_6H_6 + CCl_4 sample is smaller than that in C_6H_{12} + CCl_4 sample. This fact suggests that the muon transfer rate for carbon atoms of C_6H_6 is higher than that for carbon atoms of C_6H_{12}. Despite using different particle, this result is consistent with the previous study for pion transfer in the same sample system [1].

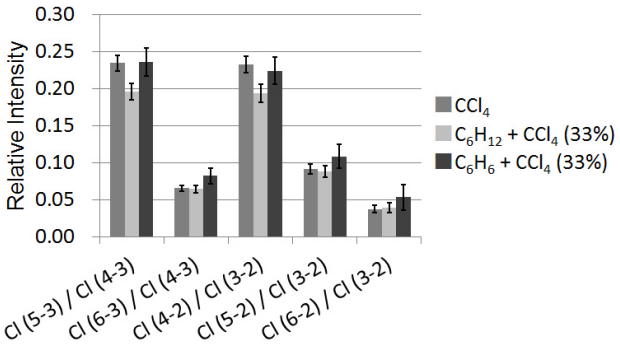

Fig. 1. Muonic chlorine X-ray structure. Cl (n–n′) means muonic Cl X-ray emitted with muon deexcitation from principal quantum number n to n′.

[1] A. Shinohara *et al.*, Hyperfine Interact. **106**, 301 (1997).

Research for Fusion Reaction Mechanisms with Deformed Nuclei

S. Ueno[1], K. Toda[1], A. Asano[1], N. Takahashi[2], Y. Kasamatsu[2], T. Yokokita[2], A. Yokoyama[3],
[1]Graduate School of Natural Science and Technology, Kanazawa Univ.
[2]Graduate School of Science, Osaka Univ.
[3]Institute of Science and Engineering, Kanazawa Univ.

Abstract – In order to better understand the reaction on the fusion reaction, we have focused on the deformation of the nuclei. We have researched for the fusion reactions of $^{169}Tm+^{16}O$ [1], $^{169}Tm+^{20}Ne$, and $^{165}Ho+^{20}Ne$ [2]. The cross sections for fusion were compared between systems of different entrance channels. The results are consistent with the idea that the degree of deformation makes an effect on the rising edge of excitation functions near the Coulomb barrier.

Keywords – Fusion reaction/ Excitation function/ Deformed nucleus

I. INTRODUCTION

Heavy ion fusion reaction is often used in the synthesis of heavy elements recently. For the synthesis of trans-actinides, evaporation residues cross section is very small compared to fission. Briefly, it is important to understand the reaction mechanism and to know the conditions for efficient synthesis.

We have focused on the deformation of nuclei. In this study, in order to study the effect of the degree of nuclear deformation on the fusion reaction, we have researched for the fusion reactions of $^{169}Tm+^{16}O$ [1], $^{169}Tm+^{20}Ne$, and $^{165}Ho+^{20}Ne$ [2]. Figure 1 shows deformed nuclei in a spheroid model and Table 1 shows the degree of nuclear deformation of ^{20}Ne, ^{16}O, ^{169}Tm and ^{165}Ho based on the model. In $^{169}Tm+^{20}Ne$ and $^{165}Ho+^{20}Ne$ systems, the target nucleus ^{165}Ho is more deformed than ^{169}Tm. In $^{169}Tm+^{16}O$ and $^{169}Tm+^{20}Ne$ systems, the projectile nucleus ^{16}O is spherical, while ^{20}Ne is deformed. Both systems of $^{169}Tm+^{16}O$ and $^{159}Ho+^{20}Ne$ form the same compound nucleus, $^{185}Ir^{*}$.

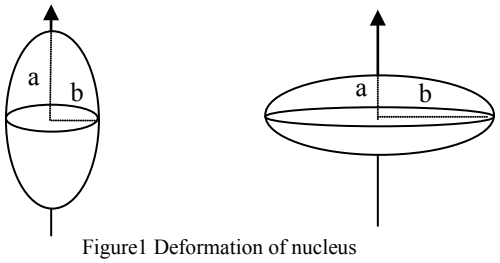

Figure1 Deformation of nucleus

Table1 Degree of deformation of relevant nuclei

	^{20}Ne	^{16}O	^{169}Tm	^{165}Ho
a/b	0.75	1.00	0.95	1.16

II. EXPERIMENTAL

The bombardment for synthesis was carried out using ^{16}O and ^{20}Ne beam supplied from the AVF cyclotron facility at Research Center for Nuclear Physics (RCNP), Osaka University. The targets were prepared by electrodeposition with standard solution on an Al foil of 2.7 mg/cm^2 thickness. For instance, the ^{169}Tm content was 4.5-5.1 mg/cm^2 in thickness. In order to achieve experiments of wide energy range in a single irradiation, energy degradation technique was used. In the present experiment using two stacks with four targets each, each target was irradiated at a different energy below 155 MeV in $^{169}Tm+^{20}Ne$ system. Typical beam intensity was 1 particle-μA. The activities produced in each target were assayed using a high resolution HPGe detector. Excitation function was made from the measured activities.

III. RESULTS AND DISCUSSION

The evaporation residues detected, for instance, in $^{169}Tm+^{20}Ne$ system were ^{185}Pt, $^{183-185}Ir$, $^{181,182}Os$ and ^{181}Re. Figure 2 shows the excitation function for fusion reaction of $^{169}Tm+^{20}Ne$, $^{169}Tm+^{16}O$ [1] and $^{165}Ho+^{20}Ne$ [2] compared with the theoretical calculations using code HIVAP taking into consideration degree of deformation of nucleus. In order to compare the systems between different entrance channels, let the value obtained by subtracting the Coulomb barrier [3] from the incident energy, ($E_{cm}-B_c$), be the horizontal axis in the figure. Comparing $^{169}Tm+^{16}O$, $^{169}Tm+^{20}Ne$ and $^{159}Ho+^{20}N$ systems, more deformed system of $^{159}Ho+^{20}Ne$ induced fusion reaction from lower incident energy. Comparing $^{169}Tm+^{20}Ne$ and $^{165}Ho+^{20}Ne$ systems, starting points for fusion reaction were nearly the same. The trends were reproduced by HIVAP calculation.

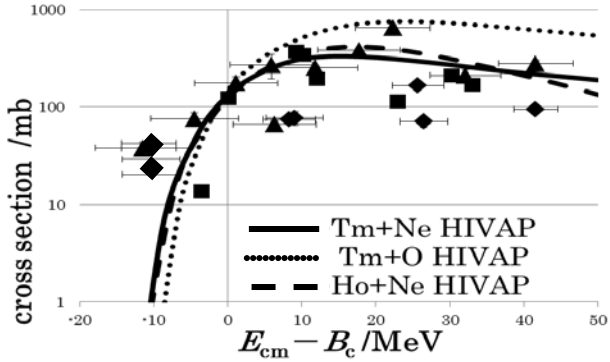

Figure2 Excitation function of $^{169}Tm+^{20}Ne$ (◆), $^{169}Tm+^{16}O$ (■) [1] and $^{165}Ho+^{20}Ne$ (▲) [2] compared to theoretical values of each system

[1] A. Asano, master thesis of Kanazawa Univ. (2010)
[2] K. Toda, master thesis of Kanazawa Univ. (2013)
[3] R. Bass, *Nuclear Reactions with Heavy Ions*, Springer-Verlag, New York (1980)

Extraction behavior of Nb and Ta in HF solutions with tributyl phosphate

M. Murakami[1,2], S. Tsuto[1], K. Ooe[1], H. Haba[2], J. Kanaya[2], S. Goto[1], and H. Kudo[1]
[1]Department of Chemistry, Faculty of Science, Niigata University, Niigata 950-2181, Japan
[2]Nishina Center for Accelerator-Based Science, RIKEN, Saitama 351-0198, Japan

Abstract – Extrtaction behavior of carrier-free Nb and Ta with tributyl phosphate (TBP) from HF solutions was studied by a batch method. Tantalum is extracted well to an organic phase, while Nb is left in an aqueous phase at 0.053–1.0 M HF concentrations. The similar extraction trends of Nb and Ta are shown in the solid phase extraction using a TBP resin. The extraction equilibria in the solid phase extraction are attained within ~10 s.

Keywords – niobium, tantalum, extraction, tributyl phosphate

I. INTRODUCTION

In the synthesis experiment of an element 115, chemically separated 27-h spontaneously fissioning nuclide was assigned to ^{268}Db which is the descendant of ^{288}115 [1,2]. To clarify this 27-h nuclide is actually Db, further chemical investigations are needed for both of known nuclides of dubnium, ^{262}Db ($T_{1/2}$ = 34 s), and 27-h spontaneously fissioning nuclide.

Tributyl phosphate (TBP) is one of the most effective extractants used for industrial separation of Nb and Ta [3]. In this work, solvent extraction behavior of Nb and Ta with TBP was first studied by a batch method. Solid phase extraction with a TBP resin was also performed to examine the feasibility of this resin to an automated rapid reversed-phase chromatography apparatus for ^{262}Db.

II. EXPERIMENTAL

The radiotracers ^{95g}Nb ($T_{1/2}$ = 34.991 d) and ^{179}Ta ($T_{1/2}$ = 1.82 y) were produced in the bombardments of 14-MeV proton beam supplied by the RIKEN AVF cyclotron on ^{nat}Zr and ^{nat}Hf target foils, respectively.

In the experiment of the solvent extraction, 1 mL of HF solution containing ^{95g}Nb and ^{179}Ta tracers were shaken with 1 mL of TBP−1,2-dichloroethane solution for 180 min at 25°C. After centrifugation, 700 μL of each phase was transferred to an polypropylene tube separately, and then subjected to γ- and X-ray measurements with a Ge detector. The distribution ratios (D) of Nb and Ta were deduced from the observed radioactivities.

The solid phase extraction was performed with following procedures. TBP resin was prepared by adsorbing TBP on a support material (MCI GEL CHP20/P30, Mitsubishi Chemical Co.) [4]. A portion of 20 to 30 mg of the TBP resin was shaken with 400 μL of HF solution containing ^{95g}Nb and ^{179}Ta tracers for 6 s to 60 min. After filtration, 200 μL aliquot was transferred to a polypropylene tube. The distribution coefficients of Nb and Ta were calculated with the observed radioactivities and the weight of the used resin.

III. RESULTS AND DISCUSSION

Figure 1 shows the dependence of the D values of Nb and Ta on the initial HF concentration ($[HF]_{ini}$) with 1.8 M TBP − 1,2-dichloroethane solution as an organic phase. Tantalum was extracted well at the $[HF]_{ini}$ of 0.053 to 1.0 M, while Nb was left in an aqueous phase.

The number of TBP molecules combined with the Nb and Ta compounds was examined by varying the TBP concentration at the constant $[HF]_{ini}$. The number of combined TBP molecules was found to be 3 for Ta at $[HF]_{ini} \leq 2.7$ M. This agrees with the results in Refs. [3,4]. Although the number of TBP molecules combined with the Nb compound is reported as 3 [3], our results show that the number is 2 independently of $[HF]_{ini}$. This results show that Nb and Ta are extracted with different chemical forms.

Using the 48 wt-% TBP resin, the dependence of the distribution coefficients of Ta on $[HF]_{ini}$ was similar to that of the D values in the liquid-liquid solvent extraction. Niobium was not extracted at ≤ 10 M. The time required for the extraction equilibrium was less than 12 s for both of Nb and Ta. This indicates that the present extraction system could be applicable to an on-line experiment with the short-lived ^{262}Db.

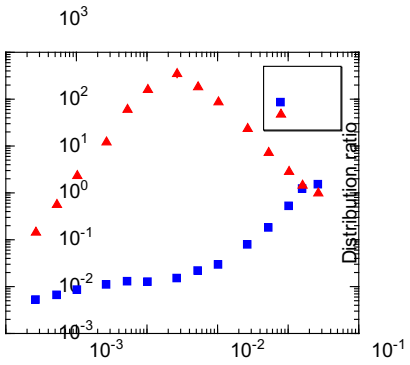

Fig. 1. Distribution ratios of Nb and Ta.

[1] S. N. Dmitriev et al., Mendeleev Commun. **15**, 1 (2005).
[2] N. J. Stoyer et al., Nucl. Phys. A **787**, 388c (2007).
[3] Z. Zhu and C. Y. Cheng, Hydrometallurgy **107**, 1 (2011).
[4] H.Haba *et al.*, Radiochim. Acta **95**, 1 (2007).
[5] S. Nishimura et al., Trans. JIM **5**, 79 (1964).

A MODIFIED METHOD FOR SYNTHESIS OF [γ-^{32}P] LABELLED ADENOSIN TRIPHOSPHATE

Wira Y Rahman[1]*, Endang Sarmini[1], Herlina[1], Triyanto[1], Rien Ritawidya[1], Abdul Mutalib[1] and Santi Nurbaiti[2]

[1] Center for Radioisotope and Radiopharmaceuticals (PRR) - BATAN)
[2]Biochemistry Research Division, faculty of Mathematics and Natural Sciences, Institut Teknologi Bandung, Jl. Ganesha 10 Bandung, Indonesia, 40132
*Tel/fax : (6221)7563141, email: wira@batan.go.id

ABSTRACT

Adenosine triphosphate-labelled with γ-^{32}P (γ-^{32}P]-ATP) has been widely used in the biotechnology research, usually as a tracer to study aspects of physiological and pathological processes. In order to support biotechnology research in Indonesia, a process for production of [γ-32P]-ATP in accordance with a more simple glycolysis enzymatic reaction utilizing glyceraldehid 3-phosphate dehydrogenase, 3-phosphoglyceryc phosphokinase and lactate dehydrogenase has been conducted. DL-glyceraldehydde 3-phosphate, *Adenosine Diphosphate (ADP) and $H_3{}^{32}PO_4$ was used as precursors for this reaction. Purification of [γ-^{32}P]-ATP was performed by using DEAE-Sephadex column chromatography. The results showed that radiochemical purity of [γ-^{32}P]-ATP was 99,49% with radioactivity was 1,175 mCi for 20 minutes enzymatic reaction. The result suggested that this modification method can be used for producing [γ-^{32}P]-ATP to support the provision of radiolabeled nucleotide for biotechnology research in Indonesia.*

Key words *: labeled nucleotide [γ-^{32}P]-ATP, synthesis, enzymatic reaction, DEAE-Sephadex column chromatography*

Production of ^{88}Nb and ^{170}Ta for chemical studies of element 105 Db using the GARIS gas-jet system

M. Huang,[1] M. Asai,[2] H. Haba,[1] D. Kaji,[1] J. Kanaya,[1] Y. Kasamatsu,[3] H. Kikunaga,[4] Y. Kikutani,[3] Y. Komori,[3] H. Kudo,[5] Y. Kudou,[1] K. Morimoto,[1] K. Morita,[1] M. Murakami,[5] K. Nakamura,[3] K. Ozeki,[1] R. Sakai,[1] A. Shinohara,[3] T. Sumita,[1] K. Tanaka,[1] A. Toyoshima,[2] K. Tsukada,[2] Y. Wakabayashi[1] and A. Yoneda[2]

[1]Nishina Center for Accelerator-Based Science, RIKEN
[2]Advanced Science Research Center, JAEA
[3]Graduate School of Science, Osaka University
[4]Research Center for Electron Photon Science, Tohoku University
[5]Department of Chemistry, Niigata University

Abstract – We developed a production technology for radioisotopes of Ta and Nb for chemical studies of element 105, Db, using the RIKEN gas-filled recoil ion separator, GARIS. Isotopes of ^{170}Ta and ^{88}Nb produced via the ^{nat}Gd(^{19}F, xn)^{170}Ta and ^{nat}Ge(^{19}F, xn)^{88}Nb reactions, respectively, were successfully extracted by the gas-jet method to a chemistry laboratory after physical separation by GARIS.

Keywords – superheavy element chemistry, Nb, Ta, Db, GARIS, gas-jet method, recoil transfer chamber

We plan to study chemical properties of element 105, Db, produced in the ^{248}Cm(^{19}F,5*n*)^{262}Db reaction using the gas-jet transport system coupled to the RIKEN gas-filled recoil ion separator, GARIS[1]. It is important to perform Db chemistry together with Ta and Nb under identical conditions to find different chemical behavior among the homologues. In this work, we tried to produce isotopes of ^{170}Ta ($T_{1/2}$ = 6.76 min) and ^{88}Nb ($T_{1/2}$ = 14.55 min) in the ^{nat}Gd(^{19}F, *xn*)^{170}Ta and ^{nat}Ge(^{19}F, *xn*)^{88}Nb reactions, respectively, using the GARIS gas-jet system.

A 106.4-MeV $^{19}F^{9+}$ beam was extracted from the RIKEN linear accelerator. A ^{nat}Ge target of 0.29 mg/cm^2 thickness was prepared by vacuum evaporation onto a 0.89 mg/cm^2 Ti backing foil, while a $^{nat}Gd_2O_3$ target of 0.34 mg/cm^2 was prepared by electro-deposition on a 0.87 mg/cm^2 Ti foil. The two arc-shaped Ge targets and two Gd_2O_3 were mounted together with four 0.95 mg/cm^2 Ti blank foils on a rotating wheel of 100-mm diameter, which was rotated at 1000 rpm. The beam energy was 103 MeV in the middle of the target and the typical intensity was approximately 3 particle μA (pμA). The working He pressure of GARIS was 33 Pa. At the focal plane of GARIS, a recoil transfer chamber (RTC) of 100-mm inner diameter and 0~100-mm adjustable depth was installed. Evaporation residues separated with GARIS were passed through a 0.5-μm Mylar window, thermalized in RTC, and were transported by the He/KCl-aerosol-gas-jet system to a chemistry laboratory. The He flow rate was 2.0 L/min, and the inner pressure of RTC was 47 kPa. After collection of the aerosols on a glass filter (ADVANTEC GB-100R) for 1 and 3 min for ^{170}Ta and ^{88}Nb, respectively, the filters were subjected to γ-ray spectrometry using a Ge detector. The magnetic setting of GARIS was varied in the magnetic rigidity ($B\rho$) range of 1.51–1.80 Tm for ^{170}Ta and 0.850–0.979 Tm for ^{88}Nb. In the GARIS separation of ^{88}Nb at low $B\rho$ values, the beam particles with lower charge states broke the thin Mylar foil of RTC. Thus, we installed a retractable Al shutter of 2-mm thickness and 30×100-mm^2 size at the focal plane to protect the Mylar foil from the undesired beam particles. The gas-jet efficiencies are very sensitive to the depth of RTC and recoil ranges of the evaporation residues in RTC. To effectively collect ^{88}Nb atoms in RTC, a 3-μm Al degrader foil was used to reduce their recoil ranges before entering the RTC.

The 221.2-keV and 671.2-keV γ-rays are useful for chemical studies of ^{170}Ta and ^{88}Nb, respectively. Yield distributions of ^{170}Ta and ^{88}Nb related to $B\rho$ are displayed in Fig. 1. The optimal $B\rho$ of 1.64±0.01 and 0.936±0.001 Tm were determined for ^{170}Ta and ^{88}Nb, respectively. Under the optimal $B\rho$ and with the 100-mm depth RTC, the production yields of ^{170}Ta and ^{88}Nb in the chemistry laboratory were evaluated to be 8.65±0.56 and 0.61±0.02 kBq/pμA after 1-min and 3-min aerosol collection, respectively. The gas-jet efficiency of ^{88}Nb was 41±2%, while that of ^{170}Ta was 77±3%.

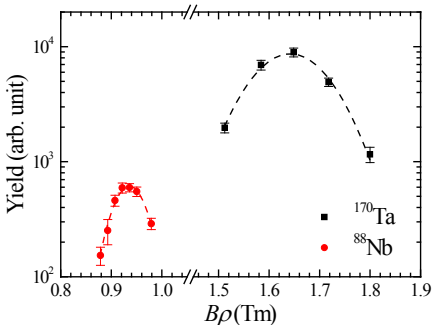

Fig.1. Yields of ^{170}Ta and ^{88}Nb as a function of $B\rho$.

[1] H. Haba et al.: Chem. Lett. **38**, 426 (2009).

Half-life measurement of ^{7}Be in several materials

T. Ohtsuki
Research Center for Electron Photon Science, Tohoku University
1-2-1, Mikamine, Taihaku, Sendai, 982-0826, Japan

Abstract – The formation of atom-doped C60 and C70 etc. has been investigated by using several types of radionuclides produced by nuclear reactions. From the trace of the radioactivities after high performance liquid chromatography (HPLC), it was found that formation of endohedral fullerenes of Be atom is possible by a recoil process following the nuclear reaction. The decay rate of ^{7}Be electron capture (EC) was measured in C 7 0 and Be metal with a reference method. The half-lives of ^{7}Be endohedral C70 and ^{7}Be in Be metal (Be metal(^{7}Be)) were found to be 52.45±0.04 and 53.25±0.04 days, respectively. This amounts to a 1.5% difference in the EC-decay half-life between ^{7}Be@C70 and Be metal(^{7}Be). The results are a reflection of the different electron wave-functions in nuclear site for ^{7}Be inside C70 compared to when ^{7}Be is in a Be metal. The further theoretical interpretation is needed for these experimental results.

Keywords – Electron Capture Decay, Beryllium-7, Half-life

I. INTRODUCTION

A long-standing challenge has been to establish the degree to which manipulation of the environmental factors can in practice change nuclear decay rates in experiments to determine the decay rate of ^{7}Be compounds. In addition, there have been several observations of variations in the half-life with host metals, chemical forms, and pressure. From the early data, the half-life of ^{7}Be as a function of different chemical forms and/or host materials have been limited almost to within 0.2%. In recent studies, however, large variations have been observed as a function of different chemical forms and pressures. Therefore, a precise measurement is still needed to obtain the absolute decay rate in different circumstances.

After the discovery of C_{60} and the subsequent successful production of several kinds of fullerenes, endohedral fullerenes which have one or more atoms inside the C_{60}, C_{70}, cages etc. currently have attracted great interest. If their mass production becomes possible, they would have many interesting applications such as stable molecular devices in nano-meter scales and/or as functionalized materials in many fields. We have examined the formation of endohedral fullerenes by a nuclear recoil implantation of several foreign atoms following nuclear reactions[1,2]. We found that the ^{7}Be atom can be endohedrally doped to create the ^{7}Be endohedral fullerenes.

Because of the unique chemical form of fullerenes and/or several factors contributing to give rise to this environment; many π-electrons of $C_{60}(C_{70})$, and special dynamic motions inside $C_{60}(C_{70})$ etc., the electron contact density on the ^{7}Be nuclei can be affected significantly by the electron environment of $C_{60}(C_{70})$. Therefore, it is intriguing to measure the half-life of the ^{7}Be inside $C_{60}(C_{70})$; "how does the EC decay rate in ^{7}Be change inside the $C_{60}(C_{70})$ cage relative to other situations?"

So far, we compared the half-life of ^{7}Be when it is encapsulated in a C_{60} cage to that of ^{7}Be in Be metal as a reference. We found a surprisingly shorter half-life of ^{7}Be inside C_{60}[3,4]. This fact implied that the ^{7}Be atoms are located in a unique environment inside C_{60} cage. Furthermore, in order to see the size effect of fullerenes, we demonstrate the change of decay rete of ^{7}Be in ^{7}Be@C_{70} and in Be metal [Be metal(^{7}Be)]. The decay rate of ^{7}Be electron capture (EC) was measured in C 7 0 and Be metal with a reference method. The half-lives of ^{7}Be endohedral C70 and ^{7}Be in Be metal (Be metal(^{7}Be)) were found to be 52.45±0.04 and 53.25±0.04 days, respectively.

[1] T. Ohtsuki *et al*., Physical Review Letters 77 (1996) 3522.

[2] T. Ohtsuki *et al*., Physical Review Letters, 81 (1998) 967-970.

[3] T. Ohtsuki *et al*., Physical Review Letters 93 (2004) 112501.

[4] T. Ohtsuki *et al*., Physical Review Letters 98 (2007) 252501

APSORC'13 - 5th Asia-Pacific Symposium on Radiochemistry
Kanazawa, Japan, 22-27 September 2013

Verification of anticlockwise gyre in the semi-closed water area of Lake Nakaumi, southwest Japan, by using $^{224}Ra/^{228}Ra$ activity ratios

Ritsuo Nomura[1],* Mutsuo Inoue[2], Hisaki Kofuji[3] and Shota Ikeda[1]
[1] Foraminiferal Laboratory, Faculty of Education, Shimane University, Matsue 690-8504 Japan
[2] Institute of Nature and Environmental Technology, Kanazawa University, Wake, Nomi, Ishikawa 923-1224 Japan
[3] Mutsu Marine Laboratory, Japan Marine Science Foundation, Minato, Mutsu, Aomori, 035-0064 Japan

Abstract –
The Honjyo area in Lake Nakaumi is a semi-closed brackish water area where some mixing of up-flowing marine water and down-flowing lake water take place. A large-scale gyre that caused by the residual circulation was once indicated by a temporal algal blooming that spread over the semi-closed Honjyo area in brackish Lake Nakaumi. In order to verify this type of water circulation, we examined ^{224}Ra ($t_{1/2}$=3.66 d)/^{228}Ra ($t_{1/2}$=5.75 y) activity ratios of both upper and lower waters that differentiated by a well-developed halocline. The $^{224}Ra/^{228}Ra$ ratios in the upper water were lowest in the central area, suggesting the formation of anticlockwise gyre. The ratios in the lower water were rather uniform, but a basin-wide anticlockwise flow of water is also indicated. The $^{224}Ra/^{228}Ra$ ratio is clearly effective to trace the water flow for both the deep and surface waters.

Keywords – $^{224}Ra/^{228}Ra$ ratio, Water flow, Lake Nakaumi

I. INTRODUCTION

Estuarine biota has been critically influenced by an increased eutrophication in Japan. The environmental and biological interaction is complicate, but the water characters and the dynamic water movement are major factor to understand the total environment of estuarine water.

The Honjyo area, occupying ~20 % of Lake Nakaumi, was closed for 28 years. This closed area is now partly opened and permitted the exchange of marine water and lake water through the opened slit [1]. After the closed area opened, the original massive low salinity water changed to form a density stratification of bottom and surface waters. In order to clarify the deep and surface water dynamics, we analyzed $^{224}Ra/^{228}Ra$ ratio of both deep and surface waters to understand the water residence time and the circulation of water.

A. Methods of study

Ten sampling locations were set in and out of the Honjyo area (Fig. 1). We used Mn-fiber to collect Ra from lake water (40-60 L) prefiltered with a polypropylene filter cartridge (~1 L/min; 0.5 μm median pore size). Mn-fiber was dried and then ashed within 24 hours. Ash powder was completely sealed in the styrene bottle.

γ-Spectrometry was performed using a coaxial-type Ge-detector. The ^{224}Ra and ^{228}Ra activities were evaluated from the γ-ray peaks of ^{212}Pb (235 keV) and ^{228}Ac (338 and 911 keV), respectively. The first γ-ray counting time for ^{224}Ra and ^{228}Ra was 18,000 seconds and the second counting time was 85,000 seconds. Owing to the short half-life of ^{224}Ra, first γ-ray counting for ^{224}Ra was conducted between 3-5 days after the sampling.

II. RESULTS AND DISCUSSION

Both the upper and lower waters in the Honjyo area show lower $^{224}Ra/^{228}Ra$ ratio, compared to that in the Sakai Channel. The ratios of the upper water show the range between 0.02-0.15, and those of the lower water are 0.08-0.20. These ratios are similar to the ratio of the Nakaumi water. It is noted that the $^{224}Ra/^{228}Ra$ ratio of the upper water shows regional difference, which is higher in western and northern sides, while the central and eastern sides are lower. The $^{224}Ra/^{228}Ra$ ratios of lower water are characterized by similar ratios, excepting the place near the Ohmisaki slit.

In 2010, algae blooming spread over the surface of the Honjyo area, showed a large-scaled anticlockwise gyre in the area. Our reconstructed surface water flow, using $^{224}Ra/^{228}Ra$ ratios, is similar to the large-scale anticlockwise gyre shown by the algae powder. The $^{224}Ra/^{228}Ra$ ratios in the lower water are rather uniformly distributed, but the lower water may form a large-scale anticlockwise flow over the basin.

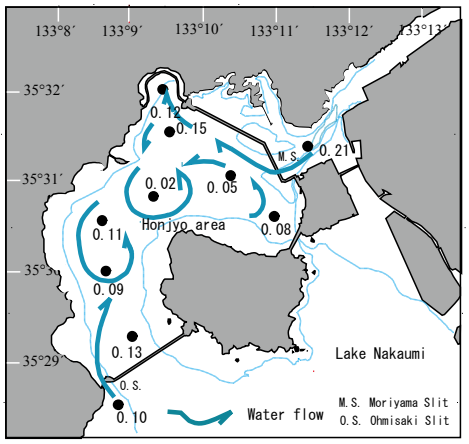

Figure 1. Distribution of $^{224}Ra/^{228}Ra$ ratios in the Honjyo area and the supposed flow of upper water.

[1] Nomura, R. et al., 2013. Opening of the closed water area and consequent changes of $^{228}Ra/^{226}Ra$ activity ratios in coastal lagoon Lake Nakaumi, Southwest Japan. Applied Radiation and Isotopes. DOI: 10.1016/j.apradiso.2013.03.069

APSORC'13 - 5th Asia-Pacific Symposium on Radiochemistry
Kanazawa, Japan, 22-27 September 2013

Effect of hydroxylated fullerene on U(VI) Adsorption onto oxidized multi-walled carbon nanotubes

Jing WANG[1], Zhan LI[2], Peng LIU[1], Wei QI[1], Juanjuan BI[1], Wangsuo WU[1]*
1 Radiochemistry Laboratory, School of Nuclear Science and Technology, Lanzhou University, Lanzhou 73000, China
2 Institute of Modern Physics, Chinese Academy of Sciences, Lanzhou 73000, China

Abstract –Herein, hydroxylated fullerene ($C_{60}(OH)_n$) was chosen as the third phase to investigate its impact on U(VI) adsorption onto carbon nanotubes. The results showed that the drastic effect of $C_{60}(OH)_n$ on U(VI) adsorption of oMWCNTs was not significant at low concentration of $C_{60}(OH)_n$, whereas a negative effect was observed at higher concentration. The adsorption of U(VI) onto oMWCNTs was enhanced with increasing pH values at pH < 6, but decreased after pH reached 6. The main mechanism may be the adsorbed Cu(II) on oMWCNTs is "squeezed" down to the solution by the adsorption of $C_{60}(OH)_n$ onto oMWCNTs. The double sorption site model was applied to simulate the adsorption isotherms of U(VI) in the presence of $C_{60}(OH)_n$ and fitted the experimental data well. This provides reference for studying the interactions between carbon nanomaterials and radionuclide in various conditions of natural environment. Meanwhile, it also brings theoretical basis for studying the biological safety problems caused by multi-component environment pollution.

Keywords –Effect, Hydroxylated fullerene, U(VI) adsorption, Oxidized multi-walled carbon nanotubes

I. INTRODUCTION

Carbon nanotubes has potential application in the disposal of nuclear fuel reprocessing, due to the large specific surface area, the surface is easy to be modified, resistant to heat and radiation. As far as we known, the study concerning the mechanism for radionuclide selective adsorption on a variety of carbon nanomaterials in the ternary system was sparse. However, it is difficult to achieve the adsorption contribution of each carbon nanomaterial when they are all chosen as adsorbent in the experiment. Two different water-soluble carbon nanomaterial must be selected as the adsorbent to resolve this problem.

$$A\% = \frac{C_2}{C_0} + \frac{e^{C_1}}{C_0} \times e^{(k \cdot b \cdot C_f)} \qquad (1)$$

Where Co (mg/L) is the initial concentration of U(VI) before adsorption; Cs (mg/g) for the equilibrium concentration of U(VI) in the solid phase after adsorption; Ce (mg/L) is the equilibrium concentration of U(VI) in the liquid phase; Cf (mg/L) is definited as the initial concentration of C60(OH)n; b is the parameter for characterization the adsorption of C60(OH)n, it depends on the species and surface character of C60(OH)n and the nature of oMWCNTs; C_1 and C_2 are the performance parameters for the sorption characterization of oMWCNTs, these parameters depend on the surface character of oMWCNTs and the nature and species of U(VI); k represents the rate constant.

Table 1 Parameters of double adsorption site model*

m/V(g·L^{-1})	DSSM model			
	C_2/C_0	e^{C_1}/C_0	k · b	R^2
1	267.26	-165.72	-773.41	0.9485
0.5	-4148.21	4246.26	12867.49	0.9739
0.25	-10.97	104.89	127.13	0.9757
0.1	-7.72	185.38	55.43	0.9457

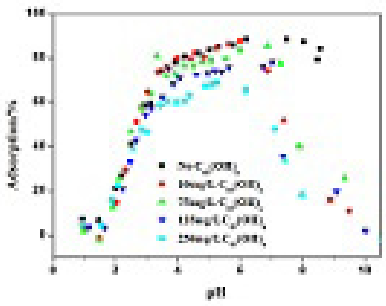

Fig. 1 Effect of $C_{60}(OH)_n$ on U(VI) adsorption onto oMWCNTs as a function of pH, *m/V* =0.5 g/L, *T* = 25±1 ºC, *I*=0.01 mol/L $NaNO_3$, C[UO_2^{2+}]initial =1.12×10^{-4} mol/L.

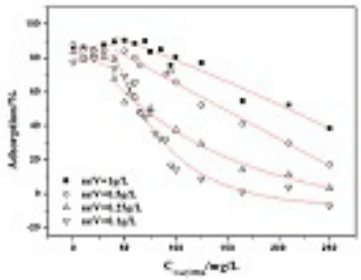

Fig. 2 Effect of oMWCNTs dosage on U(VI) adsorption onto oMWCNTs as a function of $C_{60}(OH)_n$ initial concentrations, pH=7.00±0.10, *I*=0.01 mol/L $NaNO_3$, *T* = 25±1 ºC, C[UO_2^{2+}]initial =1.12×10^{-4} mol/L.

*Corresponding author: Wangsuo Wu,
Tel & Fax:+8609318913594,
E-mail:wuws@lzu.edu.cn(W.Wu).

APSORC'13 - 5th Asia-Pacific Symposium on Radiochemistry
Kanazawa, Japan, 22-27 September 2013

Corrosion of Copper in Water and Colloid Formation under Intense Radiation Field

Kotaro Bessho[1], Yuichi Oki[2], Naoya Akimune[3], Hiroshi Matsumura[1], Kazuyoshi Masumoto[1], Shun Sekimoto[2], Naoyuki Osada[4], Norikazu Kinoshita[5], Hideaki Monjushiro[1], Seiichi Shibata[2]
[1] Radiation Science Center, High Energy Accelerator Research Organization (KEK),
[2] Research Reactor Institute, Kyoto University (KURRI), [3] Graduate School of Engineering, Kyoto University,
[4] Graduate School of Engineering, Tohoku University, [5] Institute of Technology, Shimizu Corporation

Abstract – Radiation effects on corrosion of copper in water and colloid formation were investigated. Irradiation experiments using ^{60}Co γ-ray irradiation facility and electron LINAC demonstrated that high-energy photons promote corrosion and elution of copper into water and formation of copper-related colloids / particles in water phase.

Keywords – Radiation effect, Corrosion, Colloid

I. INTRODUCTION

At high-energy accelerator facilities, colloid formation in cooling water is an important subject for radiation management at high-energy accelerator facilities, because the presence of colloidal species complicates the behavior of radionuclides in the cooling water systems [1]. It's possible that intense radiation field inside accelerator facilities affects the corrosion of metal components and formation of metal-related colloid in the cooling water. Effects of radiation on corrosion of copper and formation of copper-related colloid in water were studied.

II. EXPERIMENTS

Irradiation experiments were carried out at the ^{60}Co γ-ray irradiation facility or the electron linear accelerator (e-LINAC) at the Research Reactor Institute, Kyoto University (KURRI). Cu vessels (Inside:19ϕ x 75 mm) filled with pure water (26 ml) were irradiated by γ-rays from ^{60}Co source, or bremsstrahlung and neutrons generated by a 30 MeV electron beam striking a Ta target assembly. At the ^{60}Co γ-ray irradiation facility, samples were irradiated by γ-ray with the dose rates of 2.9 kGy/h or 21 kGy/h for 2 to 240 h. At the e-LINAC facility, irradiation experiments were carried out with several beam-current conditions, and the irradiation times were varied between 2 to 24 h.

After the irradiations, water samples in the Cu containers were collected and filtrated with four kinds of ultrafiltration (UF) units for particle size separation. Estimated pore sizes of the UF units were 200 nm, 16 nm, 7 nm, and 3 nm. Elemental concentrations of Cu in each UF filtrate and original samples before UF were determined by ICP-AES analyses.

III. RESULTS AND DISCUSSION

Figure 1 shows soluble and size-separated colloidal concentrations of Cu in water without irradiation or after the irradiation at the γ-ray irradiation facility or the e-LINAC facility. The results for the LINAC experiments were obtained at the downstream (0-deg) sample position, where flux of neutrons can be neglected compared to flux of bremsstrahlung. The results demonstrate that irradiation of high-energy photons (γ-ray or bremsstrahlung) clearly affects the elution of Cu into water and formation of Cu-related colloid / particle in water phase.

Concentration of soluble Cu species increased with photon intensity. Formation of colloidal species was also noticeable at intense photon environment. Furthermore, qualitative evaluations using water-quality test kits clarified that H_2O_2 and O_3 were generated in water by irradiating γ-ray or bremsstrahlung. These results imply that high-energy photons produce active species, such as H_2O_2, O_3 and OH radicals, in water. These active species may affect various processes, such as corrosion of Cu materials, transfer of Cu species into water as a soluble species or colloidal species, and growth of colloidal species in water phase.

Time dependence of size-profiles for Cu species formed at constant dose rates imply that dissolution of Cu materials in water and formation of Cu-related colloid occurring in intense radiation environments progress in the time scale of several hours to hundreds hours.

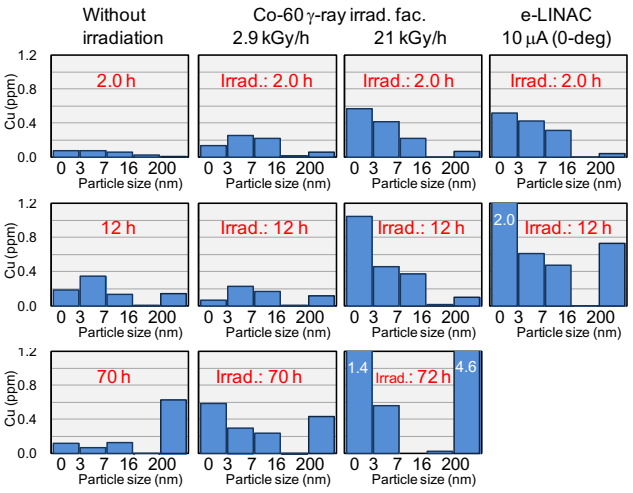

Figure 1 Soluble (0-3 nm) and colloidal concentrations (3-7, 7-16, 16-200 nm) of Cu in water without irradiation, after the irradiation at Co-60 γ-ray irradiation facility, and after the irradiation at electron LINAC. Irradiation time : 2.0 h, 12 h

[1] K. Bessho *et al.*, Eleventh Meeting of the Task-Force on Shielding Aspects of Accelerators, Targets and Irradiation Facilities (2012)

Study on Unattached Fraction of Radon Progeny and its Environmental Influence Factors

Lu GUO[1], Lei ZHANG[2], Qiuju GUO[1]
[1]State Key Laboratory of Nuclear Physics and Technology, Peking University, Beijing 100871,China
[2]Solid Dosimetric Detector and Method Laboratory, Beijing 102205, China

Abstract – *The exposure of radon and its progeny contributes more than half of the natural radiation exposure received by the public. The unattached fraction of radon progeny is an important parameter in radiation dose estimation through dosimetric process; however, not so much data has been reported. For a better understanding on temporal variation and its environmental influence factors of the unattached fraction of radon progeny, a series of field measurements were performed periodically by adopting a new developed integrating monitor for measuring unattached fraction of radon progeny, and an instrument for measuring aerosol concentration in both indoor and outdoor environments.*

It was shown by the measurement results that the ranges of unattached fraction of radon progeny in indoor and outdoor environments all over the year were 8.4%~16.5% and 9.4%~28.2%, respectively. Seasonal and diurnal variations of the unattached fraction of radon progeny were also analyzed. It comes to the conclusion that during the winter season the unattached fraction of radon progeny is stable in indoor environment because of the little change on aerosol concentration、temperature and humidity indoor in Beijing area, while on the other hand, it changes a lot in outdoor environment due to the great undulation of atmospheric factors, and the average of the unattached fraction of radon progeny is higher in outdoor environments than that of indoors. While in summer, the unattached fraction of radon progeny in indoor environment was close to the values of outdoor environment, and both of them had lower average than that in winter.

Keywords – radon; unattached fraction; aerosol; dose conversation factor

APSORC'13 - 5th Asia-Pacific Symposium on Radiochemistry
Kanazawa, Japan, 22-27 September 2013

Preliminary Study on Measuring Radon Progeny Concentration Using Alpha/Beta Spectroscopic Method

Abdumomin Kadir[1], Lei Zhang[2], Qiuju Guo[1], and Juncheng Liang[3]
[1] State Key Laboratory of Nuclear Physics and Technology, School of Physics, Peking University, Beijing, 100871, China
[2]Solid Dosimetric Detector and Method Laboratory, Beijing, 102205, China
[3]Ionizing Radiation and Medical Science, National Institute of Metrology, Beijing, 100013, China

Abstract – The accurate measurement of radon progeny concentration is essential for dose evaluation of radon exposure. Alpha/beta spectroscopic methods have great advantage comparing with traditional total counting methods as well as alpha-spectrum methods. This work introduces a radon progeny measurement method using alpha/beta spectroscopy. Sample 10 min with unit flow rate (1 L/min), 1 min delay and then record the alpha/beta spectroscopy at 3 min internals for 30 min, the uncertainty of this method is 9.3% in a typical indoor environment (C_{Rn}=40 Bq/m^3, F=0.4). Experiment comparison results confirm that this method could greatly improve the measurement precision of radon progeny concentration.

Keywords – radon progeny; spectroscopic method; least-square calculation; accurate measurement;

The Measurement Comparability of ^{134}Cs and ^{137}Cs in Foodstuff Samples in Japan - Result of Inter-Laboratory Experiment for Certification of Certified Reference Material

Tsutomu Miura[1], Yoshitaka Minai[2], Shoji Hirai[3], Hiroshi Iwamoto[4], Chushiro Yonezawa[5], Yoshinobu Uematsu[6], Akira Okada[7], Masami Shibukawa[8], Koichi Chiba[1], Kiyoshi Kitamura[9], Takahiro Yamada[10], Kazutoshi Kakita[11], Isao Kojima[11]

[1]National Metrology Institute of Japan, AIST, [2] Musashi University, [3]Tokyo City University, [4]Environmental Technology Service Co, Ltd., [5]Japan Institute of International Affairs, [6]Japan Accreditation Board, [7]TERM, [8]Saitama University, [9]Japan Chemical Analysis Center, [10]Japan Radioisotope Association, [11]The Japan Society for Analytical Chemistry

Abstract – The measurement comparability of ^{134}Cs and ^{137}Cs in foodstuff samples in Japan was evaluated based on the inter-laboratory experiment for certification of certified reference material (CRM) for environmental radioactivity analysis.

Keywords – measurement comparability, certified reference material, Environmental radioactivity, ^{134}Cs, ^{137}Cs, inter-laboratory experiment method, Uncertainty

I. INTRODUCTION

Following the mega earthquake, tsunami, and the accident at the Fukushima No.1 nuclear power plant on March 11, 2011, a massive amount of radioisotopes were released in the environment. This situation required urgent measurements of radioactive isotopes in foodstuff samples for human health. The CRM is essential to accurate and precise measurement of radioisotopes in the samples. The Japan Society of Analytical Chemistry was developed the certified reference material of brown rice (JSAC0731 and JSAC0732) and bovine muscle flakes (JSAC0751 and JSAC0752) for measuring radioactive isotopes of ^{134}Cs and ^{137}Cs support by Grant-in-aid Japan Science and Technology Agency. The certification of the ^{134}Cs, ^{137}Cs and ^{40}K in candidate CRM of brown rice and bovine muscle for environmental radioactivity analysis was performed by the inter-laboratory experiment method. Twelve laboratories, including the research institutes, JCSS (Japan Calibration Service System) accredited calibration labs, universities, and industrial testing labs in Japan participated in the inter-laboratory experiment for certification. The certified values and associated expanded uncertainties (k=2) of ^{134}Cs, ^{137}Cs, and ^{40}K in brown rice CRM were 141 Bq kg^{-1} ± 9 Bq kg^{-1}, 210 Bq kg^{-1} ± 13 Bq kg^{-1}, and 75 Bq kg^{-1} ± 7 Bq kg^{-1}, respectively [1]. And also, the certified values and associated expanded uncertainties (k=2) of ^{134}Cs, ^{137}Cs, and ^{40}K in bovine muscle CRM were 174 Bq kg^{-1} ± 12 Bq kg^{-1}, 297 Bq kg^{-1} ±20 Bq kg^{-1}, and 276 Bq kg^{-1} ± 46 Bq kg^{-1}, respectively [2].

In this paper, we present a measurement comparability of ^{134}Cs and ^{137}Cs in foodstuff samples in Japan resulting from that of the inter-laboratory experiments.

Instruments and methods

All participants of the inter-laboratory experiments measured ^{134}Cs, ^{137}Cs, and ^{40}K in the candidate CRM using the Ge semiconductor detector.

Results and discussions

The example of the results of inter-laboratory experiments is shown in Fig.1. In that case, the z-score of the all reported values ranged from -3 to 3, the all data were used for calculation of the certified value.

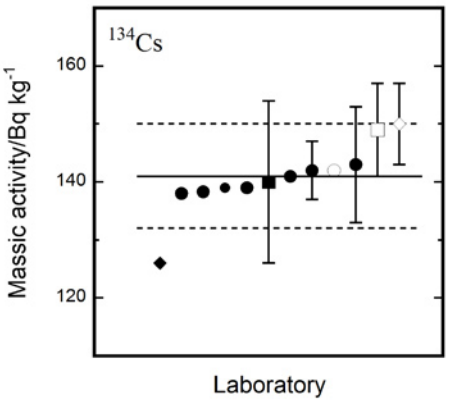

Fig.1 The result of inter-laboratory experiment of ^{134}Cs in JSAC 0731 brown rice CRM.

Acknowledgement

Our deepest appreciation goes to participants the inter-laboratory experiment for certification of CRMs.

APSORC'13 HEADING (WITHOUT NUMBER)

[1] Certificate of JSAC 0731, 0732 Brown rice certified reference material for environmental radioactivity, www.jsac.or.jp/srm/CRMJSAC0731.
[2] Certificate of JSAC 0751, 0752 Bovine muscle flakes certified reference material for environmental radioactivity www.jsac.or.jp/srm/CRMJSAC0751.

APSORC'13 - 5th Asia-Pacific Symposium on Radiochemistry
Kanazawa, Japan, 22-27 September 2013

Synthesis and Characterization of Volatile Technetium Compound

Bradley C. Childs[1], Frederic Poineau[2], Ken R. Czerwinski[2]
[1]University of Nevada Las Vegas, Las Vegas, Nevada 89154, USA

Abstract – Technetium-99 is an important fission ($T_{1/2}$= 2.13.105 y) product of the nuclear industry. Technetium in its highest oxidation state (VII) is highly mobile and can represent a threat to the environment [1]. There are over 55 million gallons of high level mixed waste located at the Hanford site. Waste tanks at the Hanford site contain Tc that could potentially leak, and in the context of management of technetium, a glass waste form was proposed to counteract the issue [2]. In the process of synthesizing melt glass between the temperatures of 600 °C and 1100 °C, volatile technetium compounds were observed in the reaction tube. These compounds displayed characteristic colors based upon the reaction environments of either breathing air or nitrogen gas. A breathing air atmosphere produces a red compound that adheres to the walls of the reaction tube. An atmosphere of nitrogen gas produces a white compound that was observed on the walls of the reaction tube.

Keywords – Technetium, Red, Volatile,

I. INTRODUCTION

A study of how technetium behaves as a waste-form and the speciation that correlates with the waste-form has garnered much attention. One of the proposed methods to create a waste-form was vitrification. The main issue with vitrication is dealing with volatile products that form in the process of manufacturing the glass from vitrification. The temperatures that are reached allow for radioactive compounds to become airborne and can present a problem when trying to retain all of the radioactive material. As it pertains to technetium, Tc_2O_7 boils at 311 °C and TcO_2 boils at temperatures above 900 °C which is problematic because melting temperatures exceed the boiling points of those compounds very easily [3]. Most speciation studies go into how the glass is formed, but the focus of the study at hand is to look at the volatilized species.

A. Vitrification Process

The process that was used to produce volatile species involves making glass material. Melt glass formers based on the LAWE4H batch composition were used while loading 1% technetium by mass to this mixture by way of sodium pertechnetate ($NaTcO_4$) [4]. A temperature range between 600 °C and 1100 °C will be used to produce the material. Two different environments will be created while producing volatile species. The first of which will be breathing air. Under these conditions we expect to see a red volatile species (Fig.1). The second environment will be nitrogen gas. It is expected that a white volatile species will be observed from this synthesis (Fig.2).

B. Additional Synthetic Routes

One way to determine the exact species being volatilized is to observe the technetium compound being used in the batch synthesis material. $NaTcO_4$ will also be observed without adding it to the batch material to see if volatile species are still produced in the same manner. Other pertechnetate salts will be observed as well with and without the batch material.

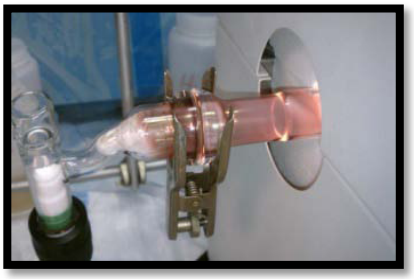

Fig.1: Volatile Red Compound

Fig.2: Volatile White Compound

REFERENCES

[1] Y. Liu, J. Terry and S. Jurisson, *Radiochim. Acta*, 2007, **95**, 717–725
[2] W.W. Lukens et al., Dissimilar behavior of technetium and rhenium in borosilicate waste glass as determined by X-ray absorption spectroscopy. Chem. Mater. 19, (2007) 55-56.
[3] J.G. Darab and P.A. Smith *Chem. Mater.* 1996, *8,* 1004-1021.
[4] DM-100 Melter Testing to Support LAW Glass Formulation Correlation Development," K. Abel and J. Westsik, WTP Test Specification, 24590-WTP-TSP RT-04-0004, Rev. 0, 1/12/05.

APSORC'13 - 5th Asia-Pacific Symposium on Radiochemistry
Kanazawa, Japan, 22-27 September 2013

Time Variation of Concentrations of Radioactive Cesium-134, 137 and Iodine-129 in the Ohori River, Chiba Prefecture, Japan

Nao Shibayama[1], Keisuke Sueki[2], Kimikazu Sasa [2,3], Yukihiko Satou[1], Tsutomu Takahashi[3], Masumi Matsumura[3], Hiroyuki Matsuzaki[4], Michio Murakami[5], Rey Yamashita[6], Mahua Saha[6], Hideshige Takada[6], Yukio Koibuchi[7], Soulichan Lamxay[7], Taikan Oki[8]

[1]Graduate School of Pure and Applied Sciences, Univ. of Tsukuba
[2]Faculty of Pure and Applied Sciences, Univ. of Tsukuba
[3]Research Facility Center for Science and Technology, Univ. of Tsukuba
[4]MALT, The Univ. of Tokyo
[5] "Wisdom of Water" (Suntory), The Univ. of Tokyo
[6]Tokyo Univ. of Agri. & Tech.
[7]Graduate School of Frontier Sciences, The Univ. of Tokyo
[8]Insitute of Industrial Science, The Univ. of Tokyo

Abstract

Radioactive nuclides emitted from the Fukushima Dai-ichi nuclear power plant were observed for the long term in Ohori River, Chiba Prefecture, Japan. In this presentation, we report time variation of concentrations of ^{134}Cs, ^{137}Cs and ^{129}I in the suspended soils (SS) and dissolved matter (DM) from the flow of the river were measured. The concentrations of radioactive cesium 134 and 137 in SS were gradually decreasing in long term observation and rising on the rainy day. The DM/SS ratios of ^{137}Cs were almost constant over time. In the DM, the ^{129}I data showed strong correlation with cesium data.

Keywords

Cesium-134, 137 ; Iodine-129 ; time variation ; river water

I. INTRODUCTION

Radioactive cesium and iodine emitted from the Fukushima Dai-ichi nuclear power plant were detected from environmental water, reflecting an aspect of dynamics of these radioactive nuclides in the environment. In the metropolitan area, comparatively high concentration of radioactive cesium isotopes were detected from sediment of Ohori River in Chiba Prefecture[1]. In this work, the long-term variations of the concentrations of the radioactive cesium and iodine in the suspended soils (SS) and dissolved matter (DM) were measured for Ohori River, and the trend of nuclides was discussed.

II. METHODS

The SS samples of two or three weeks are collected by the SS Auto-Sampler[2] which installed at the middle of river near the Showa-bridge, and the river water samples are collected every two or three weeks in the same place from May, 2012 at Ohori River. The river water was filtrated. The SS was defined as residue of 0.7 μm filter and the DM was defined as the component passing through the 0.2 μm filter. The concentrations of ^{134}Cs and ^{137}Cs were determined from the γ-ray spectrum obtained by HPGe detectors. ^{129}I in the river was investigated about the same samples by AMS at MALT, The Univ. of Tokyo[3].

III. RESULTS AND DISCUSSION

Time variations of concentration of radioactive cesium in the SS of Ohori River are shown in Fig.1. The average concentrations of radioactive cesium were gradually decreasing in long term observation. The concentration of radioactive nuclides in the SS sampled by Auto-Sampler was treated as average for a certain period. The momentary concentrations of radionuclides in the SS were obtained from the river water sampled every two or three weeks. In most points, the momentary concentration was lower than the average concentration, but a few points which corrected in rainy differed from the tendency due to rain fall. The DM/SS ratios of ^{137}Cs were almost constant, which may considered as the equilibrium constant of cesium between SS and DM. In the DM, the ^{129}I data showed strong correlation with cesium data. The iodine data, however, is insufficient.

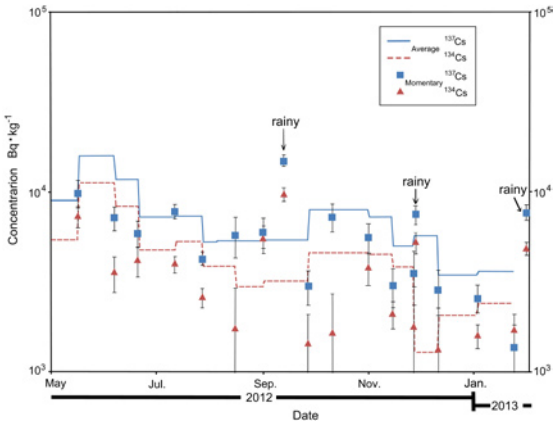

Fig.1. Time variation of concentration of radioactive cesium in SS of Ohori River. Solid line and dashed line show the average concentration of ^{137}Cs and ^{134}Cs, respectively. Square points and triangular points show momentary concentrations of ^{137}Cs and ^{134}Cs, respectively.

REFERENCES

[1] Ministry of Environment, 2011, http://www.env.go.jp/jishin/monitoring/result_pw111222-1.pdf
[2] Phillips et al. (2000) Hydrol. Process. 14, 2589-2602.
[3] H. Matsuzaki et al., Nucl. Instr. and Meth. B, 259, 2007, 721–726.

Ra isotopes in Na-Cl type groundwater in Japan

Junpei Tomita[1, a], Takahiro Takada[1], Seiya Nagao[1], Masayoshi Yamamoto[1]
[1] Low Level Radioactivity Laboratory, Institute of Nature and Environmental Technology, Kanazawa University, Wake, Nomi, Ishikawa 923-1224, Japan
[a] Department of Radiation Protection, Nuclear Science Research Institute, Japan Atomic Energy Agency, Tokai-mura, Ibaraki 319-1195, Japan.

Abstract – Radium isotopes (^{226}Ra and ^{228}Ra) were measured for Na-Cl type groundwater samples collected from Hokkaido, Aomori, Akita and Yamagata Prefectures in Japan. The ^{226}Ra contents varied in the wide range from 9 - 5000 mBq kg^{-1} and their values were roughly correlated to the total dissolved solid (TDS). Activity ratios of ^{228}Ra/^{226}Ra in groundwater ranged from 0.3 – 4.2 and most of them clustered around those of ^{232}Th/^{238}U of common rocks in Japan. These observations agreed well with the previous results from Ishikawa, Toyama and Niigata Prefectures, and overall indicated that Ra was mainly transported into the groundwater by α-recoil process and its concentration in groundwater was constrained by adsorption-desorption reaction depending on salinity.

Keywords – Ra isotopes, Na-Cl type groundwater, α-recoil, adsorption-desorption reaction

I. INTRODUCTION

Radium isotopes (^{226}Ra ($T_{1/2}$=1600 y) and ^{228}Ra ($T_{1/2}$= 5.75 y)) in groundwater have been investigated worldwide from the various viewpoints such as geochemical interest and radiation protection. Activities of Ra isotopes in groundwater vary widely, and anomalously high ^{226}Ra contents over several tens of Bq kg^{-1} have been found in saline waters and brines.

In Japan, Ra isotopes in groundwater have been investigated mainly in relation to the radioactive hot spring, and groundwaters with high ^{226}Ra concentration over 1 Bq kg^{-1} have been found at hot springs such as Arima and Masutomi. Since these hot springs are commonly originated from granite areas where have relatively high U contents, it was considered that such higher ^{226}Ra in water was attributed to the U in granite. Recently, Na-Cl type groundwaters with intermediate salinity (ca.1-36‰) have been obtained from the deep wells with the development of more sophisticated drilling techniques. We have studied the distribution of Ra isotope concentrations in these Na-Cl type groundwaters from coastal area and sedimentary basin in Ishikawa, Toyama and Niigata Prefectures facing to the Japan Sea of Central Japan, and found that some of them contained relatively high ^{226}Ra over 1 Bq kg^{-1} even in coastal areas and sedimentary basin.

Authors are interested in clarifying the geochemical mechanism of such high ^{226}Ra occurrence, and expanded research to groundwater at Hokkaido and Tohoku Districts (Aomori, Akita and Yamagata Prefectures). In this study, we report the Ra contents in Na-Cl type groundwaters from these areas. Constraining factors which Ra content becomes higher in groundwater will be mainly discussed, including the results obtained previously from other areas such as Ishikawa, Toyama and Niigata Prefectures.

II. MATERIAL AND METHODS

Na-Cl type groundwater samples were collected from the coastal area and sedimentary basin in Hokkaido, Aomori, Akita and Yamagata Prefectures in Japan. Radium isotopes were co-precipitated with $BaSO_4$, and their activities were determined by γ-ray spectrometry.

III. RESULTS AND DISCUSSION

Activities of ^{226}Ra in groundwater from Hokkaido, Aomori, Akita and Yamagata Prefectures were observed in the wide range from 9 - 5000 mBq kg^{-1}. These ^{226}Ra activities in groundwater samples showed an increasing tendency with increasing total dissolved solid (TDS) (Fig. 1). Activity ratios of ^{228}Ra/^{226}Ra of them varied from 0.3 – 4.2, and most of them clustered around 0.5 - 2. These ratios were nearly similar to those of ^{232}Th/^{238}U of common rocks in Japan. These observations agreed well with the previous results from Ishikawa, Toyama and Niigata Prefectures.

Ra isotopes are supplied into groundwater by some processes: 1) decay of dissolved parent nuclides (Th is considered as insoluble element); 2) weathering and/or dissolution of aquifer rock; 3) α-recoil at water-rock interface; and 4) desorption reaction at water-rock interface.

Results both relationships between ^{226}Ra and TDS and activity ratios of ^{228}Ra/^{226}Ra in groundwater samples obtained here indicated that Ra was mainly ejected into the groundwater by α-recoil process and its Ra was constrained by adsorption-desorption reaction depending on salinity.

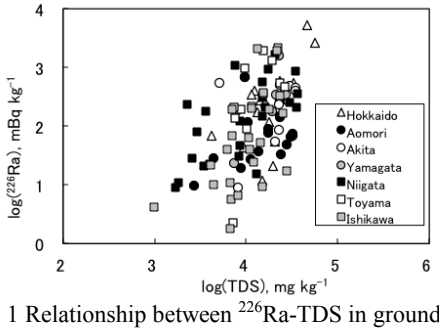

Fig. 1 Relationship between ^{226}Ra-TDS in groundwater

A new method to estimate $^{210}Po/^{210}Pb$ activity ratio in atmospheric aerosol by alpha spectrometry

N. Momoshima[1], S. Nishio[2], K. Hibino[2], S. Sugihara[1]
[1] Radioisotope Center, Kyushu University, Hakozaki, Higashi-ku, Fukuoka 812-8581, Japan
[2] Graduate School of Science and Technology, Kumamoto University, Kurokami, Kumamoto 860-8555, Japan

Keywords – aerosol, ^{210}Po ^{210}Pb activity ratio, alpha spectrometry

Various kinds of radionuclides are observed in the atmosphere, among them radon and its daughter nuclides attached to aerosol are most abandon and the daughter nuclides finally decay to ^{210}Pb within a few hours. The formed ^{210}Pb (22.3 y) decays to ^{210}Bi (5 d) followed by ^{210}Po (138 d). The half life of ^{210}Po is rather long compared to the removal process functioning to atmospheric aerosols; therefore $^{210}Po/^{210}Pb$ activity ratio as well as $^{210}Bi/^{210}Pb$ activity ratio is usable to estimate residence time of aerosol in the atmosphere.

The growth curves of ^{210}Po from ^{210}Pb in aerosol are shown in Fig.1 as a function of initial $^{210}Po/^{210}Pb$ activity ratios. The growth pattern differs depending upon the initial $^{210}Po/^{210}Pb$ activity ratio. The initial activity ratio varies in the environment due to additional input of ^{210}Po to atmosphere from such as volcanic release, fire burning of vegetation etc. Atmospheric migration of soil dusts increases the initial activity ratio because of secular radioactive equilibrium in soil. Under the general environmental circumstances major radionuclide in aerosol would be ^{210}Pb and then, ^{210}Po is considered to be the main alpha particle emitted from aerosol. If we measure a growth of ^{210}Po activity with time and compared with growth pattern shown in Fig. 1, we can estimate the $^{210}Po/^{210}Pb$ activity ratio of the aerosol samples.

The theoretical calculation of ^{210}Pb-^{210}Bi-^{210}Po equilibrium suggests that $^{210}Po/^{210}Pb$ slightly depends on initial $^{210}Bi/^{210}Pb$ activity ratio. The measurement time of a few days would be necessary for alpha spectrometry to obtain statistically acceptable counts. Then, the ^{210}Po growth pattern dependent on the initial $^{210}Bi/^{210}Pb$ activity ratio would be obscure. However, the proposed method is simple and no chemical separation is necessary.

The growth of ^{210}Po activity in the aerosol collected on a membrane filter and measured several times with a silicon surface barrier detector of an alpha spectrometer is shown in Fig. 2 as an example. The growth pattern is analyzed under the assumption that the initial $^{210}Bi/^{210}Pb$ activity ratio is 0.6, which would be the representative value in the general environment [1]. The least square fitting was carried out to obtain the initial ^{210}Pb and ^{210}Po counts. The measurements were done at the identical geometrical configuration between the detector and the sample, and in a series of measurements the same detector of the same alpha spectrometer system was used.

[1] Rangarajan, C., J. Environ. Radioactivity, 15, 193-206(1992)

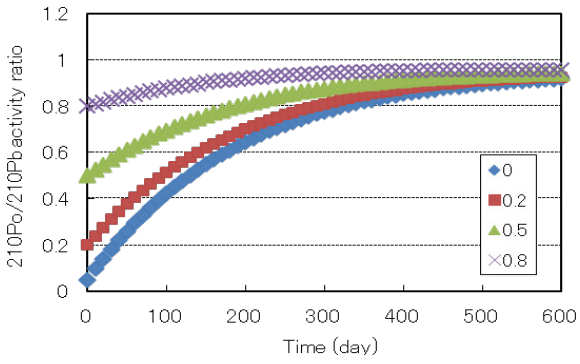

Fig. 1 Theoretical change in $^{210}Po/^{210}Pb$ activity ratio with time at different initial $^{210}Po/^{210}Pb$ activity ratio.

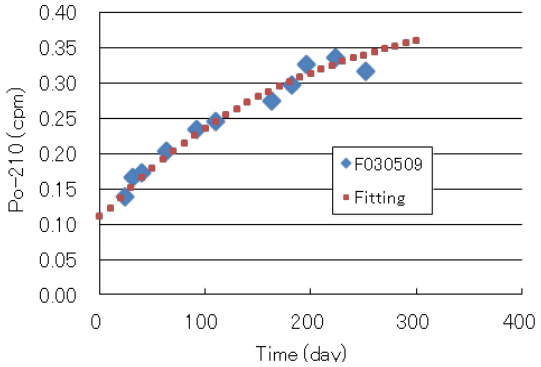

Fig. 2 Counts of ^{210}Po measured with the alpha spectrometer for the aerosol collected on a membrane filter and the theoretical counts obtained by least square fitting.

APSORC'13 - 5th Asia-Pacific Symposium on Radiochemistry
Kanazawa, Japan, 22-27 September 2013

Sedimentary environment inferred from sedimentation rates by ^{210}Pb and ^{137}Cs and their inventories in Mutsu Bay, Japan

Kazuhito Hamataka[1], Seiya Nagao[1], Michio Kato[2], Isao Kudo[3], Masayoshi Yamamoto[1]
[1] Low Level Radioactivity Laboratory, KINET, Kanazawa University, Ishikawa 923-1224, Japan
[2] Graduate School of Science, Kanazawa University, Kanazawa, Ishikawa 920-1192, Japan
[3] Graduate School of Fisheries Sciences, Hokkaido University, Sapporo 060-0808, Japan

Abstract –Fourteen sediment cores were collected from Mutsu Bay, Aomori in Japan, and excess ^{210}Pb and ^{137}Cs were measured γ-spectrometrically. The spatial distributions of sedimentation rates by ^{210}Pb$_{ex}$ and ^{137}Cs and their inventories were studied in order to clarify whole pictures about the sedimentary environment of Mutsu Bay. Excessively post-depositional mixing (up to a depth of 10-15 cm) of surface sediments by bioturbation was observed on the ^{210}Pb$_{ex}$ depth profiles in cores from the offshore areas. The sedimentation rates calculated varied in the wide range from 0.04 to 0.2 g/cm^2/y. The sedimentation rates using ^{137}Cs method could not be applied. Apart from the ^{210}Pb$_{ex}$ inventories from the nearshore area, the responding inventories (17-30 kBq/m^2) from the offshore area were higher than the reported value of ca.15 kBq/m^2 in the surrounding soils, indicating that the sediment focusing due to the inner current etc., to the deeper area from the surrounding nearshore area, affects the sediment accumulation in the offshore area.

Keywords –Mutsu Bay, Aomori, sedimentation rate, inventory, ^{210}Pb, ^{137}Cs, sedimentary environment

I. INTRODUCTION

Semi-enclosed bay is sensitive to human activity and change of natural environment, and these directly and strongly impact in its sedimentary environment.

Mutsu Bay (surface area of 1580 km^2, average depth of 34 m, and maximum depth of 75 m), which is located in the north of Honshu in Japan, is indirectly connected with the open sea by a narrow channel through which seawater flows in and out the bay. The east floor of Mutsu Bay is relatively flat and shallow (40 m deep on average). The coastal areas are excessively populated and extensive scallop farming has been popularly practiced since 1970s. The present–day, death of scallop due to overcrowded cultivation and generation of red tides by declining water quality are going on, and muds are markedly accumulating in the offshore areas (Minoura *et al*. (1992)).

We have been interested in clarifying whole pictures about such sedimentary environment of Mutsu Bay, investigating the sediment rates by using radioactive ^{210}Pb and ^{137}Cs and their inventories in sediments.

II. MATERIAL AND METHODS

Core sampling: The core sediment samples were collected during cruises in May and August 2011, and June and September 2012. A small gravity corer (3.5 or 8.0 cm in diameter) was used to collect surface sediments (20-40 cm long) at 14 locations (Fig. 1). The obtained cores were immediately cut every 1 cm from top along the core, and after taking them to laboratory the samples were freeze-dried.

Measurements of ^{210}Pb and ^{137}Cs: The samples were then sieved through a 2-mm mesh to remove pebbles and fragments of shell, and pulverized in an agate mortar to obtain homogeneous samples. An aliquot of 5-10 g of sample was packed into a plastic vessel and stored for more than 3 weeks. The ^{210}Pb, ^{226}Ra (from daughter nuclide ^{214}Pb) and ^{137}Cs were measured by a low–background γ-ray spectrometer with a high pure Ge detector (planar or well type). The spectrometer was calibrated with standards prepared by the New Brunswick Laboratory (NBL) reference materials No. 42-1 (4.04% uranium), and analytical grade KCl. Unsupported ^{210}Pb activity (^{210}Pb$_{ex}$) was calculated from the difference between the total ^{210}Pb and the ^{226}Ra (from ^{214}Bi) contents.

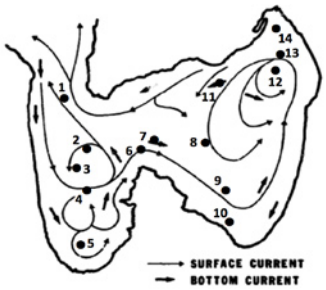

Fig. 1 Sampling sites in Mutsu Bay

III. RESULTS AND DISCUSSION

To date, activity measurements of ^{210}Pb and ^{137}Cs were finished for cores from St.1 to St.10. Overall, the sediments (Sts. Sts. 2-4 and 6-8) from the offshore area were mostly mud, while sand and coarser sediments, with their low mud contents, are restricted to the nearshore area. Surface mixed layers (up to a depth of 10-15 cm) were observed on the ^{210}Pb$_{ex}$ depth profiles from the offshore area, evidencing the excessively post-depositional mixing of surface sediments by bioturbation and so on. For other sites, ^{210}Pb$_{ex}$ concentrations declined more or less exponentially with depth. Sedimentation rates calculated for these cores varied in the wide range from 0.04 to 0.2 g/cm^2/y. Sedimentation rates using ^{137}Cs method could not be applied. A generally increasing trend in sedimentation rate after the late 1970s, when correspond to the rapid increase of scallop-production activity, was clearly observed at St.10.

Excess ^{210}Pb and ^{137}Cs inventories were calculated as the sum of ^{210}Pb$_{ex}$ and ^{137}Cs through a sediment core, respectively. The ^{210}Pb$_{ex}$ inventories ranged from 7-30 kBq/m^2. Apart from the values (7-9 kBq/m^2) from the nearshore areas, the responding inventories (17-30 kBq/m^2) for cores (Sts. 2-4 and 6-8) from the offshore areas were somewhat higher than the reported value of ca.15 kBq/m^2 estimated for the surrounding soils, indicating that the sediment focusing due to the inner current etc., to the deeper area from the surrounding nearshore area, affects the sediment accumulation in the offshore area. The ^{137}Cs inventories (0.08-0.14 kBq/m^2) were clearly lower than its inventories (around 3 kBq/m^2) in the surrounding soils. Further works are going on organic contents and grain-size of sediments.

K. Minoura et al. (1992), *Marine Geology,* 103, 487-502.

Distribution of radiocarbon in Japanese agricultural soils

Nobuyoshi Ishii, Keiko Tagami, Shigeo Uchida
Office of Biospheric Assessment for Waste Disposal, National Institute of Radiological Sciences

Abstract – Distributions of C-14 in solid, liquid, and gas phases were determined by batch sorption tests using 142 Japanese agricultural soil samples. The agricultural soils used were classified into "paddy" and "upland" soils. Each of the soil samples was suspended in deionized water containing [1, 2-C-14] sodium acetate and shake-incubated for 7 days. After the incubation, the distributions of C-14 in solid, liquid and gas phases were approximately 35%, 5% and 60% of the spiked C-14, respectively. These results suggested that if the C-14 of acetate migrated from a TRU repository site to agricultural soils, most of the C-14 would be released into the air and the rest would be distributed in the soil solid phase. The distribution of C-14 in gas phase was lower for upland soils than for paddy soils..

Keywords – TRU waste, Radiocarbon, Distribution, Agricultural soils

I. INTRODUCTION

Transuranic (TRU) waste is generated during the operation and dismantling of reprocessing facilities and mixed oxide (MOX) fuel fabrication facilities, and the waste contains radionuclides that have long half-lives. The dominant nuclides contributing to the dose from TRU waste are C-14 and I-129 [1]. These radionuclides, therefore, are very important in safety assessments for geological repositories of TRU waste.

C-14 could be released from a geological repository over a timescale of several thousand years. Because there is little information regarding reliable migration and realistic transport models, the possible migration of C-14 from a TRU repository site to the biosphere through groundwater presents some concern. It is, therefore, required to clarify the behavior of C-14 in the environment due to the reduction of exposure to C-14.

In general the environmental behavior of chemicals is influenced by various factors such as land use, soil type, temperature, pH, oxidative conditions and so on. The behavior of C-14 may differ between paddy and upland soils. In this study, distribution of C-14 for both Japanese paddy and uplands was determined and compared. The relationships among the distribution of C-14 and selected soil properties were discussed.

II. MATERIALS AND METHODS

A total of 142 agricultural soils (63 paddy soils and 79 upland soils) were collected throughout Japan. The soil samples were dried at room temperature, and then passed through a 2 mm mesh sieve to obtain fine particles.

[1,2-C-14] sodium acetate was used as the chemical form of C-14. This solution was diluted with deionized water to a specific activity of 1.8 kBq mL^{-1} and was filter-sterilized to remove microorganisms [2]. The specific activity corresponded to 4.2 x 10^{-1} nmol mL^{-1}.

For batch culture experiments, 0.5-g of air-dried soil sample was soaked with a 5-mL of the radioactive solution. The culture was shake-incubated at 25℃ for 7 days in the dark. After the incubation, the C-14 activities of the culture were determined to estimate the distribution of C-14 in solid, liquid and gas phases by measuring C-14 in solid, liquid phase with a liquid scintillation counter.

III. RESULTS AND DISCUSSION

Distribution of C-14 in solid, liquid and gas phases were determined on day 7 of incubation. The mean values of those distributions were 59.1 ± 8.6% in as phase, 35.4 ± 7.7% in solid phase, and 5.5 ± 5.4% in liquid phase. For each phase, a positive excess kurtosis was found (2.7 for solid, 7.1 for liquid and 4.2 for gas), and the interquartile range, which is the difference between the third and first quartiles, was less than 10%. Results of these statistical analyses mean that the distribution of C-14 in each phase had small variation ranges for Japanese agricultural soils. It should, however, note that there were big differences between the two extreme values for each phase. These values were far from the average and thus must be paid attention in safety assessments for geological repositories of TRU waste.

Distribution in liquid phase was correlated positively with pH of the culture solution. Similar results were found in our previous study [3].

Significant differences in the distribution of C-14 between paddy and upland soils were found for all phases. Distributions in solid and liquid phases were higher for the upland soils than for paddy soils, but, on the other hand, distribution in gas phase was lower for upland soils than for paddy soils. The difference in distribution in liquid phase may be explained by pH of the solution because pH of the upland samples was significantly higher than that of the paddy samples.

This work was supported by the Agency for Natural Resources and Energy, the Ministry of Economy, Trade and Industry (METI), Japan.

REFERENCES

[1] JAEA, FEPC, Second progress report on research and development for TRU waste disposal in Japan –Repository design, safety assessment and means of implementation in the generic phase-, JAEA-Review 2007-010, FEPC TRU-TR2-2007-01(2007).

[2] N. Ishii, S. Uchida, "Bacteria contributing to behaviour of radiocarbon in sodium acetate," Radiat. Prot. Dosimetry. 146, 151-154 (2011).

[3] N. Ishii, H. Koiso, H. Takeda, S. Uchida, "Partitioning of ^{14}C into solid, liquid and gas phases for various paddy soils in Japan," J. Nucl. Sci. Technol., 47, 238-243 (2010).

APSORC'13 - 5th Asia-Pacific Symposium on Radiochemistry
Kanazawa, Japan, 22-27 September 2013

Lateral distributions of $^{228}Th/^{228}Ra$ and $^{228}Ra/^{226}Ra$ ratios in surface waters of the Sea of Japan and their physical implications

Y. Furusawa[1], M. Inoue[1], S. Nagao[1], M. Yamamoto[1], Y. Hamajima[1], H. Kofuji[1], K. Yoshida[1]
Y. Nakano[1], K. Fujimoto[2], A. Morimoto[3], T. Takikawa[4], Y. Isoda[5]
[1]Low Level Radioactivity Laboratory, Kanazawa University
[2] Fisheries Research Agency, National Research Institute of Fisheries Science
[3]Hydrospheric Atmospheric Research Center, Nagoya University
[4]National Fisheries University
[5]Graduate School of Fisheries Sciences, Hokkaido University

Abstract –
We examined $^{228}Th/^{228}Ra$ and $^{228}Ra/^{226}Ra$ ratios in surface waters from the Sea of Japan by low background γ-spectrometry. These lateral distributions clarified the aspects of physical movement of geochemical species on surface.

Keywords –
$^{228}Th/^{228}Ra$ ratio, $^{228}Ra/^{226}Ra$ ratio, Sea of Japan

I. INTRODUCTION

Many researchers have studied the flow pattern of the Tsushima Warm Current (TWC), a major feature of the flow patterns in the Sea of Japan, using various techniques [1]. However, the origin and characteristics of the circulation pattern of the TWC have not yet been well clarified because of the markedly complicated seasonal variation in the circulation. The seasonal variation in the $^{228}Ra/^{226}Ra$ ratio recorded for the surface waters of the Sea of Japan is considered to be mainly controlled by the remarkable changes in the mixing ratio of the ^{228}Ra-poor Kuroshio ($^{228}Ra/^{226}Ra$ = 0.2) and the ^{228}Ra-rich continental shelf waters ($^{228}Ra/^{226}Ra$ = 3.5) within the East China Sea (ECS) [2]. Activity of particle-reactive ^{228}Th (half-life, 1.91 y) in seawater is governed by biogenic particle behavior, and therefore the combination of ^{228}Th and ^{228}Ra activities ($^{228}Th/^{228}Ra$ ratio) in seawater samples is useful for the study of scavenging processes in the Sea of Japan.

II. METHOD AND SAMPLING SITE

We collected 165 surface water samples (20 L) during the research expeditions of T/V *Oshoro Maru*, R/Vs *Mizuho Maru*, *Tansei Maru*, *Soyo Maru*, and *Tenyo Maru* (Fig. 1). Low-background γ-spectrometry was performed on the samples using Ge-detectors at the Ogoya Underground Laboratory in Japan [3, 4].

III. RESULTS AND DISCUSSION

Along the Tsushima Strait, the $^{228}Ra/^{226}Ra$ ratio of samples on the transect A gradually increased from south to north (from 0.8 to 2.3). On the transect B, the $^{228}Ra/^{226}Ra$ ratio of coastal-side waters (0.6-0.8) was lower than that of offshore-side waters (1.2). This reflects a higher mixing ratio of the Kuroshio water in the Honshu Island side. On the other hand, $^{228}Th/^{228}Ra$ ratio of waters on the transect A exhibited gradual decrease (<0.01 to 0.12) from south to north, dominantly reflecting a higher flux of biogenic particles in shelf water [5]. In this study, we examined the lateral distributions of $^{228}Th/^{228}Ra$ ratio as well as $^{228}Ra/^{226}Ra$ ratio on surface of the Sea of Japan and clarify the circulation patterns of particles and water masses. This is an operation that we are currently engaged in, by obtaining additional surface water samples.

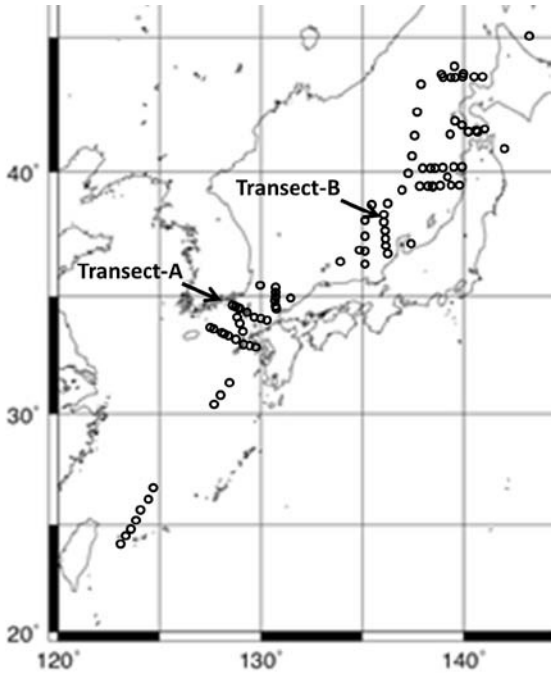

Fig. 1. Sample locations for seawater

References
[1] Hase *et al.* (1999) *J. Oceanogr.* **55**, 217-234
[2] Nozaki *et al.* (1989) *Geophys. Res. Lett.* **16**, 1297-1300
[3] Y. Nakano *et al.* (2008) *J. Oceanogr.* **64**, 713-717
[4] Y. Hamajima & K. Komura (2004) *Appl. Radiat. Isot.* **61**, 179-183
[5] M. Inoue *et al.* (2012) *Geochem. J.* **46**, 311-320

Vertical profiles of ^{228}Ra and ^{226}Ra activities in the Sea of Japan and their implications for water circulation

M. Inoue[1], M. Minakawa[2,*], K. Yoshida[1], Y. Nakano[1], H. Kofuji[1], S. Nagao[1], M. Yamamoto[1], Y. Hamajima[1]

[1]Low Level Radioactivity Laboratory, Kanazawa University
[2]Fisheries Research Agency, National Research Institute of Fisheries Science
*present address; National Research Institute of Aquaculture

Abstract-

By employing low-background γ-spectrometry combined with minimal radiochemical processing, we examined vertical profiles of ^{226}Ra ($t_{1/2}$ = 1600 y) and ^{228}Ra (5.75 y) activities in water columns in the Sea of Japan. The results indicate continuous delivery of ^{228}Ra to the Deep Proper Water (DPW), and clarify aspects of the transport of ^{226}Ra and ^{228}Ra by water circulation.

Keywords- ^{226}Ra, ^{228}Ra, Deep Proper Water, residence time, low-background γ-spectrometry

I. INTRODUCTION

The Sea of Japan is surrounded by the Eurasian continent and the Japanese Archipelago, and is connected to the Pacific and other marginal seas by the very shallow Tsushima, Tsugaru, and Soya Straits (≤~150 m of depth). Therefore, the deep water, so-called the Proper Water of the Sea of Japan, has no influx from a surrounding sea, indicating unique vertical water circulation [1]. ^{226}Ra and ^{228}Ra of seawater have been used as powerful tracer for studying the migration of water masses. However, standard γ-spectrometry for measuring ^{228}Ra of deep seawater usually required very large volumes (hundreds to thousands of liters) because of its low activity and previously reported data are not sufficient to allow investigating the details of the vertical distribution of ^{228}Ra in oceans. In the present study, we analyzed seawater samples from the Japan Basin, Yamato Basin, and Tsushima Basin within the Sea of Japan, for ^{226}Ra and ^{228}Ra.

II. SAMPLES and EXPERIMENTAL

We analyzed a total of seawater samples collected in water columns in the Sea of Japan for ^{226}Ra and ^{228}Ra. Low-background γ-spectrometry was performed using well-type Ge-detectors, which are located at the Ogoya Underground Laboratory, Japan [2]. Detailed explanations of these experimental procedures were presented elsewhere [3]. γ-Peaks for ^{228}Ra measurement (^{228}Ac; 338 and 911 keV) on a blank sample, which was performed our experimental procedures on 50 L of distilled water, were "not detected" level. Therefore, we corrected only least Ra-contaminated Ba-reagent blank, which accounted for <1% ^{228}Ra for our water samples.

III. RESULTS and DISCUSSION

In the Japan Basin, the ^{226}Ra activity of the water samples gradually increased from surface to the DPW (1.5-2.3 mBq/L). The ^{228}Ra activity of the water exhibited steep gradients with depth from the surface to the Upper Proper Water (1.8-0.2 mBq/L), and short-lived ^{228}Ra is continuously delivered to the DPW by the active water circulation before it radioactively decays. The results indicate continuous delivery of ^{228}Ra to the DPW, and clarify aspects of the transport of ^{226}Ra and ^{228}Ra by water circulation. The residence time of the DPW is calculated to be about 100 y.

Acknowledgements

We thank the researchers, captain, and crew of R/V *Soyo Maru* for their assistance during sampling.

References
[1] Gamo, T. and Horibe, Y. (1983) *J. Oceanogr. Soc. Jpn* **39**, 220-230:
[2] Hamajima, Y. and Komura, K. (2004) *Appl. Radiat. Isot.* **61**, 179-183:
[3] Nakano, Y. *et al*. (2008) *J. Oceanogr*. **64**, 713-717.

Induced radioactivity in air and water at medical accelerators

K. Masumoto[1], K. Takahashi[1], H. Nakamura[1], A. Toyoda[1], K. Iijima[1], K. Kosako[2], K. Oishi[2], F. Nobuhara[3]

[1]High Energy Accelerator Research Organization (KEK)
[2]Shimizu Co.
[3]Tokyo Nuclear Service Co

Abstract – Activation of air and water has been evaluated at the 10 and 15 MeV linear electron accelerator facilities. At 15 MeV irradiation, the activity of 10-min-half-life ^{13}N was observed in the case of the air in the glove box. Air and water samples were also bombarded by 250 MeV protons and 400 MeV/u carbon, and the irradiation dose was 10 Gy at the isocenter. Upon the ion-chamber monitoring of the air sampled from the glove box, ^{15}O, ^{13}N, and ^{11}C activities were mainly observed. At the end of proton and carbon irradiation, the activity of the water was found to be about 10 kBq•cm^{-3} and several kBq•cm^{-3}, respectively. From the decay analysis of the induced activity in water, ^{15}O, ^{13}N, and ^{11}C were detected.

Keywords – Activation, Air, Water, Medical accelerator

I. INTRODUCTION

Accelerators have been widely used in medical applications, especially in cancer treatment. Electron linear accelerators have been used in hospitals for the X-ray irradiation of diseased organs. Particle accelerators have also been used in recent times as a powerful tool for cancer therapy. In this work, we investigated the activation of air and water in treatment rooms in hospitals for radiation safety management. In the case of photonuclear reaction, several positron emitting radioisotopes such as ^{15}O and ^{13}N can be produced by the bremsstrahlung at higher than 15 MeV in air. In case of hadron irradiation, many radioisotopes might be produced by high-energy particles. In this work, we measured the induced activity in air and water caused by the electron and hadron accelerators employed for medical use, in order to determine whether the concentration of radioactivity was below regulated levels.

II. EXPERIMENTAL

A. Activation of air and water

(1) Electron accelerator:10 and 15MeV irradiations for 10 min were performed by Varian Clinac 2100C and Clinac iX, respectively. Doses were 40 and 60 Gy at the isocenter, respectively.
(2) Proton accelerator: 200 MeV proton beam was irradiated for 3.25 min on an area of 0.15 m × 0.15 m, and 10 Gy at the isocenter.
(3) Heavy ion accelerator: Carbon beams of 400 MeV/nucleon was irradiated for 2 min on an area of 0.15 m × 0.15 m, and 10 Gy at the isocenter.

B. Activity measurement

(1) Air: The air in a glove box of 250L was irradiated and sampled with a vacuum ionization chamber for measurement. An aerosol was also collected on a HEPA filter by an air sampler.
(2) Water: After irradiation, dose rate of water surface was monitored using a NaI(Tl) survey meter and the gamma-ray spectrum was measured using a $LaBr_3$(Ce) scintillation spectrometer.

III. RESULTS AND DISCUSSION

At the 15 MeV irradiation of bremsstrahlung, the activity of ^{13}N was 0.87 Bq•cm^{-3} at the end of the irradiation. As the activity of ^{13}N was also detected on the filter paper, NO_x fomation was presumed. Activity of water could not be detected.

In case of 250 MeV proton irradiation, activities of ^{15}O, ^{13}N, and ^{11}C were found to be 1.9, 0.6, and 0.6 Bq•cm^{-3} at the end of irradiation in air sampled from the glove box. The activity of ^{13}N was also detected on the filter paper. By the decay curve analysis of water activity obtained from the surface dose rate of the polyethylene tank, activities of ^{14}O, ^{15}O, ^{13}N, and ^{11}C were found to be 91000, 12000, 1100, and 190 Bq•cm^{-3} at the end of irradiation, respectively.

In case of carbon irradiation, we performed irradiation of air for two times and fitted the decay curve for ^{14}O, ^{15}O, ^{13}N, ^{11}C, and ^{41}Ar. Average activities of ^{14}O, ^{15}O, ^{13}N, ^{11}C, and ^{41}Ar were 0.8, 1.1, 0.08, 0.09, and 0.006 Bq•cm^{-3} at the end of irradiation. By the decay curve analysis of water activity obtained from the surface dose rate of the polyethylene tank, activities of ^{14}O, ^{15}O, ^{13}N, and ^{11}C were found to be 2100, 2000, 100 and 180 Bq•cm^{-3} at the end of irradiation, respectively.

IV. CONCLUSION

In case of 10 MeV irradiation, we could not detect the residual activity in air and water. In the case of 15 MeV irradiation, we observed ^{13}N in the air sampled from the glove box irradiated in front of the beam exit window and on the filter collected by the air samplers in the irradiation room and the maze. In the case of 250 MeV proton activation and 400 MeV/u carbon irradiation, activation of air was not excessively high and the induced activity was comparable to that induced by 15 MeV irradiation for the electron accelerator. But induced activity of water was extremely high. The main radionuclides detected were ^{13}N and ^{11}C, 10 min after irradiation with protons and ^{11}C, 20 min after irradiation with carbon

Radioactivity determination of ^{14}C and ^{3}H in solid waste samples by liquid scintillation counter

Jong-Myoung Lim[1*], Mun-Ja Kang[1], Kun-Ho Chung[1], Chang-Jong Kim[1], Geun-Sik Choi[1]
[1]Environmental Radioactivity Assessment Team, Korea Atomic Energy Research Institute
989-111 Deadeok-daero, Yuseong-gu, Daejeon, 305-353, Korea

Abstract –This study reports the comprehensive efforts made to evaluate the analytical procedure for ^{3}H and ^{14}C in solid sample. The sludge samples from National Physical Laboratory (NPL) proficiency program (Environmental Radioactivity Proficiency Test Exercise 2012) were combusted by high temperature furnace and analyzed in LSC. The various performance tests of analytical method were conducted with standard solutions. The detection limit and uncertainty of the method were also evaluated in detail. Major factors of standard uncertainty were grouped into counting error, sample homogeneity, and efficiency calibration. Finally, sensitivity tests of these major factors were performed.

Keywords – tritium, ^{14}C, radioactivity, combusting, sludge,

As an attempt to reduce social costs and apprehension arising from the radioactivity in environments, an accurate and rapid assessment of radioactivity is highly desirable. Nuclear wastes (e.g., sludge, activated carbon, oils, resins, etc.) have been consistently generated by actions to prevent the emission of radioactive pollutants from nuclear sites. To decide a proper disposal option of these nuclear wastes, we need an analytical method that can determine the radioactivity of ^{3}H and ^{14}C which exists in very low levels.

The ^{3}H in the water (tritiated water; HTO) is major chemical form in the environment. Through the natural or industrial process with organic compounds, tritium is easily converted into organic bound tritium (OBT). The HTO form is easily lost at a temperature around 120°C, whereas the strongly-bounded tritium with the form of non-HTO requires high temperature of a few hundred degrees in centigrade for complete extraction. The ^{14}C decays into ^{14}N through beta decay(E_{max}=156 kev). The main anthropogenic origin of ^{14}C is thermal neutron activation of ^{14}N in the nuclear reactor by a neutron capture reaction $^{14}N(n,p)^{14}C$. For extraction of ^{14}C which exist in lattice structure, it requires also high temperature to oxidize $^{14}CO_2$ gas.

Radioactivity of ^{3}H and ^{14}C in waste water sludge has been determined by the following combustion method. The sludge samples were combusted in a purpose-designed tubular high temperature furnace (Raddec Pyrolyser Trio^{TM}) which consist of six quartz tubes with the length of 1.5 m and the diameter of 1.5 cm. The combusting temperature was controlled stepwise up to 800°C. The ^{3}H and ^{14}C were trapped in 0.1 M HNO_3 and carbon absorber solution (Carbo-Sorb® E, Perkin Elmer), respectively. The measuring of the radioactivity was carried out in LSC (Walac 1220 Quantulus, Perkin Elmer).

This study reports the comprehensive efforts made to evaluate the analytical procedure for ^{3}H and ^{14}C in solid sample. The sludge samples from National Physical Laboratory (NPL) proficiency program (Environmental Radioactivity Proficiency Test Exercise 2012) were combusted by high temperature furnace and analyzed in LSC. The various performance tests of analytical method were conducted with standard solutions. In order to evaluate dynamic range of the method, real samples with spiking ^{3}H and ^{14}C standard solution were analyzed. Duplicated samples (n=6) were analyzed to see the repeatability of this method. The results showed that relative standard deviations for ^{3}H and ^{14}C are about 11% and 2.9%, respectively. The activity concentrations were compared statistically with the assigned values. The deviation between the two values for ^{3}H and ^{14}C are about 14.5% and 5.7%, respectively. The detection limit and uncertainty of the method were also evaluated in detail. Major factors of standard uncertainty were grouped into counting error, sample homogeneity, and efficiency calibration. Finally, sensitivity tests of these major factors were performed.

Table 1. Uncertainty budget of the analytical procedure for solid sample

	Uncertainty factor	^{3}H	^{14}H	Unit
Standard uncertainty	Counting error	0.53	2.15	%
	Sample homogeneity	5.3	1.1	
	Lab control standard	2.0	2.0	
	Efficiency calibration	5.0	5.0	
	Overall process	3.0	3.0	
Combined uncertainty		8.1	6.6	
Measured values		66.7	2.0	Bq/g
Uncertainty(k=1)		5.3	0.1	

[1] Kim, H.R., Kang, M.J., Choi, G.S. An experiment on the radioactivity characteristics of the tritium contaminated metal sample, *Annals of Nuclear Energy*, 2011. 1074- 1077.
[2] Hou, X., Roos, P. Critical comparison of radiometric and mass spectrometric methods for the determination of radionuclides in environmental, biological and nuclear waste samples. *Analytica chimica Acta* , 2008. 105-139.

*Corresponding author. E-mail: jmlim@kaeri.re.kr

Preparation of pure TiO_2 sorption material

Irena Špendlíková, Jakub Raindl, Mojmír Němec
Czech Technical University in Prague, Department of Nuclear Chemistry, Brehova 7, 115 19 Prague, Czech Republic

Abstract

Among the natural or anthropogenic radionuclides of very low concentrations nowadays measured in environmental samples, the radionuclide of ^{236}U has been recently included. In these ultra-trace analyses, the purity of sorption materials is very important and the traditional preparation procedures have to be optimized to minimize possible contamination. In the case of the determination of natural concentration of ^{236}U ($^{236}U/^{238}U \sim 10^{-10} - 10^{-14}$), the sample treatment procedure has to be modified in order to eliminate possible contamination from anthropogenic ^{236}U that may result even in more than ten thousand times higher $^{236}U/^{238}U$ ratios.

Many inorganic and organic materials have been proposed for the extraction of uranium. However, only several of them are suitable for the uranium sorption from the solutions of low uranium concentration, but relatively high salt content, such as fresh water, sea water etc. At the same time they have to meet other limiting parameters such as fast kinetics, chemical stability, and low costs. Among the inorganic sorption materials, titanium dioxide has been studied for years with promising results.

Titanium dioxides can be prepared via the hydrolysis of titanium compounds, either inorganic salts or organic derivatives, but their properties strongly depend on the preparation conditions. In classical procedures, titanium dioxides are prepared from commercial inorganic salts, such as sulphates or chlorides, or even from industrial intermediates of the titanium white production. Typically, the resulting titanium dioxides are contaminated with uranium already from the origin. Assuming that most organic compounds do not contain uranium and that it is possible to find "uranium free" water, titanium dioxide free of uranium contamination could be prepared by the hydrolysis of organic titanium derivatives.

The aim of this study was to find a suitable way of pure titanium dioxide preparation and to optimize the preparation procedure with respect to the sorption properties of the resulting material towards uranium. Therefore, an organic compound, tetrabutylorthotitanate, was used for the preparation of a series of titanium dioxide samples. The conditions of the preparation procedure slightly varied (e.g. different washing solutions – ethanol, acetone or both) but the important steps like sample drying remain unchanged.

One of the aspects which should be considered in the preparation of TiO_2-based absorbers is the fact that the sorption properties of titanium dioxide strongly depend on the crystal structure and their capacities increase in order: rutile < anatase < amorphous. Therefore, the first characterization of the new prepared materials was carried out using the X-Ray Powder Diffraction method. The presence of the organic compound residue in the materials after the hydrolysis was monitored using the thermogravimetry and IR methods and the size and shape of the particles were measured using the SEM/TEM.

Other important characteristic of new sorption material are specific surface area, sorption capacity and possible correlation among them. Specific surface area of the prepared oxides was determined by selective sorption of nitrogen gas from catalytically deoxygenated mixture of 5 H_2 : 1 N_2 at the temperature of 77 K. Sorption capacities for uranium were deduced from their sorption isotherms determined with fixed uranium concentration (20 $mmol.L^{-1}$) and variable values of V/m (10 - 1400 $mL.g^{-1}$).

Based on this characterization, the most promising material has been chosen. In the future study, this material will be prepared in larger quantity using "uranium free" water and used for the uranium concentration from environmental samples and for the consecutive determination of $^{236}U/^{238}U$ ratios using Accelerator Mass Spectrometry which will outline the contamination with anthropogenic ^{236}U and/or its natural abundance.

Keywords

Titanium dioxide, uranium sorption, ^{236}U

APSORC'13 - 5th Asia-Pacific Symposium on Radiochemistry
Kanazawa, Japan, 22-27 September 2013

Mössbauer Study of Iron Carbide Nanoparticles Produced by Sonochemical Synthesis

R. Miyatani[1], Y. Yamada[1], Y. Kobayashi[2,3]
[1]Department of Chemistry, Tokyo University of Science
[2]Department of Engineering Science, The University of Electro-Communications, [3]RIKEN

Abstract – Iron carbide nanoparticles were synthesized by ultrasonic irradiation of iron pentacarbonyl or ferrocene in diphenylmethane. Mössbauer spectra of the as-prepared particles measured at room-temperature and 6 K indicated only one doublet. The particles were annealed at 600 °C under argon for 2 h, and the Mössbauer spectrum measured at room-temperature consisted of Fe_3C, α-Fe, and a paramagnetic component.

Keywords – Sonochemistry, Iron carbide, Iron pentacarbonyl, Ferrocene, Nanoparticles

I. INTRODUCTION

Iron carbide nanoparticles of various compositions have been studied extensively due to their magnetic properties. Recently, Fe/Fe_3C nanoparticles were synthesized by sonicating iron pentacarbonyl $Fe(CO)_5$ in diphenylmethane and subsequent annealing [1]. But the mechanism of the sonochemical reaction and the effect of annealing are yet to be investigated. In this study, we performed sonolysis of $Fe(CO)_5$ in diphenylmethane and both the as-prepared nanoparticles and the particles after annealing were measured. The similar experiments were performed using ferrocene $FeCp_2$ in order to investigate the difference of the products depended on precursors.

II. EXPERIMENT

0.1mol of $Fe(CO)_5$ in diphenylmethane was irradiated using a high intensity ultrasonic horn (Ti-horn, 20 kHz) under argon flow for 1 h. 15 mmol of $FeCp_2$ in diphenylmethane was also sonicated under argon flow for 6 h. After the sonication, the products were centrifuged, washed with hexane and dried in vacuum. The product was annealed under argon flow for 2 h. The product was investigated by Mössbauer spectroscopy, X-ray diffraction (XRD), and transmission electron microscope (TEM).

III. RESULTS AND DISCUSSION

Nanoparticles were produced by sonolysis of $Fe(CO)_5$ in diphenylmethane. Mössbauer spectra were measured at 293 K and 7 K, and there observed only one doublet; $\delta = 0.35$ mm/s, $\Delta E_q = 0.94$ mm/s at 293 K and $\delta = 0.48$ mm/s, $\Delta E_q = 0.94$ mm/s at 7 K. Thus, the product was a paramagnetic compound. The XRD patterns with broad peaks and the TEM images showed that the nanoparticles were amorphous. Then, the sample were annealed at 300 °C, also the Mössbauer spectrum exhibited a doublet ($\delta = 0.35$ mm/s, $\Delta E_q = 0.88$ mm/s) at 293 K. However, Mössbauer spectrum measured at 6 K of the sample consisted of two sextets ($\delta = 0.45$ mm/s, $H = 491$ kOe and $\delta = 0.42$ mm/s, $H = 428$ kOe) and a doublet ($\delta = 0.41$ mm/s, $\Delta E_q = 1.12$ mm/s). The some of the XRD patterns of the sample corresponded to those of Fe_3O_4. It was presumed that the particles after annealing consisted of Fe/O/C. Room-temperature Mössbauer spectrum of the sample annealed at 700 °C showed only one sextet ($\delta = 0.35$ mm/s, $H = 511$ kOe) which was assigned to α-Fe_2O_3.

Next, nanoparticles were produced by sonolysis of $FeCp_2$ in diphenylmethane in order to eliminate the effects of oxygen in the sample. Mössbauer spectra measured at room temperature showed a doublet ($\delta = 0.36$ mm/s, $\Delta E_q = 0.94$ mm/s) (Fig.1a) while the spectrum measured at 6 K also showed one doublet ($\delta = 0.44$ mm/s, $\Delta E_q = 0.98$ mm/s). However, Mössbauer spectrum of the sample after annealing at 600 °C showed two sextets and a doublet (Fig.1b). The sextets were assigned to cementite Fe_3C ($\delta = 0.20$ mm/s, $H = 211$ kOe) and α-Fe ($\delta = 0.02$ mm/s, $H = 333$ kOe). Iron oxides were not found in the sample produced from $FeCp_2$.

IV. CONCLUSION

Nanoparticles produced by ultrasonic irradiation of $Fe(CO)_5$ in diphenylmethane consisted of Fe/O/C, whereas the nanoparticles produced by sonolysis of $FeCp_2$ in diphenylmethane did not contain oxygen. As-prepared particles were paramagnetic amorphous, and the particles with magnetic nature were produced after annealing. $FeCp_2$ is an adequate starting material to produce iron carbide particles.

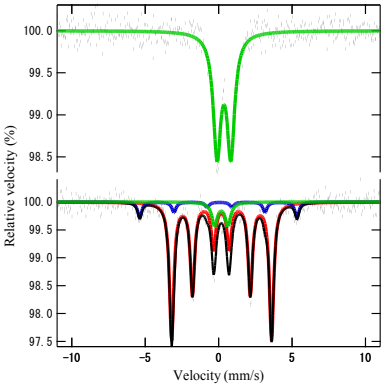

Fig.1 Room-temperature mössbauer spectra of (a) as-prepared nanoparticles produced by sonolysis of $FeCp_2$ in diphenylmethane and (b) the sample after annealing at 600 °C under argon flow for 2 h.

[1] S. I. Nikitenko, Yu. Koltypin, I. Felner, I. Yeshurun, A. I. Shames, J. Z. Jiang, V. Markovich, G. Gorodetsky, and A. Gedanken, *J.Phys. Chem. B*. 108, 7620-7626 (2004)

MÖSSBAUER STUDY OF IRON FLUORIDE FILMS PRODUCED BY PULSED LASER DEPOSITION

K. Shiga[1], Y. Yamada[1], Y. Kobayashi[2,3]
[1]Department of Chemistry, Tokyo University of Science
[2]Department of Engineering Science, The University of Electro-Communications, [3]RIKEN

Abstract – Iron fluoride thin films were produced by a reaction of laser-evaporated iron atoms with sulfur hexafluoride gas. The composition of thin films changed varying a pressure of ambient SF_6 gas: FeF_3 was obtained at a high pressure while FeF_2 was obtained at a low pressure. It was also demonstrated that the crystalline size of FeF_3 in the film was controlled by the substrate temperature while PLD.

Keywords – Iron fluoride, Film, Pulsed laser deposition, Mössbauer spectroscopy

I. INTRODUCTION

Pulsed laser deposition PLD in an ambient gas is a very useful method to produce compound films controlling the compositions [1-4]. In this study, we performed PLD of Fe metal in SF_6 atmosphere to produce iron fluoride films deposited onto Al substrates, and their structures and compositions were investigated. While SF_6 is known as an inert gas, it decomposes to produce F atoms in a plasma plume produced by the laser ablation followed by a production of iron fluorides.

II. EXPERIMENTAL

A block of Fe metal in a vessel filled with pure SF_6 gas was irradiated using Nd: YAG laser (523 nm, 85 mJ/pulse, 10 Hz) for 110000 pulses, and the laser-evaporated Fe atoms were deposited onto an Al substrate. The SF_6 atmosphere was maintained at a desired pressure between 1 and 5 Pa, and the Al substrate was kept at desired temperature between 298 and 873 K using a heater. The synthesized iron fluoride films were investigated by Mössbauer spectroscopy, powder X-ray diffraction (XRD), and scanning electron microscopy (SEM).

III. RESULTS AND DISCUSSION

PLD of Fe onto Al substrate at 298 K was performed in a SF_6 ambient gas of 5 Pa to produce an iron fluoride film. The Mössbauer spectrum of the film was measured at 298 K (Fig. 1a) and only one doublet (δ = 0.49 mm/s, ΔE_q = 0.58 mm/s) was observed. When the same sample was measured at 6 K (Fig. 1b), Mössbauer spectrum changed to show a sextet (δ = 0.59 mm/s, $H\iota$ = 561 kOe) which was assigned to FeF_3. It was considered that the crystalline size of FeF_3 in the film was very small showing the superparamagnetic nature at a high temperature. The XRD pattern of the sample showed broad lines, and it was also confirmed that the film consisted of small crystalline. Next, PLD of Fe in SF_6 of 5 Pa onto the Al substrate at 873 K was performed. The Mössbauer spectrum of the film measured at 298 K (Fig. 2a) showed a sextet (δ = 0.49 mm/s, $H\iota$ = 395 kOe) of FeF_3 as well as an unassigned doublet (δ = 0.46 mm/s, ΔE_q = 1.71 mm/s). The crystal growth on the substrate surface was enhanced by increasing the substrate temperature while deposition to show the sextet at 298 K. SEM images of the films revealed that the film produced at 873 K had rugged surface because of the crystal growth, whereas the film produced at 293 K had a smooth surface. Similar experiment was performed at a low pressure 1 Pa of SF_6, and the Mössbauer spectra measured at room temperature (Fig. 2b) showed a doublet (δ = 1.39 mm/s, ΔE_q = 2.76 mm/s) of FeF_2. The assignments of the films were also confirmed by the XRD patterns. The composition of the films clearly depended on the ambient SF_6 pressures.

IV. CONCLUSION

PLD of Fe in SF_6 gas produced FeF_3 or FeF_2 films. The crystalline size in the film was controlled by the substrate temperature while deposition. Composition of films was controlled by the pressure of ambient gas.

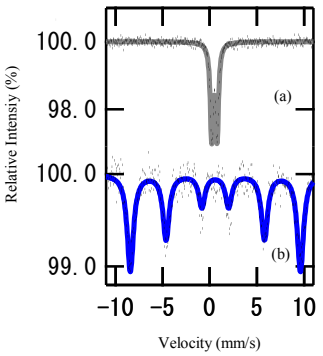

Fig.1 Mössbauer spectra of an iron fluoride film produced by PLD onto an Al substrate at 298 K in 5 Pa of SF_6 ambient gas. The film was measured at (a) 298 K and (b) 6 K.

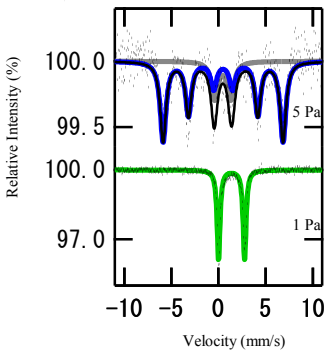

Fig.2 Room-temperature Mössbauer spectra of iron fluoride thin films produced by PLD onto an Al substrate at 873 K.
The pressures of SF_6 are indicated in the figure.

[1] D. Yokoyama, K. Namiki, H. Fukasawa, J. Miyazaki, K. Nomura, Y. Yamada, J. Radioanal. Nucl. Chem., 272, (2007) 631
[2] Y. Yamada, H. Yoshida, K. Kouno, J. Phys.: Conf. Ser. 217, 012096 (2010)
[3] Y. Yamada, H. Yoshida, Y. Kobayashi, Hyper. Int. 198, (2010) 55
[4] R. Usui, Y. Yamada, Y. Kobayashi, Hyper. Int. **205** (2012) 13

APSORC'13 - 5th Asia-Pacific Symposium on Radiochemistry
Kanazawa, Japan, 22-27 September 2013

Iron sulfide particles synthesized in liquid phase

R. Shimizu[1], Y. Yamada[1], Y. Kobayashi[2,3]
[1]Department of Chemistry, Tokyo University of Science
[2]Department of Engineering Science, The University of Electro-Communications, [3]RIKEN

Abstract – Iron sulfide particles were prepared by a polyol method using ferrocene as a precursor. The composition of the particles changed varying a mixture ratio of 1,2-hexadecanediol and 1-octadecanethiol. Iron (III) sulfide (Fe_2S_3) which has not been available in normal conditions was obtained.

Keywords – Iron (III) sulfide, Particles, Mössbauer spectroscopy, polyol method

I. INTRODUCTION

Generally, iron sulfide is stable having divalent iron Fe(II), and few Fe(III) sulfides have been reported. As the iron (III) sulfide have been appeared in an amorphous form, and thus, the existence has been the subject of discussion. Mössbauer spectra of Fe(III) sulfide (Fe_2S_3) was reported in a literature [1], but the crystal structure was not clear. An unstable phase could be stabilized in a form of small particles. In this study, we synthesized iron sulfide particles using a polyol method, and their Mössbauer spectra were measured.

II. EXPERIMENTAL

A mixture of ferrocene (2 mmol), oleylamine (30 mL), 1,2-hexadecanediol (HD), and 1-octadecanethiol (OT) (varying the mixture ratio of HD / OT = 0 mmol / 8 mmol, 8 mmol / 2 mmol, 8 mmol / 4 mmol, 8 mmol / 8 mmol) was heated to reflux for 2 h at 320 °C under a flow of argon. Particles were washed three times with ethanol and hexane after air cooling. The synthesized iron sulfide particles were investigated by Mössbauer spectroscopy, powder X-ray diffraction (XRD), and scanning electron microscopy (SEM).

III. RESULTS AND DISCUSSION

Fig. 1 shows SEM images of iron sulfide particles. Particle size changed dramatically by a presence of polyol: the particles produced without HD were ~ 1 μm (Fig. 1a), whereas the particle produced with HD were 100 ~ 200 nm (Fig. 1b).

Fig. 2 shows the Mössbauer spectra measured at room temperature of iron sulfide particles obtained in various mixture ratio of HD / OT. The particles produced without HD were assigned to $Fe_{1-x}S$ (pyrrotite) (Fig. 2a). When the small amount of OT (2 mmol) was added, two sets of sextet were observed, which were assigned to FeS (troilite) and α-Fe (Fig. 2d). Two sets of doublet (δ = 0.38 mm/s, ΔE_q = 0.73 mm/s and δ = 0.44 mm/s, ΔE_q = 0.47 mm/s) were observed in all the samples produced under the conditions with HD (Fig. 2b-d). Mössbauer parameters of the doublets had the similar values of iron (III) sulfide (Fe_2S_3) reported in the literature [1].

XRD patterns of the samples were shown in Fig. 3, and the yields of FeS, $Fe_{1-x}S$ and α-Fe were in good agreement with the results obtained by the Mössbauer spectra. Besides these well assigned XRD patterns, unassigned XRD patterns were observed. The peaks marked 'X' in Fig. 3 may correspond to Fe_2S_3 with a long-range periodic structure which were observed for the first time.

IV. CONCLUSION

Iron sulfide particles were prepared by the polyol method. Iron(III) sulfide (Fe_2S_3) particles having a long-range periodic structure were found. The Mössbauer spectra of Fe_2S_3 showed that it was paramagnetic.

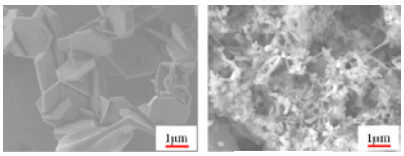

Fig. 1. SEM images of the iron sulfide particles synthesized with the molar ratio of HD / OT (a) 0/ 8 and (b) 8 / 4.

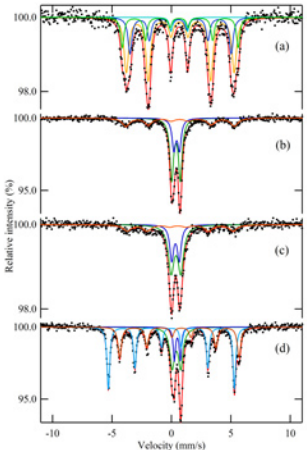

Fig. 2. Room-temperature Mössbauer spectra of the iron sulfide particles synthesized in a mixture of HD / OT = (a) 0 / 8, (b) 8 / 8, (c) 8 / 4, and (d) 8 / 2.

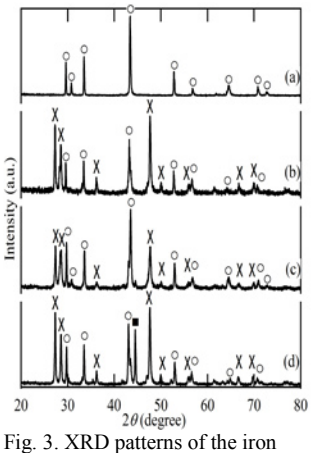

Fig. 3. XRD patterns of the iron sulfide particles synthesized in a mixture of HD / OT (a) 0 / 8, (b) 8 / 8, (c) 8 / 4, and (d) 8 / 2. (○) FeS or $Fe_{1-x}S$, (■) α-Fe, (×) unidentified peaks

[1] A. H. Stiller, B. Jack MaCormick, P. Russell, P. A. Montano, J. Am. Chem. Soc. 100, 2553-2554 (1978)

APSORC'13 - 5th Asia-Pacific Symposium on Radiochemistry
Kanazawa, Japan, 22-27 September 2013

Mössbauer and XRD studies of NiCuZn ferrites By Sol-Gel auto-combustion

Chenglong Lei[1], Qing Lin[1,2]*, Haifu Huang[3], Hui Zhang[1], Yun He[1]
[1]*College of Physics and Technology, Guangxi Normal University, Guilin 541004, China*
[2]*Department of Information Technology, Hainan Medical College, Haikou 571101, China*
[3]*Nanjing National Laboratory of Microstructures and Jiangsu Provincial Laboratory for NanoTechnology,,Department of Physics, Nanjing University, Nanjing 210093, China*
e-mail:hy@gxnu.edu.cn

Abstract:
The $Ni_{0.6}Cu_{0.2}Zn_{0.2}Ce_xFe_{2-x}O_4$ ferrites（$0\le x\le 0.85$） have been prepared by Sol-Gel auto-combustion method and we have investigated the effect of impurity CeO_2 phase to the microstructure and hyperfine magnetic field in spinel ferrite. The results of XRD patterns confirm the average crystallite size of samples decreases with Ce^{3+} substitution increasing and the lattice parameters vary as a function of x content. ^{57}Fe Mössbauer spectra at room temperature for all samples confirm the [Fe^{3+}- O^{2-}-Fe^{3+}] super exchange interaction decrease due to cerium substitution. For low temperature auto-combustion samples it reveals one normal sextet line and one doublet line $x\le 0.25$, which shows well-resolved ferromagnetic order. Lattice defects are determined and Mössbauer spectrums vary from magnetic sextet to relaxation doublet at $x\ge 0.45$ due to a mass of CeO_2 phase. In contrast, the Mössbauer spectra for the samples sintered at 800℃/3h detect the secondary phaseα -Fe_2O_3 where the cation distribution occurs and it collapses to paramagnetic doublet($x\ge 0.85$). Ce^{3+} substitution has its maximum limit values of super exchange interaction and high sintering temperature will affect this interaction.

Keywords: NiCuZn ferrite, Rare earth, Cerium substitution, Mössbauer, XRD

I. RESULTS AND DISCUSSION

We have successfully prepared ferrite system Ce^{3+} doped $Ni_{0.6}Cu_{0.2}Zn_{0.2}Fe_2O_4$ by Sol-Gel auto-combustion method. The XRD patterns of ferrite as-brunt and sintered at 800℃/3h powders are shown in Fig.1-3, respectively.

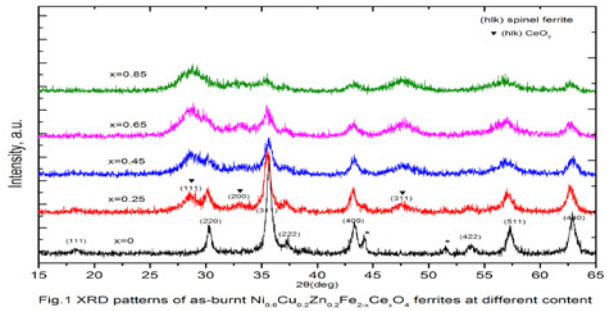

Fig.1 XRD patterns of as-burnt $Ni_{0.6}Cu_{0.2}Zn_{0.2}Fe_{2-x}Ce_xO_4$ ferrites at different content

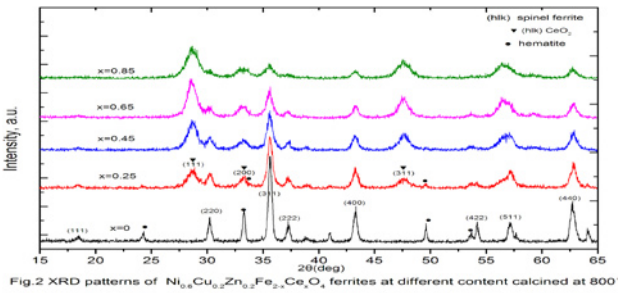

Fig.2 XRD patterns of $Ni_{0.6}Cu_{0.2}Zn_{0.2}Fe_{2-x}Ce_xO_4$ ferrites at different content calcined at 800℃

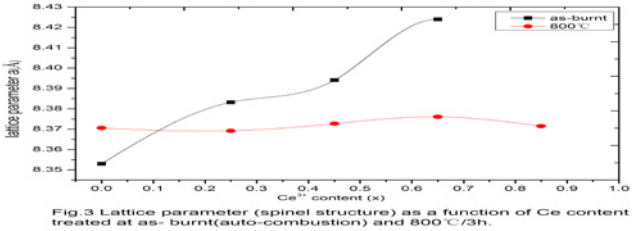

Fig.3 Lattice parameter (spinel structure) as a function of Ce content treated at as- burnt(auto-combustion) and 800℃/3h.

Fig.4 and Fig.5 show the Mössbauer spectra (RT) of $Ni_{0.6}Cu_{0.2}Zn_{0.2}Ce_xFe_{2-x}O_4$ nanocrystalline ferrites measured at room temperatures , respectively.

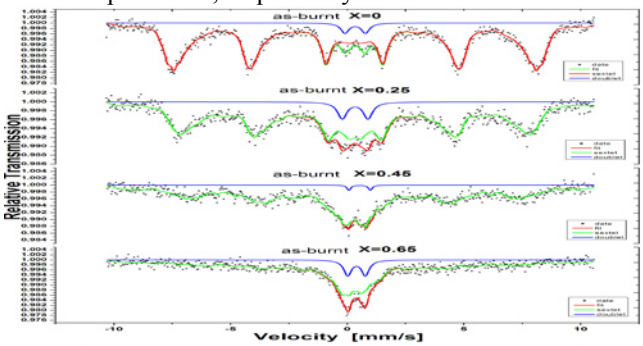

Fig.4 The Mossbauer spectra at room temperature of as-burnt $Ni_{0.6}Cu_{0.2}Zn_{0.2}Ce_xFe_{2-x}O_4$ at different content

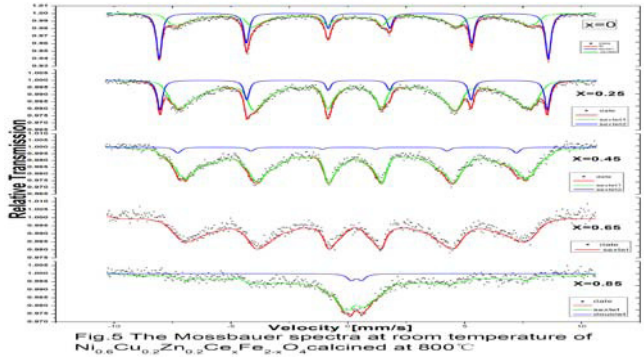

Fig.5 The Mossbauer spectra at room temperature of $Ni_{0.6}Cu_{0.2}Zn_{0.2}Ce_xFe_{2-x}O_4$calcined at 800℃

The lattice parameter changes as a function of the cerium substitution. The Mössbauer spectra (RT) results illustrate that only after low temperature auto-combustion the samples exhibit ferromagnetism and a super para-magnetism.

[1] Aphesteguy, J.C., et al., *Characterization of nanosized spinel ferrite powders synthesized by coprecipitation and autocombustion method.* Journal of Alloys and Compounds, 2010. 495(2): p. 509-512.
[2] Nedkov, I., R.E. Vandenberghe, and A. Zaleski, *Surface magnetic disorder in nanostructured $Ni_{0.5}Zn_{0.5}Fe_2O_4$ particles.* Journal of Magnetism and Magnetic Materials, 2010. 322(18): p. 2732-2736.
[3] S.I.Moussa, R.R.Sheha, E.A.Saad, N.A.Tadros, Synthesis and characterization of magnetic nano-material for removal of Eu^{3+} ions from aqueous solutions, *Journal of Radioanalytical and Nuclear Chemistry*, 2013. 295: 929–935.

Thermal Stability of Locally-Associated Al and In Impurities in Zinc Oxide

S. Komatsuda[1], W. Sato[1,2], and Y. Ohkubo[3]
[1]Graduate School of Natural Science and Technology, Kanazawa University
[2]Institute of Science and Engineering, Kanazawa University
[3]Research Reactor Institute, Kyoto University

Abstract – Local structures in 100 ppm Al-doped ZnO were investigated by means of the time-differential perturbed angular correlation method. From distinct perturbation patterns obtained for the samples annealed in different conditions, we found that the ^{111}In, which is strongly associated with Al ions in ZnO, gradually breaks the interaction and occupies the defect-free substitutional Zn site in high-temperature vacuum.

Keywords – Al-doped ZnO, electric field gradient, In-111, perturbed angular correlation

I. INTRODUCTION

Zinc Oxide (ZnO) doped with group 13 elements (Al, Ga, In) as impurity donors is expected to be applied to functional devices as *n*-type semiconductors. For a practical use of ZnO as a conduction-controlling device, it is of great importance to study the physical and chemical states of the dilute impurity ions in ZnO. The time-differential perturbed angular correlation method (TDPAC) is very suited for that purpose because it can directly provide atomic-level information of impurity atoms. In our previous TDPAC studies, we found that Al ions and ^{111}In probe doped in ZnO can form local associations even at extremely dilute concentrations[1]. In this work, we have investigated the stability of the interaction between Al and In impurities in various conditions.

II. EXPERIMENTS

For the synthesis of 100 ppm Al-doped ZnO, stoichiometric amounts of $Al(NO_3)_3 \cdot 9H_2O$ and ZnO powder were mixed in ethanol. The suspension was heated to evaporate the ethanol until dryness. The powders were pressed into disks and sintered in air at 1273 K for 3 h. For TDPAC measurements, commercially available ^{111}In solution was added in droplets onto each of the sintered disks at the concentration of 100 ppt. The disks again underwent heat treatment in air at 1373 K for 2 h. Then the disk samples were ground into powder, and sealed in a quartz tube in vacuum respectively. The samples underwent further heat treatment in vacuum at 1023 K and 1173 K for 24 h. The TDPAC measurements were carried out for the 171-245 keV cascade γ rays of ^{111}Cd($\leftarrow^{111}$In) probe with the intermediate state of I = 5/2 having a half-life of 85.0 ns.

III. RESULTS

Figure 1(a) shows a TDPAC spectrum obtained for the sample heat-treated in air. The directional anisotropy, $R(t)$, is plotted as a function of the time interval between the cascade γ-ray emissions, t, during which the probe is perturbed by the outer surrounding field. This spectrum shows that 100 ppm Al and 100 ppt ^{111}In are locally-associated in ZnO matrix, suggesting that there is a strong attractive force between Al and In in ZnO[1]. Figure 1(b) and 1(c) show TDPAC spectra obtained for the samples annealed in vacuum at 1023 K and 1173 K respectively, for 24 h after the probe was doped. For the spectrum in Fig. 1(b), two different components appearing in the spectra for the Fig. 1(a) and undoped ZnO[2] were observed. The component appearing in the spectrum for undoped ZnO has become more visible in Fig.1 (c). These observations imply that in high-temperature vacuum, the probe resides solely at the substitutional Zn site being independent of the field produced by Al ions. Showing TDPAC spectra of the samples annealed in various conditions, we discuss the stability of locally-associated Al and In impurities doped in ZnO.

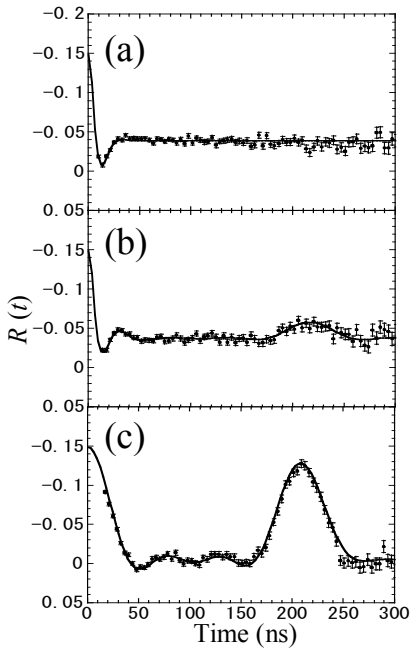

Fig.1 Room temperature TDPAC spectra of ^{111}Cd($\leftarrow^{111}$In) embedded in 100 ppm Al-doped ZnO annealed (a) in air at 1373K, (b) in vacuum at 1023 K, and (c) in vacuum at 1173K.

[1] S. Komatsuda, W. Sato, S. Kawata, and Y. Ohkubo, J. Phys. Soc. Jpn. **80**, (2011) 095001.
[2] W. Sato, Y. Itsuki, S. Morimoto, H. Susuki, S. Nasu, A. Shinohara, and Y. Ohkubo, Phys. Rev. B **78** (2008) 045319.

Structure and Antimony-121 Mössbauer Spectra of Hypervalent Antimony Compounds with an Antimony–Gold Bond in Equatorial Position

Masashi Takahashi, Asumi Sato, Shiro Matsukawa
Department of Chemistry, Toho University
Funabashi, Chiba 274-8510 Japan

Abstract – Hypervalent antimony compounds having Sb–Au bond in equatorial position are studied. [$Rf_2SbAu(PPh_3)_2$] (Rf = $C_6H_4C(CF_3)_2O^-$) has a short Sb–Au bond (2.6813 Å). ^{121}Sb Mössbauer spectrum of [$Rf_2SbAu(SMe_2)$] indicates a large electron density along the Sb–Au bond. These results suggests a dative interaction of the gold fragments to hypervalent antimony atom.

Keywords –Mössbauer Spectroscopy, Hypervalent Compound, Dative Bond, Antimony, Gold

I. INTRODUCTION

Since the first report on the ruthenaboratrane, in which the boron atom at the pivot position of a tripodal ligand acts as the Lewis acid [1] , unconventional metal to ligand donation (M→□) attracts keen interests. Although the investigations are mostly carried out using the electron deficient borane ligands such as $R_nB(C_6H_4PR'_2)_{3-n}$, the heavier main group elements such as phosphorus, antimony, silicon and tin can be used as the Lewis acidic point because these elements accept the electron pair to form hypervalent compounds. Indeed quite recently Wade and Gabbai have demonstrated such M→□ interactions using [$(C_6H_4PPh_2)_3$ SbAuI] (**1**) [2]. On the other hand we have already suggested that the existence of electron flow from organometallic fragment to antimony atom in the hypervalent antimony compounds $Rf_2SbMCpL_n$ [M = Fe, Ru, Cr, Mo, W; L = CO, PPh_3 etc; Rf = $C_6H_4C(CF_3)_2O^-$] (**2**) using ^{121}Sb Mössbauer spectroscopy. [3] These results inspired us to extend our investigation to the Au fragments.

II. EXPERIMENTAL

material: Rf_2SbAuL (L = SMe_2, PPh_3) were prepared by the reaction of $[Rf_2Sb]^-$ with AuLCl using a modified method for [$Rf_2SbFeCpL_n$]. The compounds were characterized using ^{1}H, ^{19}F and ^{31}P NMR.
Structural determination: X-ray diffraction data were collected on a SMART APEX (Bruker) at 150 K. Data were processed as routine.
^{121}Sb Mössbauer spectrum: Mössbauer spectrum was measured at 20 K using a $Ca^{121}SnO_3$ source on a Mössbauer measurement system from Wissel (MDU-1200, DFG-1200, MVC-450, CMCA-550). The spectrum was analyzed using a MossWin software. The value of the isomer shift was given relative to InSb.

III. RESULTS AND DISCUSSION

The reaction product with $AuCl(PPh_3)_2$ was confirmed to be [$Rf_2SbAu(PPh_3)_2$] (Fig. 1), which has unexpectedly a three coordinated gold atom. The antimony atom adopts trigonal bipyramidal geometry as expected. The Sb–Au length (2.6813 Å) is shorter than that of (**1**) (2.7086 Å). The Sb–O and Sb–C lengths are slightly longer than those of **2**. The O–Sb–O and C–Sb–C angle is almost the same to those of **2**. These results suggest the high electron density along the equatorial Sb–Au bond due to the strong electron donation from gold atom. Two phosphine ligands at gold atom should afford the electron density to Sb atom effectively and might stabilize the Sb–Au bond.

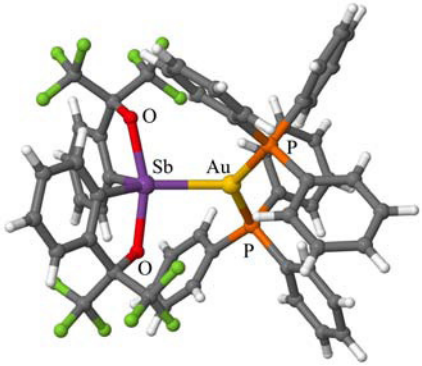

Figure 1 Crystal Structure of [Rf_2Sb–$Au(PPh_3)_2$] Sb–O = 2.1095, 2.1237; Sb–C = 2.123, 2.123 Å; O–Sb–O = 161.75; C–Sb–O = 107.10°.

Fig. 2 shows the Mössbauer spectra of [$Rf_2SbAu(SMe_2)$] (**3**). As expected 3 has a large negative quadrupole coupling constant (–23.91 mm s^{-1}) and a large asymmetry parameter (0.67). The isomer shift value (2.63 mm s^{-1}) is an intermediate value between typical Sb(V) and Sb(III) complexes. The Mössbauer parameters indicate considerable electron density is present along the Sb–Au bond, suggesting a strong electron donation of gold atom.

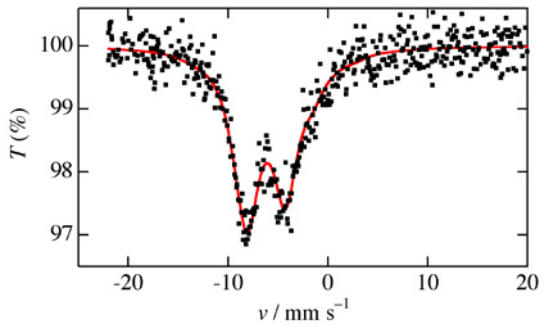

Figure 2 ^{121}Sb Mössbauer spectrum of [$Rf_2SbAu(SMe_2)$] at 20 K.

[1] Hill, A. F. et al. *Angew. Chem. Int. Ed.* **1999**, *38*, 2759.
[2] Wade, C. R.; Gabbai, F. P. *Angew. Chem. Int. Ed.* **2011**, *50*, 7369.
[3] Takahashi, M. et al. *Z. Naturforsch.* **2001**, *57a*, 631.

APSORC'13 - 5th Asia-Pacific Symposium on Radiochemistry
Kanazawa, Japan, 22-27 September 2013

Local Structure of ^{57}Mn/^{57}Fe Implanted into Lithium Hydride

Jun Miyazaki[1], Takashi Nagatomo[2], Yoshio Kobayashi[3, 4], Michael K. Kubo[5], Yasuhiro Yamada[6], Mototsugu Mihara[7], Wataru Sato[8], Kazuya Mae[5], Shinji Sato[9], Atsushi Kitagawa[9]
[1]College of Industrial Technology, Nihon University
[2]J-PARC Center, High Energy Accelerator Research Organization
[3]Department of Engineering Science, The University of Electro-Communications
[4]RIKEN Nishina Center for Accelerator-Based Science, RIKEN
[5]The Division of Arts and Sciences, International Christian University
[6]Department of Chemistry, Tokyo University of Science
[7]Department of Physics, Osaka University
[8]Institute of Science and Engineering, Kanazawa University
[9]Department of Accelerator and Medical Physics, National Institute of Radiological Sciences

Abstract – We report the in-beam Mössbauer Spectra of ^{57}Mn implanted into polycrystalline LiH at under room temperature. As compared with the result of DFT calculations, ^{57}Fe atoms were implanted into Li or H substitutional site in LiH crystal. With an increase the sample temperature, we could observe the decrease of lattice defects.

Keywords – In-beam Mössbauer Spectroscopy, β-decay of ^{57}Mn, Lithium hydride, DFT Calculations

I. INTRODUCTION

In-beam Mössbauer spectroscopy is a powerful technique to obtain the direct information on exotic chemical or physical state of the nuclear probe that was implanted into the sample such as metal or inorganic solid. Lithium hydride (LiH) is an ionic solid having the rock salt type crystal structure in which one Li^+ cation is surrounded by six H^- anions. In our previous study[1], we reported the in-beam Mössbauer spectra of ^{57}Mn implanted into LiH from room temperature to over 800 K. In this study, we report the spectra under room temperature and discus the local structure of ^{57}Mn/^{57}Fe implanted into LiH.

II. EXPERIMENTAL

The measurements were performed using Heavy Ion Medical Accelerator in Chiba (HIMAC) at National Institute of Radiological Science (NIRS) in Chiba, Japan. ^{57}Mn beam (E =~ 260*A* MeV) was produced from the projectile fragment process of nuclear collisions between ^{58}Fe ions (500*A* MeV, ~ 1×10^6 particles per beam) and ^{9}Be nuclei in a 27 mm thick production target. The beam pulse was generated every 3.3 s with a ~300 ms duration and with 1×10^6 particles/pulse. The energy of the ^{57}Mn nuclei was adjusted using energy degraders to stop the ions at an appropriated depth in the sample. The polycrystalline LiH (Wako Pure Chemical) was mounted on a cold finger or BN heater in a vacuum chamber in order to control the sample temperature from 11 K to over 800 K. A parallel-plate avalanche counter (PPAC) was employed as a detector. The anti-coincidence method that uses a plastic scintillation detector to detect and reject extraneous β-rays was employed to obtain high-quality in-beam Mössbauer spectra with improved S/N ratios.

III. RESULTS AND DISCUSSION

In-beam Mössbauer spectra of ^{57}Mn/^{57}Fe implanted into LiH at 11, 274, 294 K were shown in Fig. 1. Obtained spectra were fitted with some single lines and doublet lines. In the spectra at 3 temperatures, the single line peaks of S (IS = -0.54 mm/s) and S' (IS = 0.07 mm/s) were observed. As compared with the result from DFT calculations, S is assigned to be in ^{57}Fe at the substitutional Li site and S' is assigned to be in ^{57}Fe at the stubstitutional H site in LiH crystal. Symmetrical doublet peaks of D1 (IS = -0.59 mm/s, ΔE_Q = 0.57 mm/s) and D' (IS = -0.03 mm/s, ΔE_Q = 0.58 mm/s) were also observed, and new doublet peak of D2 (IS = -0.60 mm/s, ΔE_Q = 2.34 mm/s) was observed at 11K (Fig.1c). In the result from DFT calculations, doublet peaks are assigned to be in ^{57}Fe at the substitutional Li or H site with a neighboring atom deficiency. The temperature dependence of the relative intensities in this study suggests that the lattice defects recover with an increase temperature.

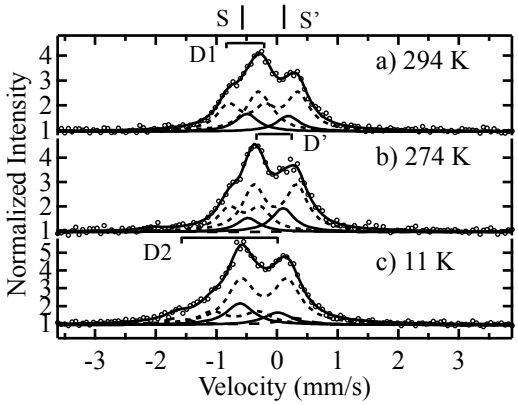

Fig.1 In-beam Mössbauer spectra of ^{57}Mn implanted into LiH

[1] T. Nagatomo *et al.*, *Hyperfine Interact*, **204**, 125-128 (2012)

Evaluation of Vacancy-Type Defects in ZnO by the Positron Annihilation Lifetime Spectroscopy

R. Ono[1], T. Togimitsu[1], and W. Sato[1,2]
[1]Graduate School of Natural Science and Technology, Kanazawa University
[2]Institute of Science and Engineering, Kanazawa University

Abstract – Annealing-temperature dependence of the formation of vacancy-type defects in ZnO has been studied by means of the positron annihilation lifetime spectroscopy. It was found that the lifetime does not drastically change for ZnO samples annealed at the temperature range below 600 ℃, whereas annealing-temperature dependence of the lifetime was observed above 600 ℃, showing the minimum value at 1000 ℃.

Keywords – positron annihilation lifetime spectroscopy, ZnO, annealing effect, vacancy, grain boundary

I. INTRODUCTION

Zinc oxide (ZnO) is an intrinsic n-type semiconductor having optoelectronic properties. Because vacancy-type defects brought about in the formation process of ZnO is known to affect the intrinsic properties, for future applications, it is important to understand various behaviors of defects in ZnO such as generation, recovery, agglomeration and diffusion. For the evaluation of their vacancy-type defects, positron annihilation lifetime spectroscopy (PALS) is one of the most powerful methods and we have applied this spectroscopy to part of our studies on local structures of ZnO. In the present study, we examined annealing-temperature dependence of positron lifetime to evaluate the concentration and size of vacancy-type defects formed in ZnO.

II. EXPERIMENTS

Polycrystalline ZnO powders (purity 99.99%) were pressed into pellets at 75 MPa. They were annealed in air at different temperatures ranging from 200 to 1200℃ for 2h. A ^{22}Na (as in NaCl) positron source covered with Kapton film was sandwiched with the sample disks. Positron annihilation lifetime was measured with a conventional circuit at room temperature. BaF_2 scintillators were used for the detection of 1275- and 511-keV γ rays.

III. RESULTS

It was found from the PALS measurements that the lifetime does not drastically change for ZnO samples annealed at the temperature range between 200 to 600℃. However, obvious temperature dependence was seen for those annealed at higher temperatures. In Fig.1 is shown the PALS spectra obtained for the ZnO samples annealed (a) at 600℃ and (b) at 1000℃. The spectra reproduced by the lines named A are made up of three different decay components as numbered 1-3. Components 1 and 2 originate from self absorption in the source materials, and Component 3 corresponds to positron annihilations in the ZnO samples. The lifetime of Component 3 is the average of those in the bulk and defects in ZnO samples. It is obvious from the slopes of the decay curves of Component 3 that the lifetime of positrons in ZnO annealed at 1000℃ is shorter than that for 600℃. The short lifetime can be explained as a result of the recovery of vacancy-type defects. Particle growth arising from the heat treatment may be another cause of the lifetime shortening because the amount of vacancy-like defects present in grain boundaries is considered to become less by the phenomenon. The positron lifetime, to the contrary, increases in ZnO samples annealed at temperatures above 1000℃. The reason for the increase has not been understood yet. For the total understanding of the defect formation process, further data acquisition at other sample-preparation conditions is now underway.

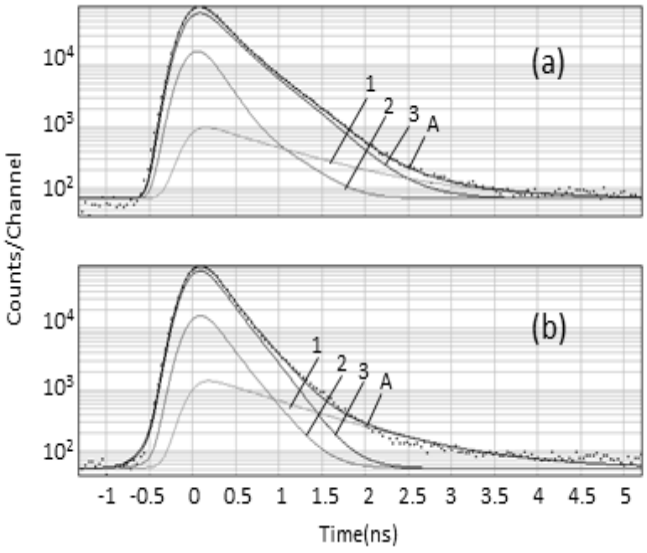

Fig.1 PALS spectra for ZnO pellets annealed (a) at 600℃ and (b) at 1000℃.

APSORC'13 - 5th Asia-Pacific Symposium on Radiochemistry
Kanazawa, Japan, 22-27 September 2013

Determination of ultratrace-levels of ^{99}Tc using ICP-QMS in the low level radioactive waste samples

Te-Yen Su, Tsuey-Lin Tsai, Hsin-Chieh Wu, Lee-Chung Men
Chemistry Division, Institute of Nuclear Energy Research, Longtan, Taoyuan 32546, Taiwan, R.O.C.

Abstract –A rapid, accurate and less labor intensive approach was developed to determine ^{99}Tc in the low level radioactive wastes (LLW). Only 0.1 g of solid radwastes was firstly dissolved using microwave digestion and then the specific TEVA resin was used for chemical separation to remove most of the matrices piror to inductively coupled plasma- quadrupole mass spectrometry (ICP-QMS) measurement. The minimum detectable activity (MDA) of ICP-QMS for the determination of ^{99}Tc in LLW samples was 8.5 mBq g^{-1} (13.6 pg g^{-1}), which was comparable to that of double-focusing magnetic sector field inductively coupled plasma mass spectrometry (ICP-SFMS), 5.3 mBq g^{-1}. The sensitivity of the ICP-QMS method for the determination of ^{99}Tc was much superior to that of the alternative radiochemical methods (e.g., liquid scintillation analyzer; LSA) when accounting for the data acquisition time for identical, low-concentration samples. Approximately 88 % of the chemical recovery was achieved and this developed technique was successfully applied to LLW samples for ^{99}Tc measurement within 5 minutes.

Keywords –^{99}Tc; inductively coupled plasma-quadrupole mass spectrometry (ICP-QMS); low level radioactive wastes (LLW)

APSORC'13 - 5th Asia-Pacific Symposium on Radiochemistry
Kanazawa, Japan, 22-27 September 2013

Development of an Automatic Prompt Gamma-ray Activation Analysis System

Takahito OSAWA[1]
[1]Neutron Imaging and Quantum Beam Analysis Group, Quantum Beam Science Directorate,
Japan Atomic Energy Agency (JAEA),

Abstract – An automatic prompt gamma-ray activation analysis system was developed and installed at the Japan Research Reactor No. 3 Modified (JRR-3M). The main control software, referred to as AutoPGA, was developed using LabVIEW 2011 and the hand-made program can control all functions of the analytical system. The core of the new system is an automatic sample exchanger and measurement system with several additional automatic control functions integrated into the system. Up to fourteen samples can be automatically measured by the system.

Keywords – Prompt gamma-ray analysis; Automatic analysis; Revolute robot; LabVIEW

Prompt gamma-ray analysis (PGA) using a neutron beam generated by a nuclear reactor is a convenient and nondestructive elemental analytical technique. PGA can be widely used in various science and technology fields [e.g. 1], because the analytical methods have high sensitivity for certain specific light elements.

The PGA system at the JRR-3M at the Japan Atomic Energy Agency (JAEA) was constructed in 1992 [2]. Although the system using cold and thermal neutron beams achieved a very low gamma-ray background level, it was outdated because no improvements had been made since its construction. In this study, an automatic system for PGA was developed in order to update the old analytical system and improve its measurement efficiency.

The new automatic PGA system is mainly composed of two computers (PC1 and PC2), four programs, a six-axis vertical revolute joint robot (Mitsubishi RV-3SD, Fig.1), and data acquisition devices. Although the inside of the shielding body is not changed most of the devices and systems on the outside of the shielding body are completely improved in this work. The core of the new system is an automatic sample exchanging and measurement system, and several automatic control functions: such as helium flow control, neutron flux recording, internet functions, and machine vision, have been integrated into the system.

In the system, fourteen samples hung on the center of Teflon frames with Teflon strings that can be placed onto a sample stand. Each sample frame is selected and introduced into a Teflon sample box using a revolute joint robot. Opening and closing of the loading hatch is enabled with compressed air and air bulbs that are controlled using a digital output module. A physical interlock on the loading hatch that synchronizes with the neutron beam shutter is operated by a single-pole single-throw relay, and the relay can also control the opening and closing of the neutron beam shutter.

Fig.1 A revolute joint robot of the automatic PGA system

A robot sequence program written in MELFA BASIC V was designed by the author. The AutoPGA program is installed in PC1 and controls the entire series of automatic analytical operations. When the user clicks the start button AutoPGA starts the servomechanism of the robot and initiates the sequence program. It then closes the neutron beam shutter, releases the interlock, and opens the loading hatch. When the machine vision system judges that the lid is not placed in the correct position, the sequence program stops working. The robot begins operating, and the Teflon lid on the Teflon sample box is removed and placed on a lid stand. The robot selects the sample frame and introduces it into the sample box and then places the lid on the sample box. The loading hatch is closed, the neutron shutter is opened, and the measurement is begun. An existing measurement program (SEIKO EG&G Spectrum Navigator) is installed in PC2 and is used for the measurements. In the automatic analysis, a batch processing mode is utilized that calls a communication program (PGA-Talk created by the author) after each measurement. PGA-Talk sends a signal to PC1 via TCP, and AutoPGA recognizes the completion of the gamma-ray recording and begins to exchange the sample. When the sample exchange is complete, AutoPGA sends a signal to PC2 and PGA-Talk is automatically shut down. Spectrum Navigator then begins the measurement of the next sample.

[1] T. Osawa, Y. Hatsukawa, P. W. U. Appel, H. Matsue, Nucl. Instrum. Meth. Phys. Res. B 269 (2011), pp. 717-720.
[2] C. Yonezawa, A.K.H. Wood, M. Hoshi, Y. Ito and E. Tachikawa, Nucl. Instr. and Meth. A 329 (1993), pp. 207-216.

APSORC'13 - 5th Asia-Pacific Symposium on Radiochemistry
Kanazawa, Japan, 22-27 September 2013

Concentration of Heavy Metal Elements in Chinese Medicine by INAA

S. Ishihara[1], E. Furuta[2], N. Iwasaki[1], Y. Yoshihara[3], R.Okumura[4], Y.Iinuma[4]
[1] Ochanomizu University, Facility of Sciences
[2]Ochanomizu University, Graduate School of Humanities and Sciences
[3]Ochanomizu University, Facility of Human Life and Environmental Sciences
[4]Kyoto University, Research Reactor Institute

Abstract – *An instrumental neutron activation analysis of Chinese medicines and medicinal herbs was performed, in which they have possibilities to contain toxic elements. By the preliminary experiments, there were some medicines that arsenic and mercury were included by observing gamma-ray spectroscopy with neutron irradiation. The Chinese medicine can be purchased through the Internet easily; however, it is considered that some regulations may be necessary.*

Keywords – Chinese medicine, Arsenic, Mercury, INAA

I. INTRODUCTION

Chinese medicine is used all over the world because of its safer image than Western pharmaceutical products. It is possible to purchase everywhere through the Internet. However, a few reports mentioned some of them included some kinds of toxic elements like arsenic (As), lead (Pb), mercury (Hg) and cadmium (Cd) [1]. Chinese medicines and medicinal herbs may be taken in continuously for a long term. So, if they include some toxic elements, it develops a health problem. Therefore, many kinds of Chinese medicines and medicinal herbs which can be purchased in an Asian area were analyzed by neutron activation at the KUR for the purpose of clarifying the actual situation. The preliminary experimental results were shown in the presentation.

II. EXPERIMANTAL

Many kinds of Chinese medicine and medicinal herbs were purchased from 5 routes to analyze the heavy metal elements; 1. 12 kinds of Chinese medicines were sold with a prescription by a hospital doctor in China; they were not sold to public in a market, 2. 8 kinds of Chinese medicines were bought through the Internet from China, 3. 11 kinds of Chinese medicines were bought at a market of Korea, 4. 47 kinds of medicinal herbs were bought at a market of Vietnam, and 5. 25 kinds of Chinese medicines were bought at a medical corner of a super market in Japan; they were produced in Japan. Each of them was enclosed almost 100 mg in a double polyethylene bag. The standard samples used were JA-2 and JR-2 of rock standard. The samples were put in capsules with standards and irradiated 5MW × 10 min or 1MW × 30 min at KUR. After cooling among 5 days, the capsules were opened to take out samples, each sample was enclosed in a new polyethylene bag, and then started measurement of medium and long half-life radionuclides.

III. RESULTS

Table shows the results of 4 elements in the samples from route-1. Among 12 kinds of Chinese medicines, 6 kinds of them included As, and 5 kinds of them included Hg. On the other hand, these 4 elements were not included in 2 of them. Other elements detected were sodium, potassium, calcium, scandium, iron, manganese, lanthanum, and selenium and these elements were included a few ten ppm except for calcium of a few thousand ppm.

Table Four elements concentrations in 10 Chinese medicines (ppm)

Sample	^{51}Cr	^{60}Co	^{76}As	^{203}Hg
牛黄解毒片 Niuhuang Jiedu Pian			7.1%	
青果丸 Fluit, Lonicera	8.0	1.1		
十全大と丸 Shiquan Dabu Wan	3.3	1.6		1.7
天麻首烏片 Tenma Shouwu Pian		1.8	1.9	
麻仁丸 Cannabis sativa				47
六神丸 (Musk) Liu Shen Wan			6.7%	6.7%
胃气痛片 Weiqitong Pian	76	1.8	14	3.8
黄迸上清片 Hou –Hashi			2.8	
木香順气丸 Muxiang Shunqi Wan		1.4		4.9
六味地黄丸 Rehmannia glutinosa			1.6	

IV. CONCLUSION

Some of Chinese medicines included high concentration of toxic elements such as As and Hg. It is considered that a regulation how to sell or a limitation of the purchase method is necessary.

[1] Agilent Technologies; www.agilent.com/chem/jp

Application of instrumental neutron activation analysis to assess dietary intake of selenium in Korean adults from meat and eggs

Jong-Hwa Moon[1], Sun-Ha Kim[1], Yong-Sam Chung[1], Ok-Hee Lee[2]
[1]Korea Atomic Energy Research Institute, Daedeok-daero 989-111, Yuseong-gu, Daejeon, 305-353, Korea
[2]Dept of Food Science and Nutrition, Yongin University, 470, Samga-dong, Cheoin-Gu, Yongin, 449-714, Korea

Abstract – Selenium is a key constituent of enzyme in glutathione peroxidase, which is effective in decreasing various types of oxidative stress, Thus, the adequacy of selenium intake is very important in decreasing the risks of various degenerating diseases such as cardiovascular disease, or certain cancers. Lately, the intake of animal foods is increasing among Koreans owing to a dietary transition toward a western style. This study was conducted to measure the selenium content in meat and eggs, and then assessed the selenium intake from these foods. Forty frequently eaten items among meat and eggs were analyzed using an Instrumental Neutron Activation Analysis. The selenium content in 100g of raw meat and eggs ranged from 8.1ug to 50.9ug. In particular, 100g of beef contained 12.4ug to 50.9ug of selenium; pork, 11.2ug to 22.6ug chicken, 10.2ug to 13.7ug and eggs, 28.6ug to 43.0ug. Thus, beef viscera and chicken eggs contain the highest amounts of selenium among these groups. 100g of Pork belly, the most frequently eaten meat type among Koreans, contains 14.6ug of selenium. An evaluation of dietary selenium intake shows that the total selenium supply from meats and eggs was 28.4ug/day and 27.5 ug/day in adult men and women, respectively. These are over one-half of the Korean RNI(Recommended Daily Intake) of 55ug/day.

Keywords–Instrumental Neutron Activation Analysis, Selenium, Meat and Eggs, Dietary Intake

I. INTRODUCTION

As the biological activity of food selenium in humans is dependent, sometimes to a very large degree, on the source and chemical form of the selenium consumed, an increased intake of animal food can facilitate meats and eggs as important sources for selenium intake in Koreans. Considering these points, an evaluation of selenium intake in Koreans from animal foods is very important. This study was conducted to analyze the selenium contents in meats and eggs, and to assess the consumption pattern of selenium in Koreans from these animal foods.

II. EXPERIMENTAL

The number of meat items used in the selenium analysis was 13 items for raw beef, 8 items for raw pork, 3 items for raw chicken, 4 items for raw eggs, and 12 items for the processed meat products, respectively. Most of the foods were bought between September 2009 and February 2010. All domestically produced and imported meats and eggs in a raw or processed state were purchased from markets with a nationwide network around Seoul and Keunggido. The meat sample was ground using a blender with a titanium blade, and freeze-dried in a lyophilizer at various times of 24 - 96 hours. The analysis of selenium was performed by instrumental neutron activation analysis using the HANARO research reactor.

III. RESULTS

The selenium contents in the different parts of beef were ranged from 12.4ug to 50.9ug in 100g of the edible portions, where the highest value was shown with beef liver. The selenium contents in raw Korean pork ranged from 11.2ug to 22.6ug in 100g of food, showing a difference according to the pork region. Pork belly, the most frequently eaten meat among Koreans, contained selenium at an amount of 14.6ug at 100g. The raw chicken contained selenium with a range of 10.2ug to 13.7ug in 100g, showing only a small difference by the chicken part. The selenium contents in the frequently eaten eggs were in the range of 28.6ug 43.0ug for 100g. Eggs were distinct in that they contained the highest amount of selenium among the meats with a range of 38.9ug to 43.0ug for chicken eggs, and of 28.6ug for the quail egg per 100g of eggs. The processed pork products contained selenium in a range of 8.8 - 14.9 ug for 100g, which is lower than the raw unprepared pork meat. Among the pork products, Pyeonuk and pork hocks, cooked pork products, showed selenium contents of 19.4 and 21.1ug for 100g, respectively. The prepared chicken, mostly from fast food eateries, contained selenium in a range of 7.4 to 11.5ug for 100g. An evaluation of dietary selenium intake shows that the total selenium supply from meat and eggs was 28.4ug/day and 27.5ug/day in adult men and women, respectively. These are over one-half of the Korean RNI (Recommended Daily Intake) of 55ug/day.

ACKNOWLEDGEMENT

This work was carried out under the Nuclear Research and Development Program of the Korean Ministry of Education, Science, and Technology.

REFERENCES

[1] J Rotruck JT, Pope AL, Ganther HE, Swanson AB, Hafeman DG, Hoekstra WG. Selenium: biochemical role as a component of glutathione peroxidase. Science 1973, 179:588-90.
[2] The Korean Nutrition Society, Dietary Reference Intake for Koreans, Seoul, 2010, p 481-97.

APSORC'13 - 5th Asia-Pacific Symposium on Radiochemistry
Kanazawa, Japan, 22-27 September 2013

Evaluation of Hypoxia at Dredged Trenches in Tokyo Bay by Determination of Redox Sensitive Elements in the Sediments

T. Yamagata[1], K. Shozugawa[1], R. Okumura[2], K. Takamiya[2], M. Matsuo[1]
[1]Graduate School of Arts and Sciences, The Univ. of Tokyo
[2]Research Reactor Institute, Kyoto Univ.

Abstract – Sediment samples were collected from Tokyo Bay, and the concentrations of some elements were determined by instrumental neutron activation analysis (INAA).Though hypoxia has been observed in dredged trenches, it is suggested that upper layers of the sediments are more oxidative than lower layers.

Keywords – Hypoxia, Sediment in Tokyo Bay, Instrumental neutron activation analysis (INAA)

I. INTRODUCTION

Hypoxia is water mass contained little dissolved oxygen (DO) (< 2 ml of O_2 / liter) [1], which is known as dead zone in coastal sea. At the seabed in Tokyo Bay, large-scale dredging operations had been done in 1970s. In particular, the dredged trenches off Makuhari have the maximum area and depth. In dredged trenches severe hypoxia has been observed in annual summer seasons, and the hypoxia has disappeared in winter. But the influence of dredged trenches on hypoxia is not revealed yet. Therefore, it is important to estimate the interannual variations of hypoxia by analyzing sediments.

To evaluate the sedimentary environment such as redox conditions, the method using the Th/U-Ce/U plot based on the data obtained by INAA was reported by Honda et al [2]. It is very useful because the correlation coefficient between the Th/U and Ce/U ratios is high, but it hasn't been used for evaluating the sedimentary environment at dredged trenches, where the conditions are unique. In this study, sediment cores were collected from the Makuhari dredged trenches in Tokyo Bay. Concentrations of U, Th, and Ce in the sediments were analyzed by INAA. And then the sedimentary environment is discussed in connection with the depth profiles of the elements and the Th/U-Ce/U plot.

II. EXPERIMENTAL

The sediment samples were collected at dredged trenches (water depth 25.5 m and 18.9 m) and reference site (non-dredged seabed, water depth 10.7 m) off Makuhari in Tokyo Bay on August 2012. Sediments were collected by a core sampler at each point. Water quality data were also obtained by a multichannel water quality meter and an oxidation-reduction potentiometer. All cores were cut in the vertical direction at 0.6 – 3.0 cm intervals after freezing.

Approximately 30 mg of freeze-dried sediments were packed in double polyethylene film bags. All samples were irradiated at the pneumatic tube, Kyoto University Reactor (KUR). Two types of gamma-ray measurement were carried out depending on half-lives of elements. For analysis of U, samples were irradiated for 20 min at 1 MW or 4 min at 5 MW, and then gamma-ray was measured for 1200 seconds (live time) by Ge detector after 3 days cooling. Regarding Th and Ce, samples were irradiated for 20 min at 1 MW or 4 min at 5 MW, and the measurement time of gamma-ray was for 9000 seconds (live time) after 3 weeks cooling.

III. RESULTS AND DISCUSSION

The DO in the seawater at dredged trenches and reference site (non-dredged area) indicated the similar vertical distribution at each station. From the depth of 8 m, the DO decreased suddenly. And below the depth of 10 m, the water became anoxic in dredged trenches. It turned out that strong hypoxia has developed at the dredged trenches.

From the depth profiles in dredged trenches, the Th/U and Ce/U ratios are higher in the upper layers than in the lower layers. It is said that the concentrations of Th and Ce in sediments increase when condition of seawater is oxidative. On the other hand, the concentration of U increases when condition is reductive. It is considered that the sedimentary environment of the upper layers is more oxidative than the lower layers.

Figure shows the Th/U-Ce/U plots of the sediments. The correlation coefficient between the Th/U and Ce/U ratios is high enough. Therefore, this method is also useful for evaluating the hypoxia at dredged trenches, in which the environment changes drastically on each summer and winter season.

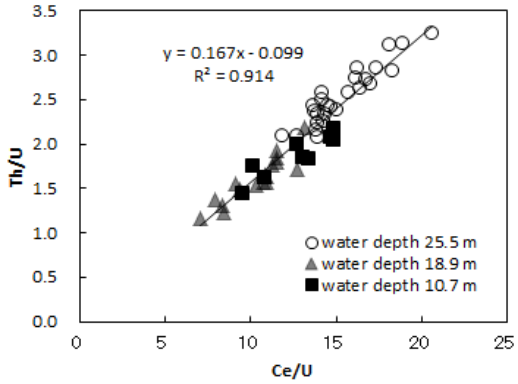

Fig. Th/U-Ce/U plots of the sediments collected from Tokyo Bay

[1] R. J. Diaz and R. Rosenberg, Science, 321, 926-929 (2008).
[2] T. Honda and K. Kimura, Bull. Soc. Sea Water Sci., Japan, 57, 166-180 (2003) (in Japanese).

APSORC'13 - 5th Asia-Pacific Symposium on Radiochemistry
Kanazawa, Japan, 22-27 September 2013

Determination of ultra trace amounts of Mn in iron meteorites by preconcentration neutron activation analysis

Y. Tanaka[1], Y. Arai[1], T. Imamura[1], Y. Oura[1]
[1]Department of Chemistry, Tokyo Metropolitan University

I. INTRODUCTION

Meteorites contain cosmogenic nuclides produced by a nuclear reaction with cosmic rays. Cosmogenic nuclides are useful for determination of exposure and terrestrial ages. In general, only radionuclides and noble gas stable-isotopes can be detected as cosmogenic nuclides. Although it is difficult to detect cosmogenic stable nuclides in stony meteorites, some cosmogenic stable nuclides could be detected in iron meteorites, which consist of mainly an iron–nickel alloy, since iron meteorites have little geochemical lithophile elements. Among such stable nuclides we focus on Mn.

Natural Mn is a monoisotopic (^{55}Mn) element. But iron meteorites have also a cosmogenic radioisotope, ^{53}Mn, which has longest half life among detectable cosmogenic radionuclides. One of practical methods for determination of ^{53}Mn is a preconcentration neutron activation analysis (preNAA) using ^{53}Mn(n, γ)^{54}Mn reaction. We suggested that ^{55}Mn content should be required for determination of ultra trace ^{53}Mn in iron meteorites by preNAA because of correction of ^{55}Mn(n, 2n)^{54}Mn. But accurate concentration in iron meteorites is rarely reported. Almost ^{53}Mn in iron meteorites is extrapolated to be comsogenic by ^{45}Sc contents [1]. If accurate ^{55}Mn concentration can be determined, ^{55}Mn-^{53}Mn system for exposure age will be also established. And estimation of original ^{55}Mn concentration is interesting for considering a differentiation of planets. Determination of ^{55}Mn in iron meteorites by NAA is well known to be interfered by ^{56}Fe(n, p)^{56}Mn reaction. Therefore, the removal of iron prior to irradiation or irradiation at a channel with high Cd ratio is required. Thus we tried to determine ^{55}Mn concentration in iron meteorites by preNAA using well thermalized neutrons.

II. EXPERIMENTAL

Using radiotracers, a chemical procedure using an ion-exchange method was developed for separation of Mn from iron meteorites based on one by Fujimoto and Shimura [2]. After dissolution of a sample in 2 M HF, the HF solution was loaded on a cation exchange resin. Adsorbed Mn was eluted by 8M HCl, and then Mn in HCl - 2-propanol solution was purified by an anion exchange method. This procedure was applied to Japan steel standard samples and Gibeon iron meteorites followed by irradiation of separated Mn fraction for 4 hours at the thermal column pneumatic transport system (Tc-Pn) and for 1 hour at Pn-2 in Kyoto University Research Reactor (KUR). In addition, sensitivity of ^{55}Mn(n, γ)^{56}Mn and contribution of ^{56}Fe(n, p)^{56}Mn at Tc-Pn in KUR and at PN-3 in the Japan Research Reactor-3 (JRR-3), Japan Atomic Energy Agency were evaluated by using Mn standard and Ti plate, respectively.

III. RESULT AND DISCUSSION

In Mn fraction irradiated for 1 h at Pn-2, no ^{59}Fe and ^{60}Co was observed. Our chemical procedure removed > 99.99% of Fe and Co and > 99.5% of Ni, Ir and Cr, and overall procedure blank of Mn was about 30 ng. Determined Mn concentration in steel standards (JSS003-5 and JSS001-5) and Gibeon meteorites are shown in Table 1. Low determination values in Run-1 were guessed to be caused by low chemical yield. In Run-2 a chemical yield was estimated to be 91% and determined concentrations on Mn in steel standards were consistent with certified values. It is concluded that down to 30 ppb of Mn can be determined by our method.

Sensitivities of Mn were 930 cps/μg and 2400 cps/μg for 4 h irradiation at Tc-Pn and 20 min irradiation at Pn-3, respectively. And contributions of (n, p) reaction were corresponding 16 ngMn/gFe and 97 ngMn/gFe for Tc-Pn and PN-3, respectively. Since Fe was sufficiently removed, contribution of ^{56}Fe(n, p) reaction was more than 150 times smaller than the present procedure blank. A detection limit of Mn by preNAA was 30 ppb, assuming that a half of induced ^{56}Mn is resulted by a blank. Even INAA using Tc-Pn can determine such concentration of Mn. Reducing a procedure blank is highly required for lower detection limit.

TABLE 1: Result of Mn content

Sample	Unit	INAA*	preNAA run1	preNAA run2	Certified Value
JSS003-5	ppm	24.9 ± 0.2	19.8 ± 0.4	26.0 ± 0.3	27 ± 1
JSS001-5	ppb	36.1 ± 2.2		27.5 ± 2.2	30 ± 10
Gibeon	ppb		273 ± 9	415 ± 7	

*Corrected for (n, p) reaction.

[1] Oura et al., Proc. Radiochim. Acta 1.383 (2011).
[2] K. Fujimoto and M. Shimura, Bunseki Kagaku 50, 175 (2001).

Instrumental photon activation analysis of geological and cosmochemical samples

Naoki Shirai[1], Shun Sekimoto[2], Mitsuru Ebihara[1]
[1]Tokyo Metropolitan University
[2]Kyoto University Research Reactor Institute

I. INTRODUCTION

Bulk chemical compositions for terrestrial and cosmochemical materials are significantly important to elucidate the formation, evolution processes and magmatism of planetary bodies. Compared to geological samples, cosmochemical samples pose several severe requirements to their analytical methods for chemical compositions. High sensitivity and accuracy for as many as elements as possible are required for analytical methods applied to such samples because of the limitation of sample amounts usable for analysis. Non-destructive analysis for many elements is equally favorable. Nuclear analytical methods represented by prompt gamma-ray analysis (PGA), instrumental neutron activation analysis (INAA) and instrumental photon activation analysis (IPAA) meet almost all these requirements. Among these nuclear analytical methods, INAA has been commonly used as an analytical tool in comomochemistry for a long time, while PGA and IPAA have not been very often applied to cosmochemical samples.

In PAA, (γ,n) reaction is used for determination of elemental abundances which is an opposite reaction ((n, γ) reaction) used in INAA. Thus, IPAA could determine elemental abundances which cannot or hardly be determined by INAA. Ebihara et al. [1] examined the suitability of PAA by analyzing cosmochemical samples (chondrites) and concluded that PAA is as effective as NAA for analyzing chondritic meteorites. Usually samples are irradiated by using 30 MeV electrons in IPAA. However, corrections of interferences caused by secondary nuclear reactions such as (γ,p) and (γ,pn) are necessary. Although the sensitivity obtained by activation with 20 MeV electrons are suppressed compared to the activation with 30 MeV electrons, activation with 20 MeV electrons reduces the degree of such interferences. In this study, we performed IPAA by using a linear electron accelerator at Kyoto University Research Reactor Institute (KURRI) and compared the results obtained the activation with 20 MeV with those for activation with 30 MeV.

II. EXPERIMENTAL

In this study, four Geological Survey Japan standards materials (JA-2, JB-3, JR-1 and JG-1) were analyzed. In addition to these terrestrial geological samples, the Allende meteorite was analyzed as a cosmochemical samples. Each samples was taken into a sample container (9 mmϕ) made of highly Al foil (Al: 99.5 %, Niraco Co., Ltd). In addition to rock samples, chemical reagents were irradiated to correct the spectral interferences. Five to ten samples were stacked, among which thin foil disks (9 mmϕ) of Au were placed for as monitoring the intensity of photon. Samples in a block were put in a quartz tube. Irradiations were performed by using a linear electron accelerator at KURRI. Electrons were accelerated by the linear accelerator to about 20 and 30 MeV. After irradiation (about 30 hrs), samples were taken into new Al foil and measured for gamma rays several times with different cooling intervals at KURRI and the Laboratory of Radioisotopes, Tokyo Metropolitan University. Elemental abundances were determined by comparison method by using JB-1.

III. RESULTS AND DISCUSSION

Table 1 shows the interfering reactions and their contributions to nuclides produced by corresponding reactions for activation with 20 MeV and 30 MeV electrons. As shown in Table 1, significant contributions from interfering reactions were found in activation with 30 MeV electrons. Thus, determinations of Cr, Co and Mn abundances need the correction of corresponding interferences. As expected, contributions from interfering reactions with 20 MeV electrons were lower than those in activation with 30 MeV electrons.

A total of 17 elements (Ca, Sc, Ti, Cr, Mn, Fe, Co, Ni, Zn, As, Rb, Y, Zr, Nb, Cs, Ba and Ce) were determined in geological reference standard materials and the Allende meteorite. Our Cr and Mn values obtained from activation with 30 MeV electrons were different from literature values. Improper corrections of the interfering reactions were responsible for these differences. In contrast, our Cr and Mn values obtained from activation with 20 MeV electrons were in good agreement with literature values. For other elements, there were no differences between the two sets of our values obtained from the activations with 20 and 30 MeV electrons, which were consistent with literature values.

Table 1. Interfering reaction and correction rate for interference.

Element interfered	Reaction used for determination	Interfering reaction	Correction rate 30 MeV	Correction rate 20 MeV
Cr	$^{52}Cr(\gamma,n)^{51}Cr$	$^{56}Fe(\gamma,\alpha n)^{51}Cr$	0.036 mgCr/gFe	-
Co	$^{59}Co(\gamma,n)^{58}Co$	$^{60}Ni(\gamma,pn)^{58}Co$	3.7 mgCo/gNi	0.88 mgCo/gNi
Mn	$^{55}Mn(\gamma,n)^{54}Mn$	$^{56}Fe(\gamma,pn)^{54}Mn$	6.2 mgMn/gFe	0.1 mgMn/gFe

Reference: [1] Ebihara M. et al. (2000) J. Radioanal. Nucl. Chem., 244 (3), 491-496.

Monte Carlo Calculation of Chloride Diffusion in Concrete

A. A. Naqvi[1], Khateeb-ur-Rehman[1], M. Maslehuddin[2], O.S.B. Al-Amoudi[3] and M. Raashid[1]
[1]Department of Physics, [2]Center for Engineering Research, and [3]Department of Civil and Environmental Engineering
King Fahd University of Petroleum and Minerals, Dhahran, Saudi Arabia

Abstract – Coefficient of chloride diffusion is calculated by applying the Fick's second law of diffusion to a chloride concentration profile. Then from the signal strength for various chlorine gamma-ray energies was then calculated at the detector. of the portable D-D neutron generator based PGNAA setup. An excellent agreement was noted between the reported results of the calculations for the ^{252}Cf neutron source-based portable PGNAA setup and the D-D portable *neutron generator based PGNAA setup developed by the authors.*

Keywords –Coefficient of chloride diffusion ; Fick's second law of diffusion; DD based Portable neutron generator based PGNAA setup; detector chloride signal strength calculation

I. INTRODUCTION

Corrosion of reinforcing steel is mainly caused due to the chloride ions. These ions either diffuse to the steel surface from the service environment or they are contributed by the mixture ingredients. The penetration of chloride ions from the service environment is a diffusion controlled process [1]. Consequently, the coefficient of chloride diffusion is calculated by applying the Fick's second law of diffusion to a chloride concentration profile. A prompt gamma-ray neutron activation (PGNAA) setup has been designed utilizing a portable neutron generator by the authors [2]. The setup, which mainly consists of a D-D portable neutron source along with its moderator placed side by side with a shielded gamma-ray detector, allows the determination of chloride concentration in a concrete structure from one side. The D-D portable PGNAA setup has been modeled for the determination of chlorine concentration at various depths using a MCNP simulation code following the procedure described elsewhere [1] for a ^{252}Cf neutron source based PGNAA setup.

.

In the reported study, the chloride diffusion profile was modeled for several values of diffusion coefficients as a function of time. These chloride concentrations are then utilized as an input to the MCNP based model [1]. The signal strength for various chlorine gamma-ray energies was then calculated at the detector. An excellent agreement was noted between the reported results of the calculations for the ^{252}Cf neutron source-based portable PGNAA setup [1] and the D-D portable neutron generator based PGNAA setup developed by the authors

[1] Livingston, R.A., Al-Sheikhly, M., Mohamed, A.B. "Numerical simulation of the PGNA signal from chlorine diffusion gradients in concrete," *Applied Radiation and Isotopes*, Vol. 68 (2010), pp. 679–682.

[2] Naqvi, A. A., Kalakada, Z., Al-Matouq, F.A., Maslehuddin, M. and Al-Amoudi, O.S.B., "Chlorine detection in fly ash concrete using a Portable Neutron Generator," *Applied Radiation and Isotopes,* Vol. 70(2012), pp.1671-4.

APSORC'13 - 5th Asia-Pacific Symposium on Radiochemistry
Kanazawa, Japan, 22-27 September 2013

Catalysis Induced by Radiation in Fatty Acids Adsorbed on Clay Minerals

A. Negron-Mendoza[1]*, S. Ramos-Bernal[1], M. Colin-Garcia[2] and F.G. Mosqueira[3]
[1]Instituto de Ciencias Nucleares, Universidad Nacional Autonoma de Mexico, UNAM. A.P. 70-543, México, D.F. 04510, México.
Instituto de Geología, Universidad Nacional Autonoma de Mexico, México, D.F. 04510, México
[3]Dirección General de Divulgación de la Ciencia, Universidad Nacional Autonoma de Mexico, D.F. 04510, México

Abstract – We have studied the behavior of small fatty and dicarboxylic acids adsorbed in sodium-montmorillonite and exposed to gamma radiation. It is observed that the radiation-induced decomposition of the clay-acid system goes along a definitive path (oxidation) rather than following several modes of simultaneous decomposition, as in the case of the radiolysis without the clay. This preferential synthesis promotes the formation of a hydrocarbon compound with one carbon atom less than the parent compound

Keywords –Decarboxylation reaction, carboxylic acids, gamma radiation, montmorillonite, $^{14}CO_2$

I. INTRODUCTION

The adsorption of certain organic compounds by clays gives rise to the transformation of the adsorbate by the action of clays. These kinds of reactions play an important role in many natural and industrial processes. In the context of oil and gas exploration, for example, the source and trap of petroleum hydrocarbons frequently are clay-rich rocks. Clay-water based muds are also seen as environmental friendly alternatives to toxic oil-based fluids [1].

In this perspective, several investigators [2, 3] have studied the thermal decomposition of fatty acids in the presence of clay minerals. The differences found by several workers for the distribution patterns of hydrocarbons may be caused largely by thermal alteration. In addition, radioactive bombardment alters these sediments. It is an important subject that has not been extensively studied.

The modification by ionizing radiation of the activity of heterogeneous catalysis is a relatively new problem in radiation chemistry. The sensitization of radiation-chemical reactions by solid surfaces may increase the catalytic activity of the clay. The aim of this paper is to study the radiation-induced decomposition of carboxylic acids adsorbed in a clay mineral as an example of heterogeneous radiation catalysis that can be correlated to natural and industrial processes.

II. MATERIALS AND METHODS

The experimental part is divided in two stages: (1) Radiolysis of aqueous solutions of the carboxylic acids, (2) Study of heterogeneous radiolysis of the water-carboxylic acid-clay system

(1) Aqueous solutions of carboxylic acids (0.1 mol L^{-1}), oxygen free, prepared in a glass syringe (acetic, succinic, aconitic); (2) Aqueous solutions of acids containing 0.3 g of the clay were prepared. The addition of the clay into the solution was in an oxygen-free bag, with continues agitation. (3) For gas analysis, 0.1 g of the clay was evacuated for one hour and 1 mL of the solution was added, in an oxygen-free bag. The samples were in special glass tubes with a stopcock that was connected to a Toepler pump. We used blanks to correct the yield of gas samples. Some runs were made with 14-carbon label acetic acid ($CH_3{}^{14}COOH$) to show that the CO_2 obtained was from the target acid. $^{14}CO_2$ was measured by a scintillation technique. The irradiations were carried out in a high intensity gamma source of ^{60}Co (Gammabeam 651 PT). The radiation doses were from 46. kGy to 300 kGy

III. RESULTS AND REMARKS

The irradiation of aqueous carboxylic acid produced many compounds, for example for acetic acid, the total yield of polycarboxylic acids was 22% and for succinic acid was about 35%. The principal feature of these series of radiolysis experiments was the production of the dimer of the acid, as the principal way of decomposition of the target compound, but many other acids were formed. For example, in the radiolysis of acetic acid (CH_3CO_2H), the main product was succinic acid $(CH_2CO_2H)_2$, the dimeric product. The formation of CO_2 from the decarboxylation reaction was only 7%. The decomposition of the target compound increased as a function of the dose.

The radiolysis performed in presence of clay decreased considerably the number of formed products. For example, in acetic acid, the production of polycarboxylic acids was 4.8 % and the formation of carbon dioxide increased to 81 %.

The main result obtained shows that the radiolysis of the system clay-acid goes along a defined path rather than showing various pathways of decomposition. The main pathway was the decarboxylation of the target compound rather than condensation/dimerization reactions.

ACKNOLEDGEMENTS

This work was supported by PAPIIT Grant No. IN110513 and the CONACyT Grant No. 168579/11.

REFERENCES

[1] Skipper, N. Hannon, A., and Buchanan, P. ISIS Experimental Report, Rutherford Appleton Laboratory, RB 1205 (2001).
[2] Eisma, E. and Jurg, W.J. in G. Eglinton and M.J. Murphy (Editors) Organic Geochemistry, Springer Verlag, New York, (1969).
[3] Simoyama, A. and Johns, W.D., Nature, 232, 14 (1971).

APSORC'13 - 5th Asia-Pacific Symposium on Radiochemistry
Kanazawa, Japan, 22-27 September 2013

Preliminary Study for Highly Sensitive Airborne Radioiodine Monitor

Yoshimune Ogata[1], Tadashi Yamasaki[2], Ryuji Hanafusa[3]
[1]Nagoya University
[2]CEPCO
[3]Fuji Electric

Abstract – Airborne radioiodine monitoring has a problem in that conventional radioiodine gas monitors have inadequate sensitivity. To solve the problem, we designed a highly sensitive gas monitor. The higher counting efficiency and lower background brought sufficient sensitivity. The properties of the monitor were investigated using air including gaseous ^{125}I. The minimum detectable activity concentration for ^{125}I was 1×10^{-4} Bq cm^{-3} for one minute counting, which corresponded to one tenth of the legal limit of ^{125}I for the radiation controlled areas in Japan.

Keywords – Radioiodine, Gas monitor, Highly sensitivity

I. INTRODUCTION

There are several issues regard with airborne radioiodines. It caused significant social fear that large amount of ^{131}I was released from the nuclear disaster of Fukushima Daiichi NPP, TEPCO. On the other hand, small amounts of ^{129}I are gradually released from nuclear reprocessing plants and decommissioning sites of NPPs. Another issue is the contamination of patient rooms by exhalation of ^{131}I from patients undergoing thyroid gland therapy. Furthermore, ^{125}I is frequently used for radioimmunoassay and research programs in medical examination facilities and/or research laboratories. To guarantee radiation safety, radioiodine concentration should be measured.

However, the legal limits of airborne radioiodine are quite low, and conventional gas monitors have inadequate sensitivity to measure such low-level airborne radioiodine[1]. One method for detecting low-level airborne radioiodine is to adsorb the radioiodine with activated charcoal by air suctioning, and measure it with laboratory detectors. But, since it is carried out in a batch process, it needs a relatively long time to obtain results.

Highly sensitive, real-time airborne radioiodine monitor are required for safety work in radiation areas and for environmental safety. In this study, a novel monitor to measure the airborne radioiodine was designed, which has sufficient sensitivity to detect the airborne radioiodines toward the legal limits.

II. MATERIALS AND METHODS

The detector consists of an adsorption column containing activated charcoal, a well-type NaI(Tl) scintillation detector, an air suction pump, and a flow regulator. The column was put in the well of the NaI(Tl) detector. The detector was surrounded by a shield with lead and copper. The air was introduced into the bottom of the column and suctioned by an air pump.

The electric signal from the detector was collected with a multichannel analyzer (MCA) through an amplifier. The MCA had two modes: a pulse height analysis (PHA) mode, and a multichannel scaling (MCS) mode. The PHA mode was used for the initial settings, and the MCS mode was used for the time-series measurements as continuous monitoring.

The characteristics of the system were investigated using ^{125}I. Before application of the airborne iodine monitoring, the counting efficiency of the detector was estimated using a set of ^{125}I solutions with several volumes. The activities of the solutions were estimated according to coincidence method[2]. Then, sample air including gaseous ^{125}I in a balloon was drawn into the detector. The concentration of ^{125}I in the air and the adsorption factor of the column were estimated using a set of tandem adsorption column. The minimum detectable concentration (MDC) of the system was evaluated by the experimental results.

III. RESULTS AND DISCUSSION

The counting efficiencies of the detector for ^{125}I were 50% – 85%, which depended on the sample height. The adsorption factor for iodine was higher than 99%. The ^{125}I concentration prepared in the balloon was 3.5×10^{-4} Bq cm$^{-3}_{\text{-air}}$.

When the flow rate was 3 L min^{-1}, the MDC is estimated as 1×10^{-4} Bq cm^{-3} for one minute counting, which was one tenth of the legal limits of the air in radiation controlled areas, 1×10^{-3} Bq cm^{-3}. In the case of 15 minute counting, the MDC is estimated as 2×10^{-6} Bq cm^{-3}, which was one fourth the legal limits of the exhausted air, 8×10^{-6} Bq cm^{-3}. Lower MDCs will be expected by improving of the detection arrangement.

This detection system can be used for ^{129}I monitoring as it is, and it needs a minor modification for ^{131}I monitoring. The MDCs of this system were almost two orders of magnitude lower than conventional radioiodine gas monitors. The system will be effective in radioactive gas monitoring applications in decommissioning sites, nuclear plants, medical and laboratorial facilities, and environment in general.

[1] Matsuda. N., Effluent monitor – Technical guideline for safe management of radioiodine. Japanese J Radiation Safety Management, 8 (2), 162 (2009) (in Japanese).
[2] Horrocks, D,. et al., Theoretical considerations for standardization of ^{125}I by the coincidence method. Nucl. Instrum. Methods, 124 (2), 585-589 (1975).

Radiation synthesis and cesium removal of cellulose microsphere based hybrid adsorbent

Long Zhao[1*], Yanliang Chen[1], Yuezhou wei[1]
[1] *School of Nuclear Science and Engineering, Shanghai Jiao Tong University, Shanghai 200240, China*
Corresponding author: Fax: (+86) 213420-7654; E-mail address:* ***ryuuchou@sjtu.edu.cn*

Abstract –A novel cellulose-based hybrid adsorbent was successfully prepared by radiation-induced grafting of glycidyl methacrylate (GMA) onto the surface of cellulose microspheres, followed by epoxy ring-opening reaction to introduce ammonium 12-molybdo phosphate (AMP). The characterization of the obtained adsorbent was investigated in detail. To evaluate the adsorption performance of the novel adsorbent, batch and column mode adsorption experiment against cesium (Cs) was conducted.
Keywords –radiation grafting; ammonium12-molybdophosphate; cellulose microsphere; cesium; adsorption

I. INTRODUCTION

It is well known that the leakage and spread of ^{137}Cs generated from the accident of atomic power plant such as Fukushima nuclear disaster can affect human health, and lead to severe environmental problem [1-2]. Several techniques have been employed for treating Cs containing aqueous solutions, which include adsorption, reverse osmosis, extraction and precipitation. Among these methods, adsorption has the advantages on high efficiency, easy handling, availability of different adsorbents and cost effectiveness.

Ammonium 12-molybdophosphate (AMP), which shows high selectivity toward Cs ion, can act as one of the most promising adsorbent materials for this purpose. [3]. However, AMP is still not employed on a large scale because of its fine powder form which hinders simple column operation. To overcome this disadvantage, in this study, we proposed a novel hybrid adsorbent which could be easily prepared by radiation grafting. In current work, AMP can be introduced onto glycidyl methacrylate (GMA) grafted cellulose microsphere surface through epoxy ring-opening reaction. The whole preparation procedures are rather simple.

To evaluate the adsorption performance of the novel adsorbent, batch and column mode adsorption experiments by using a nonradioactive Cs solution will be conducted.

In this report, the synthesis conditions and adsorption properties of the novel adsorbent prepared by radiation grafting are introduced in detail.

II. EXPERIMENTAL AND RESULTS

Adsorbent was prepared by pre-irradiation grafting polymerization. Initially, trunk polymer was sealed in polyethylene bags purged with nitrogen gas. The sample bags were irradiated by EB generated from an accelerator, at a voltage of 750 keV and a dose rate of 10 kGy per pass under the cooling of dry-ice. After getting rid of oxygen by nitrogen flow, monomer solution was injected into the sample bags. The grafting reaction was then performed in a water bath at desired temperature and reaction time. The homopolymer and unreacted monomer were removed by eligible solvent and then grafted polymers were dried in vacuum. Thereafter, the grafted cellulose microsphere with GMA having epoxy groups was reacted with AMP in a turbid liquid state at 80°C for 18h. The resulting adsorbent was washed with water and dried in vacuum and kept for further use. The structure of the resulting adsorbent was confirmed by micro-FTIR spectra, TG and XPS analysis.

The batch adsorption of Cs has been investigated as a function of contact time, pH, Cs and NaCl concentration. A column-mode adsorption test was carried out using 15ml volume column at a flow rate of space velocity $10h^{-1}$ for initial Cs of 5 mg L^{-1} at pH5.4. The concentration of Cs was measured by atomic absorption spectrophotometer (AAS) and Inductively Coupled Plasma Mass Spectrometer (ICP-MS).

It was found that adsorption equilibrium could be achieved within 30 min for initial Cs of 5 mg L^{-1}. It is believed that the functional groups concentrated in surface result in such quick adsorption. Cs uptake of adsorbent depends on solution pH, with a maximum Cs uptake at pH 5.4. The adsorption kinetics was well described by the pseudo-second order model equation, and the adsorption isotherm was better fitted by the Langmuir mode. Fig.1. showed the breakthrough curves of column adsorption experiment. The breakthrough curve indicated that the Cs adsorption amount at the breakthrough point was 0.75g-Cs/L-adsorbent, and the Cs can be completely removed till the flux reached roughly 150 bed volumes.

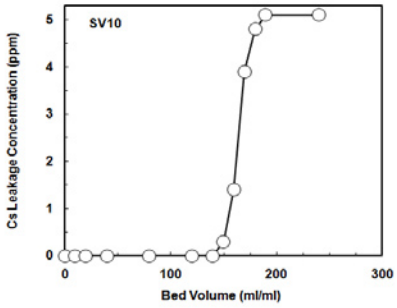

Fig.1. Breakthrough curves of adsorbent.

Lastly, it was found that 80% adsorption capacity can be kept even though the adsorbent was exposed to 1000kGy γ-irradiation. These results suggested that obtained adsorbent could be used to removal Cs from wastewater.

REFERENCES

[1] *IAEA Technical Report Series*, *No. 356* (1993).
[2] K. Takeshita and T. Ogata, *J. Ion Exchange.23,*1 (2012).
[3] W. Faubel and S. A. Ali, *Radiochim. Acta*, *40*, 49 (1986).

Study about separation mechanism of endohedral metallofullerenes with Lewis acid

K. Chiba[1], T. Hamano[1], E. Takeuchi[1], K. Akiyama[1], S. Kubuki[1], and H. Shinohara[2]

[1]Department of Chemistry, Tokyo Metropolitan University, Hachioji, 192-0397, Japan

[2]Graduate School of Science, Nagoya University, Nagoya 464-8602, Japan

Keywords – Metallofullerene, Lewis acid, Separation

I. INTRODUCTION

Recently, a method for the separation and purification of endohedral metallofullerenes (EMFs) with Lewis acid was reported[1]. It is found that EMFs in fullerene crude extract are selectively oxidized with Lewis acid and separated with especially high yield (>99 %) by the liquid Lewis acid such as $TiCl_4$ and $SnCl_4$. On the other hand, the method using solid Lewis acids like $AlCl_3$ needs long time for the separation compared to liquid Lewis acid and the separation efficiency is decreased to around 40 % for the same reaction time. Based on the previous study, it is presumed that homogeneous diffusion of Lewis acid in crude extract solution lead to the efficient interaction between EMFs and Lewis acid.

In this session, we will report the effect of diffusion of $AlCl_3$ to the separation and the detail of separation mechanism of EMFs.

II. EXPERIMENTAL

Soot containing La EMFs were produced by arc discharge method with La/C composite rods (La:C=1:130). The produced soot were dissolved to 1,2,4,-trichlorobenzene (TCB), and then refluxed for 12 hours. The TCB solution including crude extracts of fullerenes was filtered and evaporated to dryness. After that, the crude extracts were re-dissolved to *o*-dichlorobenzene (DCB). EMFs of ^{141}Ce, which are known to behave as with La EMFs, were added to these solutions as a radioactive tracer. Chlorobenzene solution of $AlCl_3$ ($AlCl_3$/CB) was added to the crude extract. These mixed solutions were stirred and then separated by PTFE membrane filter (pore diameter is 0.2 μm, Millex, Merck Millipore). The EMFs remaining on the filter were washed by water and acetone. After that, DCB was passed through the filter to recover the EMFs. The gamma-ray emitted from ^{141}Ce in the samples was measured for the determination of separation efficiency by germanium semiconductor detector (GMX25, SEIKO EG&G).

$AlCl_3$/CB was also added to purified La@C_{82} DCB solutions and their vis-NIR absorption spectra were measured (UV-3600, SHIMADZU) in order to investigate the electronic states of the EMF.

III. RESULTS AND DISCUSSION

In comparison of the radioactivity of ^{141}Ce at before / after separation, the efficiency with $AlCl_3$/CB was determined as about 40 %. This is corresponding to that with solid $AlCl_3$. It suggests that the separation efficiency is not much affected by homogeneous diffusion of Lewis acid.

In the vis-NIR spectra of the mixed solution of La@C_{82} and $AlCl_3$/CB, two characteristic absorption bands at 1000, 1400 nm of La@C_{82} were disappeared but new band was raised at 1300 nm after 5 min of adding $AlCl_3$/CB. This result indicate that neutral La@C_{82} is immediately oxidized by the addition of Lewis acid and cationic species of La@C_{82} is produced within 5 minute.

Detail of the mechanism of separation will be discussed in the session.

[1] K. Akiyama *et al., J. Am. Chem. Soc.,* **134,** 9762-9767, (2012).

CRYSTAL STRUCTURE AND SPIN STATE OF MIXED-CRYSTALS OF $Fe(NCS)_x(NCBH_3)_{2-x}(bpp)_2$ (bpp = 1,3-BIS(4-PYRIDYL)PROPANE)

Haruka Dote[1], Hiroki Yasuhara[1], Satoru Nakashima[2]
[1]Graduate School of Science, Hiroshima University
[2]Natural Science Center for Basic Research and Development (N-BARD), Hiroshima University

Abstract
New mixed crystals, $Fe(NCS)_x(NCBH_3)_{(2-x)}(bpp)_2$ were synthesized. ^{57}Fe Mössbauer spectroscopy showed that the ratio of low-spin state in the $Fe(NCBH_3)_2$ unit changed with the change of x. The results revealed that the high spin site of $Fe(NCS)_2$ unit affects the spin state of $Fe(NCBH_3)_2$ unit.

Keywords
Mössbauer spectroscopy, mixed crystals, spin-crossover, assembled complexes

I. INTRODUCTION

Self-assembled coordination polymers containing transition metal ions and organic bridging ligands have attracted intensive interests because of their potential abilities for selective inclusion and transformation of ions and molecules.[1)] It is possible to construct various structures for porous assembled iron complexes bridged by bis(4–pyridyl) type ligand. We have studied iron complexes bridged by 1,3–bis(4–pyridyl)propane (bpp), which has three methylenes, by using single crystal X–ray diffraction analysis, Mössbauer spectroscopy, and SQUID measurements. $Fe(NCX)_2(bpp)_2$ (X = S, Se, and BH_3) had a 2D interpenetrated structure and the $NCBH_3$ complex showed a spin–crossover phenomenon.[2)] We also synthesized $Fe(NCX)_2(bpp)_2 \cdot 2(benzene)$ (X = S, Se, and BH_3). They had a 1D structure and were in temperature-independent Fe^{II} high-spin state. Both 2D interpenetrated and 1D structures were converted to each other by desorption and adsorption of benzene molecules.[3)] Recently, we discussed the spin state of the mixed crystals with zinc or cobalt ion both in the 2D interpenetrated and 1D structures for the assembled complexes bridged by bpp.[4)] In the present study, we discussed the structure of the mixed crystals of iron with NCS and $NCBH_3$ for the assembled complexes bridged by bpp, and then we discussed the spin state of the mixed crystals.

Ⅱ. Results and Discussions

Elemental analysis of $Fe(NCS)_X(NCBH_3)_{2-X}(bpp)_2$ showed that x is 0.25, 0.65, 0.95, 1.15, 1.1, 1.25, 1.4, 1.7, 1.8, and 1.9, when the preparation ratio of x is 0.2, 0.4, 0.6, 0.8, 1, 1.1, 1.2, 1.4, 1.6,and 1.8, respectively. This reveals that the obtained crystals show a trend that the ratio of NCS increases compared with the preparation ratio. All the mixed crystals showed the similar powder X-ray diffraction patterns, and the (002) diffractions of the mixed crystals are not the superposition of those from $Fe(NCS)_2(bpp)_2$ and $Fe(NCBH_3)_2(bpp)_2$. The (002) diffractions are shifted to higher degree by increasing ratio of NCS.

We carried out single crystal X-ray diffraction analysis of $Fe(NCS)_{1.8}(NCBH_3)_{0.2}(bpp)_2$. By comparing $Fe(NCS)_{1.8}(NCBH_3)_{0.2}(bpp)_2$ with $Fe(NCS)_2(bpp)_2$, and $Fe(NCBH_3)_2bpp_2$, we found that the structure is similar to $Fe(NCS)_2(bpp)_2$ but has shorter b-axis and longer c-axis. The result is consistent with the result of powder X-ray diffraction.

We measured Mössbauer spectra of the present mixed crystals. All the spectra consist of $Fe(NCS)_2$ unit and $Fe(NCBH_3)_2$ unit. Fig. 1 shows that ratio of $NCBH_3$ and fraction of low spin in mixed anion crystal. The result reveals that the ratio of low-spin state in the $Fe(NCBH_3)_2$ unit changed with the change of x and revealed the high-spin site of $Fe(NCS)_2$ unit affects the spin state of $Fe(NCBH_3)_2$ unit. The results suggest the chemical pressure effect, in which $Fe(NCS)_2$ unit next to $Fe(NCBH_3)_2$ unit makes $Fe(NCBH_3)_2$ unit to become high spin from low spin at low temperature.

Ⅲ. Conclusion

We synthesized new mixed anion crystals, $Fe(NCS)_x(NCBH_3)_{(2-x)}(bpp)_2$. ^{57}Fe Mössbauer spectroscopy showed that the high-spin site of $Fe(NCS)_2$ unit affects the spin state of $Fe(NCBH_3)_2$ unit.

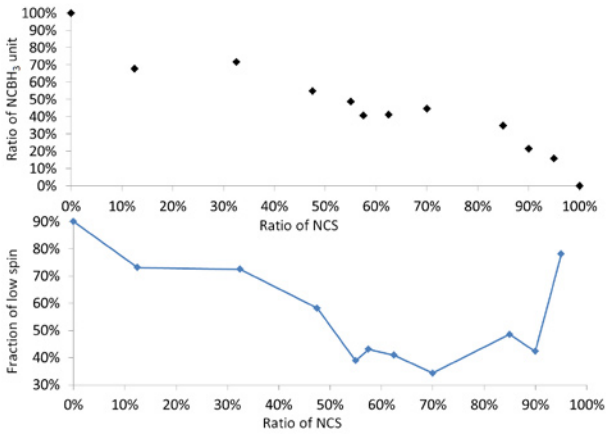

Fig 1. Ratio of $NCBH_3$ and fraction of low spin in mixed anion crystal

[1] B. Moulton, M. J. Zaworotko, Chem Rev., 101 (2001) 1629
[2] M. Atsuchi, H. Higashikawa, Y. Yoshida, S. Nakashima, and K. Inoue, Chem. Lett., 36 (2007) 1064.
[3] M. Atsuchi, K. Inoue, and S. Nakashima, Inorg. Chim. Acta, 370 (2011) 82
[4] S. Nakashima, T. Dote, M. Atsuchi, and K. Inoue, J. Phys., C217, 01035 (2010).

Analysis of Fragments of a Roman Mask using Mössbauer spectroscopy

Paulo de Souza[1,2], G. Klingelhöfer[3], P Gütlich[3], M. Egg[4]
[1]University of Tasmania, Hobart TAS 7001 Australia
[2]Commonwealth Scientific and Industrial Research Organisation, Hobart TAS 7001 Australia
[3]Johannes Gutenberg-Universität Mainz D-55128 Germany
[4]Römisch-Germanisches Zentralmuseum, Mainz D-55116 Germany

Abstract – *A fragmented roman mask was found in excavations at "Villa von Allmend", Saarland, Germany. The mask is made of iron, covered externally by bronze. Such objects were used in war games during the height Roman times. During the excavations around the mask other metallic objects were also found. Some clearly belong to the mask, such as the left ear (Figure 1, top left), among other fragments that cannot be associated with the mask without further investigation. Some of these fragments were investigated using backscattering Mössbauer spectroscopy. The objective was to determine whether the fragment was a piece of the roman mask or was part of another object laying in the excavated area, and shed additional light on the manufacturing process of the mask itself.*

The current communication discusses the results of the analysis of fragments from this roman mask using the miniaturised Mössbauer spectrometer (MIMOS II). This instrument was developed by Dr. Klingelhöfer's research group in Mainz for space exploration [1] and was successfully used onboard NASA's Mars Exploration Rovers [2]. Thanks to MIMOS II portability, robustness, low-power consumption and relative good radiation shielding, in situ characterization became possible. These advantages of MIMOS II were explored in a number of outdoor applications [3, and references therein]. In archaeology the instrument has been applied in the analysis of rock paintings [3] and on a greek Vase [4].

On this roman mask, the results yield the understanding of the provenance of fragments and were used to guide the process of its restoration. The Mössbauer spectra on pieces that clearly belong to the mas show the presence of many iron oxides including wüstite (FeO_{1-x}). Wüstite has been interpreted as the indication of production of 'brand patina' on the surface of the object. This oxide phase could be produced by fast cooling under reducing atmosphere (e.g., putting the hot metal in a bath of animal fat). Patina was a surface treatment used by romans to improve resistance to corrosion and for aesthetics purposes. Therefore, the absence of wüstite would imply in a possible mismatch with the original mask.

Keywords – Mössbauer spectroscopy, archaeology.

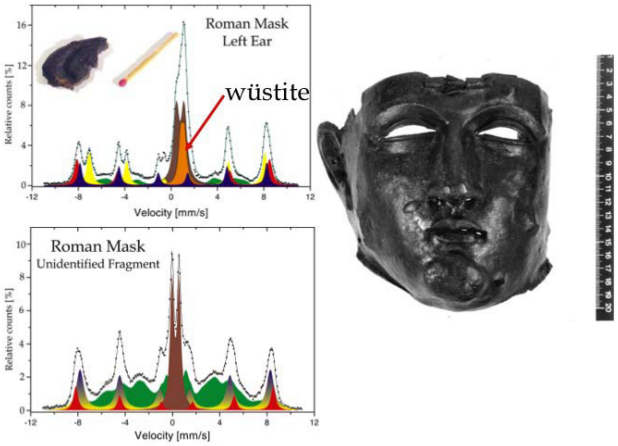

Fig. 1. Room temperature Mössbauer spectra of some of the studied metallic fragments. On the top, the left ear of the mask; on the bottom, an unidentified fragment (probably from the metallic box where it was placed), and on the left, the final appearance of the reconstructed mask.

REFERENCES

[1] G. Klingelhöfer, R. V. Morris, B. Bernhardt, D. Rodionov, P. A. de Souza, S. W. Squyres, J. Foh, E. Kankeleit, R. Gellert, C. Schröder, S. Linkin, E. Evlanov, B. Zubkov, O. Prilutski (2003) The Athena MIMOS II Mössbauer Spectrometer Investigation. ***Journal of Geophysical Research***, v. 108, No. E12, 8067. doi: 10.1029/2003JE002138.

[2] G. Klingelhöfer, R. V. Morris, B. Bernhardt, C. Schröder, D. Rodionov, P. A. de Souza, A. Yen, R. Gellert, E. N. Evlanov, B. Zubkov, J. Foh, U. Bonnes, E. Kankeleit, P. Gutlich, D. W. Ming, F. Renz, T. Wdowiak, S. W. Squyres, R. E. Arvidson (2004) Jarosite and Hematite at Meridiani Planum from Opportunity's Mössbauer Spectrometer. ***Science***, 306,1740-1745. doi: 10.1126/science.1104653.

[3] C. Schröder, G. Klingelhöfer, R. V. Morris, B. Bernhardt, M. Blumers, I. Fleischer, D. S. Rodionov, J. Gironés López, P. A. de Souza (2010) Field-portable Mössbauer Spectroscopy on Earth, the Moon, Mars, and Beyond, ***Geochemistry: Exploration, Environment, Analysis***, 11 (2011) 2, 129-143. doi: 10.1144/1467-7873/09-IAGS-018.

[4] P. A. de Souza, B. Bernhardt, G. Klingelhöfer, P. Gütlich (2003) Surface Analysis in Archaeology Using the Miniaturized Mössbauer Spectrometer MIMOS II. ***Hyperfine Interactions***, v. 151, 125-130. doi: 10.1023/A:1025444209059.

Synthesis of ^{14}C labeled C_{60} with higher specific activity

T. Tadai[1], K. Akiyama[1], H. Aoshima[2], R. Ibuki[2], S. Kubuki[1]
[1]Department of Chemistry, Tokyo Metropolitan University, Hachioji, 192-0397, Japan
[2]Vitamin C60 BioResearch Corporation, Chuo-ku, Tokyo 103-0028, Japan

Keywords Keywords – ^{14}C-labeled C_{60}

I. INTRODUCTION

Recently, Fullerenes and their derivatives have been attracted to the medical and cosmetics fields. However, there are some problems for the application of fullerenes, such as nano toxicity. To overcome these problems, further study about drug disposition is required. As one of the most useful technique, the radioactive tracer method using ^{14}C-labeled C_{60} is applicable for this purpose. Synthesis of ^{14}C-labeled C_{60} has been reported so far [1, 2]. However, synthesis of ^{14}C-labeled C_{60} with higher specific radioactivity is desired for the detail study. In this session, we will report the development of synthesis and the properties of produced ^{14}C-labeled C_{60} such as specific radioactivity.

II. EXPERIMENTAL

$Ba^{14}CO_3$ (0.2 mmol, 57 mCi/mmol) was mixed with $PbCl_2$ and AgCl and then put into the electric furnace for heating at 450 ^oC to produce labeled CO_2 under He gas flow. The produced CO_2 gas was stored in the plastic bag, and then introduced to the Et_2O solution of 2-lithiofuran to produce the furoic acid. The produced furoic acid was reduced with $LiAlH_4$ in THF solution to obtain the labeled furfuryl alcohol. This alcohol was condensed by the evaporator, and then dissolved into *o*-dichlorobenzene (*o*-DCB). For the polymerization of this alcohol, *p*-toluenesulfonic acid was added into this *o*-DCB solution. The polymer solution was adsorbed on a porous carbon rod (PC5060G, Tokai Carbon Inc.) and dried at 200 ^oC under He gas stream for 1 hour. After that, carbon rod was set into fullerene generator and sintered by the electric resistance heating method. The resulting ^{14}C-impregnated graphite electrode was then employed as an anode for the arc discharge for the fullerene production. The soot containing ^{14}C-labeled C_{60} were recovered from the generator as a CS_2 solution and then filtered to remove the insoluble substances. The ^{14}C-labeled C_{60} was purified from these filtered crude fullerenes by HPLC (Buckyprep, Nakarai tesque Inc.). Their total weight and specific radioactivity were determined by UV/vis absorption and liquid scintillation counter (LSC).

III. RESULTS AND DISCUSSION

The yield of ^{14}C was estimated from the radioactivity in $Ba^{14}CO_3$ and in obtained C_{60}, and found to be 0.73 %. This is about 3 times larger than that of previously reported value [1]. As the results of UV/vis absorption measurement, the total weight of purified C_{60} is found to be about 3 mg. The specific radioactivity of these C_{60} estimated from the radioactivity determined by the results of LSC measurement and total weight of $C_{60,}$ were found to be 18.4 mCi/mmol. Enrichment of ^{14}C for this sample was about ^{14}C: ^{12}C = 1: 200. This value is the highest among that of previous reports and indicate that the most enriched ^{14}C-labeled C_{60} is produced by our method.

[1] W. A. Scrivens, *et al., J.Am.Chem.Soc.,*116, 4517-4518, 1994.
[2] S. R. Wilson, *et al., Fullerene Sci. & Technol.,* 4, 43-48, 1996.

Adsorption Behavior of Zr and Hf to TTA-resin in Microcolumn for Determining the Forming Ability of Rf Monofluoride Complex

Y. Kitayama[1], Y. Shigeyoshi[1], A. Yokoyama[2], A. Toyoshima[3], K. Tsukada[3], K. Ooe[4], E. Maeda[1], H. Kimura[1], H. Kikunaga[5], Y. Kudou[6], J. Kanaya[6], M. Huang[6], and H. Haba[6]

*1 Graduate School of Natural Science and Technology, Kanazawa University
*2 Institute of Science and Engineering, Kanazawa University
*3 Japan Atomic Energy Research Institute
*4 Institute of Science and Technology, Niigata University
*5 Research Center for Electron Photon Science, Tohoku University
*6 Nishina Center for Accelerator-Based Sience, RIKEN

Abstract — *We study aqueous chemistry of Rf to determine the forming ability of monofluolide complex of Rf. Reversed-phase chromato-graphic behaviors of non-carrier tracers of Zr and Hf with TTA-resin were observed for simulation of the Rf experiment. Although we obtained good adsorption behavior and short equilibrium time for the batch experiment, the chemical system in microcolumn does not appear to come to equilibrium and needs further improvement.*

Keywords — *Reversed-phase chromatography, Zirconium(Zr), Hafnium(Hf), Rutherfordium(Rf)*

I. INTRODUCTION

Rutherfordium (Rf) has attracted a lot of attention in research on the chemical properties of a super heavy element. For the purpose of its speciation in aqueous solution, we aim to observe the chemical behavior of Rf by means of reversed-phase chromatography with a chelate extractant of 2-thenoyl-trifluoroacetone (TTA) as the stationary phase. It extracts quadrivalent metal ions preferentially, and, that is, it will make possible determination of a specific complex formation constant of Rf. [1]

In this work, we observed chemical equilibrium times and distribution coefficients of non-carrier tracers of Zr and Hf with TTA-resin in the acid solutions of HF/HNO_3 for simulation of the Rf experiment. Then, on-line reversed-phase chromatography of Zr was performed with Automated Rapid Chemistry Apparatus (ARCA), which was also used for an on-line chemical system for the Rf experiment.

II. EXPERIMENTAL

In the batch experiments with ^{88}Zr and ^{175}Hf tracers, we observed equilibrium times and distribution coefficients on TTA-resin in the solution of 9.5×10^{-5} – 10^{-1} M HF / 10^{-1} M HNO_3 , 1×10^{-4} M HF / 10^{-2} –10^{-1} M HNO_3. and 1.0×10^{-4} M HF / 10^{-2} –10^{-1} M HNO_3 by assaying in γ-ray spectrometry with a Ge detector.

In the on-line experiment, an reversed-phase chromato-graphy was performed with the ^{89m}Zr atoms produced in the ^{89}Y (p, n) reaction at the RIKEN K70 AVF cyclotron. They were transported with KCl/He gas jet and collected in ARCA. They were dissolved in acid solutions of HF/HNO_3, and the solutions were introduced in the microcolumns (1.6mm ϕ × 7mm) filled up with TTA-resin at flow rate of 0.1-1 mL/min. The solutions eluted through TTA-resin were collected and subjected to γ-ray spectrometry by using a Ge detector.

III. RESULTS AND DISCUSSION

The batch experiment demonstrated that the best perfor-mance in adsorption was obtained for TTA (octanol) resin on Kel-F resin and TTA (octanol) on CHP20/P20 resin. The equilibration was attained in less than 1 min for the cases. Besides, it was found that the results of experimental with TTA resin agree with those of solvent extraction behavior for Zr and Hf at the lower acid concentrations.

In the on-line experiment, an example of the obtained elution curves is shown in Fig. 1 for TTA on CHP20/P20 resin with a ^{89m}Zr tracer. It shows the tracer atoms are adsorbed on the resin. However, the equilibration times in the on-line experiment appears to be not as short as we had expected from the batch experiment; K_d value from the on-line experiment was observed lower than that for the batch experiment. Therefore, we should find better conditions for shorter equilibration time for the experimental with Rf.

In conclusion, reversed-phase chromatography with TTA resin has the potential for speciation of a Rf chemical species although the resin preparation needs further improvement to optimize the experimental condition for Rf. Thus far we have succeeded in introducing ^{261}Rf into ARCA system and its measurement by α -ray spectrometry.

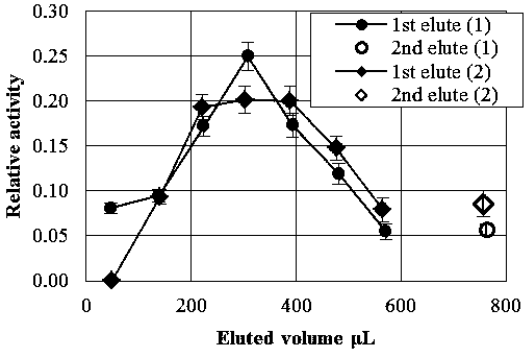

Fig. 1. An example of elution curve of Zr on the TTA resin.
The conditions were 1.0×10^{-4}M in [HF], 0.01M in [HNO_3] for the 1st elute and 1.0×10^{-4}M in [HF], 0.01M in [HNO_3] for the 2nd elute at 0.1 mL/min in flow rate

Reference:

[1] M. Araki, T. Nanri., Y. Takeda, M. Nishio, M. Nishikawa, Y. Kasamatsu, Y. Ezaki, Y. Kudou, H. Haba, and A. Yokoyama: RIKEN Accel. Prog. Rep. **43**, 271 (2010).